Copyright is owned by the Author of the thesis. Permission is given for a copy to be downloaded by an individual for the purpose of research and private study only. The thesis may not be reproduced elsewhere without the permission of the Author.

Transcriptional regulation in mouse macrophages: the role of enhancers in macrophage activation and infection

A thesis presented in partial fulfilment of the requirements for the degree of

Doctor of Philosophy

in

Genetics

at Massey University, Albany Campus, New Zealand.

Elena Denisenko

2018

Abstract

Macrophages are sentinel cells essential for tissue homeostasis and host defence. Owing to their plasticity, macrophages acquire a range of functional phenotypes in response to microenvironmental stimuli. Of those, M(IFN-γ) and M(IL-4/IL-13) macrophage activation states are well known for their opposing pro- and anti-inflammatory roles. Imbalance in these populations of macrophages has been implicated in progression of various diseases. Macrophages also comprise the first line of an organism's defence against *Mycobacterium tuberculosis*, the causative agent of tuberculosis; interactions between the bacteria and host macrophages define the infection outcome.

The area of mammalian transcriptional regulation progressed remarkably with recent advances in high-throughput technologies. Enhancers emerged as crucial regulatory DNA elements capable of activating transcription of target genes at distance in an orientation-independent manner. A recent discovery revealed that enhancers can be transcribed themselves into enhancer RNAs, or eRNAs. Enhancers were shown to be pervasive, yet the associated regulatory patterns remain largely unknown and require further research.

In this thesis, we investigated *in silico* transcribed enhancers in mouse tissues and cell lines, with a particular focus on macrophages. We have performed a large-scale study to identify transcribed enhancers across multiple tissues and to characterise their

properties. In macrophages, we have established the most accurate, to our knowledge, genome-wide catalogue of transcribed enhancers and enhancer-gene regulatory interactions. We have inferred enhancers that might drive transcriptional responses of protein-coding genes upon M(IFN-γ) and M(IL-4/IL-13) macrophage activation, and demonstrated stimuli specificity of regulatory associations. We have conducted the first to our knowledge study of the role of transcribed enhancers in macrophage response to *Mycobacterium tuberculosis* infection. Taken together, the present work provides new insights into genome-wide enhancer-mediated transcriptional control of macrophage protein-coding genes in different conditions. Given the increasing promise for enhancer- and chromatin-directed therapy, this work paves the way for further studies towards host-directed therapies and novel treatments for tuberculosis and immune diseases associated with macrophage dysfunction.

Acknowledgements

First and foremost, I would like to express my deepest gratitude to my mentor and supervisor Dr. Sebastian Schmeier, for his continuous guidance and support all the way through this journey. For invaluable contributions of time and ideas, fruitful discussions, enthusiasm and encouragement, and for all the exciting and rewarding research opportunities I was given.

I would like to thank my co-supervisor Dr. Olin Silander for helpful discussions and his insightful comments on my work.

I am grateful to our collaborators Prof. Frank Brombacher, Dr. Reto Guler, and Dr. Harukazu Suzuki for the data and for their valuable feedback.

My study would not have been possible without a PhD scholarship from the Institute of Natural and Mathematical Sciences, which I am profoundly grateful for.

Last but not least, I would like to express my special appreciation to my family for their endless love and support. I am eternally grateful to my parents for all the hard work, for giving me all the best opportunities so early in life, and for supporting my decisions ever since. A special thank you goes to my husband, for his understanding, love and support through time and space, and for giving everything the right meaning.

List of publications

The results presented in Chapter 3 of this thesis were published as:

- Denisenko, E., Guler, R., Mhlanga, M. M., Suzuki, H., Brombacher, F., Schmeier, S. (2017). Genome-wide profiling of transcribed enhancers during macrophage activation. *Epigenetics & Chromatin*, 10(1), 50.

In addition to the work presented in this thesis, the author has made significant contributions to the following publications:

- Denisenko, E., Ho, D., Tamgue, O., Ozturk, M., Suzuki, H., Brombacher, F., Guler R., Schmeier, S. (2016). IRNdb: the database of immunologically relevant non-coding RNAs. *Database*, 2016, baw138.
- Hon, C. C., Ramilowski, J. A., Harshbarger, J., Bertin, N., Rackham, O. J., Gough, J., Denisenko, E., Schmeier, S., . . ., Forrest, A. R. (2017). An atlas of human long non-coding RNAs with accurate 5' ends. *Nature,* 543(7644), 199-204.
- Hoeppner, M. P., Denisenko, E., Gardner, P. P., Schmeier, S., Poole, A. M. (2018). An evaluation of function of multicopy non-coding RNAs in mammals using ENCODE/FANTOM data and comparative genomics. *Molecular Biology and Evolution*, 35(6), 1451-62.

Table of abbreviations

Abbreviation	Meaning
BMDM	Bone marrow-derived macrophages
bp	Base pair
CAGE	Cap analysis of gene expression
ChIP-seq	Chromatin immunoprecipitation followed by sequencing
DEG	Differentially expressed gene
DNA	Deoxyribonucleic acid
eRNA	Enhancer RNA
E-P	Enhancer-promoter
FDR	False discovery rate
GRO-seq	Global nuclear run-on sequencing
GSEA	Gene set enrichment analysis
H3K27ac	Acetylation of histone H3 at lysine 27
H3K4me1	Monomethylation of histone H3 at lysine 4
IFN-γ	Interferon gamma
IL-13	Interleukin-13
IL-4	Interleukin-4
kb	Kilobase
lncRNA	Long-noncoding RNA
LPS	Lipopolysaccharide

Abbreviation	Meaning
M.tb	*Mycobacterium tuberculosis*
Mb	Megabase
mRNA	Messenger RNA
PRR	Pattern recognition receptor
RNA	Ribonucleic acid
RNAPII	RNA polymerase II
RNA-seq	RNA sequencing (whole transcriptome shotgun sequencing)
SE	Super (stretch) enhancer
SEM	Standard error of the mean
TAD	Topologically associating domain
TB	Tuberculosis
TF	Transcription factor
TFBS	Transcription factor binding site
TLR	Toll-like receptor
TPM	Tags per million
TSS	Transcription start site
TT-seq	Transient transcriptome sequencing

Table of contents

List of figures

List of tables

Chapter 1

Introduction

1.1. Macrophage biology

Macrophages are phagocytic cells that have a central role in both tissue homeostasis and immune responses, performing tissue-specific functions and protecting the organism against invading pathogens (Murray & Wynn, 2011). Below we present a brief overview of macrophage biology, starting from macrophage origins, through their broad functions, to their role in tuberculosis infection.

1.1.1. Macrophages in tissues

Macrophages are generated both during embryonic development and in adult organisms. During organogenesis in embryos, macrophages originate from erythromyeloid progenitor cells that are derived from the embryonic yolk sac and foetal liver (Ginhoux & Guilliams, 2016; Gordon & Pluddemann, 2017). Later on, bone marrow haemopoietic stem cells give rise to blood monocytes, which can differentiate into

macrophages (Ginhoux & Guilliams, 2016; Gordon & Pluddemann, 2017). Macrophage precursors are recruited to tissues where they differentiate into various specialised populations of tissue resident macrophages (Ginhoux & Guilliams, 2016; Gordon & Pluddemann, 2017).

In tissues, the resident macrophages interact with other tissue cell-types and perform phagocytic, homeostatic, regenerative, and metabolic functions (Ginhoux & Guilliams, 2016; Gordon & Pluddemann, 2017). For instance, osteoclasts represent one of the macrophage subpopulations in bone marrow, which is responsible for bone remodelling; Kupffer cells in the liver participate in metabolism; alveolar macrophages in lungs are involved in particle clearance and primary interactions with airborne pathogens (Gordon & Pluddemann, 2017). Macrophage populations are highly heterogeneous and often various subpopulations co-exist even within one tissue. This is achieved due to the high plasticity of macrophages and their ability to alter their phenotypes and acquire specific functions in response to environmental conditions (Ginhoux, Schultze, Murray, Ochando, & Biswas, 2016).

1.1.2. Macrophages in immune responses

Macrophages constantly scan the tissues where they reside, and sense potential pathogens with a variety of receptors they express (Gasteiger et al., 2017). In addition, macrophages are specifically recruited to sites of injury, inflammation or infection (Gordon & Pluddemann, 2017). They serve as sentinel cells that both mediate innate immune responses and initiate adaptive immune responses (Murray & Wynn, 2011).

As innate immune system cells, macrophages represent the first line of defence against invading pathogens, and mediate immediate but nonspecific response (Murray &

Wynn, 2011). Upon recognition of a pathogen, macrophages can engulf and kill it (Murray & Wynn, 2011). In addition, this encounter induces the production and release of cytokines and chemokines by macrophages (Arango Duque & Descoteaux, 2014). These signalling molecules regulate inflammation by binding to cognate receptors on various immune cells and inducing these cells or attracting them to the site of inflammation (Arango Duque & Descoteaux, 2014). In addition, upon phagocytosis of foreign material, macrophages can digest it and present its antigens to T cells, hence, participating in the initiation of adaptive immune response (Arango Duque & Descoteaux, 2014). In contrast to the innate immune response, the adaptive response is specific to a pathogen and establishes immunological memory (Gasteiger et al., 2017).

Besides initiating immune response, macrophages are crucial at its later stage for resolution of immune response-related processes (Murray & Wynn, 2011). Once the pathogen is eliminated, the immune response has to be converted into wound healing and tissue-repair processes, and processes to restore tissue homeostasis. These processes are also mediated by macrophages. However, these macrophages must acquire a regulatory or suppressive phenotype (Murray & Wynn, 2011). In order for macrophages to perform these opposite functions, they must be appropriately activated, or polarised, in response to environmental signals.

1.1.3. Macrophage activation states

Macrophages respond to a wide range of external stimuli by changing their phenotype and physiology (Mosser & Edwards, 2008). Macrophages acquire heterogeneous activation states that exert functional programmes tailored for specific microenvironments (Mosser & Edwards, 2008). A spectrum of macrophage phenotypes

has been observed, with macrophages activated in response to interferon-γ, M(IFN-γ), and interleukin-4/interleukin-13, M(IL-4/IL-13), representing two extreme states (**Figure 1.1**) (Ginhoux et al., 2016; Murray et al., 2014).

M(IFN-γ) macrophages, often referred to as classically activated macrophages, are pro-inflammatory macrophages characterised by efficient antigen presentation, high bactericidal activity, and the production of pro-inflammatory cytokines, reactive oxygen and nitrogen intermediates (**Figure 1.1**) (Martinez & Gordon, 2014; Sica & Mantovani, 2012). *In vivo*, IFN-γ can be secreted by T-helper 1 cells in response to the infection with intracellular pathogens during reciprocal interactions with macrophages (Martinez & Gordon, 2014). The interaction of IFN-γ with its receptors activates Janus kinase adaptors (Jak1 and Jak2), which, in turn, activate a range of transcription factors (TFs), e.g. signal transducer and activator of transcription 1 (STAT1), as well as interferon regulatory factors (e.g. IRF1 and IRF8), which ultimately leads to the transcription of pro-inflammatory genes (Martinez & Gordon, 2014). Besides IFN-γ, other stimuli such as IFN-β and LPS, which can act via different mechanisms, are often considered as inducers of pro-inflammatory classically activated macrophages (Martinez & Gordon, 2014; N. Wang, Liang, & Zen, 2014).

M(IL-4/IL-13) macrophages, often classified as alternatively activated macrophages, are predominantly regulatory macrophages involved in homeostasis, angiogenesis, wound healing, tissue remodelling and parasitic and bacterial infection (**Figure 1.1**) (Gordon & Martinez, 2010; Herbert et al., 2004; Jenkins et al., 2013; Mosser & Edwards, 2008; Murray & Wynn, 2011). M(IL-4/IL-13) macrophages release anti-inflammatory cytokines and show less efficient antigen presentation and decreased production of pro-inflammatory cytokines when compared to M(IFN-γ) (Gordon & Martinez, 2010; Mosser & Edwards, 2008). *In vivo*, IL-4 and IL-13 can be released by T helper 2 cells and macrophages themselves in response to extracellular parasites and pathogens (Gordon & Martinez, 2010;

Hume, 2015). These cytokines act through their receptors and Jak1/Jak3 adapters to activate TFs such as STAT6, c-Myc and IRF4 (Martinez & Gordon, 2014). In addition to IL-4 and IL-13, other stimuli such as IL-10 and M-CSF have been classified as inducers of alternatively activated macrophages (Martinez & Gordon, 2014; N. Wang et al., 2014).

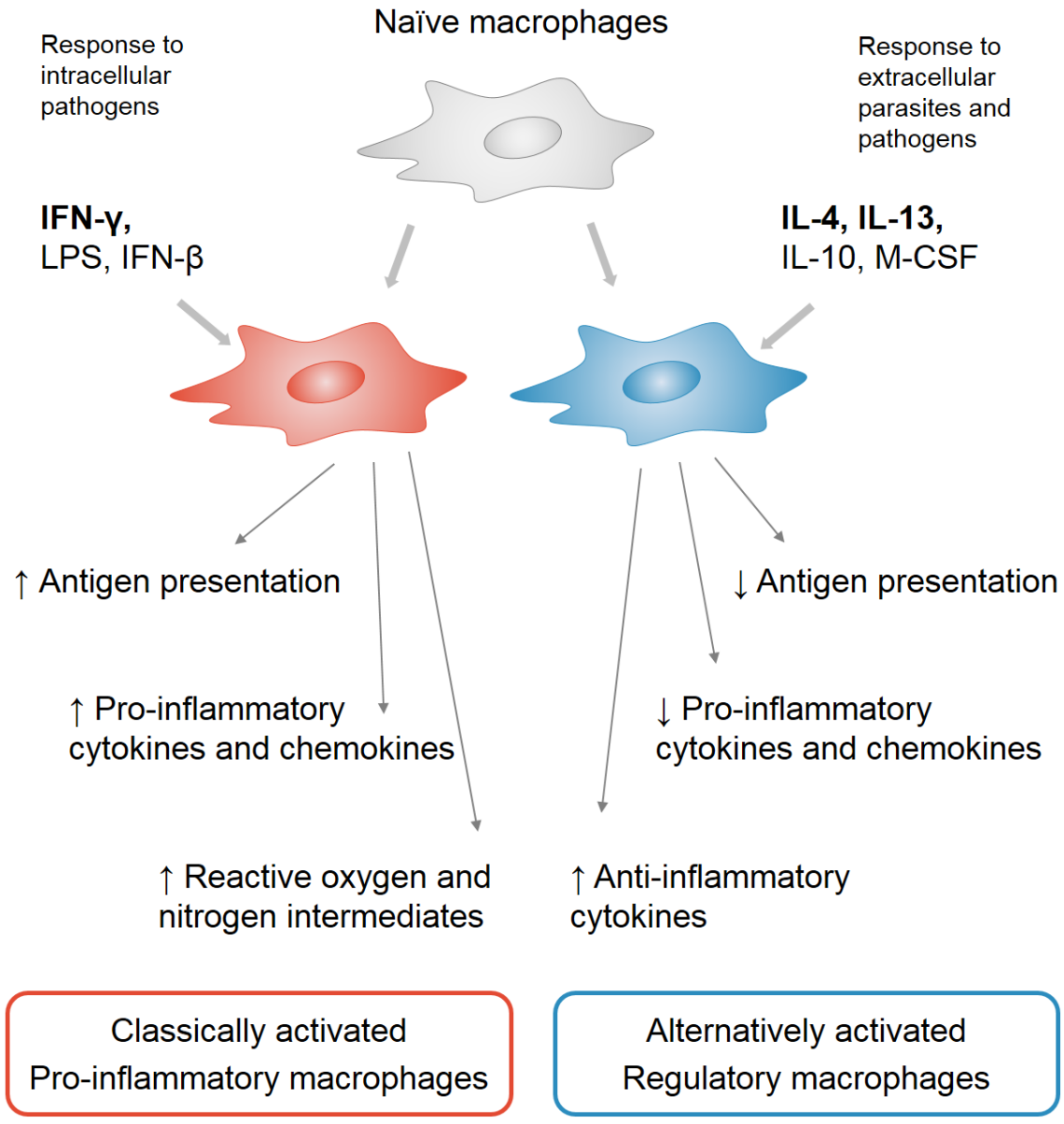

Figure 1.1. Classical and alternative macrophage activation states.

Imbalance in populations of macrophages with opposing pro- and anti-inflammatory roles has been implicated in disease progression (Murray & Wynn, 2011). For instance,

tumour microenvironments promote phenotypic switches from pro- to anti-inflammatory macrophages, which might contribute to tumour progression by inhibiting immune responses to tumour antigens (Mosser & Edwards, 2008; Murray & Wynn, 2011). Conversely, the phenotypic switch from anti- to pro-inflammatory population of macrophages might contribute to obesity and metabolic syndrome (Mosser & Edwards, 2008; Murray & Wynn, 2011; Odegaard et al., 2007). Intracellular pathogen *Mycobacterium tuberculosis*, the causative agent of tuberculosis, interferes with classical activation of macrophages to avoid its antibacterial actions, and promotes alternative activation state (Guler et al., 2015; Lugo-Villarino, Verollet, Maridonneau-Parini, & Neyrolles, 2011). Therefore, the development of techniques for the manipulation and specific targeting of macrophage populations could ultimately improve diagnosis and treatment of inflammatory diseases (Mosser & Edwards, 2008).

Multiple studies have been devoted to the identification of macrophage activation mechanisms and classification of polarisation states (Ginhoux et al., 2016; Murray et al., 2014). In order to distinguish between macrophage subpopulations, certain activation state gene markers are often employed (Murray et al., 2014). Older studies proposed to divide all macrophages into classically and alternatively activated, whereas latest insights underscore the presence of a continuous spectrum of macrophage activation states (Ginhoux et al., 2016). To advance this area of research, the cellular mechanisms responsible for macrophage activation need to be further deciphered.

1.1.4. Macrophages in the response to tuberculosis infection

1.1.4.1. Tuberculosis

Tuberculosis (TB) remains a significant global threat, which causes over one million deaths each year (Zumla et al., 2015). The causative agent of TB is *Mycobacterium tuberculosis (M.tb)*, an intracellular pathogen that persists inside host macrophages (Ernst, 2012; Xu, Wang, Gao, & Liu, 2014). Over 30% of the world's population is infected with *M.tb*, and the infection progresses to active TB in about 5-10% of cases (Xu et al., 2014; Zumla, Raviglione, Hafner, & von Reyn, 2013). The widely used BCG vaccine for TB has a limited efficacy (Ernst, 2012; Russell, Barry, & Flynn, 2010). Existing TB treatment comprises long and expensive multidrug therapy with toxic side effects, high failure and relapse rates (Baer, Rubin, & Sassetti, 2015; Dartois, 2014; Hawn, Matheson, Maley, & Vandal, 2013). In addition, only a single new drug has been introduced over the past decades (Baer et al., 2015). The infection management is complicated by the emergence of multidrug-resistant and extensive drug-resistant *M.tb* strains (Hmama, Pena-Diaz, Joseph, & Av-Gay, 2015; Russell et al., 2010). The lack of effective TB control systems is in part explained by significant gaps in our knowledge of the biology of *M.tb* and its interactions with its host (Orme, Robinson, & Cooper, 2015). Consequently, understanding the cellular pathways that underlie the initial infection and TB progression remains a scientific challenge directly applicable to human health.

The course of *M.tb* infection is initiated by the inhalation of bacteria, followed by their interaction with host cells and the eventual release of *M.tb* back to the atmosphere. One of the first lines of a host's defence against invading bacterial pathogens are macrophages (Weiss & Schaible, 2015). Interaction between macrophages and *M.tb* are

thought to define the infection outcome (Orme et al., 2015). In the lungs, *M.tb* is phagocytosed primarily by resident alveolar macrophages, which triggers a cascade of host response events (Guirado, Schlesinger, & Kaplan, 2013). Macrophages release a range of cytokines and chemokines, which serve to attract additional immune cells to the site of infection and to stimulate their activation (Guirado et al., 2013). The recruited innate immune system cells become infected with *M.tb* and accumulate to establish a macrophage-rich cell mass known as the granuloma, which serves to limit the bacterial expansion (Dartois, 2014; Guirado et al., 2013; Russell et al., 2010).

The next step in the course of infection is associated with the onset of adaptive immune response carried out primarily by T cells (R. T. Robinson, Orme, & Cooper, 2015). T cells need to accumulate at the site of infection, to be appropriately activated themselves and able to activate the infected macrophages in granuloma (R. T. Robinson et al., 2015). As a result, the expansion of the *M.tb* population is restricted, and TB enters a latent state, asymptomatic and not infectious; nevertheless, a subpopulation of *M.tb* keeps replicating (Ernst, 2012). Later in life, the latent *M.tb* might be reactivated and might progress to active symptomatic TB. The underlying causes are yet to be fully understood, but are often connected to weakened immunity (Ernst, 2012).

1.1.4.2. Interplay between host macrophages and *M.tb*

The complex interplay between host macrophages and *M.tb* is believed to be central to the control of infection and to define the infection outcome (Guirado et al., 2013; Orme et al., 2015). Macrophages phagocytise *M.tb* in order to combat the pathogen. However, *M.tb* has developed a multitude of strategies to resist host immune responses by escaping

from macrophage killing, and surviving and proliferating within these cells (Guirado et al., 2013).

Host macrophages recognise surface molecules of *M.tb* with a group of pattern recognition receptors (PRRs), such as toll-like receptors (TLRs), scavenger and mannose receptors (Stamm, Collins, & Shiloh, 2015). The recognition leads to bacterial phagocytosis and induction of signalling pathways that ultimately activate and shape immune responses (Queval, Brosch, & Simeone, 2017). Of those pathways, NF-κB and Mapk signalling play central roles in the induction of a pro-inflammatory response, as they mediate the production of pro-inflammatory cytokines and chemokines (Mogensen, 2009; Wada & Penninger, 2004). The production of Tnf is also induced by PRRs and amplifies the inflammatory response, as Tnf signalling further induces NF-κB and Mapk signalling pathways (Brenner, Blaser, & Mak, 2015). Macrophage phagocytosis of *M.tb* is followed by the formation of a membrane-enclosed phagosome, which normally serves as a compartment for destruction and digestion of the pathogen (Hmama et al., 2015). For this to happen, phagosomes must undergo maturation processes and fusions with lysosomes, which result in their acidification and acquisition of microbicidal factors, necessary for internalised particle degradation (Kinchen & Ravichandran, 2008). In addition, macrophages produce various toxic anti-bacterial compounds such as nitric oxide and reactive oxygen species, restrict the invader's access to essential nutrients such as iron and fatty acids, and employ other complex strategies to combat the pathogen (Weiss & Schaible, 2015). Macrophages require an appropriate activation in order to successfully eliminate the pathogen, i.e. classically activated macrophages, such as M(IFN-γ), have strong anti-bacterial capacities (Weiss & Schaible, 2015). Hence, the success of *M.tb* as an intracellular pathogen depends on its ability to resist the multitude of stresses exerted by the host cells.

M.tb can subvert the host response by interfering with classical activation of macrophages and inducing alternative activation (Gordon & Martinez, 2010; Muraille, Leo, & Moser, 2014). This exploitation of alternative activation might contribute to a persistent *M.tb* infection and represents one of the adaptation mechanisms of *M.tb* (Kahnert et al., 2006).

M.tb has developed a plethora of other survival strategies to circumvent host immune responses. *M.tb* can inhibit phagosomal maturation via preventing fusion with lysosomes and acidification (Hmama et al., 2015; Queval et al., 2017). Moreover, the bacteria might induce phagosomal rupture and escape to the cytosol (Queval et al., 2017). Another important survival mechanism of *M.tb* is the attenuation of macrophage antigen presentation to T cells, hence, avoiding the onset of adaptive immune response (Hmama et al., 2015). In addition, *M.tb* can control macrophage cell death pathways, however, our current understanding of this process remains limited. It is generally believed that *M.tb* interferes with apoptosis, which contributes to the pathogen elimination, and causes necrosis, which facilitates the spread of *M.tb* (Amaral, Lasunskaia, & D'Imperio-Lima, 2016). However, some evidence suggests that, on the contrary, *M.tb* might induce apoptosis that facilitates its spread, while necrosis might contribute to immune system sensing of the bacteria (Amaral et al., 2016). Hence, the mechanisms of *M.tb* survival within macrophages are multifaceted and need to be comprehensively studied and understood in order to improve on current TB treatments.

1.1.5. Conclusions and perspective

Macrophages are crucial for both tissue homeostasis and immune responses. Owing to their plasticity, macrophages acquire various activated phenotypes with distinct and

sometimes opposing functions. Imbalance in macrophage populations is involved in a range of diseases, thus, making macrophages important therapeutic targets. However, our current knowledge of macrophage activation states and mechanisms remains limited, and further studies are required to advance this area of research.

1.2. Transcriptional regulation

1.2.1. Transcriptional regulation as a fundamental mechanism of gene expression control

Expression of the genetic information in eukaryotic cells is a complex process guided by a multitude of mechanisms (Komili & Silver, 2008). Precise regulation of gene expression ensures realisation of tissue-specific functions and generation of appropriate fine-tuned responses to external stimuli (Weake & Workman, 2010). Gene expression is dynamically regulated on different levels including transcription and translation, through a wide range of molecular mechanisms such as DNA methylation (Wu & Zhang, 2014), chemical modification of RNA (Roundtree, Evans, Pan, & He, 2017), and regulation by non-coding RNAs (Bartel, 2004; Bonasio & Shiekhattar, 2014). Regulation of transcription, i.e. of the amount of RNA produced from the gene's DNA region, represents one of the first layers of gene expression control, which largely defines rapid signal-dependent expression changes (Weake & Workman, 2010).

Transcription of RNA from the DNA template is mediated by a complex molecular machinery, components of which recognise specific regulatory regions of DNA, bind them, and function together in a combinatorial manner (Hantsche & Cramer, 2016). Promoters represent a better-characterised class of such regulatory DNA regions from which RNA

transcription is initiated (Forrest et al., 2014; Lenhard, Sandelin, & Carninci, 2012). RNAs are synthesised from template DNA regions by the enzyme RNA polymerase (Borukhov & Nudler, 2008). Three distinct types of RNA polymerase transcribing different classes of genes into different types of RNAs are described in eukaryotic cells (Hantsche & Cramer, 2016). Protein-coding genes are transcribed into messenger RNAs (mRNAs) by RNA polymerase II (RNAPII), the better-studied type of RNA polymerases (Hantsche & Cramer, 2016). Other proteins and protein complexes such as TFs and cofactors are required to guide RNA polymerases and modulate their activity. TFs are DNA-binding factors that recognise and bind specific short DNA sequences (Spitz & Furlong, 2012). Cofactors interact with other components of the transcription machinery and participate in induction or repression of the corresponding gene transcription, e.g. by altering TF or RNA polymerase activity via protein modifications (Reiter, Wienerroither, & Stark, 2017).

Initiation of transcription from the promoter requires the transcription machinery to locate a promoter region, unwind the corresponding DNA duplex and to assemble a preinitiation complex (Hantsche & Cramer, 2016). Upon initiation, RNA polymerase transcribes short RNA molecules and pauses. Pause release and switch to RNA elongation requires recruitment of additional factors and formation of elongation complexes, and, possibly, another set of factors mediates termination of transcription later on (Lee & Young, 2013). Hence, RNA transcription represents a multi-step process which is thoroughly controlled at different stages.

Promoters act in concert with distal regulatory DNA elements, such as enhancers and silencers (Shlyueva, Stampfel, & Stark, 2014). Enhancers function to induce transcription of their target genes, as opposed to silencers, which suppress it (Shlyueva et al., 2014). These regions, often referred to as *cis*-regulatory elements, bind specific TFs and cofactors which can influence the functioning of transcription machinery at the target

gene (Shlyueva et al., 2014; Spitz & Furlong, 2012). Insulators represent another class of *cis*-regulatory elements, which control the accessibility of target genes to the influence of factors bound to enhancers and silencers (Gaszner & Felsenfeld, 2006; Spitz & Furlong, 2012). Hence, multiple different TFs and cofactors bound to promoters and *cis*-regulatory DNA regions are involved in the control of RNA transcription. Each of these DNA regions typically contains clusters of multiple TF binding sites, allowing for simultaneous binding of distinct TFs (Reiter et al., 2017; Spitz & Furlong, 2012). Such combinatorial TF occupancy enables precise regulation and high variability of transcriptional output, as a few TFs can form multiple combinations, each controlling transcription in response to a specific stimulus (Reiter et al., 2017; Spitz & Furlong, 2012; M. C. Thomas & Chiang, 2006).

Transcription is key for the regulation of gene expression, which enables rapid cellular responses to changing environmental conditions (Lee & Young, 2013). Numerous approaches for profiling transcriptional events on a genome scale have become available owing to the rapid development of high-throughput technologies. For over a decade, DNA microarrays have been the principal technology for genome-wide studies of gene expression (Bakalova, Ewis, & Baba, 2006). The core of the method is the hybridisation of a sample of interest to an array of predetermined DNA sequences or probes and, thus, DNA microarrays allow measuring the relative abundance of the known predefined sequences (Bakalova et al., 2006). With the recent advances and decreasing cost of next-generation sequencing, modern transcriptomics technologies, such as RNA-seq (shotgun transcriptome sequencing) (Cloonan et al., 2008; Z. Wang, Gerstein, & Snyder, 2009), are beginning to replace DNA microarrays. These technologies capture and sequence the total cell transcriptome and outperform microarrays in terms of sensitivity and specificity (Marioni, Mason, Mane, Stephens, & Gilad, 2008; C. Wang et al., 2014). In addition, they address some of the limitations of DNA microarrays such as indirect calculation of the

expression levels using fluorescence signal intensities, differences in hybridisation properties across probes and cross-hybridisation (binding of other transcripts rather than the target to a certain probe) (Cloonan et al., 2008; Draghici, Khatri, Eklund, & Szallasi, 2006). Various transcriptomics technologies have been widely applied in a range of biological problems and have dramatically improved our understanding of transcriptional changes under different conditions, regulation of transcription, and its role in health and disease.

1.2.2. Studying transcriptome with cap analysis of gene expression

Cap analysis of gene expression (CAGE) has been developed as a method for profiling actively transcribed RNAs via sequencing of their 5'-ends (Kanamori-Katayama et al., 2011; Kodzius et al., 2006; Shiraki et al., 2003). CAGE selectively identifies RNA molecules carrying 5' caps, a specific chemical modification of a guanine nucleotide which is found in some classes of RNA, including protein-coding mRNAs, and is of importance for pre-mRNA processing, nuclear export and protein translation (Ramanathan, Robb, & Chan, 2016). Given that the 5'-end corresponds to the beginning of the transcribed RNA molecule, CAGE enables identification of active transcription start sites (TSSs). Besides identification of their position, CAGE allows simultaneous quantification of the transcribed RNA molecules (Kanamori-Katayama et al., 2011; Kodzius et al., 2006; Shiraki et al., 2003). Hence, CAGE is a powerful technique that has dramatically advanced studies of transcriptional regulation in mammals (Carninci et al., 2005; Carninci et al., 2006; Forrest et al., 2014).

The experimental workflow for the modern experimental procedure, HeliScopeCAGE, is shown in **Figure 1.2** (Kanamori-Katayama et al., 2011). The workflow

starts with cDNA synthesis from the sample RNA pool (**Figure 1.2a**). Further steps include: biotinylation of RNA cap (**Figure 1.2b**), digestion of single strand RNA (**Figure 1.2c**), capture of biotinylated RNA/cDNA duplexes (**Figure 1.2d**), and removal of non-biotinylated duplexes (**Figure 1.2e**). The single strand cDNA is further released from the captured duplexes and sequenced on HeliScope Single Molecule Sequencer. The protocol does not include an amplification step; instead, sequencing of the single cDNA molecule is performed, avoiding amplification-related biases (Kanamori-Katayama et al., 2011). Sequencing on HeliScope Single Molecule Sequencer yields a set of CAGE reads which subsequenly need to be mapped to the reference genome for identification of TSS positions.

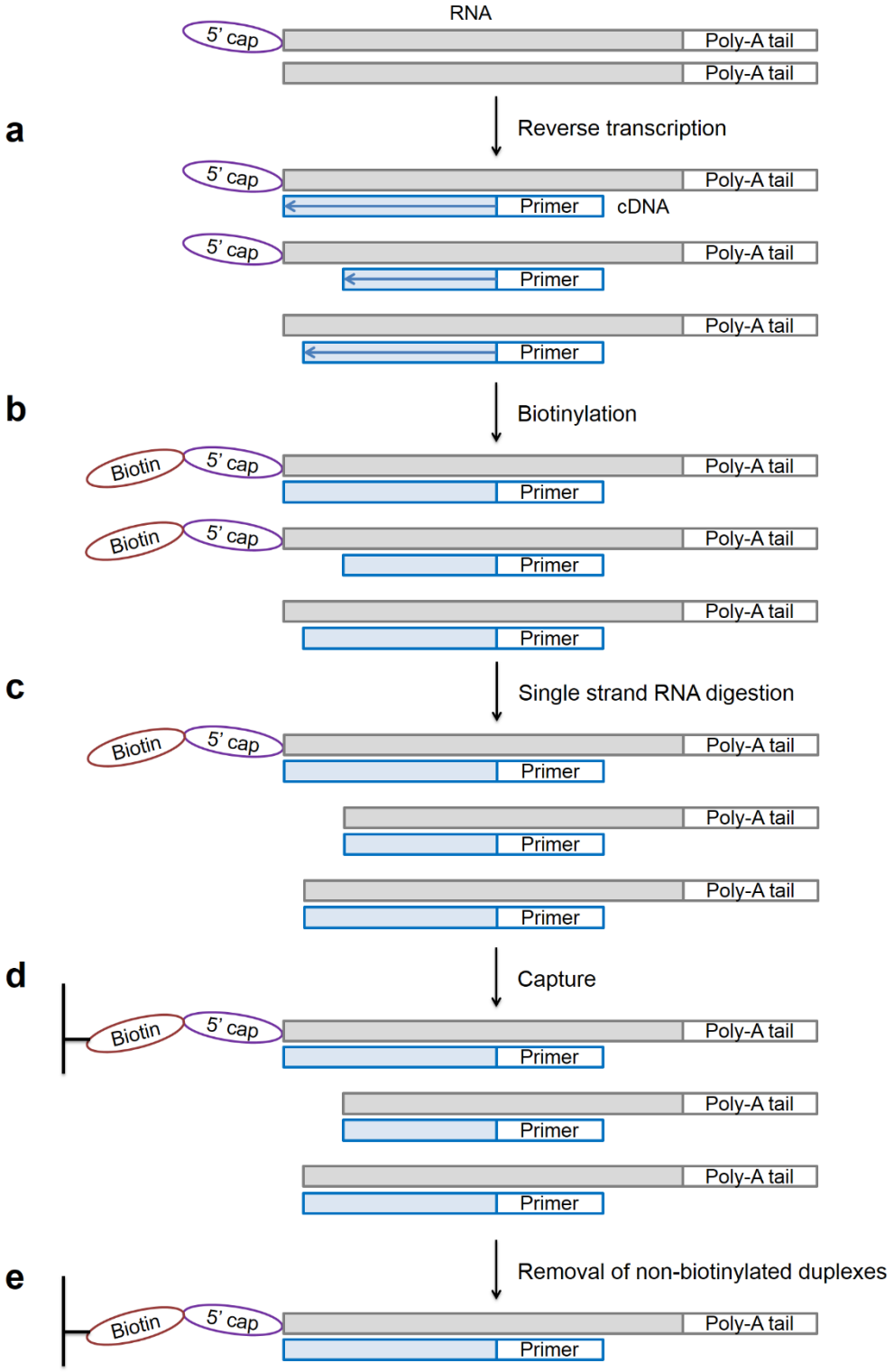

Figure 1.2. HeliScopeCAGE library preparation (Kanamori-Katayama et al., 2011). a First-strand cDNA is generated from a pool of sample RNA using random primers. **b** RNA cap is biotinylated. **c** Single strand RNA is digested using RNase I. **d** Biotinylated 5'-end-complete capped RNA with synthesised cDNA are captured on magnetic streptavidin beads. **e** Unbound 5'-end-incomplete RNA is washed away.

A remarkable advantage of CAGE is that it enables identification of TSSs at a single base-pair resolution. Owing to this property, the first influential studies using CAGE have shown that transcription in mammals is not initiated at a single nucleotide position within the promoter region (Carninci et al., 2006; Kawaji et al., 2006). Rather, a transcript might have multiple initiation positions spread across its promoter region, and at least four different shapes of such distributions were described, including distributions with a single dominant position, broad distributions with or without a dominant position, and bi- or multi-modal distributions (Carninci et al., 2006; Kawaji et al., 2006). CAGE reads representing different transcription initiation events are, thus, unevenly distributed across the genome and identification of genuine promoters represents a complex task.

Different algorithms have been employed to identify CAGE clusters or CAGE peaks – groups of CAGE reads which represent one promoter. First algorithms were based on the distance between the mapped reads. For instance, the reads which overlap with at least 1 bp could be grouped into one CAGE cluster (Carninci et al., 2006). As an alternative, an algorithm for parametric clustering of CAGE reads was developed, where the genomic regions with a given density of CAGE reads are defined as clusters (Frith et al., 2008; Ohmiya et al., 2014). The algorithm of choice might be more complex such as decomposition peak identification (DPI), which accounts for CAGE read distribution across multiple analysed samples and identifies CAGE peaks with different expression profiles across samples (Forrest et al., 2014). Another example is the use of Bayesian methodology to merge into one cluster those CAGE reads, whose expression levels across samples are indistinguishable up to measurement noise (Balwierz et al., 2009). Approaches that account for CAGE read expression profiles across different samples are currently thought to be more precise, since they distinguish even closely located promoters if they are expressed differently in different samples (Balwierz et al., 2009).

This field, however, continues to develop and standardised methods are yet to be established.

CAGE has been extensively used to map TSSs in The Encyclopaedia of DNA Elements (ENCODE) (Djebali et al., 2012) and FANTOM consortium projects (http://fantom.gsc.riken.jp/). Recently, CAGE was applied to a large set of human and mouse primary cells, cell lines, and tissues to produce a comprehensive atlas of gene expression and promoter structure, use and evolution (Forrest et al., 2014) and identify *cis*-regulatory enhancer elements (Andersson et al., 2014). In addition, CAGE has been employed for comprehensive transcriptome profiling of human mast cells (Motakis et al., 2014), monocyte subsets (Schmidl, Renner, et al., 2014), and T cells (Schmidl, Hansmann, et al., 2014). Recently, in a study by our collaborators, CAGE was used for investigation of macrophages and enabled the identification of TFs with distinct activity dynamics in different macrophage populations (Roy, Schmeier, et al., 2015).

Current limitations of CAGE technology include the inability to detect splice variation or alternative termination, as well as absence of standardised analysis protocols due to the relative novelty of the technology. However, CAGE has several advantages over other high-throughput methods such as RNA-seq or microarrays. It avoids the cross-hybridisation problem, allows direct calculation of digital transcript expression, and enables identification of TSSs at a base pair resolution (Balwierz et al., 2009). Hence, the CAGE technology is highly beneficial to transcriptome studies as it enables the genome-wide characterisation of transcription start sites.

1.3. Regulation of transcription by enhancer DNA elements

Enhancers are defined as *cis*-regulatory DNA regions that activate transcription of target genes in a distance- and orientation-independent manner (Shlyueva et al., 2014). Investigations into enhancer regions started a few decades ago from a study of a single element, SV40 virus genome DNA sequence (Banerji, Rusconi, & Schaffner, 1981). Insertion of this element into beta-globin gene recombinants resulted in ~200-fold increase in the gene expression, which was achieved upon insertion in either orientation and at many positions relative to the gene (Banerji et al., 1981). Since then, enhancers have been attracting an increased interest and have been found to be extremely widespread, with an estimation of up to one million enhancers in mammalian genomes (Creyghton et al., 2010; Heintzman et al., 2009; Romanoski, Link, Heinz, & Glass, 2015; Shen et al., 2012). Nowadays, enhancers are considered major determinants of gene expression programmes required for establishing cell-type specificity and mediating responses to extracellular signals (Kieffer-Kwon et al., 2013; W. Li, Notani, & Rosenfeld, 2016; Romanoski et al., 2015; G. D. Thomas et al., 2016). Enhancers are characterised by a set of specific features which are described below.

1.3.1. Enhancers carry specific histone marks

Histone proteins serve as a scaffold to organise DNA into a nucleosome, the basic unit of chromatin (Kouzarides, 2007). Histones can be dynamically modified at many residues by histone-modifying enzymes and these modifications change properties of the corresponding DNA regions (Kouzarides, 2007). For instance, they can result in chromatin remodelling or recruitment of non-histone proteins, ultimately influencing the

transcriptional state of the corresponding DNA region and its transcription (Kouzarides, 2007).

A decade ago it was shown that enhancer and promoter regions could be characterised by distinct histone modifications (Heintzman et al., 2007). Enhancers were found to be marked by mono-methylated histone H3 lysine 4 (H3K4me1) and lacked its tri-methylated form (H3K4me3), whereas this ratio was the opposite in promoter regions (Heintzman et al., 2007). Moreover, a genome-wide mapping of these histone modifications could reliably identify enhancer regions (Heintzman et al., 2009; Heintzman et al., 2007). Further studies showed that H3K4me1 demarcated both poised and active enhancers, while the acetylation of histone H3 lysine 27 (H3K27ac) distinguished the latter (Creyghton et al., 2010). Since then, a combination of H3K4me1 and H3K27ac histone marks has been considered as an enhancer-specific chromatin signature, with H3K4me1 being a mark of an established (or primed) enhancer which may or may not be active, and a combination of H3K4me1 and H3K27ac demarcating active enhancers. The particular mechanisms guiding deposition of H3K4me1 and H3K27ac, its functional consequences and influence on enhancer activity still remain to be elucidated (Calo & Wysocka, 2013).

1.3.2. Enhancers bind transcription factors and coactivators

Enhancer regions carry multiple DNA binding sites and can recruit TFs and transcription coactivators, RNAPII and specific proteins such as histone acetyltransferases p300 and CBP (Heintzman et al., 2007; F. Koch et al., 2011; Romanoski et al., 2015; Spitz & Furlong, 2012; Visel et al., 2009).

Among all these factors, pioneer TFs have an important role in enhancer priming, as they are capable of binding *de novo* to yet unoccupied DNA binding sites, that are inaccessible to other TFs (Zaret & Carroll, 2011). This initial binding of pioneer TFs enables binding of additional TFs and cofactors by opening the chromatin (Zaret & Carroll, 2011). Interestingly, the binding of pioneer TFs to enhancers can have a 'passive' role, in which case their binding reduces the number of additional factors that are necessary for enhancer activation, thus, enabling a rapid signal-dependent activation (Zaret & Carroll, 2011).

Besides pioneer TFs, enhancers carry binding sites for multiple other factors, and the composition of TFs and cofactors that bind an enhancer region changes dynamically during development or in response to stimuli (Spitz & Furlong, 2012). Enhancers were shown to recruit general transcription factors (TFIIA, TFIIB, TFIID, TFIIE, TFIIF, TFIIH) and RNAPII (F. Koch et al., 2011; Szutorisz, Dillon, & Tora, 2005). In this manner, enhancer regions serve as a platform for an assembly of the transcription preinitiation complex, which might further be transferred to a target gene promoter, but also mediates transcription of enhancers themselves (see 1.3.3). In addition, enhancers carry binding sites for specific TFs, such as signal-dependent terminal TFs of signaling pathways, that are responsible for a conditional activation of selected enhancers, which drive signal-specific gene expression changes (Heinz, Romanoski, Benner, & Glass, 2015).

CBP and p300 are highly similar ubiquitous transcriptional coactivators and histone acetyltransferases that extensively occupy active enhancers and some promoters (Calo & Wysocka, 2013; Holmqvist & Mannervik, 2013). CBP and p300 facilitate gene activation by TFs, possibly by mediating interactions between the transcriptional machinery and enhancer-bound TFs (Holmqvist & Mannervik, 2013). CBP and p300 acetylate various proteins, including histone H3 and, thus, mediate the deposition of H3K27ac active enhancer histone marks (Calo & Wysocka, 2013).

1.3.3. Enhancer regions are transcribed into eRNA

Enhancers can recruit RNAPII and serve as a platform for assembly of the transcription preinitiation complex. It can result in transcription of enhancer regions themselves into non-coding RNAs called eRNAs.

This novel class of RNAs was first introduced in a genome-wide study in mouse neurons (Kim et al., 2010). This study investigated enhancer regions and reported a dramatic increase in recruitment of CBP and RNAPII in response to an extracellular stimulus. This recruitment was coupled with an increased transcription of enhancers into eRNAs in a divergent bidirectional manner (**Figure 1.3**). Importantly, eRNA synthesis was suggested to occur specifically at active enhancers that were involved in a stimulus-dependent induction of mRNA transcription (Kim et al., 2010). At the same time, a different group approached the enhancer transcription phenomenon from a different perspective, by investigating all events of stimuli-induced transcription that occurred outside protein-coding genes in mouse macrophages (De Santa et al., 2010). They reported that as many as 70% of extragenic regions bound by RNAPII carried enhancer chromatin signatures (De Santa et al., 2010).

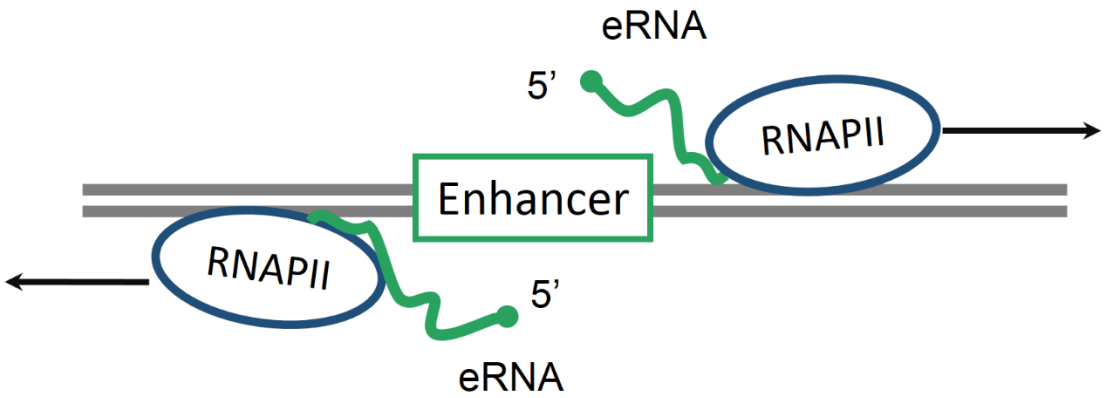

Figure 1.3. RNAPII transcribes enhancer regions in a divergent manner.

Later on, a group of studies showed that the production of eRNAs correlated with target mRNA synthesis; eRNA could serve as a robust and independent indicator of active enhancers, that are more likely to be validated *in vitro* (Andersson et al., 2014; Kim et al., 2010; Mikhaylichenko et al., 2018; Sanyal, Lajoie, Jain, & Dekker, 2012; D. Wang et al., 2011; Wu et al., 2014). Moreover, eRNA transcription can be used for a genome-wide identification of active enhancers (Andersson et al., 2014; Core et al., 2014; Melgar, Collins, & Sethupathy, 2011).

Nevertheless, the field of enhancer transcription remains controversial. First, non-transcribed enhancers still exist and seem to be functional (Cheng, Pan, Tsai, & Tsai, 2015; W. Li et al., 2016). It is unclear what percentage of enhancers can be activated without producing eRNAs and whether this is merely a consequence of inability of current methods to detect eRNA in these regions. Second, although it is believed that transcribed enhancers mostly produce eRNAs in a bidirectional manner, some unidirectional transcription has been reported (Kaikkonen et al., 2013; F. Koch et al., 2011; Kowalczyk et al., 2012; Lam, Li, Rosenfeld, & Glass, 2014; W. Li et al., 2013). Third, the functional importance of enhancer transcription is still being widely studied and debated (W. Li et al., 2016; Natoli & Andrau, 2012), and currently there are three opposing points of view:

1. Enhancer transcription can represent transcriptional noise resulting from accidental collision of RNAPII and enhancer regions;
2. The act of enhancer transcription can itself be important for gene regulation, and its effect is independent of eRNA;
3. eRNAs are functional non-coding RNAs that participate in the regulation of target gene transcription (W. Li et al., 2016; Natoli & Andrau, 2012).

There is evidence supporting each of these three opposed views (Natoli & Andrau, 2012) and it is possible that each of them holds true for a distinct class of enhancers (W. Li et al., 2016).

1.3.4. Controversy over eRNA classification and functionality

There is currently no known specific characteristic that could distinguish eRNA from other non-coding RNA classes, as eRNAs can vary in size from hundreds to thousands of base pairs, can be polyadenylated or non-polyadenylated, spliced or unspliced, and their evolutionary conservation is debated (Andersson et al., 2014; Kim et al., 2010; F. Koch et al., 2011; W. Li et al., 2016; Natoli & Andrau, 2012). Hence, eRNAs are usually defined by their genomic origin, as RNAs transcribed from an enhancer region. Detectable eRNA levels are usually low (De Santa et al., 2010; Natoli & Andrau, 2012), possibly due to their short half-life and fast degradation by RNA exosomes (Lam et al., 2014; Michel et al., 2017; Pefanis et al., 2015) or their generally low transcription initiation rates (W. Li et al., 2016).

Recent findings have complicated the eRNA definition by blurring the differences between eRNAs and other RNA classes such as long-noncoding RNAs (lncRNAs). For instance, many enhancers are transcribed into potentially functional lncRNAs, e-lncRNAs (Hon et al., 2017), some of which have a role in inflammation and immunity (Denisenko et al., 2016; Hon et al., 2017). Furthermore, it was reported that intragenic enhancers can serve as alternative promoters of protein-coding genes (Kowalczyk et al., 2012), whereas another recent study found intragenic enhancers to attenuate expression of their host genes (Cinghu et al., 2017). Therefore, various subtypes of eRNA might exist, and their respective properties are yet to be characterised.

Evidence for functional importance of several eRNAs and their contribution to enhancer action comes from studies investigating individual loci, e.g. by analysing consequences of eRNA targeted suppression (Hsieh et al., 2014; Lam et al., 2013; Melo et al., 2013). Proposed mechanisms of eRNA function include their binding to TFs (Sigova et al., 2015), participation in chromatin remodelling (Mousavi et al., 2013), or formation and stabilisation of enhancer-promoter contacts (Hsieh et al., 2014; W. Li et al., 2013; Pnueli, Rudnizky, Yosefzon, & Melamed, 2015), the importance of which is discussed in the following section. If eRNAs are indeed functional, their functionality would be restricted by the eRNA stability, with more stable e-lncRNAs being able to act in *trans*, and less stable eRNAs being restricted to the same DNA region they were derived from (W. Li et al., 2016; Rothschild & Basu, 2017). Overall, in comparison to an estimate of hundreds of thousands enhancers in a mammalian genome, the relatively few examples of functionality coming from individual eRNA studies reflect a huge gap in the knowledge of enhancer and eRNA biology.

1.3.5. Enhancers loop towards their target promoters

Although various hypotheses exist, the dominant model states that transcriptional regulation by enhancers is exerted via direct physical interaction between an enhancer and a target gene promoter, mediated by DNA looping (see **Figure 1.4a**) (Gorkin, Leung, & Ren, 2014; Shlyueva et al., 2014). Evidence supporting the looping model comes from studies investigating three-dimensional chromatin architecture (Dekker, 2008; Nolis et al., 2009; Sanyal et al., 2012). Possibly, the looping allows to increase a local concentration of TFs and cofactors (which might be delivered by enhancers to promoters), and mediates

the assembly of the transcriptional machinery (Pennacchio, Bickmore, Dean, Nobrega, & Bejerano, 2013).

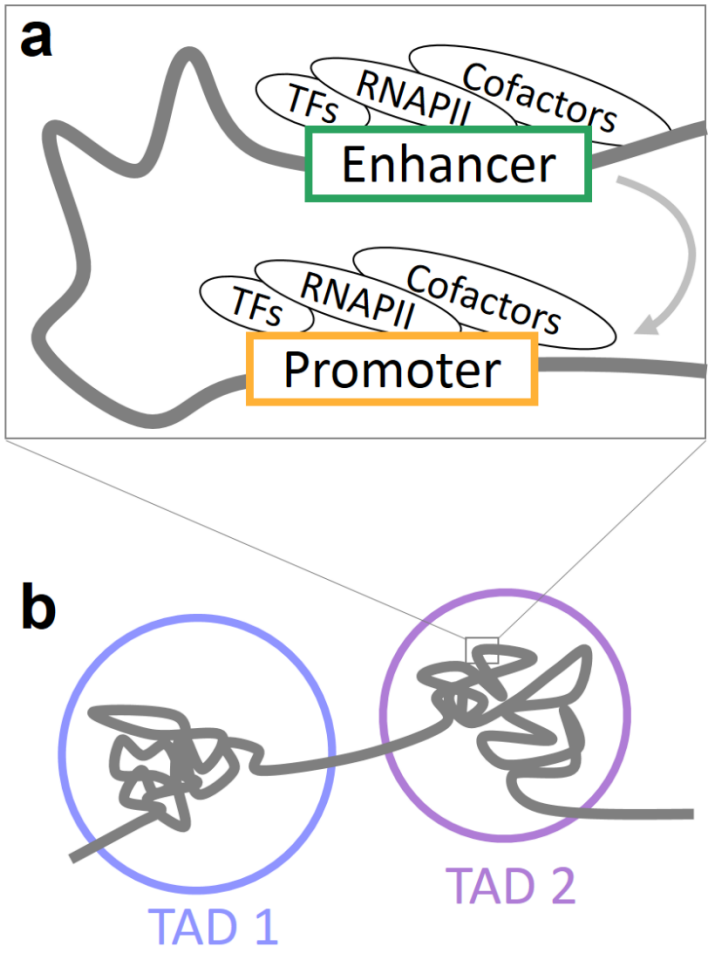

Figure 1.4. Enhancer regulation is mediated via enhancer-promoter looping within topologically associating domains (TADs).

Precise mechanisms of the loop formation and stabilisation remain to be uncovered. One of the outstanding questions is how an enhancer can locate its distant target promoter. Studies of chromosomal three-dimensional structure and discovery of its folding into stable and functional chromosomal domains has shed some light on this question. Topologically associating domains (TADs) have emerged as critical conserved units of chromatin organisation that favour internal DNA contacts, whereas regulatory

interactions between TADs are limited (see **Figure 1.4b**) (Dixon et al., 2012; Rocha, Raviram, Bonneau, & Skok, 2015). Enhancer-promoter looping is believed to occur almost exclusively within TADs, thus, effectively restricting the area for enhancer target (Dixon et al., 2012; Lupianez, Spielmann, & Mundlos, 2016; Rocha et al., 2015; Symmons et al., 2014). Identification of architectural proteins that establish and maintain genome topology, starting from larger chromosomal domains such as TADs, ending with individual enhancer-promoter DNA loops, has become an area of a growing research interest.

CTCF is one of the core architectural proteins with diverse functions (Ghirlando & Felsenfeld, 2016). First, CTCF is enriched at TAD borders, and seems to act as an insulator, which constrains between-TAD interactions, and might determine TAD establishment (Rao et al., 2014). Second, CTCF seems to act on an intra-TAD level, as its binding sites are over-represented at promoters and enhancers (Ong & Corces, 2014). CTCF might guide enhancers to their cognate promoters (Ong & Corces, 2014), and altering CTCF binding patterns changes chromatin loops and gene expression (Guo et al., 2015). Finally, CTCF can bind a variety of proteins and RNAs and might play a role in RNA splicing (Ghirlando & Felsenfeld, 2016).

Cohesin is another structural protein, which co-localises with CTCF at TAD boundaries (Rao et al., 2014). A recent study has shown that cohesin is crucial for TAD formation (Schwarzer et al., 2017). The H3K4me1 enhancer histone mark was shown to facilitate recruitment of cohesin to chromatin (Yan et al., 2018). Cohesin, together with another structural complex called Mediator, co-occupy enhancers and promoters and are believed to form between them a functional and physical bridge, or a ring (Kagey et al., 2010). The mediator complex is also a major regulator of RNAPII transcription, which

transfers regulatory signals from DNA-bound TFs to RNAPII via protein-protein interactions (Allen & Taatjes, 2015).

Some studies have implicated eRNAs in mediating the formation or stabilisation of enhancer-promoter loops. The structural role might be exerted via eRNA interaction with cohesin (W. Li et al., 2013) or the Mediator complex (Hsieh et al., 2014). In agreement, increased expression of eRNAs was reported as a precise mark of the functional looping between activated enhancer and target promoter (D. Wang et al., 2011). In another study, a significant correlation was reported between gene expression, promoter–enhancer looping and the presence of eRNAs (Sanyal et al., 2012). All in all, enhancer-promoter communication is crucial for precise transcriptional regulation, and the corresponding DNA contacts must be thoroughly controlled by architectural proteins on different structural levels.

1.3.6. Enhancer mode of action

A recent review has proposed a general model of enhancer priming and activation (W. Li et al., 2016). According to the model, pioneer TFs first bind future enhancer region to mediate chromatin opening. It enables binding of lineage-determining TFs that define enhancers in a particular cell-type. This is followed by recruitment of collaborative TFs and cofactors, including those mediating the deposition of H3K4me1 histone marks and, therefore, enhancer priming. Activation of enhancers starts with the recruitment of another set of cofactors including CBP and p300 that deposit H3K27ac marks at the enhancer site. In addition, general TFs and RNAPII are recruited, which results in eRNA transcription. Finally, other groups of cofactors mediate eRNA elongation and enhancer-promoter looping (W. Li et al., 2016). This simplistic model outlines a sequence of events

necessary for activation of a single enhancer, while modes of enhancer-promoter communication on a genome scale remain poorly understood.

Enhancer-promoter contacts are believed to occur almost exclusively within the well-conserved TADs (Lupianez et al., 2016). Notably, enhancer-promoter interactions are not limited to one-to-one contacts. Instead, an enhancer might regulate a few genes, and multiple enhancers might contribute to the activation of a gene (Beagrie & Pombo, 2016). The mechanisms and functional consequences of establishing multiple contacts remain elusive. While it is plausible that some enhancers might have overlapping and redundant activities, existing evidence suggest that, instead, many enhancers contribute together to gene expression (Schwarzer & Spitz, 2014). Integration of the signal from several enhancers might occur in different ways. Many enhancers might contact a single promoter stochastically and independently, and the more enhancers there are, the more likely the promoter is contacted by at least one of them at any given moment (Schwarzer & Spitz, 2014). Different enhancers might act sequentially and be necessary for different stages of promoter activation (Schwarzer & Spitz, 2014). Finally, multiple enhancers might be brought together in close proximity to a promoter to form a more stable conformation or to further increase local concentrations of TFs and cofactors (Schwarzer & Spitz, 2014). Irrespective of the precise mechanisms of contribution from multiple enhancers, some evidence indicate that they often act in either an additive or synergistic manner, with many enhancers conferring higher expression activity to a gene (Chepelev, Wei, Wangsa, Tang, & Zhao, 2012; Long, Prescott, & Wysocka, 2016; Shlyueva et al., 2014).

Both enhancers and enhancer-gene regulatory interactions are characterised by a remarkable tissue specificity. First, enhancer-specific histone marks were shown to vary dramatically between different cell-types (Creyghton et al., 2010; Heintzman et al., 2009; C. M. Koch et al., 2007). Second, eRNAs are expressed in a tissue-specific manner (Wu et

al., 2014). Third, three-dimensional chromatin folding and interactions show cell-type-specificity and, thus, can provide structural framework for cell-specific transcription (G. Li et al., 2012; Sanyal et al., 2012). Such tissue specificity is crucial for the establishment of cell-type- and state-specific transcriptional programmes (Kieffer-Kwon et al., 2013; Romanoski et al., 2015). Moreover, enhancer-gene interactions can be dynamically rewired during development or in response to environmental stimuli, enabling the tuning of gene expression programmes (Heinz et al., 2015; Stavreva & Hager, 2015; D. Wang et al., 2011). Hence, profiling of enhancers and their targets in various tissues and conditions is indispensable to improve our understanding of transcriptional regulation.

1.3.7. Enhancers form clusters of super or stretch enhancers

Super or stretch enhancers (SEs) have emerged as enhancer regions especially important for the regulation of genes involved in cell-specific processes and responses (Hnisz et al., 2013; Pott & Lieb, 2015). A strict definition of a SE is yet to be established, and methods of their identification vary considerably between studies (Hah et al., 2015; Hnisz et al., 2013; Parker et al., 2013; Whyte et al., 2013). However, some distinctive properties of SEs are beginning to be elucidated. SEs represent clusters of active and potent enhancers (Hnisz et al., 2015). They are often enriched for TFBSs of terminal TFs of signaling pathways, and thus, can be rapidly activated in response to the corresponding signals (Hnisz et al., 2015). This fact explains why SEs are extensively involved in regulating key cell identity genes, transcription of which needs to be dynamically tuned in response to constantly changing conditions (Hnisz et al., 2015). SEs are associated with higher levels of enhancer-specific histone marks and eRNA expression, and are occupied by more TFs and coactivators such as Mediator than typical enhancers (Hah et al., 2015; Hnisz et al.,

2013; Whyte et al., 2013; Witte, O'Shea, & Vahedi, 2015). Importantly, a recent study showed that SEs maintain especially high local concentrations of transcription stimulatory factors, which allows for their associated genes to have a reduced RNAPII transcription pausing and an increased RNAPII release into productive elongation (Henriques et al., 2018). Hence, this study provided a molecular mechanism that might ensure high expression levels of genes regulated by SEs (Henriques et al., 2018). Due to these properties, SEs have been attracting an increased interest recently, especially in studies of cell-specific functions and responses.

1.3.8. Genome-wide approaches for enhancer identification

Characterisation of enhancer properties described above gave rise to genome-wide approaches for enhancer identification (Shlyueva et al., 2014). These approaches can be classified into three major groups:

1. Profiling of enhancer-specific histone marks (Gosselin et al., 2014; Heintzman et al., 2009; Heintzman et al., 2007; Lavin et al., 2014);
2. Identification of regions bound by certain TFs or cofactors such as p300 and CBP (Ghisletti et al., 2010; Visel et al., 2009);
3. Approaches based on profiling eRNA transcripts (Andersson et al., 2014; Core et al., 2014; Hah, Murakami, Nagari, Danko, & Kraus, 2013; D. Wang et al., 2011).

The first two approaches most often employ chromatin immunoprecipitation coupled to massively parallel sequencing (ChIP-seq), a method for identification of DNA sequences bound by a protein of interest. The third approach makes use of CAGE technology described above (Kanamori-Katayama et al., 2011) or other methods such as transient transcriptome sequencing (TT-seq), global nuclear run-on sequencing (GRO-

seq), and its cap-enriched variant GRO-cap. GRO-seq profiles all nascent RNAs associated with transcriptionally engaged polymerases, by incorporating bromouridine in actively synthesized transcripts, and simultaneously blocking new transcription initiation events (Core, Waterfall, & Lis, 2008). In TT-seq, 4-thiouridine is incorporated into newly synthesized RNA within a five minutes interval, and the corresponding fragments are sequenced (Schwalb et al., 2016).

Despite the progress in these and other high-throughput techniques, the identification of enhancers remains challenging. They are scattered across the non-coding genome, and there is no single 'enhancer mark', sequence code or pattern that could robustly predict all enhancers in a given tissue and state and report their activity levels (Pennacchio et al., 2013). For instance, a multitude of studies has employed H3K4me1 and H3K27ac histone marks to identify enhancer regions and their activation state, however, this approach has known disadvantages. A group of studies showed that many enhancers can carry other histone mark, either in addition to or instead of the H3K4me1 and H3K27ac marks (Pekowska et al., 2011; Z. Wang et al., 2008; Zentner, Tesar, & Scacheri, 2011). Furthermore, H3K4me1 and H3K27ac mark broad regions, that could either include regions flanking genuine enhancers or even demarcate groups of individual enhancers, thus, hindering identification of enhancers on a base pair level (Bonn et al., 2012). Hence, additional criteria are needed to reliably identify enhancers on a genome-wide level.

Another outstanding challenge in enhancer analysis is the identification of their target genes (Levine, Cattoglio, & Tjian, 2014). First popular approaches assigned enhancers to their nearest genes, while other studies used a linear distance threshold to identify potential enhancer target genes (Andersson et al., 2014; De Santa et al., 2010; Kim et al., 2010; Ostuni et al., 2013). However, accumulating evidence suggests that linear proximity might not be an accurate predictor of enhancer-gene interactions, as many

enhancers regulate distal genes, bypassing the nearest promoter (G. Li et al., 2012; Lupianez et al., 2016; Sanyal et al., 2012). Enhancers can be located either up- or downstream of their target promoters at any distance, and might form multiple long-range interaction (Sanyal et al., 2012; Zhang et al., 2013). Hence, approaches profiling physical enhancer-promoter contact have been developed to facilitate discovery of regulatory interactions. Chromosome conformation capture (3C) has been developed to test physical interactions between a pair of genomic loci based on cross-linking of interacting genomic regions (Dekker, Rippe, Dekker, & Kleckner, 2002). Nowadays, a group of 3C-based methods exist, which differ in their scope. Of those, Hi-C is a genome-wide adaptation of 3C (Lieberman-Aiden et al., 2009), and Capture Hi-C is its modification which includes a sequence capture step to enrich for a set of genomic regions of interest, such as promoters (Dryden et al., 2014). Capture Hi-C has been used recently in a group of studies to map genome-wide enhancer-promoter contacts (Mifsud et al., 2015; Rubin et al., 2017; Schoenfelder et al., 2015). However, these approaches for chromatin interaction profiling have their own limitations (Mora, Sandve, Gabrielsen, & Eskeland, 2015). For instance, spatial proximity alone, as determined by these methods, does not necessarily imply a functional relationship (Mora et al., 2015). Cross-linking might introduce a bias due to its different efficiency for different proteins and DNA, and the fixation might cause DNA damage responses (Mora et al., 2015). Nevertheless, 3C-based methods are of high importance in studies of the genome-wide chromatin organisation and are being continuously improved.

1.3.9. Conclusions and perspective

Studies in multiple cell types unravelled the fundamental importance of enhancer regions as DNA regulatory elements. However, our current understanding of these elements remains incomplete. High tissue specificity of enhancers is a major hurdle towards establishing a comprehensive catalogue of the full enhancer population (Kieffer-Kwon et al., 2013; Romanoski et al., 2015). Moreover, emerging evidence indicates that enhancers selectively act in a stimuli- or condition-specific manner (Arner et al., 2015; Mukhopadhyay, Ramadass, Akoulitchev, & Gordon, 2014). A major challenge is, therefore, to catalogue enhancers active in different tissues and conditions and link them to their target genes.

1.4. Studies of enhancer regulation in macrophages

Given the important roles of macrophages in tissue homeostasis and immune responses, macrophages have been extensively investigated in past decades, including a set of studies of transcriptional regulation by enhancers. Here, we give a brief overview of a few landmark studies, highlighting the main insights into enhancer regulation in macrophages.

Two reports by the same research group were published in 2010 and investigated mouse BMDM response to a stimulation with lipopolysaccharide (LPS), a component of bacterial cell walls that triggers immune response in macrophages (De Santa et al., 2010; Ghisletti et al., 2010). The first study performed ChIP-seq profiling of RNAPII binding to identify transcription sites on a genome scale (De Santa et al., 2010). Of 3,216 transcribed extragenic regions with no protein-coding potential, 69% were classified as enhancers,

based on a combination of H3K4me1 and H3K4me3 histone marks (De Santa et al., 2010). This study, together with the enhancer study in neurons (Kim et al., 2010), highlighted for the first time the prevalence of RNA transcription at enhancers (De Santa et al., 2010). The second study used ChIP-seq profiling of p300 protein binding to infer 2,742 enhancer regions, 88.7% of which appeared *de novo* upon LPS treatment (Ghisletti et al., 2010). The LPS-inducible enhancer regions were strongly enriched for TF PU.1, which is involved in both macrophage differentiation and gene regulation in mature macrophages (De Santa et al., 2010; Ghisletti et al., 2010). Importantly, in Ghisletti et al. (2010) PU.1 was required for H3K4me1 deposition, and it was proposed that PU.1 might be required and sufficient for the establishment of enhancer regions. In addition to PU.1, LPS-inducible enhancers were strongly enriched for inflammatory stimulus-activated TFs, such as NF-kB, IRFs, and AP-1 (Ghisletti et al., 2010). Hence, this study reported an important finding that a combination of both lineage-specific and stimulus-activated TFs could determine enhancer activity (Ghisletti et al., 2010).

Three years later, these findings were reinstated by the same research group in an extended analysis of BMDM enhancer responses to eight stimuli (Ostuni et al., 2013). Based on ChIP-seq profiling of H3K4me1 and H3K27ac histone marks, enhancers were classified with respect to their response to the stimuli (Ostuni et al., 2013). Constitutive enhancers were defined as those carrying both histone marks before and after stimuli. Poised activated enhancers carried only H3K4me1 histone mark before stimuli, but acquired also H3K27ac mark after stimulation, in contrast to poised non-activated enhancers, which lacked H3K27ac. Repressed enhancers were defined as those losing H3K27ac after stimulation. Finally, latent enhancers, that were the main focus of the study, acquired both H3K4me1 and H3K27ac only after stimulation. Such classification revealed that enhancers were not completely established in differentiated cells and highlighted

their extremely dynamic nature. Importantly, sets of latent enhancers differed dramatically between the stimuli. Similarly to their earlier study, the authors reported that activation of latent enhancers was achieved via cooperation between stimulus-activated TFs and lineage-determining TF PU.1 (Ostuni et al., 2013).

The same conclusion was reached by a different research group in their study analysing macrophage response to TLR4 agonist (Kaikkonen et al., 2013). ChIP-seq data for H3K4me2 histone mark was used to infer enhancer regions. A total of ~32,000 enhancers were identified, with ~3,000 of those being established *de novo* upon stimulation. Macrophage lineage-determining TF PU.1 was found to collaborate with stimulus-activated TF NF-kB. This study extensively investigated kinetics of *de novo* enhancer activation. Surprisingly, it was found that enhancer transcription preceded and was necessary for H3K4me1/2 deposition (Kaikkonen et al., 2013).

Taken together, these four studies presented an extensive analysis of macrophage enhancers. The first important finding concerned the plasticity of the macrophage enhancer repertoire. Indeed, instead of being entirely pre-determined during cell differentiation, the enhancer repertoire remained highly plastic and dynamically changed in response to a stimulus in a stimuli-specific manner. The second important finding uncovered the crucial role of macrophage lineage-determining TF PU.1 in enhancer establishment. Indeed, PU.1 binding sites were found in both pre-established and *de novo* stimuli-induced enhancers. Third, an important step towards understanding the enhancer tissue-specific regulation was made by discovering the cooperative action of PU.1 with stimulus-specific TFs in establishing novel enhancer regions. Such a mechanism might ensure establishment of *de novo* enhancers in both cell-type- and stimuli-specific manner, allowing for gene expression changes triggered by a particular stimulus to differ between

cell-types (De Santa et al., 2010; Ghisletti et al., 2010; Kaikkonen et al., 2013; Ostuni et al., 2013).

Two subsequent studies investigated the enhancer repertoire in tissue macrophages (Gosselin et al., 2014; Lavin et al., 2014). Distinct population of tissue macrophages perform different tissue-specific functions, have different gene expression profiles and respond to different stimuli (Davies & Taylor, 2015). The two studies analysed two (Gosselin et al., 2014) and seven (Lavin et al., 2014) distinct populations of tissue macrophages to characterise their enhancer usage. Remarkable differences in enhancer repertoires were observed between different tissue macrophage populations. Distinct tissue microenvironments, characterised by distinct signalling factors, were found to specifically shape enhancer landscapes in macrophage populations, which in turn, drives tissue- and population-specific gene expression programmes. Tissue-specific enhancers might be established via a collaborative action of PU.1 and tissue-specific TFs induced by the local microenvironment. These findings uncovered molecular mechanisms that might be involved in tissue-dependent establishment of macrophage phenotypes (Gosselin et al., 2014; Lavin et al., 2014).

All listed studies focused primarily on the macrophage enhancer landscape and potential mechanisms of *de novo* enhancer formation upon stimulation. Little was investigated in terms of enhancer target genes, and their characterisation was limited by considering only the closest genes. None of the studies analysed thoroughly enhancer-gene interactome in naïve or stimulated macrophages. In addition, a study of enhancer regulation in macrophages in response to infection is lacking.

1.5. Project overview and research objectives

The major focus of the present work was on the role of transcribed enhancers in the regulation of transcription in mouse macrophages. This choice was motivated by a combination of two main factors. On one hand, is the rapidly growing appreciation of the importance of enhancers for transcriptional regulation. On the other hand, is a very limited understanding of how genetic programmes are controlled by transcribed enhancers in macrophages.

As outlined above, a group of prominent studies have been dedicated to enhancers as *cis*-regulatory elements in mouse macrophages. However, most of these studies paid little attention to transcription at enhancers themselves, and importantly, lacked identification and analyses of reliable enhancer target genes. Furthermore, none of these studies analysed the role of enhancers in regulating macrophage responses to tuberculosis infection. An unprecedented opportunity to address this gap was provided by the CAGE data available to us. First, it enabled identification of high-confidence transcribed enhancers. Second, CAGE allows the simultaneous quantification of gene expression, and we used this property to infer reliable enhancer target genes. Third, the available data encompassed distinct macrophage activation states, as well as tuberculosis infection, making it a unique and consistent set for investigating transcriptional programmes that are exerted in macrophages under various conditions.

The present work includes three chapters reporting our analyses and findings. In Chapter 2, we made use of publicly available CAGE data to infer transcribed enhancers on a genome-wide scale in a large collection of mouse tissues. This part of the project improved our understanding of general properties of enhancers in various tissues and

provided practical insights into approaches for the more detailed investigation of enhancers in macrophages (in Chapters 3 and 4).

In Chapter 3, we focused on a specific subset of this large collection of CAGE data, which consisted of mouse macrophage samples profiled by our collaborators. We used the transcribed enhancer regions inferred in Chapter 2 as a basis for the identification of high-confidence transcribed enhancers in mouse macrophages. Furthermore, we established a reliable mouse macrophage enhancer-target gene interactome. Using this interactome, we characterised the roles of enhancers in guiding macrophage activation and polarisation into distinct pro- and anti-inflammatory phenotypes.

In Chapter 4, we further narrowed our focus down to a subset of macrophages infected with *M.tb*. Making use of the enhancer-gene interactome established in Chapter 3, we performed, to our knowledge, for the first time, a study of the role of transcribed enhancers in macrophage response to *M.tb* infection.

The major research objectives of the present work were:

1. Identifying and characterising transcribed enhancers and their candidate target genes on a genome-wide scale in various mouse tissues;
2. Analysing the enhancer-gene interactome in naïve macrophages and its changes during macrophage activation;
3. Uncovering the role of transcribed enhancers in macrophage response to tuberculosis infection.

Chapter 2

Genome-wide profiling of transcribed enhancers in mouse tissues

2.1. Overview

Enhancers are *cis*-regulatory DNA elements that activate transcription of target genes in a position- and orientation-independent manner. Many enhancers were shown to be bidirectionally transcribed into eRNAs. This feature can be used for a genome-wide identification of such enhancer regions. The rates of eRNA production were shown to correlate with the levels of target mRNAs, and this property can be used to infer enhancer-gene regulatory interactions.

In the present study we used cap analysis of gene expression (CAGE) data for 969 mouse samples across more than 20 tissues to characterise the transcribed mouse enhancer landscape with the following objectives:

1. Identifying transcribed mouse enhancers on a genome-wide level;
2. Characterising enhancer properties in terms of location and eRNA expression;
3. Identifying and characterising candidate regulatory enhancer-target gene interactions.

2.2. Results

2.2.1. Transcribed enhancers in mouse tissues

Many active enhancer regions in mammals were shown to be transcribed into RNA molecules, known as eRNAs (De Santa et al., 2010; Kim et al., 2010), which can be profiled with CAGE technology (Kanamori-Katayama et al., 2011). Furthermore, enhancers are transcribed in a specific bidirectional manner producing divergent eRNAs (**Figure 2.1**), and the corresponding divergent clusters of CAGE-derived transcripts were used before to reliably infer transcribed enhancers in humans (Andersson et al., 2014).

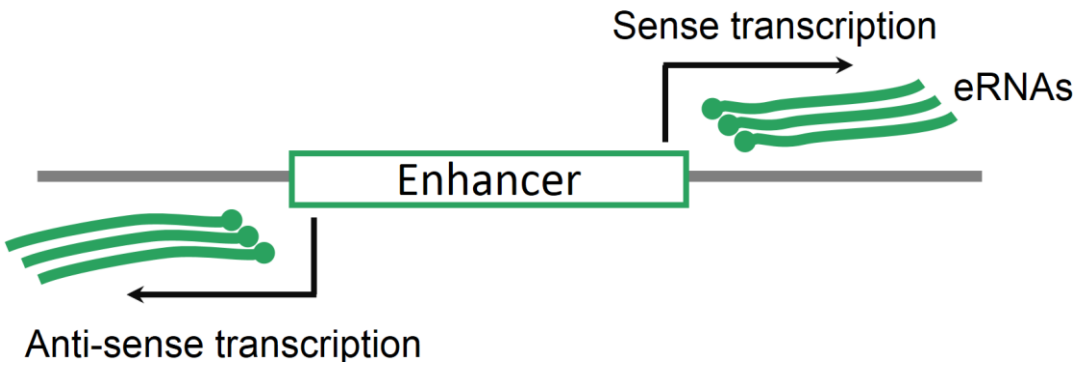

Figure 2.1. Bidirectional enhancer transcription.

To identify enhancer regions that are transcribed into eRNAs in mouse tissue, we used a large collection of CAGE mouse samples from the FANTOM5 consortium (Forrest et al.,

2014) and a previously developed enhancer identification strategy (Andersson et al., 2014) with modifications as described in 2.6. Briefly, we obtained CAGE data for 969 mouse samples in a form of mapped transcription start sites (TSSs) coupled with expression measurements (see 2.6.1). We clustered these TSSs into CAGE peaks (see 2.6.2). We further defined regions demarcated by pairs of divergently transcribed CAGE peaks as mouse enhancers and quantified expression of the corresponding CAGE transcripts (see 2.6.5). This approach yielded 42,470 transcribed mouse enhancers. Distribution of the enhancers among mouse chromosomes (**Figure 2.2**) shows that the highest numbers of enhancers were found on the longest chromosomes 1 and 2, and unexpectedly, on a shorter chromosome 11. Most of the autosomes contained around twice as many enhancers as genes, except for the chromosome 7, where 2,388 enhancers and only 2,027 genes were localised. Finally, chromosome X contained more genes that enhancers (**Figure 2.2**).

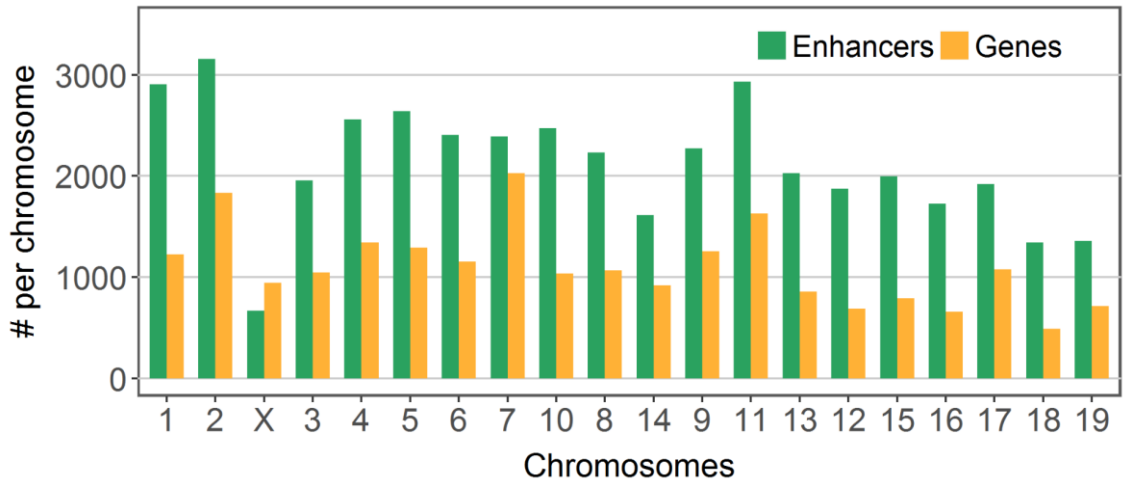

Figure 2.2. Number of transcribed mouse enhancers and Ensembl protein-coding genes per chromosome. Chromosomes are ordered by size, starting from the longest.

We compared the 42,470 transcribed mouse enhancers to *cis*-regulatory regions established in previous studies, to assess their concordance and novelty. An atlas of *cis*-regulatory sequences in 19 mouse tissues and cell types has been built based on the

presence of H3K4me1 and absence of the H3K4me3 chromatin marks, as defined by ChIP-seq profiling (Shen et al., 2012). The study reported 380,843 unique single-nucleotide positions as centres or summits of enhancer regions derived by merging individual enhancers located within 1.5 kb. Therefore, we assessed an overlap of these 1-nt positions within 1.5 kb of our transcribed enhancer and found that 64,390 (16.9%) of these summits overlapped a total of 18,112 (42.6%) of our transcribed enhancers. 3,618 additional transcribed enhancers (8.5%) were located within 3 kb of the 1-nt centres. Next we compared our transcribed enhancers with a list of 614 experimentally validated mouse enhancers from the VISTA Enhancer Browser (Visel, Minovitsky, Dubchak, & Pennacchio, 2007) and found that 205 of them (33.4%) overlapped our transcribed enhancers directly and 38 additional enhancers (6.2%) were located within a 1.5 kb window. These results are in agreement with a current state of knowledge of enhancer biology, postulating that not all regions with enhancer-specific chromatin marks are transcribed into eRNAs. Of note, about half of our transcribed enhancers were not recovered previously by ChIP-seq and might represent novel mouse enhancer regions.

We next investigated eRNA expression levels of transcribed enhancers in available FANTOM5 CAGE mouse samples and tissues. The expression across all samples and enhancers was overall low, with a median of 0 and a mean of 0.11 tags per million (TPM). Zero expression was reported (in other words, no eRNA expression was detected) in 86.8% of the observations, where one observation corresponds to the expression of an enhancer in a sample. It means that, although we identified transcribed enhancers, most of the enhancers showed eRNA expression only in a small subset of samples. Hence, we re-evaluated detectable eRNA expression, focusing on nonzero measurements alone (**Figure 2.3**). Nevertheless, such exclusion of undetectable measurements resulted in a still low eRNA expression with a median of 0.38 TPM and a mean of 0.85 TPM across all samples.

Distribution of the expression levels was similar between tissues, with the minimum median of 0.3 TPM observed in testis and kidney, and the maximum median of 0.49 TPM in the T cell induction process and 0.45 TPM in hepatocytes (**Figure 2.3**). These results might reflect the short half-lives of eRNAs (Lam et al., 2014) or their low expression levels in general.

To enable a systematic comparison of eRNA expression among tissues, we further focused only on a subset of tissues with at least 20 samples each. We deemed an enhancer transcribed in a tissue if the eRNA showed nonzero expression in at least 20% of the tissue samples. We observed a high variance in numbers of these transcribed enhancers in the ten tissues under investigation, with a minimum of 3,012 enhancers identified in J2E erythroid cells and a maximum of 12,857 enhancers in macrophages (4.3-fold difference) (**Figure 2.4a**). Comparison to protein-coding gene promoters in the same tissues showed, as expected, that expression of the promoters of protein-coding genes was overall higher (**Figure 2.4b**) (see 2.6.4 for identification of promoter expression levels with CAGE data). In addition, the number of the expressed promoters ranged from 22,909 in J2E erythroid cells to 40,093 in neurons, showing only a 1.8-fold difference (**Figure 2.4b**).

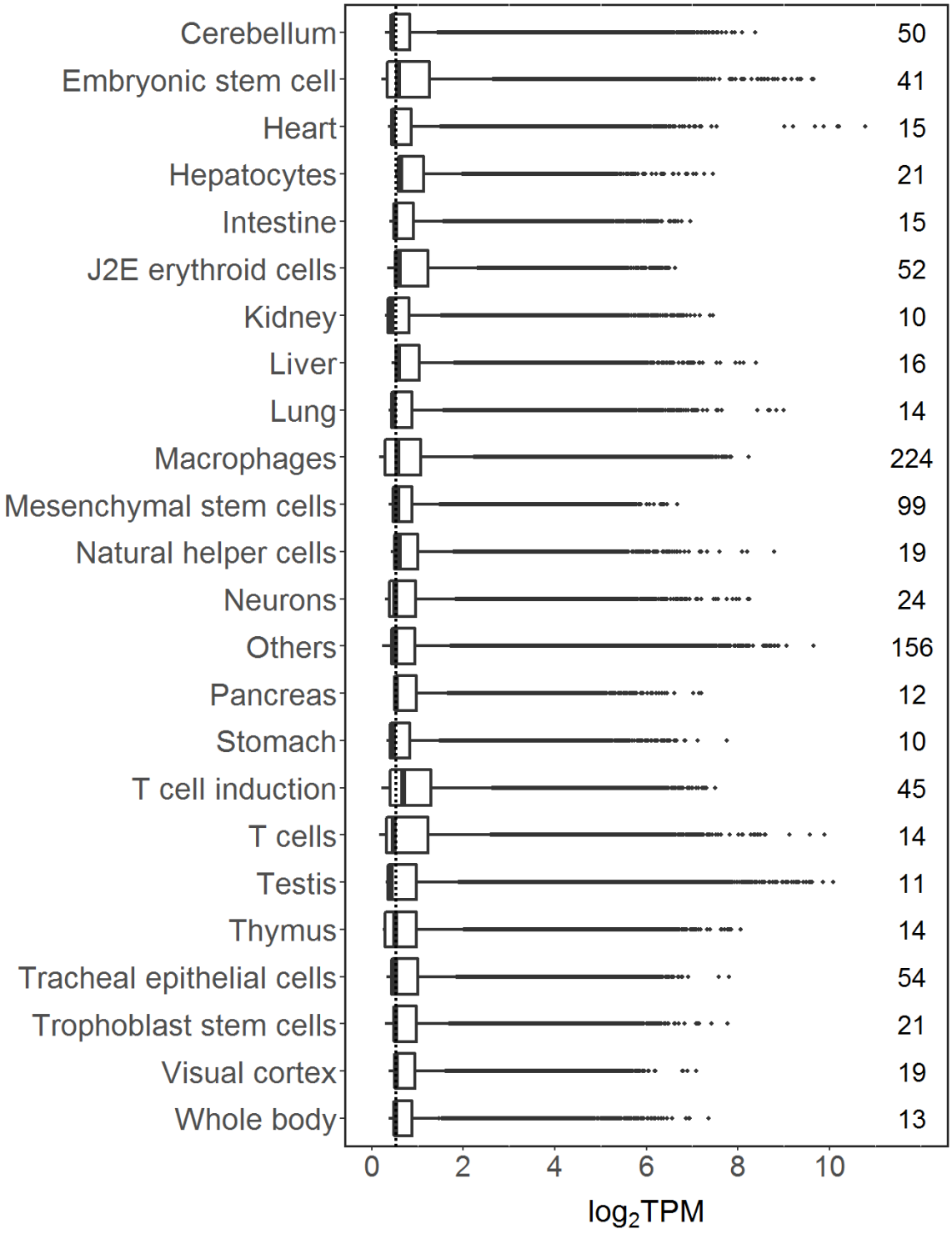

Figure 2.3. Detectable eRNAs are overall lowly expressed in mouse tissues. Tissues with at least ten samples were considered separately, the rest of the samples were combined together into an 'Others' category; numbers of samples per category are indicated. Enhancers with nonzero eRNA expression were considered in each sample. Expression in TPM was log-transformed for plotting. The edges of the boxes indicate the 25th and 75th percentiles, the lines within the boxes show the median. Dashed line shows median expression level across all tissues.

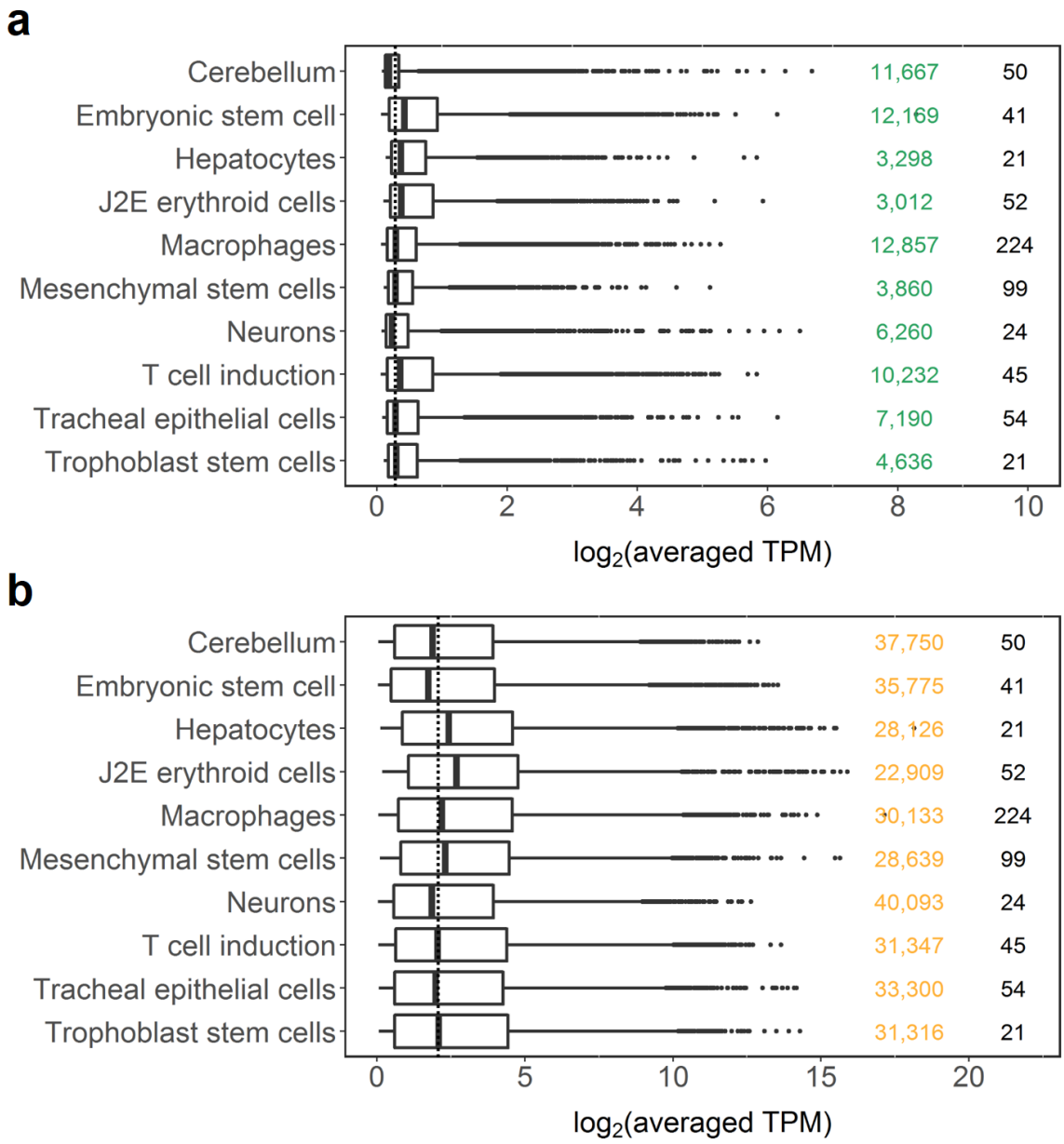

Figure 2.4. Expression of transcribed enhancer eRNAs and expressed promoters in mouse tissues. a Transcribed enhancers were selected per tissue, eRNA expression was averaged across the corresponding samples. Numbers of samples and transcribed enhancers per tissue are shown in black and green, respectively. **b** Expressed promoters were selected per tissue, expression was averaged across the corresponding samples. Numbers of samples and expressed promoters per tissue are shown in black and orange, respectively. In **a** and **b**, tissues with at least 20 samples were considered; nonzero eRNA or mRNA expression in at least 20% of the tissue samples was required for transcribed enhancers and expressed promoters, respectively. Expression in TPM was averaged across tissue samples and log-transformed; the edges of the boxes indicate the 25th and 75th percentiles, the lines within the boxes show the median; dashed lines show median expression level across all the tissues.

For each pair of the tissues, we asked what percentage of the transcribed enhancers in one of these tissues was also deemed transcribed in the other one, and vice versa. **Figure 2.5a** shows the resulting values in the form of an asymmetrical matrix. The strongest similarity among all tissue pairs was observed in neurons, where 84.3% of the transcribed enhancers were also deemed transcribed in cerebellum. The largest dissimilarity was observed in embryonic stem cells, where only 11.6% of the transcribed enhancers were also deemed transcribed in hepatocytes. Transcribed enhancers in macrophages showed the highest similarity to those transcribed during T cell induction (42.1%) and the largest dissimilarity to hepatocytes and J2E erythroid cells. In contrast, expressed promoters were more similar between tissues (**Figure 2.5b**). The lowest 55.1% of the promoters expressed in neurons were also expressed in J2E erythroid cells, and these two tissues were the most dissimilar when compared to other tissues (**Figure 2.5b**). This, however, might be explained by the fact that these two tissues showed the smallest and the largest number of expressed promoters, respectively (see above and **Figure 2.4b**). Taken together, these results indicate that the transcribed enhancers identified here are characterised by highly tissue-specific eRNA expression, which is more similar in tissues with related origins or functions.

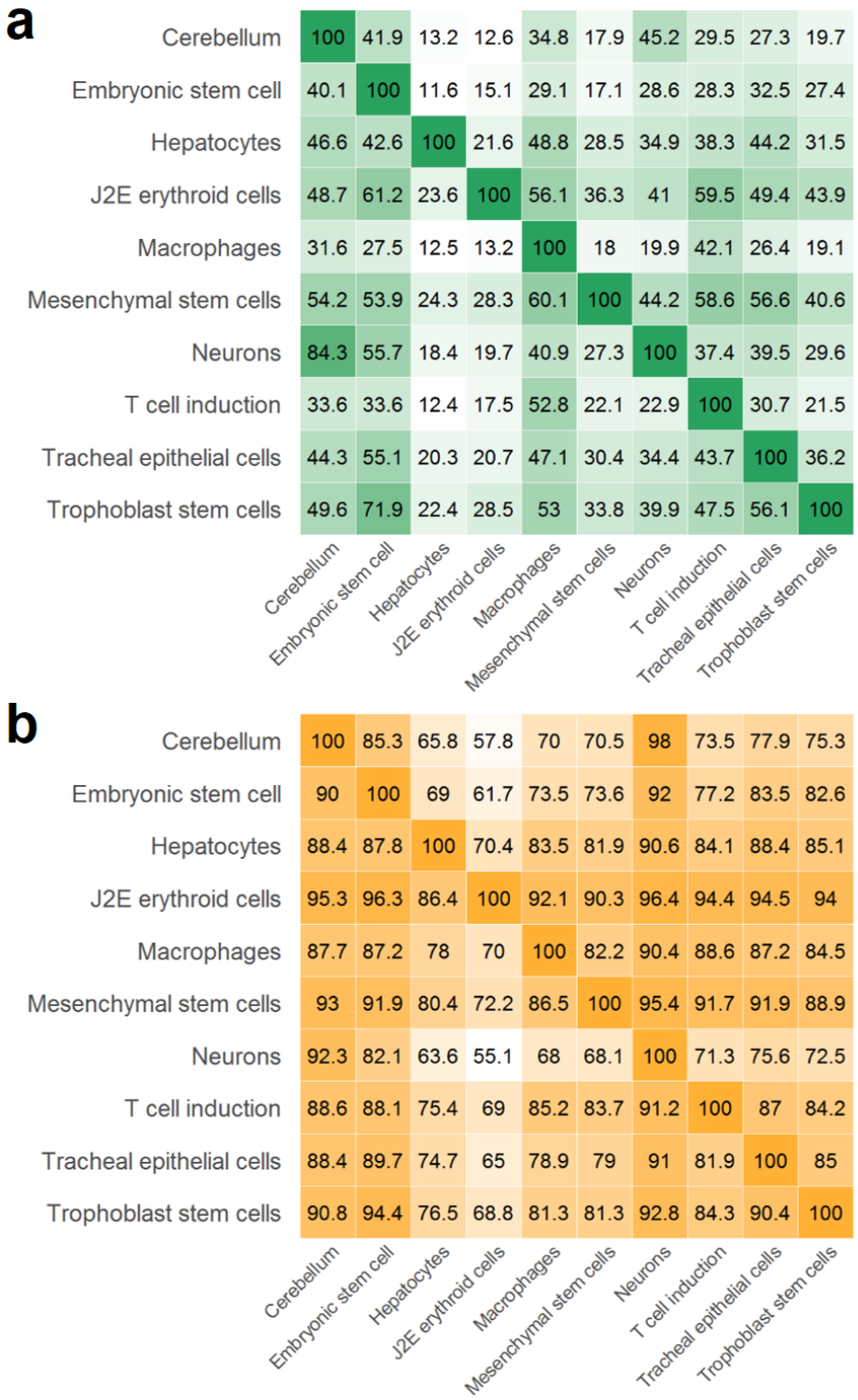

Figure 2.5. Enhancer transcription shows strong tissue-specificity as compared to promoters of protein-coding genes. Numbers indicate percentage of transcribed enhancers (in **a**) or expressed promoters (in **b**) in a tissue on the left, that were also deemed transcribed (expressed) in a tissue on the bottom. Tissues with at least 20 samples were considered; nonzero eRNA or mRNA expression in at least 20% of the tissue samples was required for transcribed enhancers and expressed promoters, respectively.

2.2.2. Enhancers in the context of chromosomal domains

Enhancer regulation is exerted via DNA looping and direct enhancer-promoter contacts (Gorkin et al., 2014; Shlyueva et al., 2014), thus, enhancers and protein-coding gene promoters should be brought into close proximity within the nucleus. These physical interactions are believed to happen within chromosomal regions called topologically associating domains (TADs) (Dixon et al., 2012). TADs are defined as DNA segments with higher frequency of physical interactions within their boundaries than with regions in different TADs and are well-conserved between tissues and species (Dixon et al., 2012). In this study, we used TAD regions inferred in mouse embryonic stem cells (Dixon et al., 2012), to identify potential enhancer target genes based on the possibility of their physical interaction (see 2.6.6).

Dixon et al. (2012) reported a total of 2,153 TADs, varying in size from 160 kb to 5.12 Mb, with a median and mean length of 880 kb and 1 Mb, respectively (**Figure 2.6a**). The size distribution varies between chromosomes with the minimum median of 640 kb on chromosome 7 and a maximum median of 1.14 Mb on chromosome 18 (**Figure 2.6b**). Chromosome 1 contains the highest number of TADs, and chromosome 19 - the lowest (**Figure 2.6c**). When combined, TAD regions cover more than 81% of each chromosome with a maximum of 94.5% for chromosome 6 (**Figure 2.6d**).

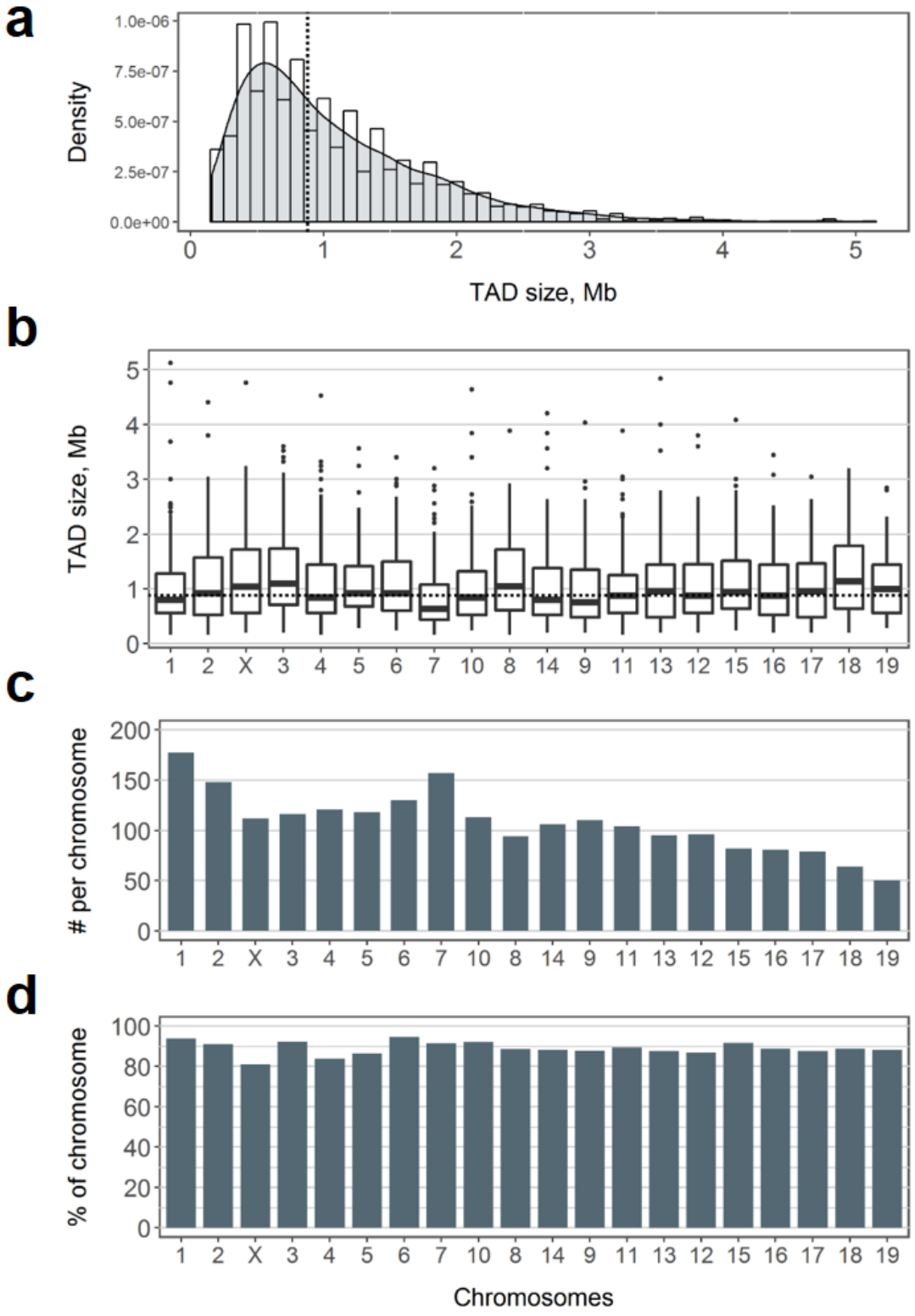

Figure 2.6. Properties of TADs. a Distribution of TAD sizes; dashed line shows the median size. **b** TAD sizes per chromosome; the edges of the boxes indicate the 25th and 75th percentiles, the lines within the boxes show the median; dashed line shows the median value across all chromosomes. **c** Number of TADs per chromosome. **d** Percentage of chromosome nucleotides covered by TADs.

Most of the transcribed enhancers and Ensembl protein-coding genes were located within TADs, with a maximum of 664 genes on the chromosome 2 and 385 enhancers on chromosome 5 being located outside of the TADs (**Figure 2.7a**). We found that the numbers of genes and enhancers per TAD were positively correlated (**Figure 2.7b**). Similarly, the numbers of genes and TADs per chromosome showed a strong positive correlation and were the highest for the longest chromosomes 1 and 2, and also for chromosome 7 (**Figure 2.7c**). Next we asked whether large TADs contained more genes and enhancers than smaller TADs. Although we observed positive correlation coefficients between TAD sizes and numbers of genes and enhancers they contain, most of the TADs with the highest numbers of genes and enhancers were of a moderate size (**Figure 2.7d** and **e**). For instance, among the top 5% of the TADs with the highest number of enhancers (52 or more), 91.2% were shorter than 2.5 Mb (**Figure 2.7d**). Similarly, among the top 5% of the TADs with the highest number of genes (24 or more), 95.5% were shorter than 2.5 Mb (**Figure 2.7e**). Taken together, these results show that the TADs inferred by Dixon et al. (2012) can be used to identify co-localised enhancers and promoters, as only a minority of them are discarded due to being located outside of the TADs. Interestingly, chromosome 7 showed distinct composition of chromosomal domains, containing more TADs of a smaller size, and the highest number of genes, when compared to other autosomes.

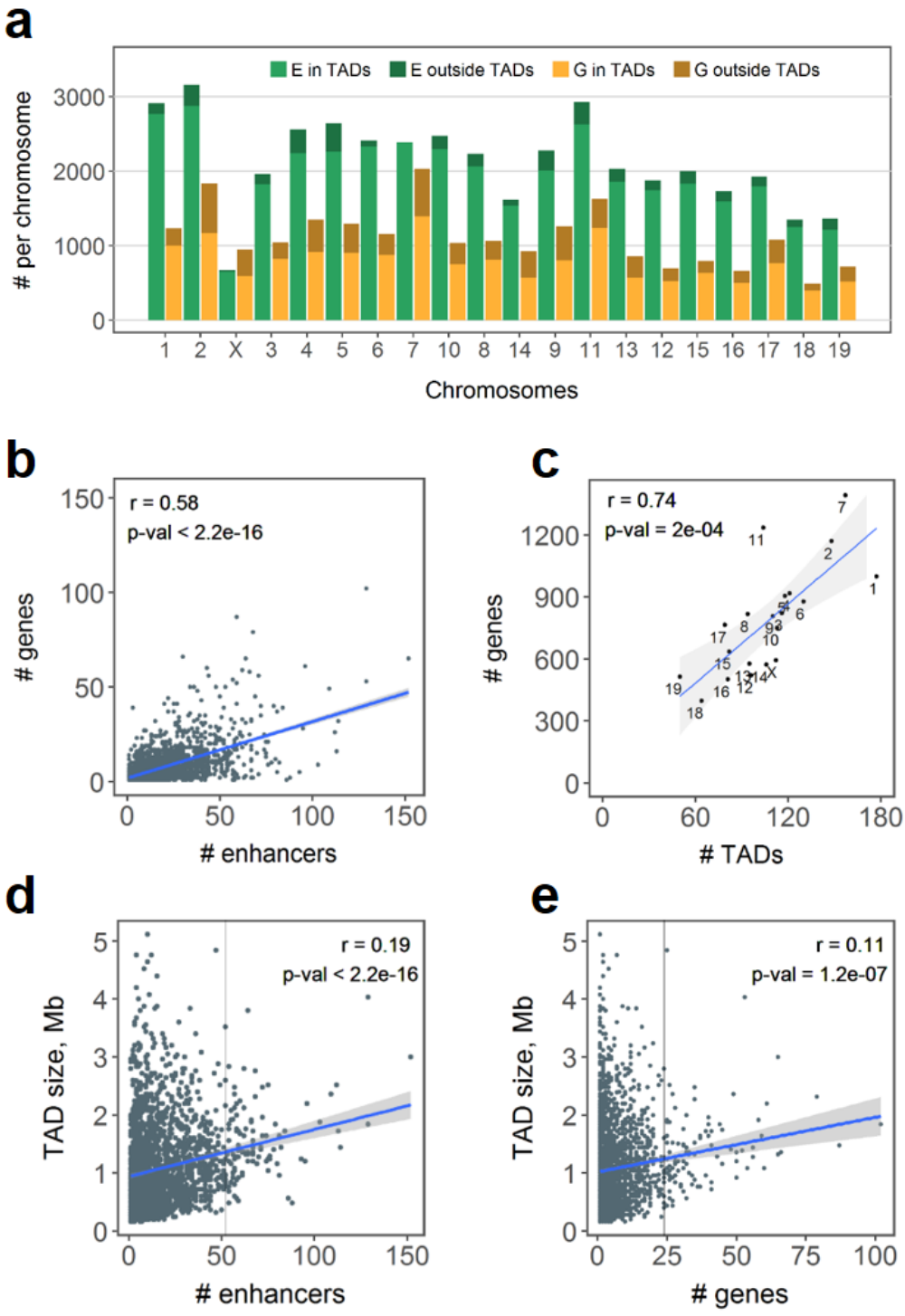

Figure 2.7. Enhancers and genes in a genomic context of TADs. a Number of enhancers and genes within and outside of TADs. **b** Number of genes and enhancers per TAD. **c** Number of genes and TADs per chromosome. **d** Number of enhancers in a TAD plotted versus the TAD size; vertical line separates top 5% of the TADs with the highest number of enhancers. **e** Number of genes in a TAD plotted versus the TAD size; vertical line separates top 5% of the TADs with the highest number of genes. In **b-e**, blue lines show linear regression with 95% confidence intervals; r is a Pearson correlation coefficient.

2.2.3. Enhancer regulation in mouse tissues

Most of the known interactions between enhancers and target promoters occur within a TAD (Lupianez et al., 2016; Rocha et al., 2015; Symmons et al., 2014) and eRNA level was shown to correlate with mRNA production of the enhancer target (Kaikkonen et al., 2013; Kim et al., 2010). Hence, we elected to use these two properties to predict enhancer target protein-coding genes in mouse tissues (see 2.6.6). As above, we focused on tissues with at least 20 samples and considered only transcribed enhancers and expressed promoters with nonzero expression in at least 20% of the tissue samples.

First, we evaluated expression correlation of all possible enhancer-promoter pairs within TADs, in each tissue separately. In each of the tissues, the median Spearman's correlation coefficient was positive (**Figure 2.8**), in agreement with the definition of a TAD as a segment of co-regulated features.

Next, we sub-selected enhancer-promoter pairs with positive correlation coefficient and deemed these pairs candidate regulatory enhancer-target promoter interactions (see 2.6.6). Interestingly, the number of candidate regulatory interactions varied dramatically between tissues, from 46,294 in hepatocytes to 282,613 in macrophages (**Figure 2.9a**), which could be explained by differences in number of TAD-based enhancer-promoter pairs (**Figure 2.9b**) stemming from differences in the number of transcribed enhancers per tissue (**Figure 2.10a**). Of note, the latter could not be attributed to different number of samples per tissue, since the corresponding correlation, albeit positive, was not statistically significant (**Figure 2.10b**). Moreover, upon removing the outlier category ("Macrophages"), the correlation coefficient dropped to -0.05 with p-value = 0.9.

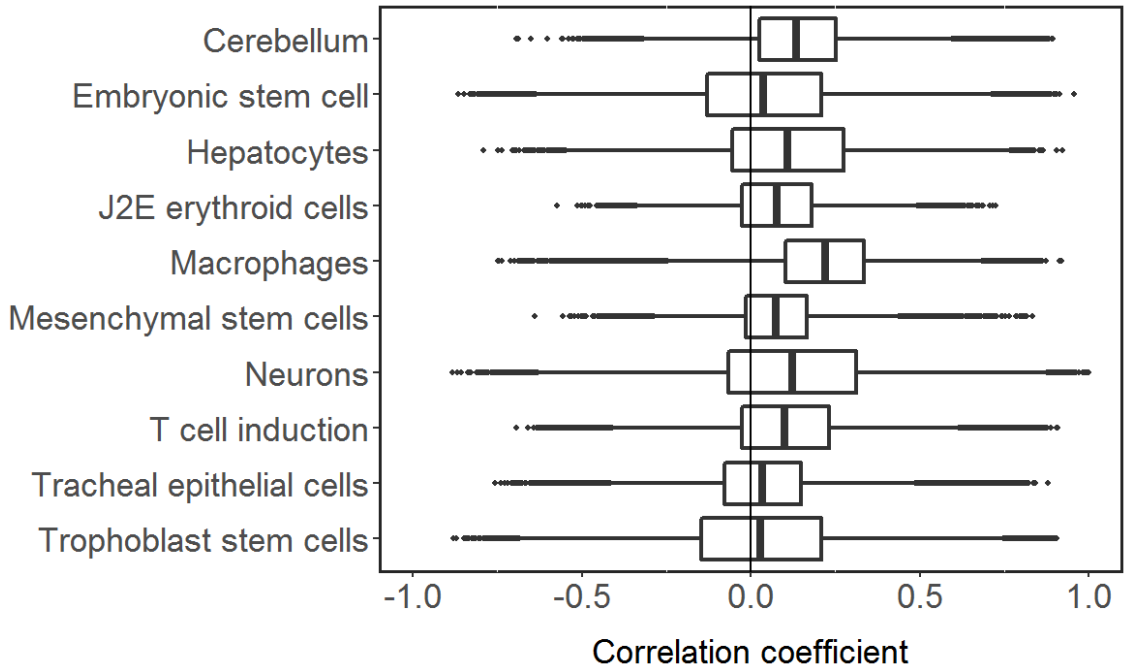

Figure 2.8 Spearman's correlation between expression of enhancer eRNAs and promoter mRNAs. All possible pairs between transcribed enhancers and expressed promoters within the same TAD were considered in each tissue separately. The edges of the boxes indicate the 25th and 75th percentiles, the lines within the boxes show the median.

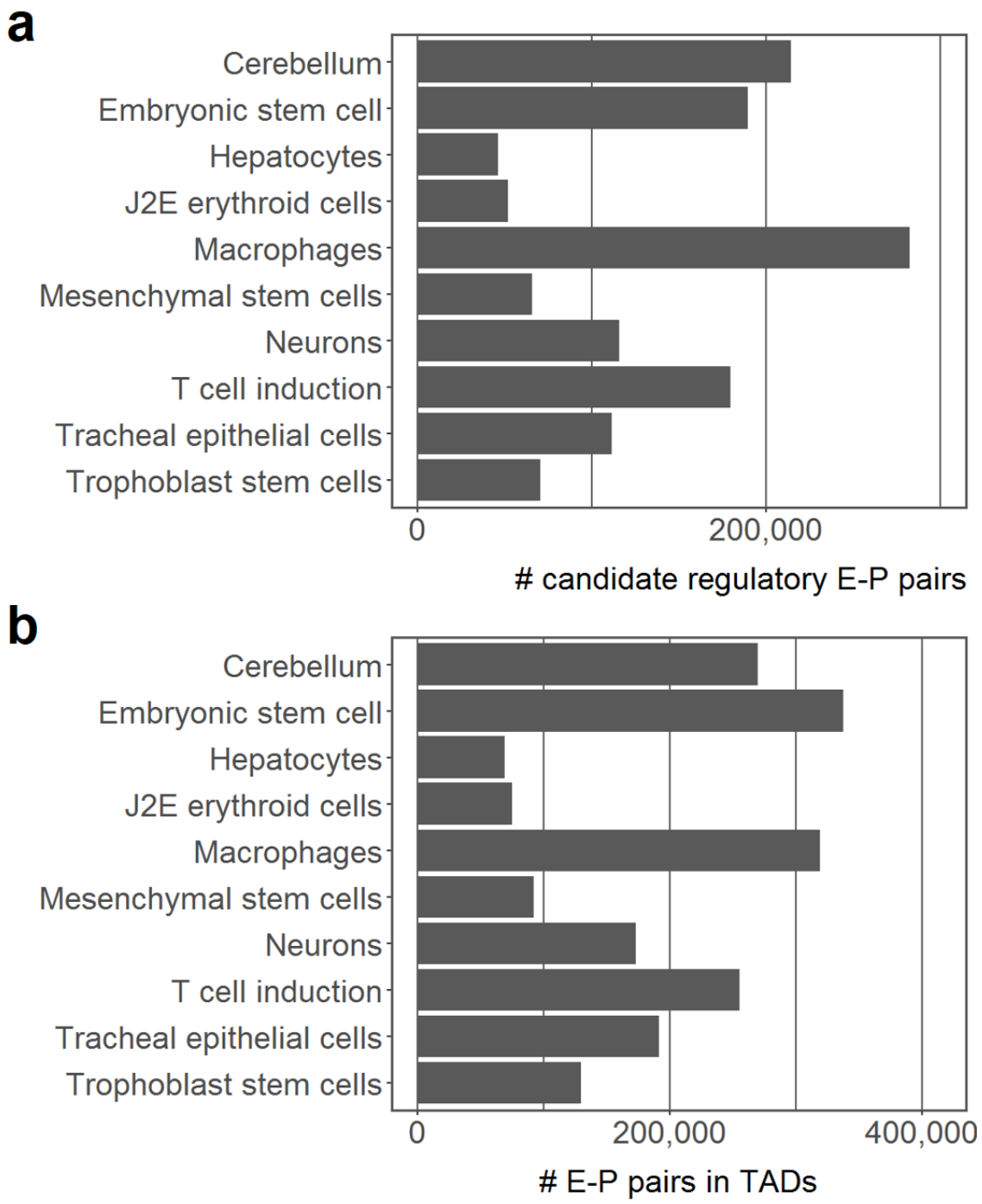

Figure 2.9. Enhancer-promoter pairs in mouse tissue. a Number of candidate enhancer-promoter (E-P) regulatory interactions; the pairs were selected based on co-localisation within a TAD and a positive correlation of expression. **b** Number of all possible E-P pairs within TADs; expressed promoters and transcribed enhancers were considered in each tissue.

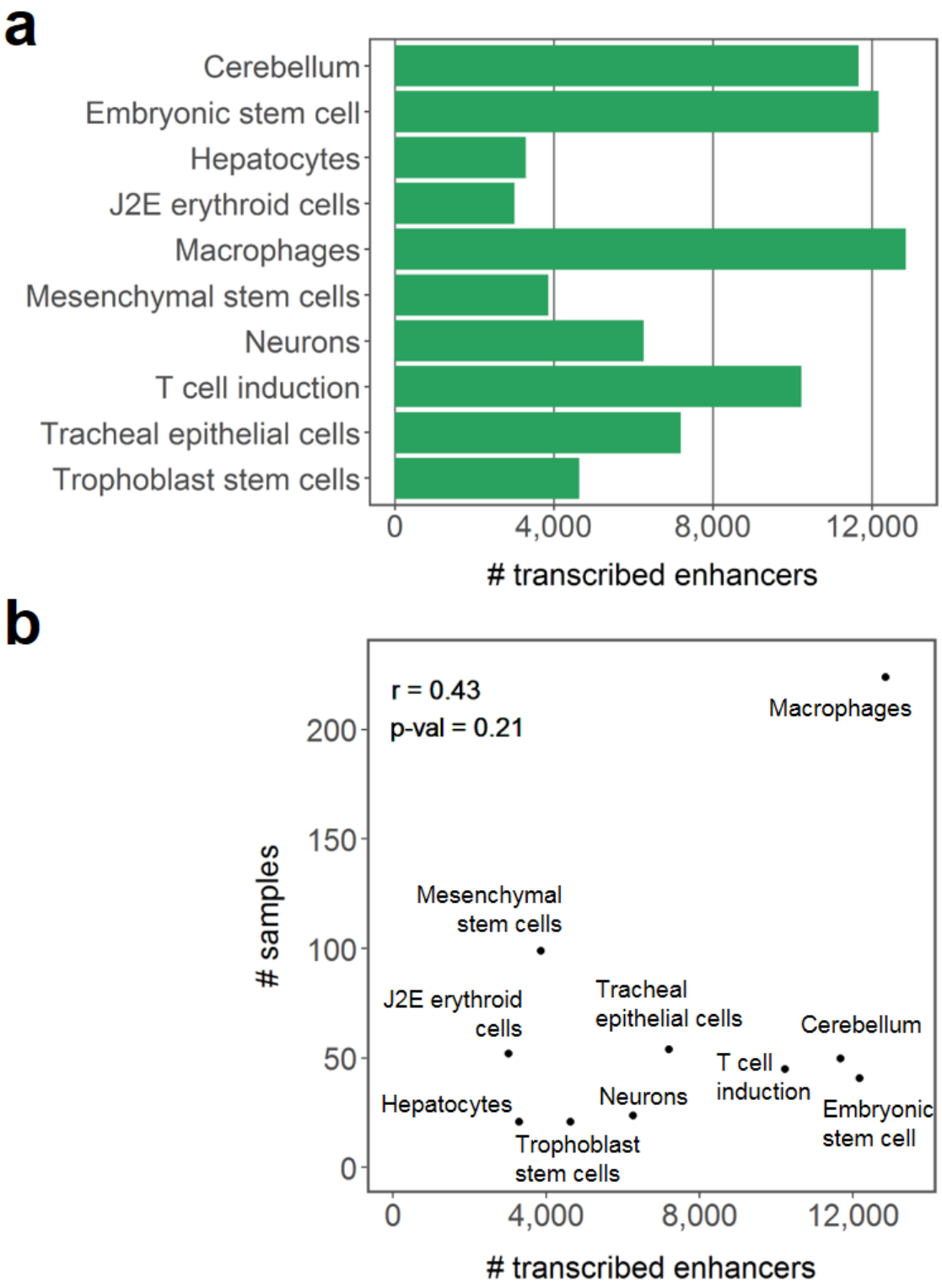

Figure 2.10. Number of transcribed enhancers. a Number of enhancers deemed transcribed in each tissue. **b** Number of transcribed enhancers plotted versus number of samples in each tissue; Pearson correlation coefficient and p-value are shown.

We further asked how the regulatory interactions were distributed among protein-coding genes in the tissues under consideration. Genes were split into 12 groups by the number of their targeting enhancers (**Figure 2.11**). Cerebellum, embryonic stem cells, macrophages, and T cell induction categories showed the largest proportion of genes targeted by more than ten enhancers (**Figure 2.11**), which could be explained by the fact that the highest number of transcribed enhancers were identified in these tissues (**Figure 2.10a**).

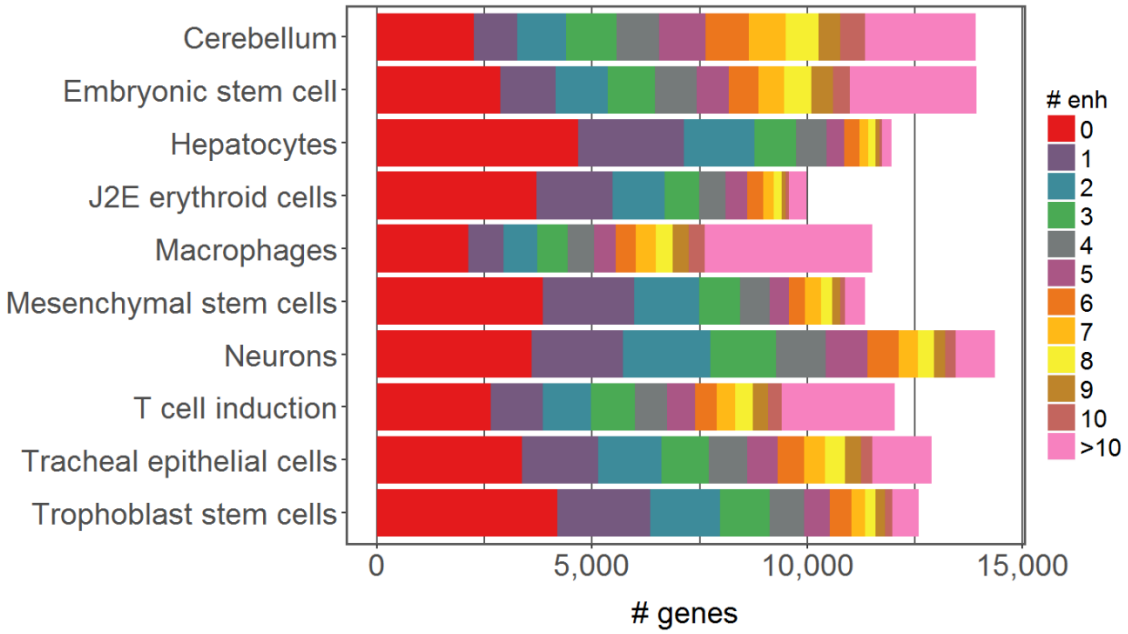

Figure 2.11. Number of genes targeted by different number of enhancers. A gene was defined as an enhancer target if at least one of its promoters formed a candidate regulatory pair with the enhancer.

We next set out to evaluate whether genes targeted by different number of enhancers showed different expression levels. We observed a trend for a higher expression in genes targeted by many enhancers (**Figure 2.12**). Two-sided Wilcoxon rank-sum test was performed in each tissue to compare expression of genes targeted by more than ten enhancers to that of genes targeted by none or a single enhancer, and all tests indicated

highly significant differences. These results support a model of additive action of enhancers where several enhancers regulate the same target gene in order to increase its transcriptional output (Chepelev et al., 2012; Shlyueva et al., 2014).

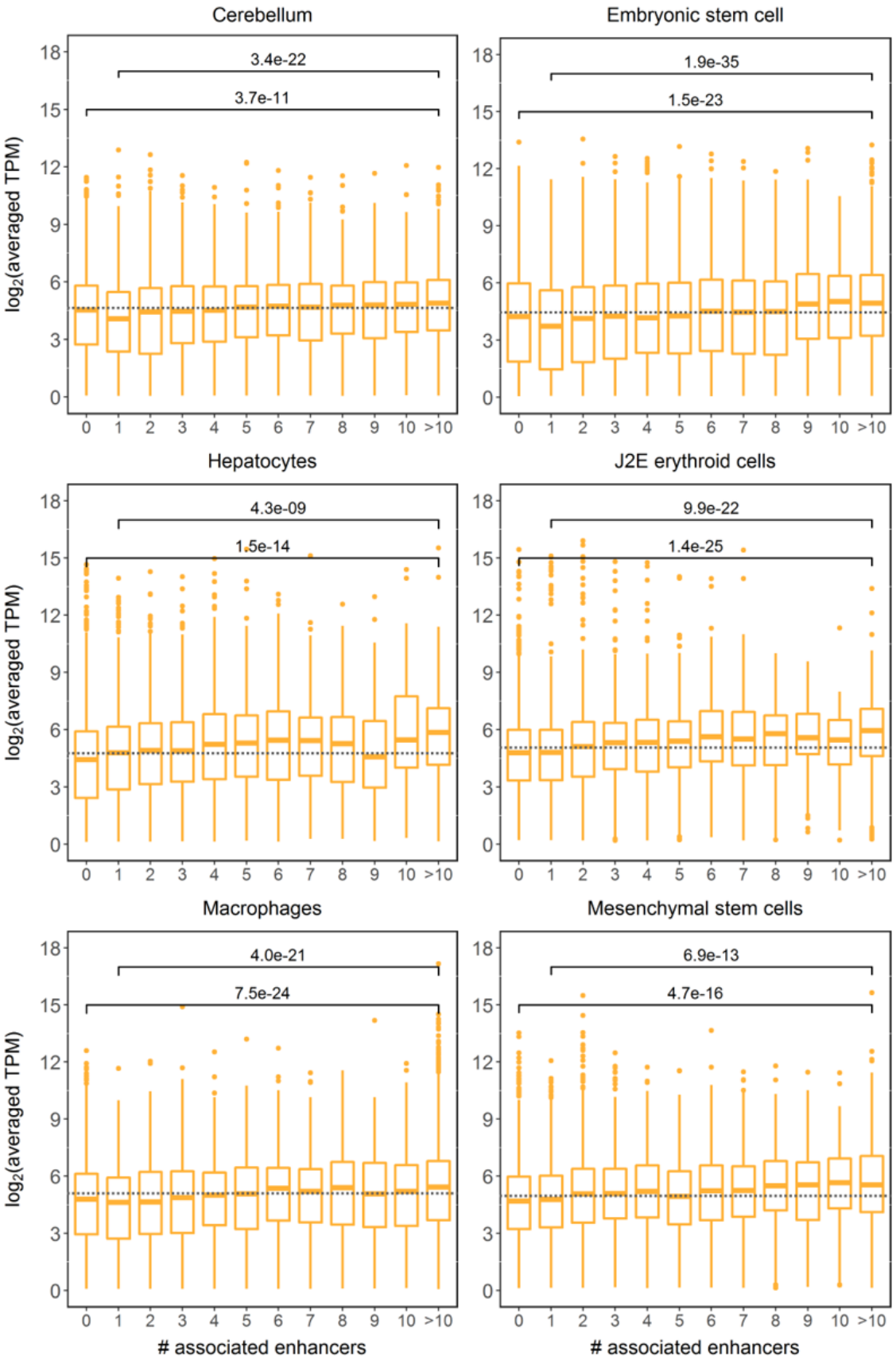

Figure 2.12. Continued on next page.

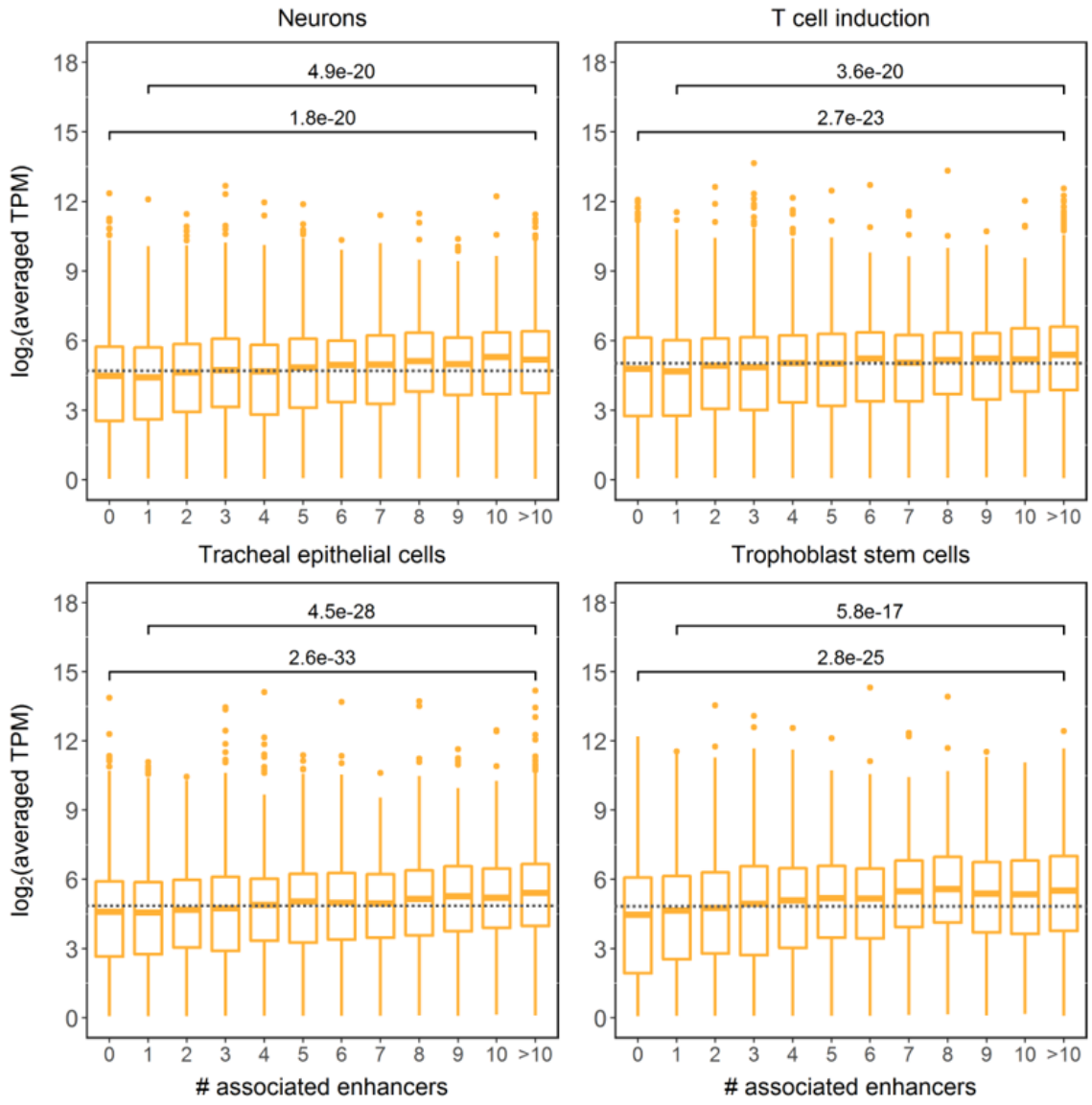

Figure 2.12. Expression of genes targeted by different number of enhancers. Expression in TPM was averaged across tissue samples and log-transformed. The edges of the boxes indicate the 25th and 75th percentiles, the lines within the boxes show the median; dashed lines indicate median expression of all genes in the corresponding tissue. P-values are based on two-sided Wilcoxon rank-sum tests.

2.3. Discussion

In this study, CAGE data were used to identify transcribed enhancers in 969 mouse samples across more than 20 tissues. Enhancer eRNAs showed lower expression and higher tissue-specificity when compared to protein-coding gene promoters. We characterised enhancer regulation in the context of TADs and found that the highest number of enhancers and genes were located within TADs of a moderate size. We identified and characterised candidate regulatory enhancer-target interactions in ten mouse tissues and demonstrated that genes interacting with many transcribed enhancers showed higher expression levels.

Shen et al. (2012) have recently built a genome-wide map of enhancers in mouse tissues based on a ChIP-seq profiling of enhancer-associated histone marks. Despite the comprehensiveness of their study, half of our CAGE-based transcribed enhancers were only identified here. These differences might arise from both methodology and sample composition and ultimately highlight the importance of combining several complementary technologies and enhancer properties to infer more reliable enhancer regions. One of the possibilities is, thus, to use a combination of transcriptomic and epigenomic data to identify transcribed enhancers with enhancer-specific chromatin signatures. Besides CAGE, other technologies for identification of actively transcribed regions might be of use for identification of transcribed enhancers. For instance, GRO-seq profiles all nascent RNAs associated with transcriptionally engaged polymerases, and its variation GRO-cap enriches for 5'-capped RNAs (Core et al., 2014; Core et al., 2008). Their advantage over CAGE is their ability to detect unstable nascent RNAs (Core et al., 2014), however, at the same time these methods have limited base resolution and require

elaborate experimental procedures which could introduce experimental bias (Murakawa et al., 2016).

We characterised location and eRNA expression of transcribed enhancers across mouse tissues (see 2.4 for the limitations of our approach). The low expression levels might reflect the instability and short half-lives of eRNAs (Lam et al., 2014; Michel et al., 2017) or their low production in general. We highlighted highly tissue-specific transcription of enhancers, as reflected in both number of transcribed enhancers and their different composition across tissues. If these dissimilarities were an artefact of our methodology, they could stem from the composition of our tissue classes. Here, we could not link the dissimilarities to the different number of samples in the tissues under consideration. Alternatively, the tissues might be composed of distinct types and groups of samples. For instance, the "Macrophages" category consists only of bone marrow-derived macrophages that were cultivated in a range of conditions, while "Neurons" were sampled from different brain parts of several donors (see **Table A2.1**, Appendix). However, enhancer regulation was reported as highly tissue specific before (Kieffer-Kwon et al., 2013; G. Li et al., 2012), and here we noted that the transcribed enhancers showed more similarities in related tissues such as neurons and cerebellum. Therefore, our findings likely reflect genuine differences in enhancer regulation across mouse tissues.

One of the outstanding challenges in enhancer analyses is the identification of their target genes (Levine et al., 2014). First popular approaches assigned enhancers to their nearest genes, while other studies used a linear distance threshold to identify potential enhancer target genes (Andersson et al., 2014; De Santa et al., 2010; Ostuni et al., 2013). However, accumulating evidence suggests that linear proximity might not be an accurate predictor of enhancer-gene interactions, as many enhancers regulate distal genes, bypassing the nearest promoter (G. Li et al., 2012; Lupianez et al., 2016; Sanyal et al., 2012).

In this study, instead of a linear proximity-based approach, we used TAD data coupled with an expression correlation-based selection (see 2.4 for related limitations).

TADs have emerged as critical units of chromatin organisation that favour internal DNA contacts, whereas regulatory interactions between TADs are limited (Rocha et al., 2015). TADs often contain co-ordinately transcribed genes (Le Dily et al., 2014; Lupianez et al., 2016; Nora et al., 2012) and the majority of characterised interactions between enhancers and target promoters occur within the same TAD (Lupianez et al., 2016; Rocha et al., 2015; Symmons et al., 2014). We found that the majority of all possible enhancer-promoter pairs within TADs had a positive correlation of expression in each tissue. On one hand, this might complicate the identification of targets based on correlation, as in the extreme case all enhancers might be selected as regulators of all genes within a TAD. On the other hand, it reflects the definition of a TAD as a segment of co-regulated features (Le Dily et al., 2014; Lupianez et al., 2016; Nora et al., 2012).

Here, we elected to use a permissive correlation threshold to infer candidate enhancer-promoter pairs within TADs. As a consequence of eRNA expression differences, we observed different numbers of candidate enhancer-promoter regulatory pairs in different tissues, again, in agreement with the known enhancer tissue-specificity (Kieffer-Kwon et al., 2013; G. Li et al., 2012). Nevertheless, in all tissues under investigation we observed a trend for a higher expression of genes targeted by many transcribed enhancers. These results support a model of additive action of enhancers where several enhancers regulate the same target gene in order to increase its transcriptional output (Chepelev et al., 2012; Shlyueva et al., 2014).

In terms of TAD, gene and enhancer distribution, chromosome 7 showed distinct characteristics, containing more TADs of a smaller size and the highest number of genes,

when compared to other autosomes. Another unexpected finding concerned a distribution of genes and enhancers in TADs of different sizes. We found that most of the TADs with the highest number of genes and enhancers were of a moderate size. Possibly, larger TADs did not arise to accommodate more genes but, instead, their length could play a role in organising chromatin structure.

2.4. Limitations

One of the objectives of this study was to identify and characterise transcribed enhancers on a genome-wide level. Hence, the landscape of non-transcribed enhancers and their interactions with the transcribed enhancers remain elusive.

This study has a list of limitations concerning the methodology of identification of transcribed enhancers, as discussed below. However, it is important to note that according to the study in human (Andersson et al., 2014), such a strategy results in a reliable prediction of enhancer regions with experimental validation rates higher than in untranscribed candidate enhancers.

First, CAGE technology has been designed to profile transcripts carrying a 5' cap (Kanamori-Katayama et al., 2011). Hence, uncapped eRNAs might be overlooked. A complementary technology, such as GRO-seq that profiles nascent RNAs irrespective of the cap (Core et al., 2008), can be used to investigate whether uncapped bidirectionally transcribed eRNAs pinpoint any enhancer regions.

Second, the enhancer identification strategy was based on detection of balanced divergent transcription of eRNAs within enhancer regions. Hence, enhancers with other transcriptional patterns are overlooked. These include so-called 1D-eRNAs transcribed in a unidirectional manner, however, they seem to represent a minor class of enhancers (F.

Koch et al., 2011; Kowalczyk et al., 2012; Lam et al., 2014; W. Li et al., 2013). To overcome this limitation, our knowledge of enhancer biology needs to be expanded, and the phenomenon of 1D-eRNAs needs to be investigated in more detail.

Third, CAGE peaks located in a close proximity to coding regions were excluded. With the current state of knowledge and genome annotation, this is a good approach that allows avoiding ambiguous annotations and decreasing the number of false positive enhancers. However, certain enhancer regions, mainly intragenic (Birnbaum et al., 2012; Cinghu et al., 2017), might be overlooked due to such filtering. To overcome this limitation, a focused study of bidirectionally transcribed enhancer-like clusters located close to coding regions might be conducted. It would require additional data types allowing to distinguish between signals of coding RNAs and eRNAs. For instance, histone modification data might be employed, but might prove to be of a limited use in this case, since ChIP-seq-derived peaks are fairly broad and do not allow to distinguish transcripts with high nucleotide resolution (Murakawa et al., 2016).

Fourth, our findings, as well as previous reports, showed that detected levels of eRNAs were generally low (Arner et al., 2015; Kim, Hemberg, & Gray, 2015). This poses additional challenges on the technology to distinguish eRNA transcription from the background noise. In cases when detected eRNA levels are low due to their rapid degradation, complementary technologies, such as GRO-seq and GRO-cap that profile nascent RNAs irrespective of their stability (Core et al., 2014; Core et al., 2008), could be employed to obtain more comprehensive transcriptomics data.

TAD regions used in this study were derived from mouse embryonic stem cells (Dixon et al., 2012). Recent studies on chromosomal domains reported that TADs are well-conserved across tissues and even species (Dixon et al., 2012; Rocha et al., 2015). This fact,

taken together with a very limited information on TADs in other mouse tissues, defined our choice. Of note, however, TADs do not cover full chromosomes. The remaining regions could represent inter-TAD boundary or unorganised chromatin regions (Dixon et al., 2012). However, these segments still contain some enhancers and protein-coding genes, thus, the TAD regions used here might be incomplete. In addition, we have restricted our analyses to TAD-based *cis*-regulatory interactions only. Still, *trans*-regulatory interactions might exist, however, our methodology in this study does not allow for their identification.

The identification and verification of enhancer-target promoter interactions could be dramatically improved by using additional types of experimental data, such as Hi-C or ChIA-PET, that provide genome-wide snapshots of closely located or interacting genomic regions (G. Li et al., 2014; Lieberman-Aiden et al., 2009). However, the availability of these types of data in the public domain remains limited, especially, when a unified data set for multiple different tissues is of interest.

All listed limitations mainly stem from the fact that the current knowledge of enhancer biology is still very limited. There is no single 'enhancer mark' or specific property that could reliably identify all enhancers in a given tissue and condition and report their activation states (Long et al., 2016; Pennacchio et al., 2013; Shlyueva et al., 2014). Moreover, the existence of such a 'mark' is doubted, as it is possible that multiple classes of enhancers with different properties occur. Thus, each existing method has its own advantages and disadvantages, and none of the current approaches for identification of either enhancers or their targets have become a gold standard yet (Andersson, 2015; Murakawa et al., 2016; Pennacchio et al., 2013; Shlyueva et al., 2014).

As an attempt to partially overcome the listed limitations, in our study of enhancer regulation in macrophages (Chapter 3 and Chapter 4), we strengthened the CAGE data with ChIP-seq-derived histone modification data and used a stricter threshold for the identification of enhancer targets.

2.5. Conclusions

In this study, we have identified transcribed enhancers across multiple mouse tissues on a genome-wide level. We were able to improve on previous studies, as more than half of these regions were not discovered using enhancer-specific chromatin modifications. We inferred enhancer target protein-coding genes using a combination of location- and correlation-based approaches, which might provide more accurate predictions (G. Li et al., 2012; Lupianez et al., 2016). Finally, we report high tissue specificity and diversity of enhancer transcription and regulatory interactions highlighting the importance of future studies of enhancers focusing on distinct cell types and conditions.

2.6. Materials and methods

2.6.1. CAGE data set

CAGE TSSs with mouse genomic coordinates and tag counts were obtained from the FANTOM5 project data repository (http://fantom.gsc.riken.jp/5/datafiles/reprocessed/mm10_v2/basic/) (Forrest et al., 2014). Data for 969 mouse samples classified as “primary_cell”, “timecourse”, “tissue”, and “cell_line” were used. The list of all samples with their corresponding tissues can be found in **Table A2.1** (Appendix).

The downloaded set of TSSs represents all reliable CAGE reads that were mapped to mouse genome by the FANTOM5 consortium as described in Forrest et al. (2014). In brief, CAGE reads which correspond to ribosomal RNA were identified by aligning to the known ribosomal DNA and were discarded. The remaining reads were mapped to mm10 mouse genome using a probabilistic mapper Delve, which places individual reads to a single position with the highest probability of the alignment, based on a pair hidden Markov model (Djebali et al., 2012; Forrest et al., 2014). Unreliable reads with a low quality of mapping and low sequence identity were discarded (Forrest et al., 2014). As a result, the genomic coordinates for all reliable reads were derived and reported as TSSs. TSS tag counts reflect the number of CAGE reads mapped to the same genomic position.

2.6.2. Identification of CAGE peaks

CAGE peaks or clusters represent genomic regions that are enriched with CAGE reads and are considered as potential promoter regions. The DPI programme (https://github.com/hkawaji/dpi1/) was used as described before (Forrest et al., 2014) to cluster CAGE TSSs into CAGE peaks. Briefly, the algorithm uses independent component analysis to decompose regions with continuous CAGE signals into separate peaks based on their profile across different samples and tissues. With the default parameters, we obtained two output files containing (i) all detected CAGE peaks and (ii) their "robust" subset enriched for promoter-associated signals. The latter includes peaks that met the FANTOM5 "robust" criteria, with a single TSS being supported by 11 or more observations (CAGE reads) and one or more TPM in at least one experiment (Forrest et al., 2014). The "robust" peaks were used to annotate protein-coding gene promoters (see 2.6.3). The full set of CAGE peaks was used for identification of enhancers (see 2.6.5). Tag counts of all

TSSs clustered into a CAGE peak were summed up to derive a total tag count for that CAGE peak.

2.6.3. Annotation of protein-coding gene promoters

To quantify expression levels of transcripts and genes of interest using CAGE data, CAGE peaks that represent their promoters need to be identified. The commonly used approach for this task is a classification by proximity (Andersson et al., 2014; De Santa et al., 2010; Kim et al., 2010; Ostuni et al., 2013).

Annotation of protein-coding gene promoters included allocation of "robust" CAGE peaks (see 2.6.2) to known protein-coding genes and transcripts. Ensembl gene model version 75 (Flicek et al., 2011) was downloaded from the UCSC Table Browser (Karolchik et al., 2004) on 11 August 2016 and was used to obtain coordinates of protein-coding transcripts and genes. A CAGE peak was deemed a promoter of an Ensembl protein-coding transcript if its 5' end was mapped within 500 bp of the 5' end of the transcript on the same strand. The transcript annotation was extended to gene annotation by combining the CAGE peaks associated with all of the gene's transcripts.

2.6.4. Calculation of promoter and gene expression

Tag counts of annotated CAGE peaks were used to estimate promoter and gene expression levels. TMM normalisation of CAGE peak tag counts was performed to derive normalised promoter expression levels in a form of TPM (M. D. Robinson, McCarthy, & Smyth, 2010). Expression of each gene was calculated as a sum of expression of the gene's promoters. A promoter was considered to be expressed in a tissue if it showed nonzero expression in at least 20% of the tissue samples.

2.6.5. Identification of mouse enhancers with CAGE data

The full set of DPI-derived CAGE peaks (see 2.6.2) was used for identification of transcribed mouse enhancers. We used a strategy similar to the one described before (Andersson et al., 2014), with a few modifications as per below. The strategy aims at inferring enhancer regions as pairs of closely located bidirectional divergent CAGE peaks. The algorithm was implemented in the R programming (http://www.R-project.org/) and Shell scripting languages.

The main steps of the algorithm are summarised in **Figure 2.13**. Briefly, at first, pairs of divergent CAGE peaks separated by at most 400 bp are identified (step 1). Second, pairs that share a CAGE peak are merged (step 2). Third, the middle position between the rightmost anti-sense strand CAGE peak and leftmost sense strand CAGE peak is identified and deemed a centre position of that locus. At step 4, the centre position is associated with two flanking 200 bp windows on sense and anti-sense strands in a divergent manner. Loci identified in this manner are further filtered. First, the sense 200 bp window is required to overlap more CAGE peaks mapped on the sense DNA strand than CAGE peaks mapped on the anti-sense strand (and in the same manner for the anti-sense 200 bp window). Second, loci are required to show a balanced bidirectional transcription (Andersson et al., 2014). The loci that passed the filtering are deemed enhancer regions, and their expression is calculated by summarising the expression of CAGE peaks overlapping each of the 200 bp windows on the same strand.

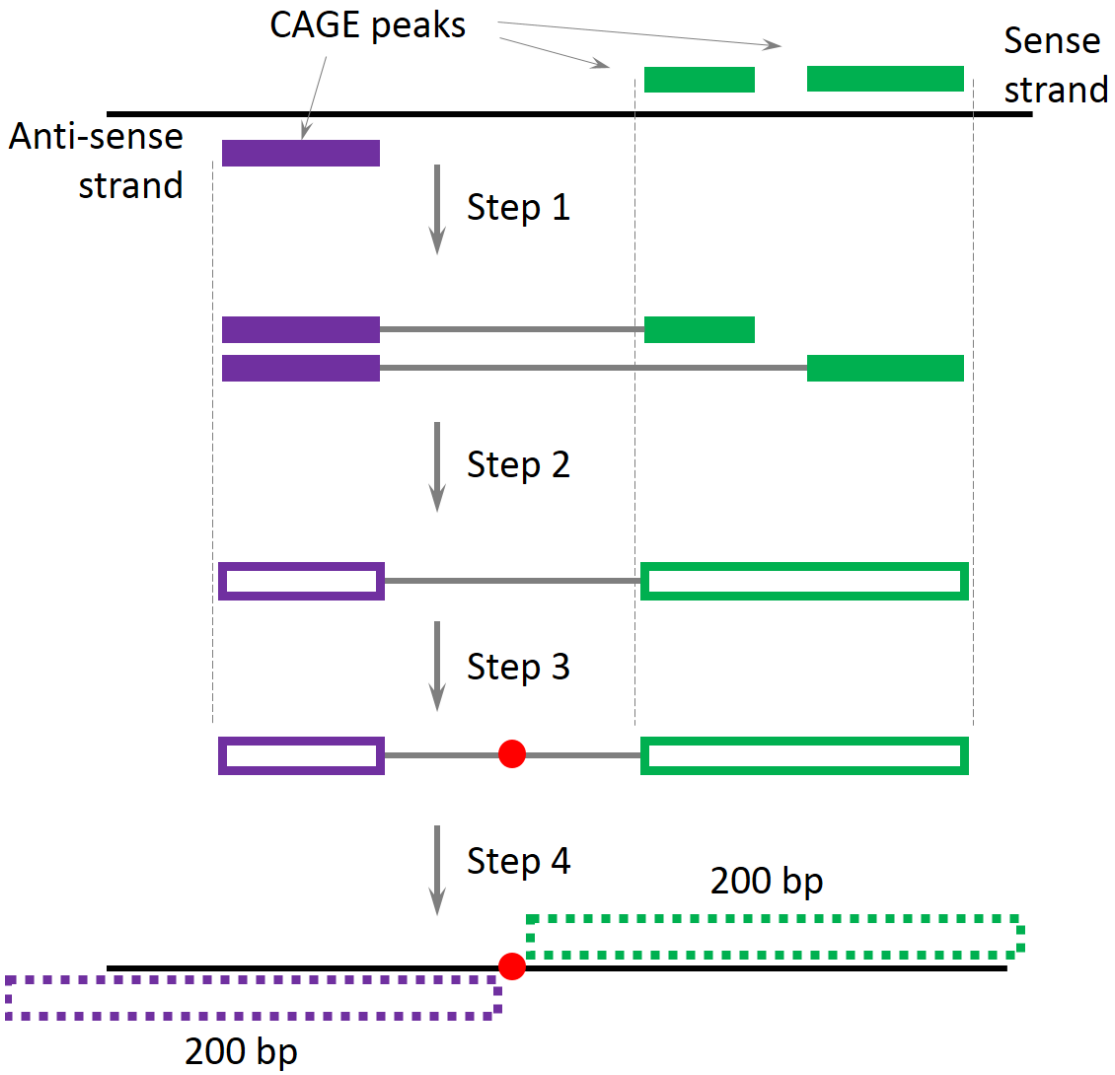

Figure 2.13. Main steps of the algorithm for identification of transcribed enhancers based on bidirectional CAGE transcription. Sense strand regions are shown in green, anti-sense stand regions are shown in purple.

In contrast to Andersson et al. (2014), we performed a positional filtering as the first (instead of the last) step of the algorithm. CAGE peaks located within 500 bp of protein-coding transcript start sites or within 200 bp of exons were excluded based on the coordinates of the Ensembl gene models, version 75 (Flicek et al., 2011). This reduced the number of CAGE peaks from 3,188,801 to 1,890,465 for the subsequent steps. Second, instead of normalising enhancer tag counts by dividing by a total library size, we used a

TMM normalisation (M. D. Robinson et al., 2010). As a result, the derived eRNA expression values are comparable to that of promoters and genes.

The algorithm yielded 42,470 transcribed mouse enhancers. An enhancer was considered to be transcribed in a particular tissue if it showed nonzero expression in at least 20% of the tissue samples.

2.6.6. Candidate regulatory enhancer-target promoter interactions

Non-overlapping TAD regions were obtained from a study in mouse embryonic stem cells (Dixon et al., 2012). For identification of candidate enhancer-promoter pairs in each tissue, we focused on tissues with at least 20 samples and considered only transcribed enhancers and expressed promoters with nonzero expression in at least 20% of the tissue samples. We first selected pairs where both enhancer and promoter were located entirely within the same TAD. Second, for all these pairs in each tissue separately, we calculated Spearman's correlation coefficient between eRNA and promoter expression across samples of that tissue. Pairs with correlation coefficient above zero were deemed candidate enhancer-promoter pairs.

2.6.7. Tools

All analyses made extensive use of the Shell scripting language and the R software (http://www.R-project.org/) with the Bioconductor packages (Gentleman et al., 2004). Most of the figures were generated with ggplot2 package for R (Wickham, 2009).

All genomic regions were either mapped to mm10 mouse genome or were converted from mm9 genomic coordinates to mm10 using the liftOver programme

(https://genome.ucsc.edu/cgi-bin/hgLiftOver). All analyses made extensive use of the BEDTools utilities (Quinlan & Hall, 2010), including tools for identification of overlapping intervals.

Chapter 3

The enhancer-gene interactome in naïve and activated macrophages

3.1. Overview

Macrophages are sentinel cells essential for tissue homeostasis and host defence. Owing to their plasticity, macrophages acquire a range of functional phenotypes in response to microenvironmental stimuli. Of those, M(IFN-γ) and M(IL-4/IL-13) macrophage activation states, sometimes referred to as classically and alternatively activated, are well known for their opposing pro- and anti-inflammatory roles. Imbalance in these populations of macrophages has been implicated in progression of various diseases.

In the present study, we use CAGE-based transcribed enhancers that we established in mouse tissues in Chapter 2. These data are combined with complementary epigenetic

data to identify transcribed enhancers in mouse bone marrow-derived macrophages (BMDM) with high confidence. The established enhancer landscape is used to study enhancer regulation in BMDM and during M(IFN-γ) and M(IL-4/IL-13) activation. This study had the following objectives:

1. Inferring a high-confidence enhancer set in mouse BMDM;
2. Establishing a high-confidence enhancer-promoter interactome in mouse BMDM;
3. Characterising the enhancer-gene interactome in mouse BMDM;
4. Identifying enhancers that might drive macrophage M(IFN-γ) and M(IL-4/IL-13) activation;
5. Characterising enhancer-gene interactome changes during M(IFN-γ) and M(IL-4/IL-13) macrophage activation;
6. Linking the macrophage response to IFN-γ and IL-4/IL-13 stimuli to enhancer-mediated transcriptional control via transcription factor activation.

3.2. Results

3.2.1. Identification of transcribed mouse macrophage enhancers

Using the FANTOM5 collection of 969 CAGE mouse samples (Forrest et al., 2014), we have identified 42,470 transcribed enhancers in mouse tissue (see Chapter 2). Among these, we selected 17,752 enhancers transcribed in our BMDM samples (see 3.6.1), by requiring an enhancer to show nonzero expression in at least 10% of samples. To refine our macrophage enhancer set, we elected to use the support of a complementary type of data, epigenomic data (**Figure 3.1**) (see 3.6.3).

The epigenomic data were derived from ChIP-seq experiments, which profiled H3K4me1 and H3K27ac histone marks in naïve BMDM and during macrophage response to a range of stimuli (Ostuni et al., 2013). Based on the presence of histone marks before and after macrophage stimulation, this study inferred enhancer regions and split them into classes of different activation states (Ostuni et al., 2013). Of the CAGE-based enhancers transcribed in BMDM, we sub-selected 11,216 enhancers (63%) that overlapped the ChIP-seq-based enhancer regions (**Figure 3.1**). Notably, of 24,718 CAGE-based mouse enhancers not transcribed in BMDM and discarded in this study (see **Figure 3.1**), only 19% overlapped the ChIP-seq-based enhancer regions, highlighting the tissue specificity of mouse enhancers.

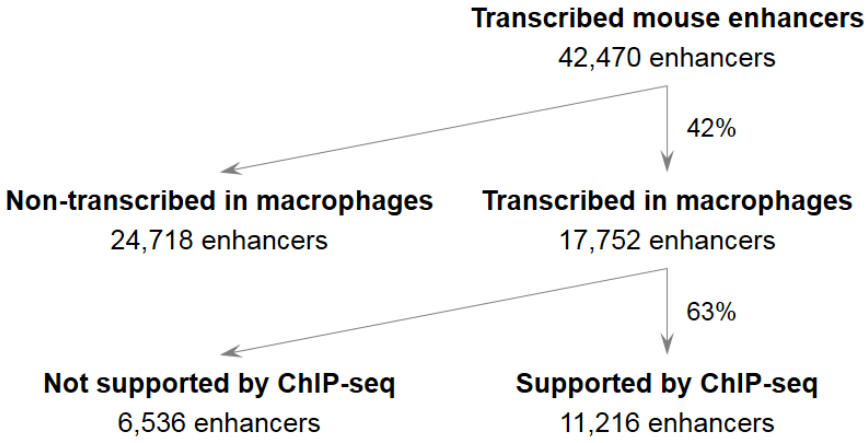

Figure 3.1. Selection of BMDM enhancer set. Of all CAGE-based transcribed mouse enhancers (see Chapter 2), we, first, selected those transcribed in BMDM samples, and, second, those supported by independent histone mark data profiled using ChIP-seq (Ostuni et al., 2013). Numbers of selected (on the right) and excluded (on the left) enhancers are shown.

We investigated the overlap of the 11,216 ChIP-seq-supported transcribed enhancers with different classes of histone mark-based enhancers, as defined by Ostuni et al. (2013). The lowest overlap of 1% was observed for "cryptic" enhancers, that did not carry any histone marks in naïve BMDM (**Table 3.1**). In addition, a low overlap of 5.2%-8.6% was found for "poised" enhancers, that carried only H3K4me1 enhancer mark in naïve

macrophages and did or did not acquire H3K27ac active enhancer histone mark upon stimulation (**Table 3.1**). The rest of the enhancer classes defined by Ostuni et al. (2013) were demarcated by H3K27ac in naïve macrophages and showed high overlaps with our CAGE-based enhancers (**Table 3.1**). A total of 93.6% of the 11,216 enhancers carried H3K27ac histone mark either before or after macrophage stimulation, in agreement with both H3K27ac and eRNA production being the properties of active enhancers.

To summarise, we identified 11,216 regions in BMDM, that were supported by both CAGE-based transcriptomic data and ChIP-seq-based epigenomic data, representing a set of high-confidence transcribed enhancer regions. Comparison to previous studies of enhancers in mouse macrophages suggests that our approach uncovered many novel enhancers. Specifically, 87.2% of our enhancers did not overlap enhancers predicted based on a combination of RNAPII binding and H3K4me1/H3K4me3 histone marks in untreated and LPS-stimulated macrophages (De Santa et al., 2010). Similarly, 73.9% of our enhancers did not overlap those inferred in a study using p300 and H3K4me1/H3K4me3 histone marks in untreated and LPS-stimulated macrophages (Ghisletti et al., 2010). Finally, 46.4% of our enhancers were not uncovered with H3K4me2 histone mark in macrophages treated with TLR4 agonist (Kaikkonen et al., 2013).

Table 3.1. Overlaps of 11,216 CAGE-based ChIP-seq-supported enhancers and histone mark-based enhancer classes. ChIP-seq-based enhancers and classes were inferred separately in LPS-treated macrophages and macrophages treated with a range of other stimuli (Ostuni et al., 2013). Combinations of histone marks before and after stimuli and number of the corresponding enhancers are shown per class.

ChIP-seq-based enhancer class (Ostuni et al., 2013)					# / % of 11,216 enhancers overlapping ChIP-seq-based enhancers		# / % of ChIP-seq-based enhancers overlapping 11,216 enhancers	
Class Name		Chromatin signature in unstimulated macrophages	Chromatin signature in stimulated macrophages	# enh.				
LPS	Constitutive Steady	H3K4me1, H3K27ac	H3K4me1, H3K27ac	9,013	3,551	31.7%	2,769	30.7%
	Cryptic		H3K4me1, H3K27ac	1,351	124	1.1%	120	8.9%
	Not Steady	H3K4me1, H3K27ac	H3K4me1, potential H3K27ac	16,287	4,620	41.2%	3,770	23.1%
	Poised Activated	H3K4me1	H3K4me1, H3K27ac	5,277	581	5.2%	512	9.7%
	Poised not Activated	H3K4me1	H3K4me1	37,629	966	8.6%	957	2.5%
Range of stimuli	Constitutive Activated	H3K4me1, H3K27ac	H3K4me1, H3K27ac	3,825	1,456	13.0%	1,140	29.8%
	Constitutive Steady	H3K4me1, H3K27ac	H3K4me1, H3K27ac	8,334	3,868	34.5%	2,736	32.8%
	Cryptic		H3K4me1, H3K27ac	1,033	116	1.0%	105	10.2%
	Poised Activated	H3K4me1	H3K4me1, H3K27ac	7,326	684	6.1%	612	8.4%
	Poised not Activated	H3K4me1	H3K4me1	27,343	667	5.9%	668	2.4%
	Repressed	H3K4me1, H3K27ac	H3K4me1	11,889	3,450	30.8%	2,823	23.7%

3.2.2. Macrophage enhancer-gene interactome

We aimed at studying enhancers that regulate expression of protein-coding genes in BMDM. We first identified pairs of enhancers and promoters located within TADs (Dixon et al., 2012), since this regulation is thought to be exerted via direct enhancer-promoter contact (Gorkin et al., 2014; Shlyueva et al., 2014). Thereafter, we refined these pairs using CAGE expression data based on the observation that eRNA and their target expression are positively correlated (Kim et al., 2010). This yielded 222,870 TAD-based enhancer-promoter (E-P) pairs, with 64,891 pairs showing significant (FDR < 10^{-4}) positive correlation of expression in macrophages (see 3.6.4 and **Figure 3.2a**). These correlation-based regulatory associations formed the basis for our further analyses and included 8,667 enhancers that we deemed actively transcribed in mouse BMDM. Interestingly, most of the TAD-based E-P pairs showed positive expression correlation (**Figure 3.2b**), which supports the definition of a TAD as a structural unit favouring internal regulatory interactions (Rocha et al., 2015). Our filtering approach further selected regulatory associations with correlation coefficient above 0.3 (**Figure 3.2b**), which we considered more reliable. The median distance between enhancers and promoters in the correlation-based E-P pairs was significantly smaller at 191,033nt as compared to 278,735nt for all TAD-based pairs (**Figure 3.2b**). In addition, we observed higher correlation coefficients in pairs of closely located paired enhancers and promoters (**Figure 3.2c**).

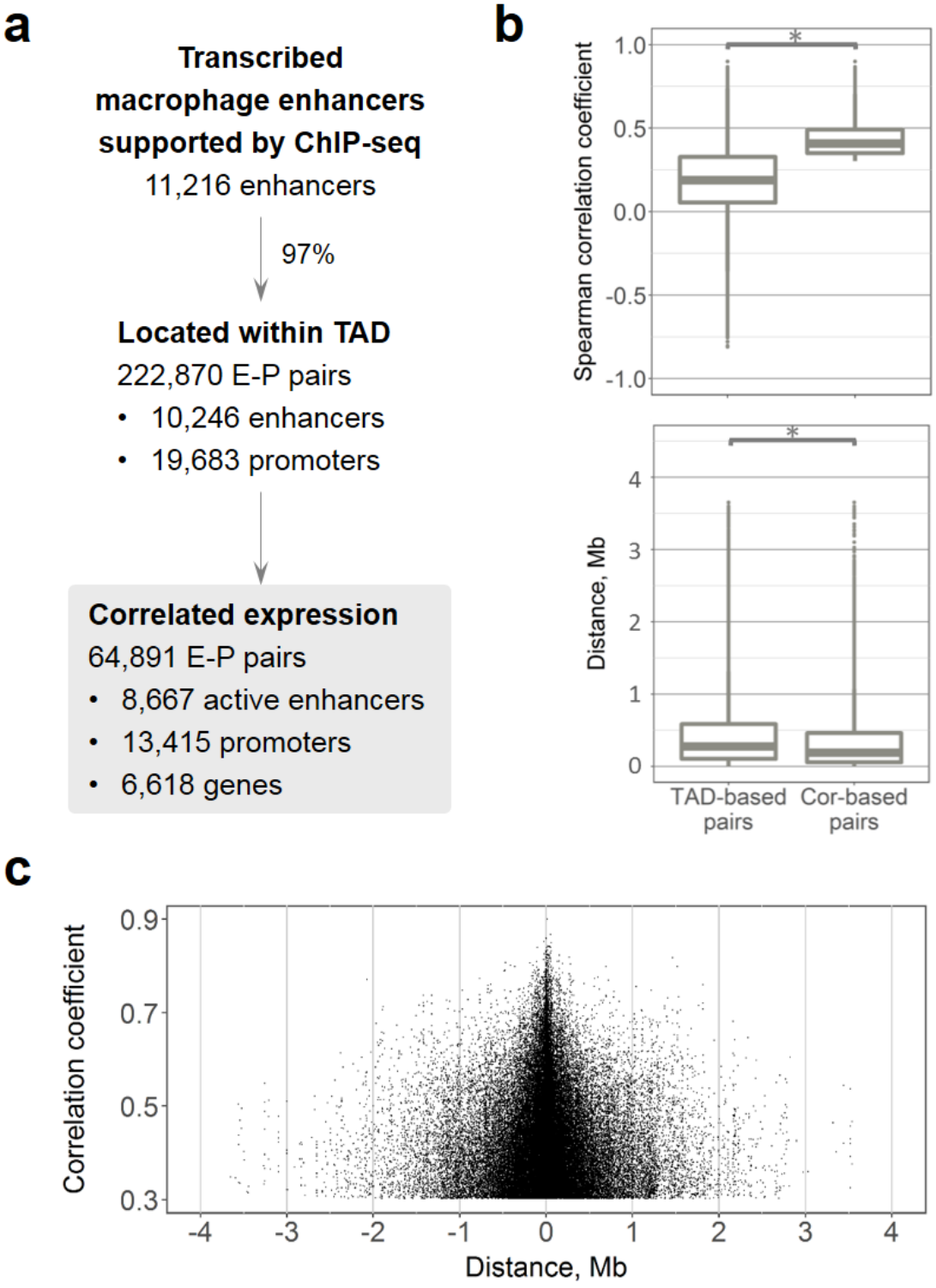

Figure 3.2. Macrophage enhancer-promoter (E-P) interactome. a Identification of E-P associations. **b** 222,870 TAD-based E-P pairs are compared to a subset of 64,891 correlation-based E-P pairs; expression correlation and distance between middle points of paired enhancers and promoters are shown; asterisks denote Wilcoxon rank sum test p-value < $2.2*10^{-16}$. **c** Spearman's correlation coefficient is plotted versus distance between middle points for the 64,891 correlation-based E-P pairs.

We further investigated associations between enhancers and target protein-coding genes. Of all 10,767 protein-coding genes with CAGE expression (see 3.6.2), 4,149 genes (38.5%) were not associated with any enhancer in our settings (**Figure 3.3a**, upper panel). Given previous evidence of additive action of enhancers (Chepelev et al., 2012; Shlyueva et al., 2014), we asked whether genes regulated by different numbers of enhancers had different gene expression levels. Genes without associated enhancers were overall lower expressed than genes associated with one (two-sided Wilcoxon signed-rank test p-value < $2.2*10^{-16}$) or more enhancers. A steady increase in gene expression concomitant with higher numbers of associated enhancers (**Figure 3.3a**, lower panel, Kruskal-Wallis rank sum test p-value < $2.2*10^{-16}$) was observed, supporting the model of additive enhancer action.

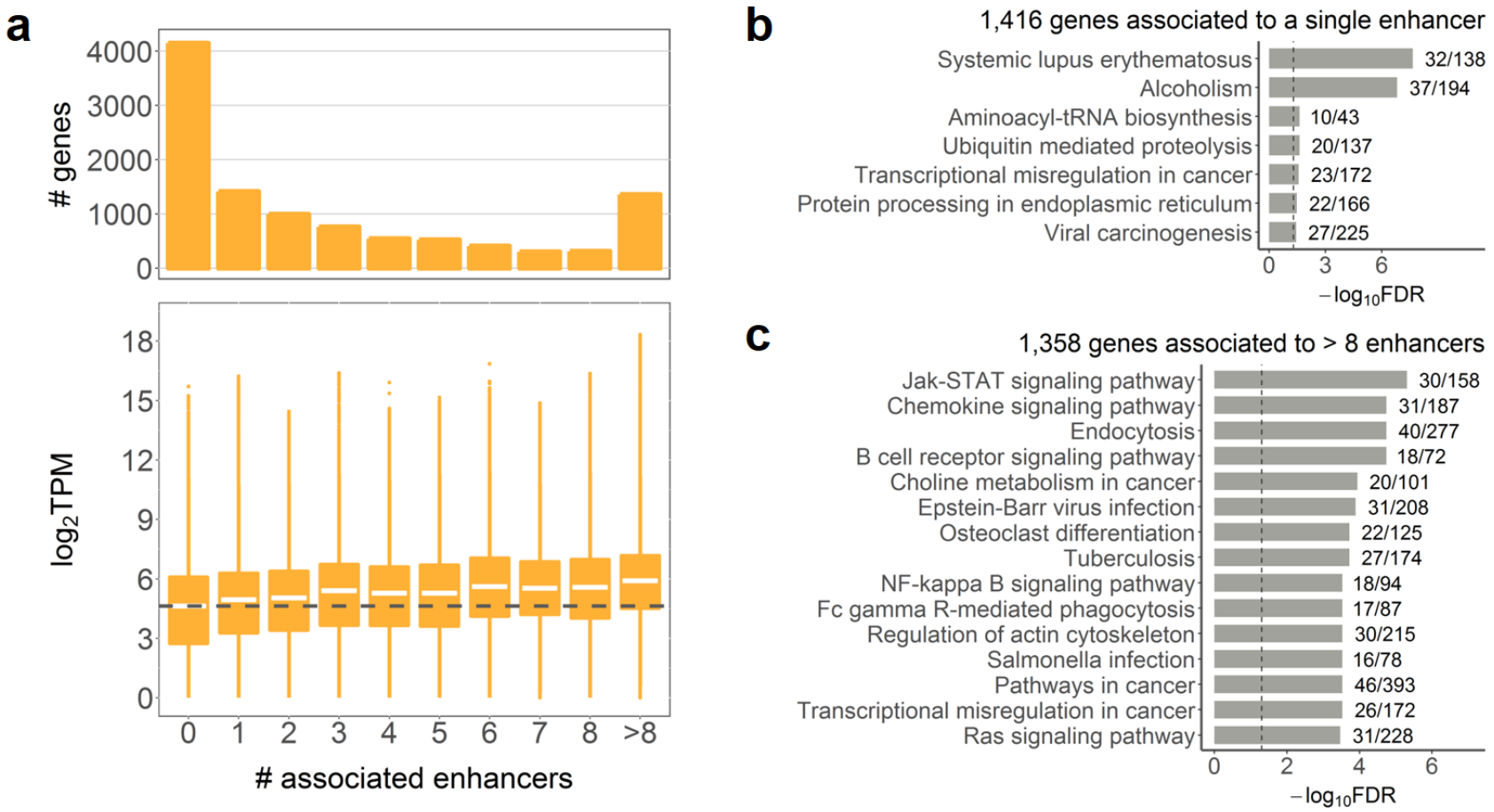

Figure 3.3. Macrophage enhancer-gene interactome. a Number and expression of genes associated with different number of enhancers. Dashed line shows median expression of genes not associated with any enhancer. **b** KEGG pathway maps significantly enriched for genes associated with a single enhancer, FDR < 0.05. **c** Top 15 KEGG pathway maps with the lowest FDR enriched for genes associated with more than 8 enhancers. In **b** and **c,** next to the bars are the numbers of genes in the KEGG pathway covered by our gene list; dashed lines indicate FDR = 0.05.

We next asked whether genes associated with different numbers of enhancers within the enhancer-gene interactome showed functional differences. Gene set enrichment analysis (GSEA, see 3.6.8) was performed for gene sets of similar size to avoid a size-related bias. The 1,416 genes associated with a single enhancer were enriched for housekeeping pathways including "Aminoacyl-tRNA biosynthesis" and "Ubiquitin mediated proteolysis", as well as a few inflammation-related pathways (**Figure 3.3b**). In contrast, the 1,358 genes associated with more than eight enhancers showed stronger enrichment for signalling pathways important for macrophage immune function, such as "Jak-STAT signalling pathway" and "Chemokine signalling pathway" (**Figure 3.3c**). GSEA for 1,306 genes associated with three or four enhancers showed enrichment for a combination of housekeeping and immune pathways (**Figure 3.4**). Finally, the larger set of 4,149 genes not associated with any enhancer showed the strongest enrichment for housekeeping pathways (**Figure 3.5**). Hence, a shift towards stronger enrichment for pathways important for macrophage immune function was a concomitant of higher numbers of associated enhancers.

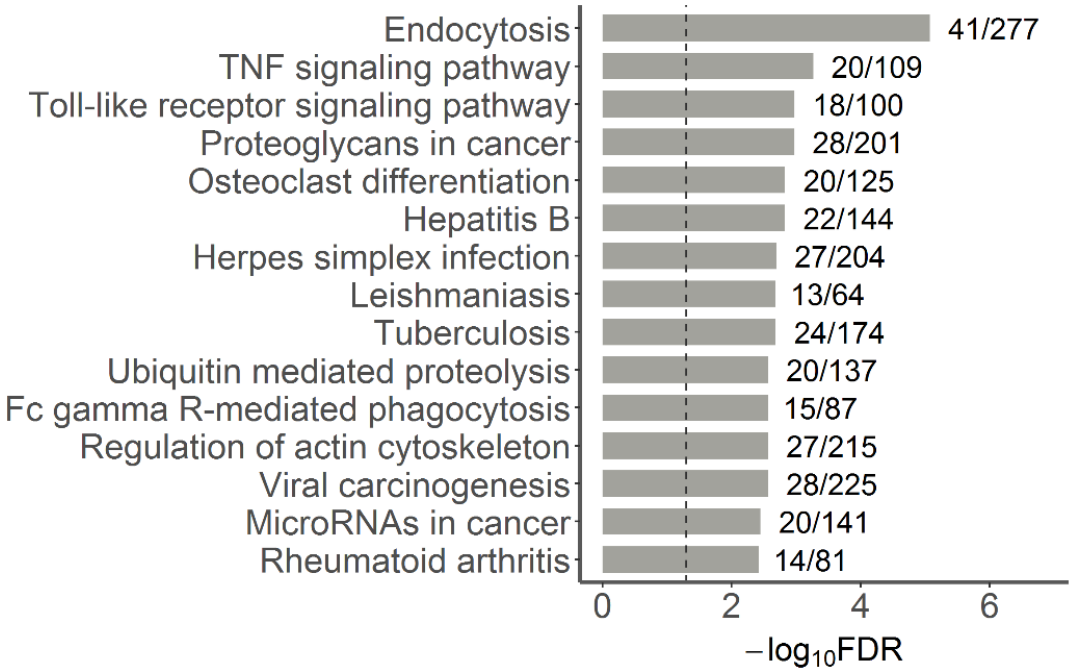

Figure 3.4. Top 15 KEGG pathway maps enriched for genes associated with 3-4 enhancers. Next to the bars are the numbers of genes in the KEGG pathway covered by our gene list; dashed lines indicate FDR = 0.05.

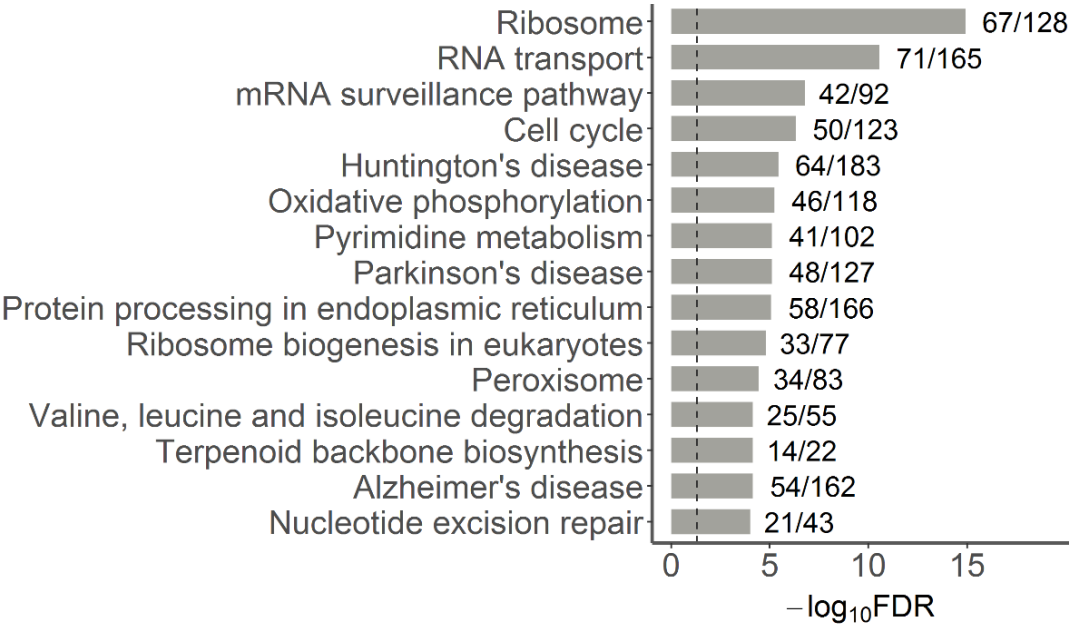

Figure 3.5. Top 15 KEGG pathway maps enriched for genes not associated with any transcribed enhancer. Next to the bars are the numbers of genes in the KEGG pathway covered by our gene list; dashed lines indicate FDR = 0.05.

3.2.3. Macrophage-specific expression

We opted for a similar strategy as developed before (Yao et al., 2015) to uncover eRNAs and genes with higher expression in macrophages as compared to other FANTOM5 mouse tissues (further referred to as macrophage specific, see 3.6.5). We identified 1,844 macrophage-specific and 8,923 non-macrophage-specific genes, and GSEA confirmed the anticipated functional differences (**Figure 3.6**).

These two sets showed significant differences in numbers of associated enhancers, with 65.6% of macrophage-specific genes being associated with more than one enhancer, whereas this proportion dropped to 44.7% for non-macrophage-specific genes (odds ratio 1.99, Fisher's exact test p-value < $2.2*10^{-16}$) (**Figure 3.7a**). These results were in agreement with our observation of stronger enrichment for macrophage-related functions in genes associated with many enhancers. Similar to the trend observed above, both macrophage-specific and non-macrophage-specific genes showed higher gene expression concomitant with higher numbers of associated enhancers, with non-macrophage-specific genes showing lower expression levels than macrophage-specific ones (**Figure 3.7b**).

Among 8,667 active enhancers, 54.7% were deemed macrophage specific (see **Figure 3.8a**, left panel, for eRNA expression levels), in agreement with known tissue specificity of enhancers (Kieffer-Kwon et al., 2013; Romanoski et al., 2015; Shen et al., 2012). Interestingly, non-macrophage-specific enhancers still showed higher eRNA expression in macrophages as compared to the non-macrophage samples (**Figure 3.8b**, left panel). This may be explained by the fact that for this analysis we excluded all enhancers that showed zero eRNA expression in the majority of our macrophage samples.

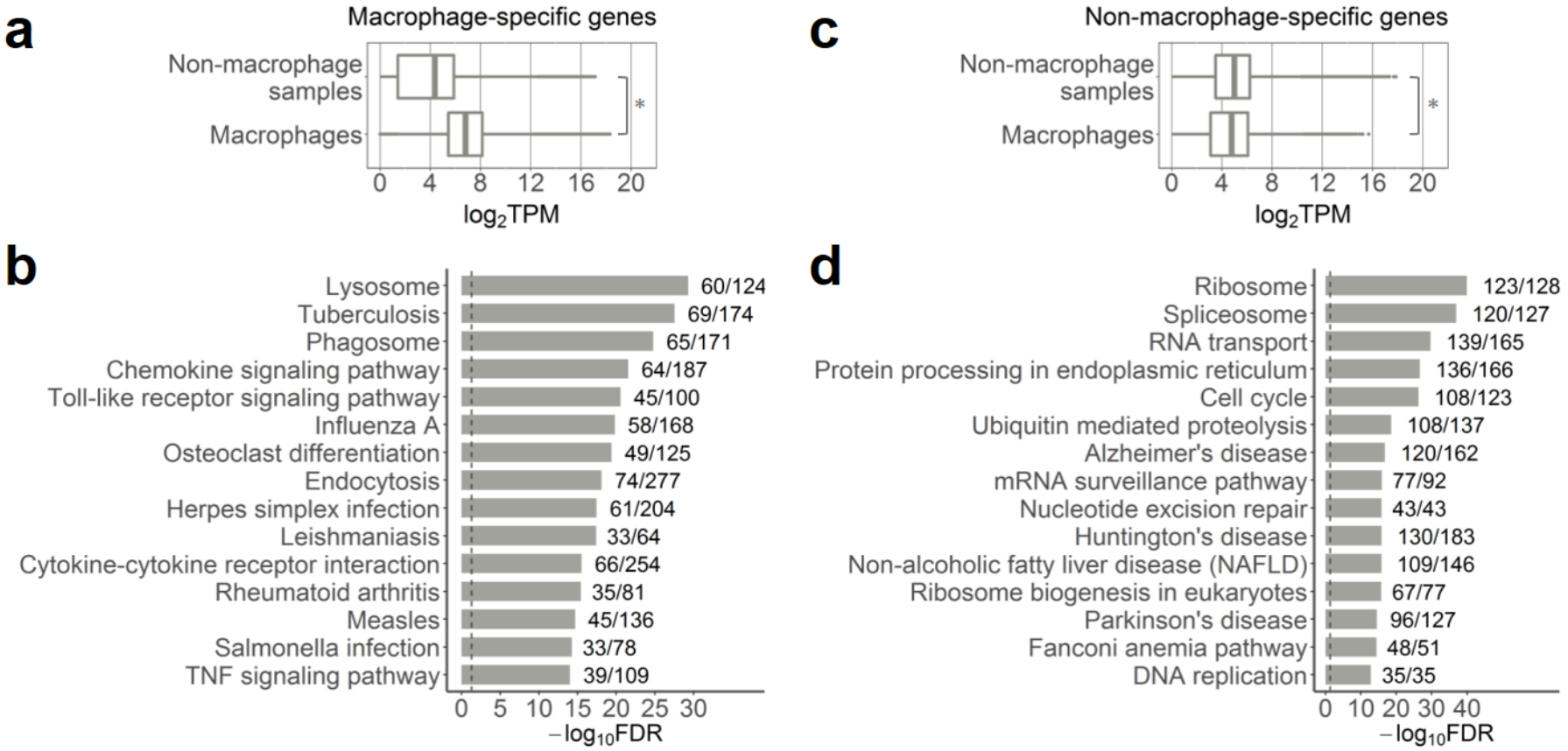

Figure 3.6. Expression and functions of macrophage-specific and non-macrophage-specific genes. a Expression of macrophage-specific genes. **b** KEGG pathway maps significantly enriched for macrophage-specific genes. **c** Expression of non-macrophage-specific genes. **d** KEGG pathway maps significantly enriched for non-macrophage-specific genes. In **a** and **c**, boxplots show expression in 184 macrophage and 744 non-macrophage samples, asterisks denote significant difference in expression (Wilcoxon signed-rank test p-value < $2.2*10^{-16}$). In **b** and **d**, top 15 KEGG terms with the lowest FDR are shown, next to the bars are the number of genes in the KEGG pathway covered by our gene list.

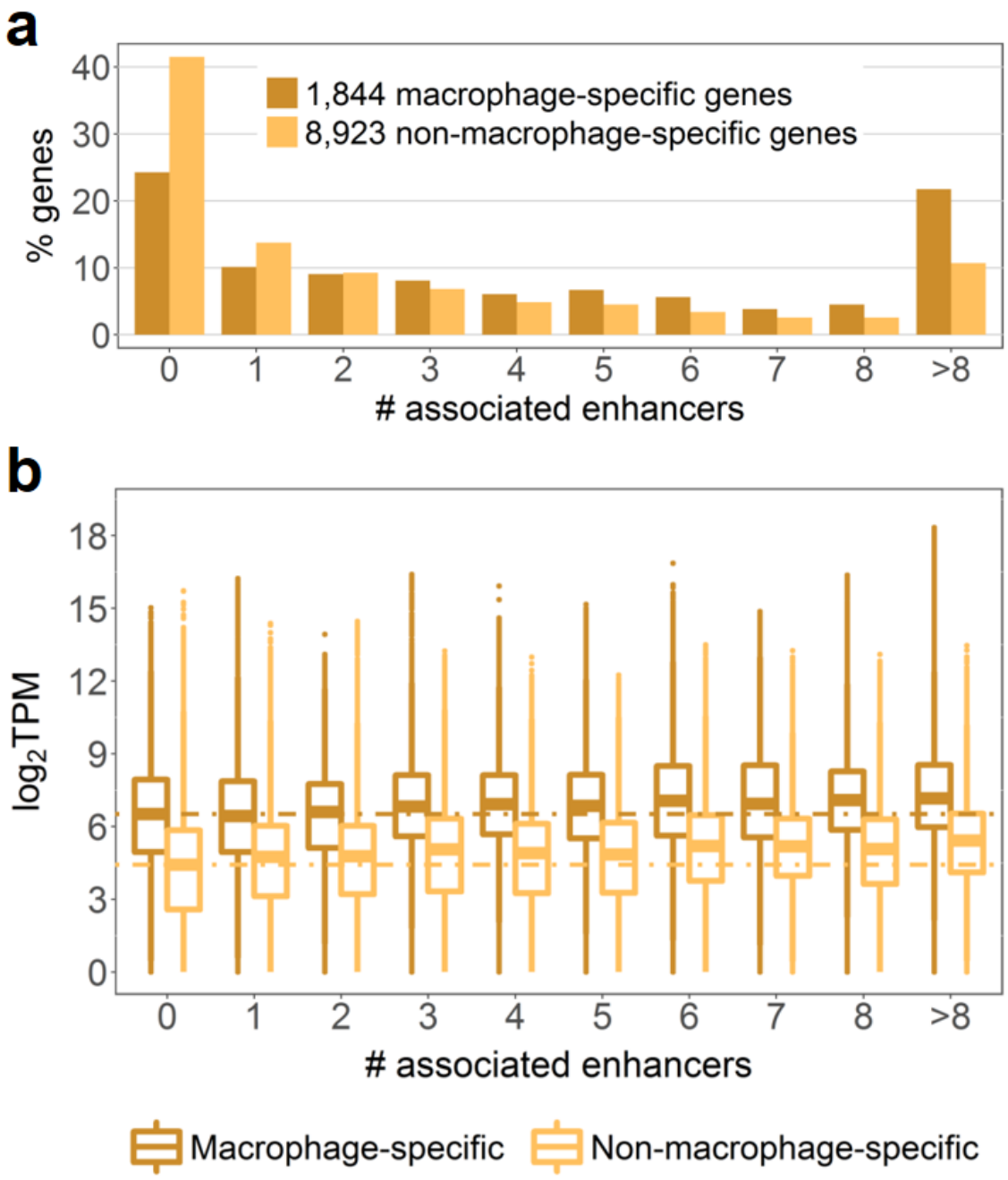

Figure 3.7. Enhancer-gene interactome of macrophage-specific and non-macrophage-specific genes. **a** Percentage of genes associated with different number of enhancers. **b** Expression of genes associated with different number of enhancers; dashed lines show median expression of genes not associated to any enhancer.

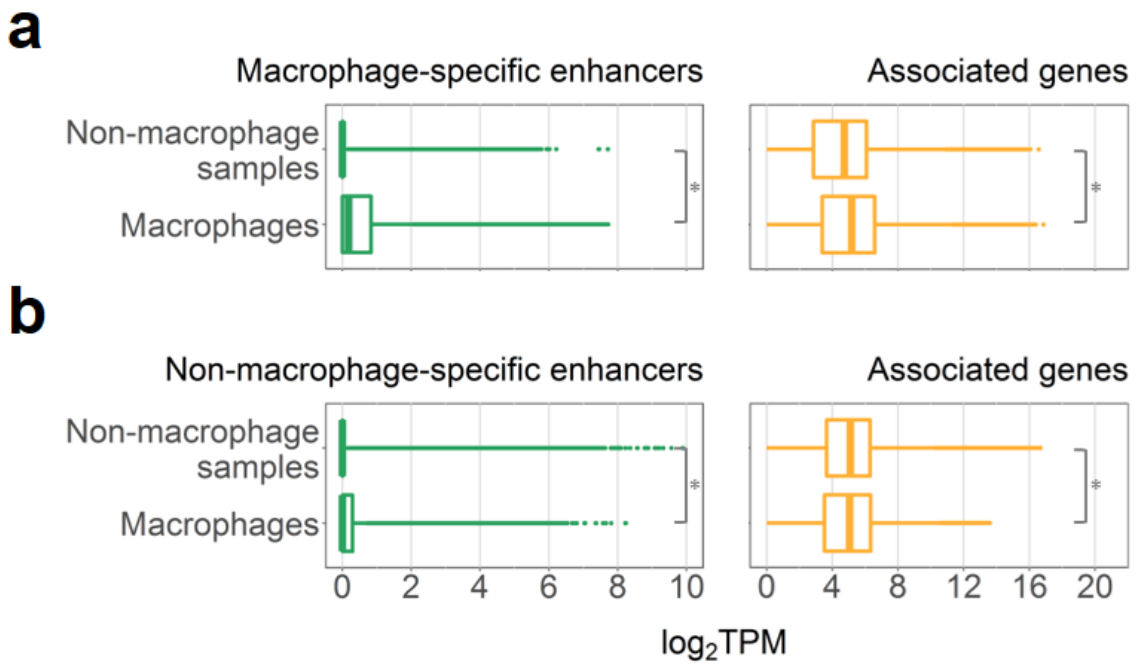

Figure 3.8. Expression of macrophage-specific and non-macrophage-specific enhancers and their associated genes. a Expression of 4,739 macrophage-specific enhancer eRNAs and 1,481 associated genes. **b** Expression of 3,928 non-macrophage-specific enhancer eRNAs and 1,207 associated genes. Expression is shown in 184 macrophage and 744 non-macrophage samples, asterisks denote Wilcoxon rank sum test p-value < 2.2*10-16.

Next, we asked whether these two enhancer sets could regulate genes with different expression and functions. Genes associated exclusively with macrophage-specific enhancers, as well as genes associated exclusively with non-macrophage-specific enhancers were sub-selected. As expected, genes associated exclusively with macrophage-specific enhancers showed overall higher expression in macrophage samples as compared to the non-macrophage samples (**Figure 3.8a**, right panel). In contrast, expression of genes associated exclusively with non-macrophage-specific enhancers was lower in macrophage samples (**Figure 3.8b**, right panel). Genes associated exclusively with non-macrophage-specific enhancers were enriched for only four KEGG pathway maps with FDR < 0.05 (**Figure 3.9a**), none of which can be considered a typical macrophage pathway. In contrast, genes associated exclusively with macrophage-specific enhancers were

enriched for both housekeeping and immune pathways (**Figure 3.10a**). This observation reflects the fact that production of macrophage-specific factors and activation of housekeeping processes that facilitate it might be both regulated by the same set of enhancers. We obtained consistent results when we repeated the analysis for a subset of 500 genes with the highest expression in macrophages (**Figure 3.9b** and **Figure 3.10b**).

Taken together, these findings demonstrate that most of the identified active enhancers in macrophages show macrophage-specific eRNA expression and regulate genes with macrophage-specific as well as housekeeping functions.

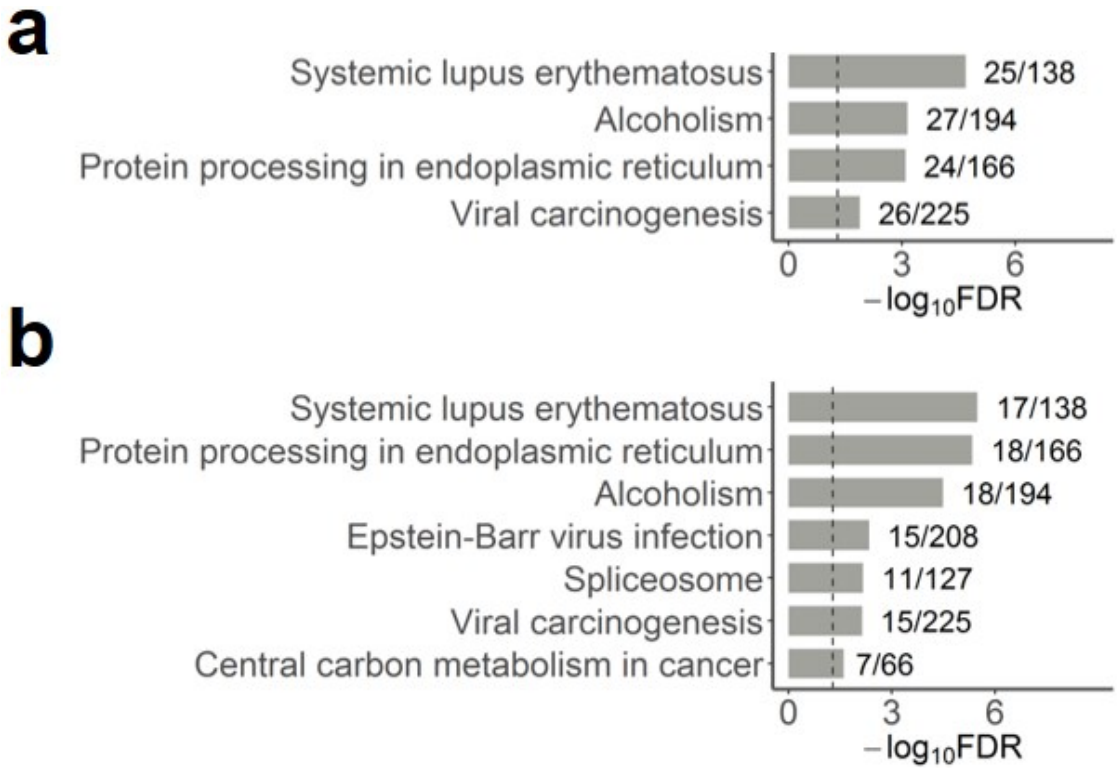

Figure 3.9. Functions of genes associated exclusively to non-macrophage-specific enhancers. a KEGG pathway maps significantly enriched for all 1,207 genes. **b** KEGG pathway maps significantly enriched for top 500 genes with the highest expression in macrophages. Next to the bars are the numbers of genes in the KEGG pathway covered by our gene list; dashed lines indicate FDR = 0.05.

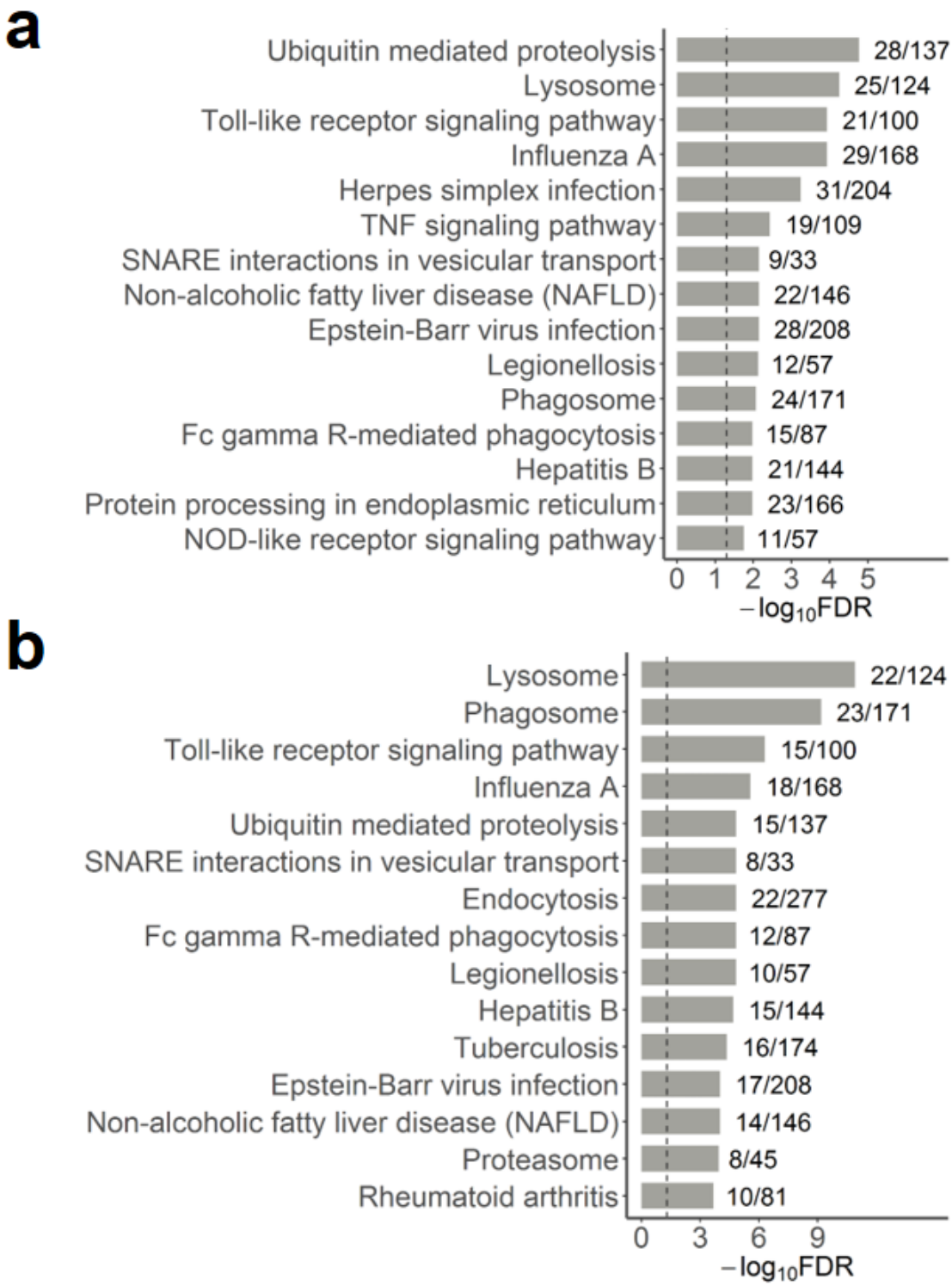

Figure 3.10. Functions of genes associated exclusively to macrophage-specific enhancers. a Top 15 KEGG pathway maps significantly enriched for all 1,481 genes. **b** Top 15 KEGG pathway maps significantly enriched for top 500 genes with the highest expression in macrophages. Next to the bars are the numbers of genes in the KEGG pathway covered by our gene list; dashed lines indicate FDR = 0.05.

3.2.4. Stimuli-induced transcriptional changes

We set out to determine transcriptional changes that were dynamically induced in M(IFN-γ) and M(IL-4/IL-13) mouse macrophages and to infer enhancers important in these processes. Time-course data used in this study are summarised in **Figure 3.11a**. M(IFN-γ)- and M(IL-4/IL-13)-responsive enhancers and genes were identified as those up-regulated upon stimulation; regulatory associations were retained for pairs with a positive correlation of expression in the corresponding activation state (see 3.6.6). In this manner, we discovered 115 M(IFN-γ)-responsive enhancers regulating 105 M(IFN-γ)-responsive genes (further referred to as sets E1 and G1), as well as 131 M(IL-4/IL-13)-responsive enhancers regulating 98 M(IL-4/IL-13)-responsive genes (sets E2 and G2) (**Figure 3.11b**). GSEA of G1 and G2 gene sets showed significant enrichment for GO terms relevant to immune system and macrophage functions (**Figure 3.11c**). These results highlight the importance of enhancer regulatory control during macrophage activation and suggest a striking influence of cytokine stimulation on activation of enhancers, which, in turn, drive some of the transcriptional responses seen during M(IFN-γ) and M(IL-4/IL-13) activation.

M(IFN-γ) and M(IL-4/IL-13) macrophages are known to possess different phenotypes and functions (Mosser & Edwards, 2008). As expected, G1 and G2 sets had only 19 genes in common. Similarly, a small overlap of only 14 enhancers was observed for E1 and E2 sets. Moreover, enhancers and genes selected as stimuli-responsive for a single activation state showed significant differences in time-course expression in M(IFN-γ) and M(IL-4/IL-13) macrophages (**Figure 3.11d**). These data indicate that M(IFN-γ) and M(IL-4/IL-13) macrophages not only differ in their gene expression profiles, but also differ in their active enhancer repertoire that likely drives observed gene expression changes.

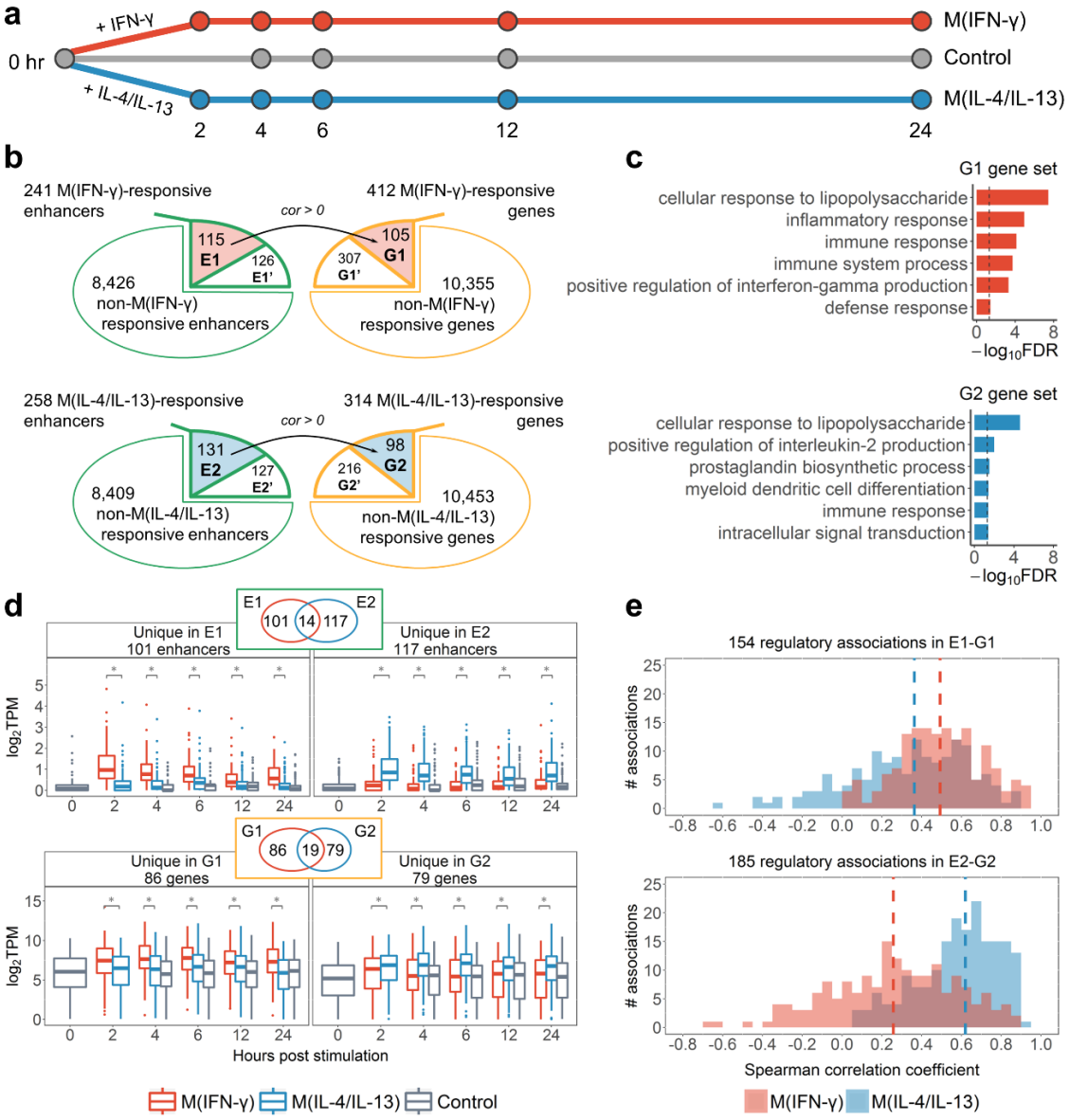

Figure 3.11. Stimuli-responsive genes and enhancers. a Time-course data used in this study. **b** Enhancer and gene sets. E1 and E2: M(IFN-γ)- and M(IL-4/IL-13)-responsive enhancers regulating M(IFN-γ)- and M(IL-4/IL-13)-responsive genes (G1 and G2), respectively; E1' and E2': M(IFN-γ)- and M(IL-4/IL-13)-responsive enhancers regulating non-stimuli-responsive genes; G1' and G2': M(IFN-γ)- and M(IL-4/IL-13)-responsive genes not regulated by stimuli-responsive enhancers. Black arrows denote regulatory associations between stimuli-responsive enhancers and genes. **c** GO terms enriched for G1 and G2 genes (all terms with FDR < 0.05 for G1; six terms with the lowest FDR for G2 are shown); dashed lines indicate FDR = 0.05. **d** Expression of stimuli-responsive eRNAs (upper panel) and genes (lower panel) unique to M(IFN-γ) or M(IL-4/IL-13). Asterisks indicate p-value < 10^{-5}, Wilcoxon signed-rank test. **e** Correlation of time-course expression of M(IFN-γ)-responsive (upper panel) and M(IL-4/IL-13)-responsive (lower panel) enhancers and genes. Vertical dashed lines show median values.

Previous studies reported and exploited positive expression correlation of eRNA and target genes (Andersson et al., 2014; Kim et al., 2010; Yao et al., 2015). Hence, we compared expression correlation of E1-G1 and E2-G2 pairs in M(IFN-γ) and M(IL-4/IL-13) macrophages (**Figure 3.11e**) to determine how correlations differ between conditions. E1-G1 pairs showed higher correlation in M(IFN-γ) macrophages as compared to M(IL-4/IL-13) (two-sided Wilcoxon signed-rank test p-value = $1.633*10^{-6}$). Similarly, correlation for E2-G2 pairs was higher in M(IL-4/IL-13) macrophages (two-sided Wilcoxon signed-rank test p-value < $2.2*10^{-16}$). Such stimuli-specific expression correlation suggests stimuli specificity of enhancer-gene regulatory associations in macrophages.

To gain an understanding of specificity of stimuli-responsive genes and enhancers to macrophages, we calculated their overlaps with macrophage-specific and non-specific genes and enhancers (**Figure 3.12**). We found that 15.6% of macrophage-specific genes and 6.8% of macrophage-specific enhancers were also stimuli responsive. Of stimuli-responsive genes, 46% were macrophage-specific. Of all stimuli-responsive enhancers, 70.1% were also macrophage specific, and this percentage was higher at 77% for E1 and 71% for E2 enhancer sets.

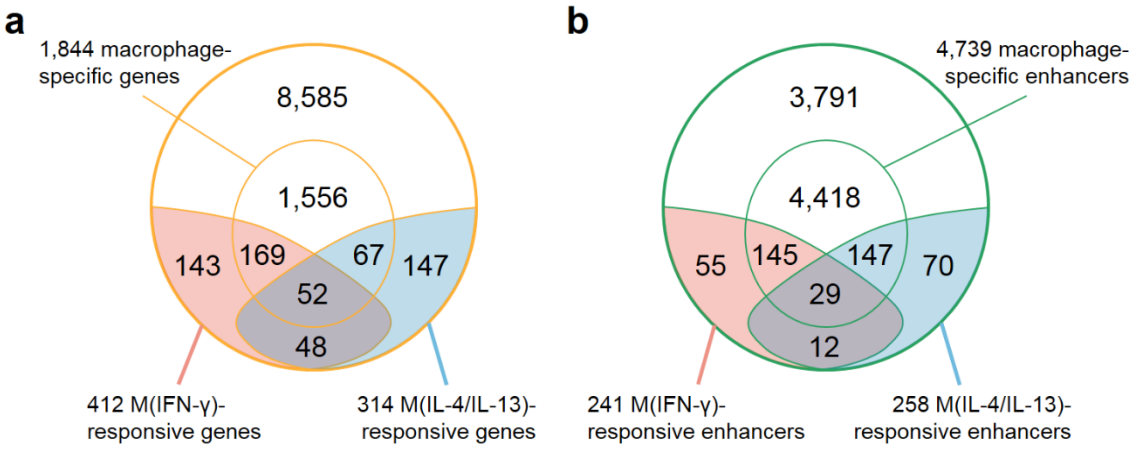

Figure 3.12. Overlaps of M(IFN-γ)- and M(IL-4/IL-13)-responsive and macrophage-specific genes and enhancers. **a** Genes, the large circle includes all 10,767 genes considered in this study. **b** Enhancers, the large circle covers all 8,667 enhancers in our BMDM interactome.

3.2.5. Marker genes of macrophage activation are regulated by stimuli-responsive enhancers

We further asked which known marker genes of classical and alternative macrophage activation (Gordon & Martinez, 2010; Jablonski et al., 2015; Martinez & Gordon, 2014; Mosser & Edwards, 2008; Murray & Wynn, 2011) were identified in M(IFN-γ) and M(IL-4/IL-13) in our setting (**Table 3.2**). Among 20 examined marker genes of classical macrophage activation, we found eight genes in the G1 set; similarly, eight of examined 26 marker genes of alternative activation were found in the G2 set (significant overlap with hypergeometric test p-value < 10^{-10}) (**Table 3.2**). The G1' set contained an additional four classical macrophage activation marker genes (Gpr18, Il12b, Il6, Inhba) and the G2' set an additional three alternative activation marker genes (Il27ra, Klf4, Myc), which, although stimuli-responsive themselves, were not associated with stimuli-responsive enhancers.

Next, we investigated the enhancer regulation of these marker genes. Given that different enhancers can modulate expression of the same gene in different conditions, we

aimed to infer potential marker enhancers that regulate marker genes specifically during either M(IFN-γ) or M(IL-4/IL-13) activation. Each of the 16 marker genes in G1 and G2 was associated with a minimum of one and maximum of nine enhancers in the E1 and E2 stimuli-responsive sets, respectively (**Table 3.2**). Of those, we identified enhancers that were selectively responsive in a single activation state and showed higher eRNA expression in this state as compared to the other one (see 3.6.7). A total of 13 M(IFN-γ) and 22 M(IL-4/IL-13) enhancers were inferred as potential activation markers (**Table 3.2**).

Table 3.2. M(IFN-γ) and M(IL-4/IL-13) macrophage activation markers. The columns list marker genes in G1 and G2, number of associated enhancers in the corresponding activation state, and potential activation marker enhancers.

M(IFN-γ) markers			M(IL-4/IL-13) markers		
Gene (G1)	***# enh. in E1***	***M(IFN-γ) marker enhancers in E1***	***Gene (G2)***	***# enh. in E2***	***M(IL-4/IL-13) marker enhancers in E2***
Cd38	1		Arg1	1	chr10:25119065..25119466
Cxcl9	3	chr5:92368373..92368774, chr5:92369052..92369453, chr5:92374704..92375105	Ccl24	1	
Cxcl10	4	chr5:92353639..92354040, chr5:92368373..92368774, chr5:92369052..92369453, chr5:92374704..92375105	Egr2	9	chr10:67595184..67595585, chr10:67598488..67598889, chr10:67628888..67629289, chr10:67636538..67636939, chr10:67694800..67695201, chr10:67695848..67696249, chr10:67712611..67713012, chr10:67713071..67713472, chr10:67715029..67715430
Cxcl11	5	chr5:92353639..92354040, chr5:92368373..92368774, chr5:92369052..92369453, chr5:92374704..92375105, chr5:92375350..92375751	Fn1	3	chr1:71938511..71938912,
Nos2	1	chr11:78916390..78916791	Igf1	7	chr10:87731929..87732330, chr10:87753519..87753920, chr10:87805812..87806213, chr10:87830718..87831119, chr10:87832100..87832501, chr10:87839444..87839845
Ptgs2	1		Irf4	2	chr13:30714614..30715015
Socs3	3		Mrc1	2	chr2:14185406..14185807, chr2:14206798..14207199
Tnf	1		Socs2	2	chr10:95232562..95232963, chr10:95236240..95236641

Interestingly, three classically activated macrophage marker genes found in M(IFN-γ), Cxcl9, Cxcl10, and Cxcl11 are located within one TAD and are co-regulated by a group

of three marker enhancers (**Figure 3.13**, see also **Figure 3.14** for a genome browser view of one of these enhancers). These enhancers, along with the two marker enhancers regulating Cxcl10 or Cxcl11 but not Cxcl9 (**Table 3.2**) are located in close proximity, in the intronic regions of the Art3 gene (**Figure 3.13c**). These enhancer regions were previously reported to show induced RNAPII binding in macrophages upon stimulation with LPS, one of the known classical macrophage activators (De Santa et al., 2010). In addition, these marker enhancer regions were shown to carry H3K4me1 enhancer histone marks in untreated macrophages (Ostuni et al., 2013). Moreover, H3K27ac histone modification, associated with active enhancers, was stronger enriched in these regions in M(IFN-γ) as compared to M(IL-4) and untreated macrophages (Ostuni et al., 2013) (**Figure 3.13c**), providing further evidence of their functionality in macrophage M(IFN-γ) activation.

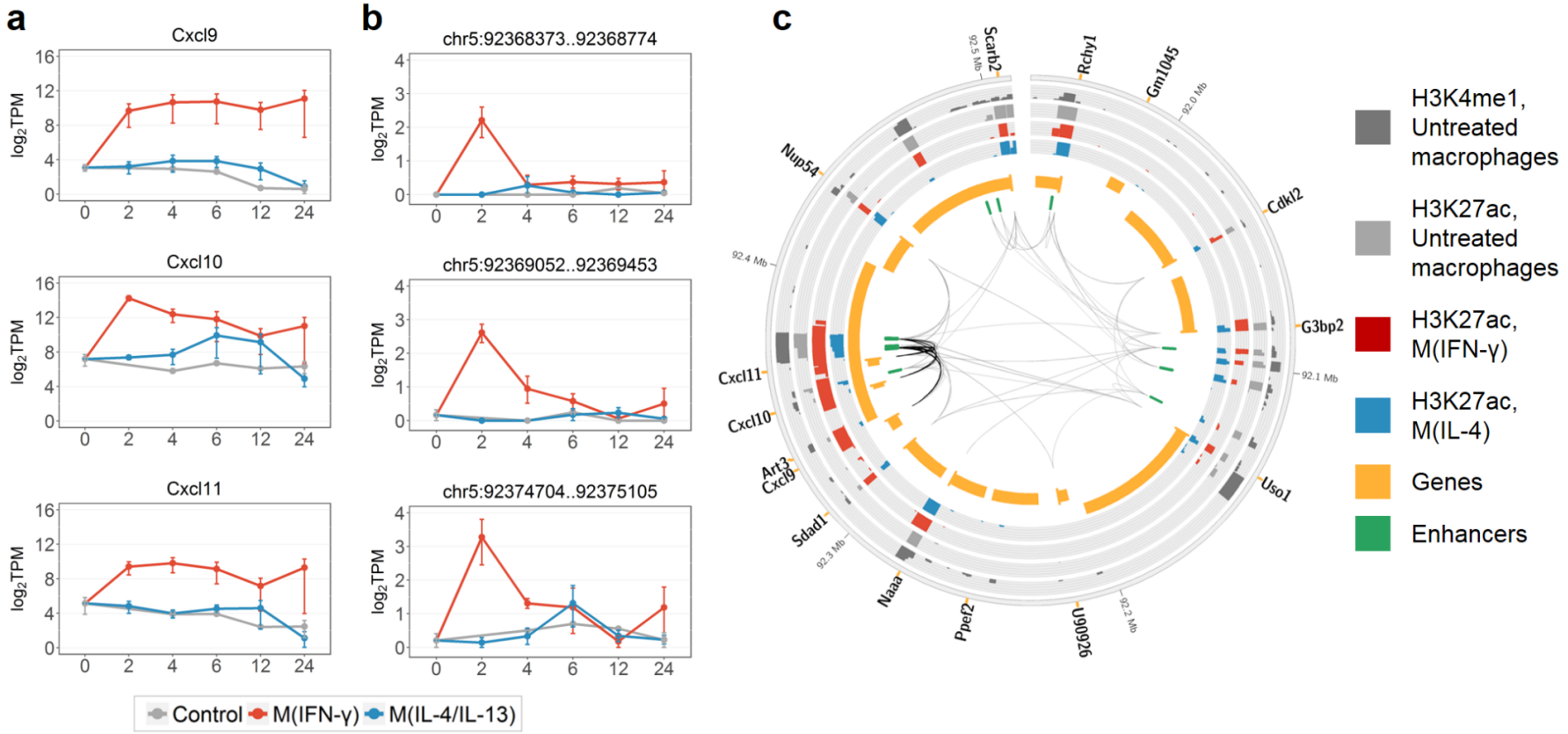

Figure 3.13. Classically activated macrophage marker genes Cxcl9, Cxcl10, and Cxcl11. **a** Expression of the genes. **b** eRNA expression of three potential marker enhancers that co-regulate Cxcl9, Cxcl10, and Cxcl11. **c** Genomic region of a TAD containing Cxcl9, Cxcl10, Cxcl11, and associated enhancers. Black links connect the marker genes with the three potential marker enhancers. Grey links denote other enhancer-gene interactions that we identified in macrophages. Genes are split into two tracks based on the strand, wide orange marks denote gene promoters; histone mark tracks show ChIP-seq peaks with the height of $-10*\log_{10}$(p-value) (Ostuni et al., 2013). In **a** and **b,** data were averaged over replicates and log-transformed, error bars are the SEM.

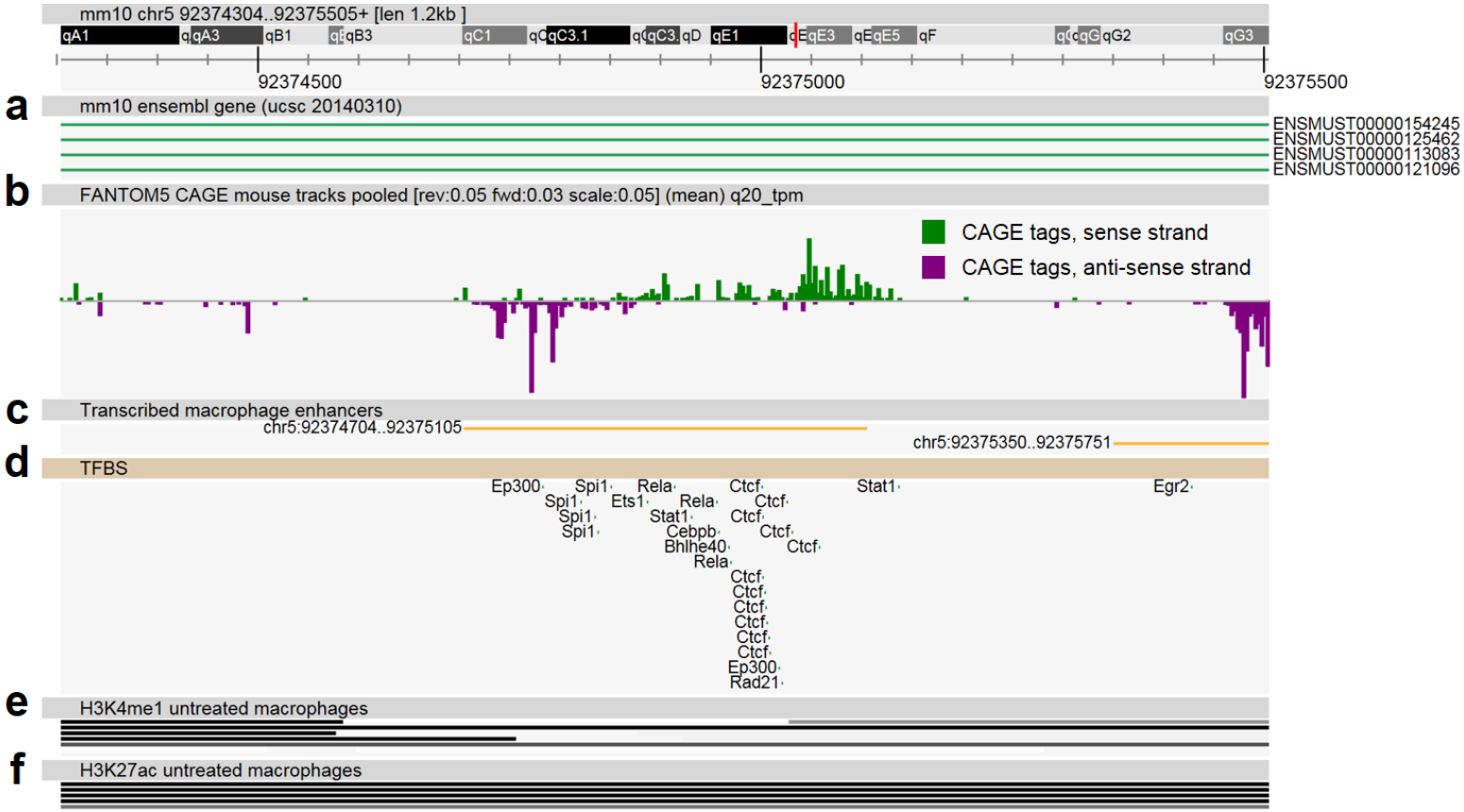

Figure 3.14. M(IFN-γ) marker enhancer associated with Cxcl9, Cxcl10, and Cxcl11 genes. ZENBU genome browser view shows the enhancer and 400 bp flanking regions. The enhancer has non-macrophage-specific eRNA expression; expression for eRNA and associated genes are shown in **Figure 3.13**. **a** The enhancer is located in an intron of the Art3 gene. **b** CAGE signal in 184 BMDM samples, split by strand. **c** Enhancer region. **d** Summits of transcription factor binding sites; based on ChIP-seq data that were used for TFBS over-representation analysis, see 3.6.9. **e, f** Significant ChIP-seq peaks for histone marks that were used to define ChIP-seq-based enhancers (Ostuni et al., 2013).

Among alternatively activated macrophage marker genes found in M(IL-4/IL-13), Arg1 as expected was substantially expressed in M(IL-4/IL-13) macrophages but had extremely low expression in M(IFN-γ) and untreated macrophages (**Figure 3.15a**). We found a single M(IL-4/IL-13)-responsive enhancer that might drive expression of Arg1 in M(IL-4/IL-13) macrophages and might serve as a marker enhancer (**Table 3.2** and **Figure 3.15b**). On the contrary, alternatively activated macrophage marker gene Egr2, a TF that activates macrophage genes (Laslo et al., 2006), was associated with as many as nine M(IL-4/IL-13) marker enhancers (**Table 3.2**). Egr2 showed immediate up-regulation in response to both IFN-γ and IL-4/IL-13 stimulation; however, in M(IL-4/IL-13) macrophages the up-regulation was sustained for up to 24 hours, whereas in M(IFN-γ) macrophages expression dropped rapidly after 2 hours (**Figure 3.16a**, upper panel). Time-course eRNA expression for two Egr2 marker enhancers with the highest expression at 2 and 4 hours is shown in **Figure 3.16a**. The distribution of all nine Egr2 marker enhancers within a TAD (**Figure 3.16b**) may suggest that the regions identified as nine individual enhancers potentially demarcate fewer regions of super or stretch enhancers (Hnisz et al., 2013; Parker et al., 2013). We observed a similar distribution for enhancers of marker gene Igf1, which is known to shape the alternatively activated macrophage phenotype and regulate immune metabolism (Spadaro et al., 2017) (**Figure 3.17**, see also **Figure 3.18** for a genome browser view of one of these enhancers with the highest expression at 2 hours). Importantly, in both Egr2 and Igf1, marker enhancer regions carried H3K4me1 in untreated macrophages and showed the strongest enrichment with H3K27ac in M(IL-4) as compared to M(IFN-γ) and untreated macrophages (Ostuni et al., 2013) (**Figure 3.16b** and **Figure 3.17c**).

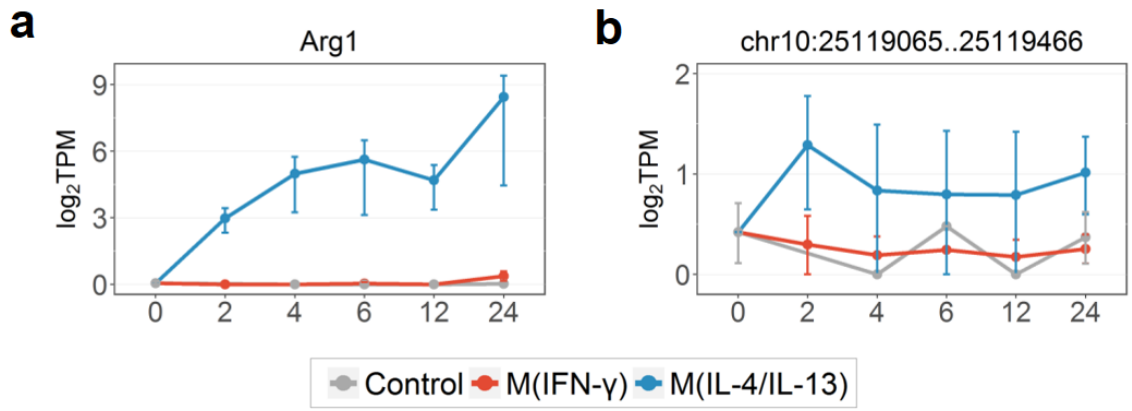

Figure 3.15. Time-course expression of Arg1 and associated M(IL-4/IL-13)-specific enhancer.

Expression data were averaged over replicates and log-transformed. Error bars are the SEM.

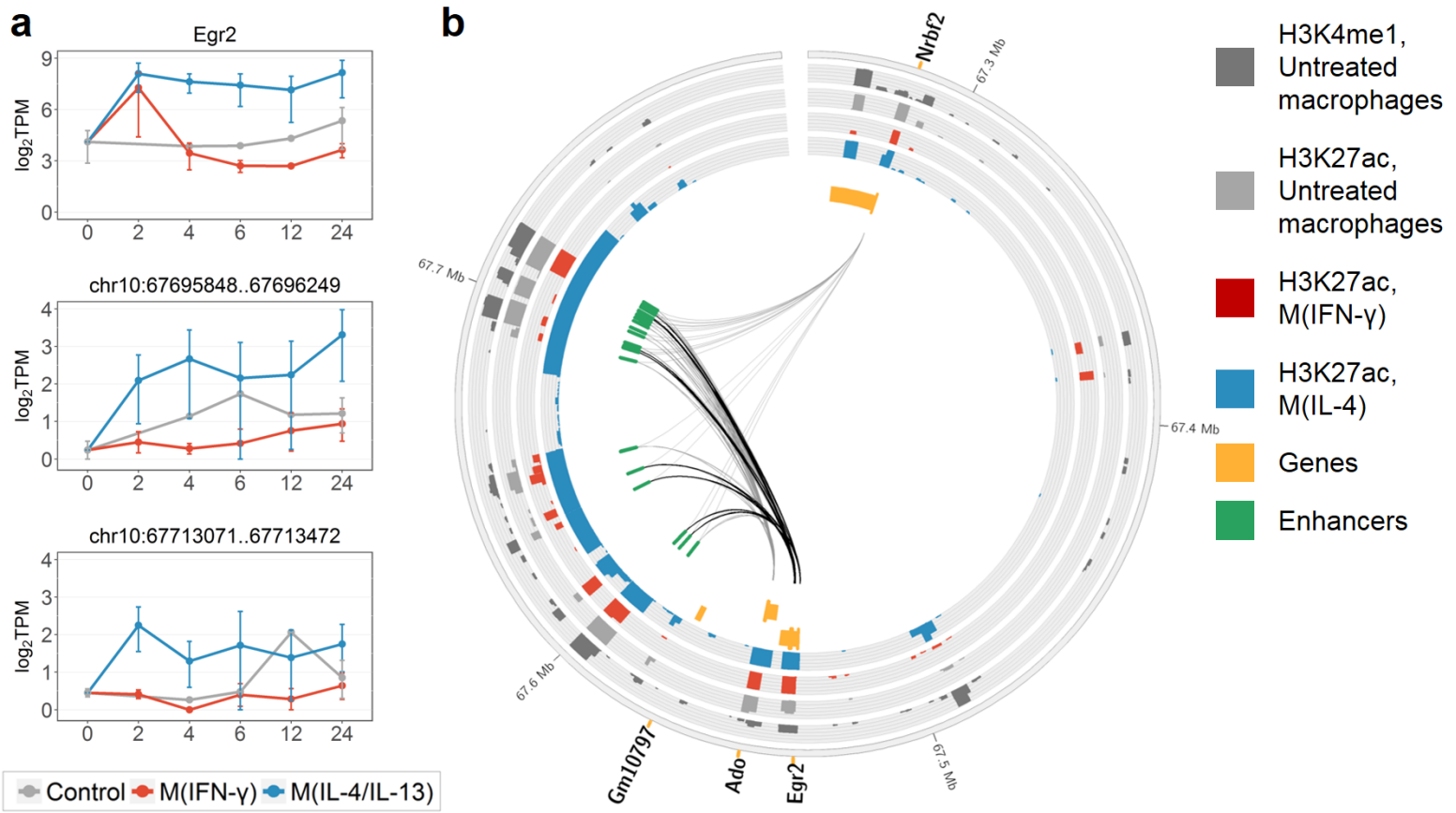

Figure 3.16. Alternatively activated macrophage marker gene Egr2. **a** Expression of the gene and two of M(IL-4/IL-13) marker enhancers associated with Egr2; data were averaged over replicates and log-transformed, error bars are the SEM. **b** Genomic region of a TAD containing Egr2 and associated enhancers. Black links connect Egr2 with the nine M(IL-4/IL-13) marker enhancers. Grey links denote other enhancer-gene interactions that we identified in macrophages. Genes are split into two tracks based on the strand, wide orange marks denote gene promoters; histone mark tracks show ChIP-seq peaks with the height of -10*$\log_{10}$(p-value) (Ostuni et al., 2013).

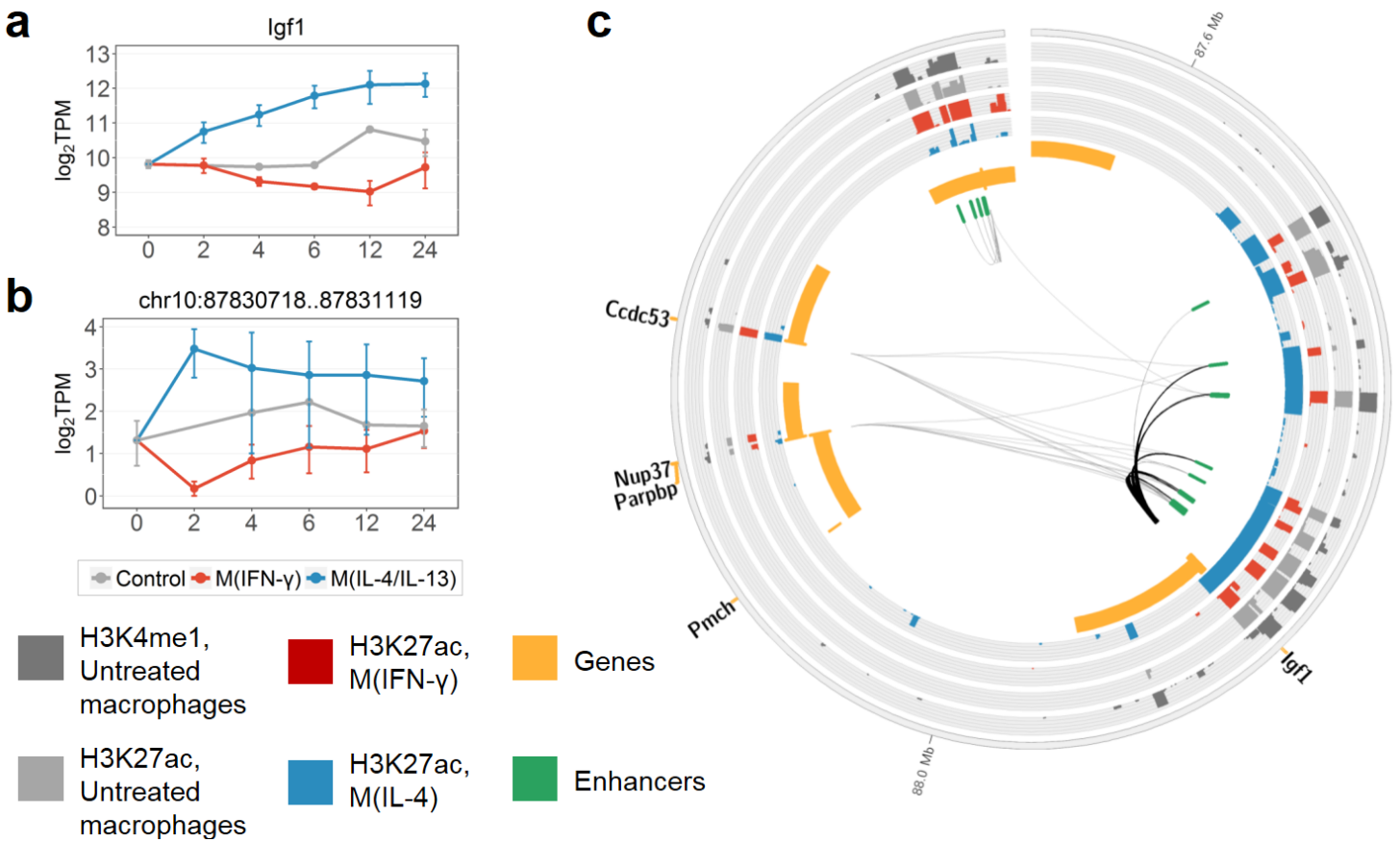

Figure 3.17. Alternatively activated macrophage marker gene Igf1. a Time-course expression of Igf1. **b** Time-course eRNA expression of Igf1-associated M(IL-4/IL-13) marker enhancer with the highest expression at 2 h. In **a** and **b,** data were averaged over replicates and log-transformed, error bars are the SEM. **c** TAD containing Igf1 marker and associated enhancers. Black links connect Igf1 to the six M(IL-4/IL-13) marker enhancers. Grey links denote other enhancer-gene interactions identified in macrophages. Genes are split into two tracks based on the strand, wide orange marks denote gene promoters; histone mark tracks show ChIP-seq peaks with the height of $-10*\log_{10}$(p-value) (Ostuni et al., 2013).

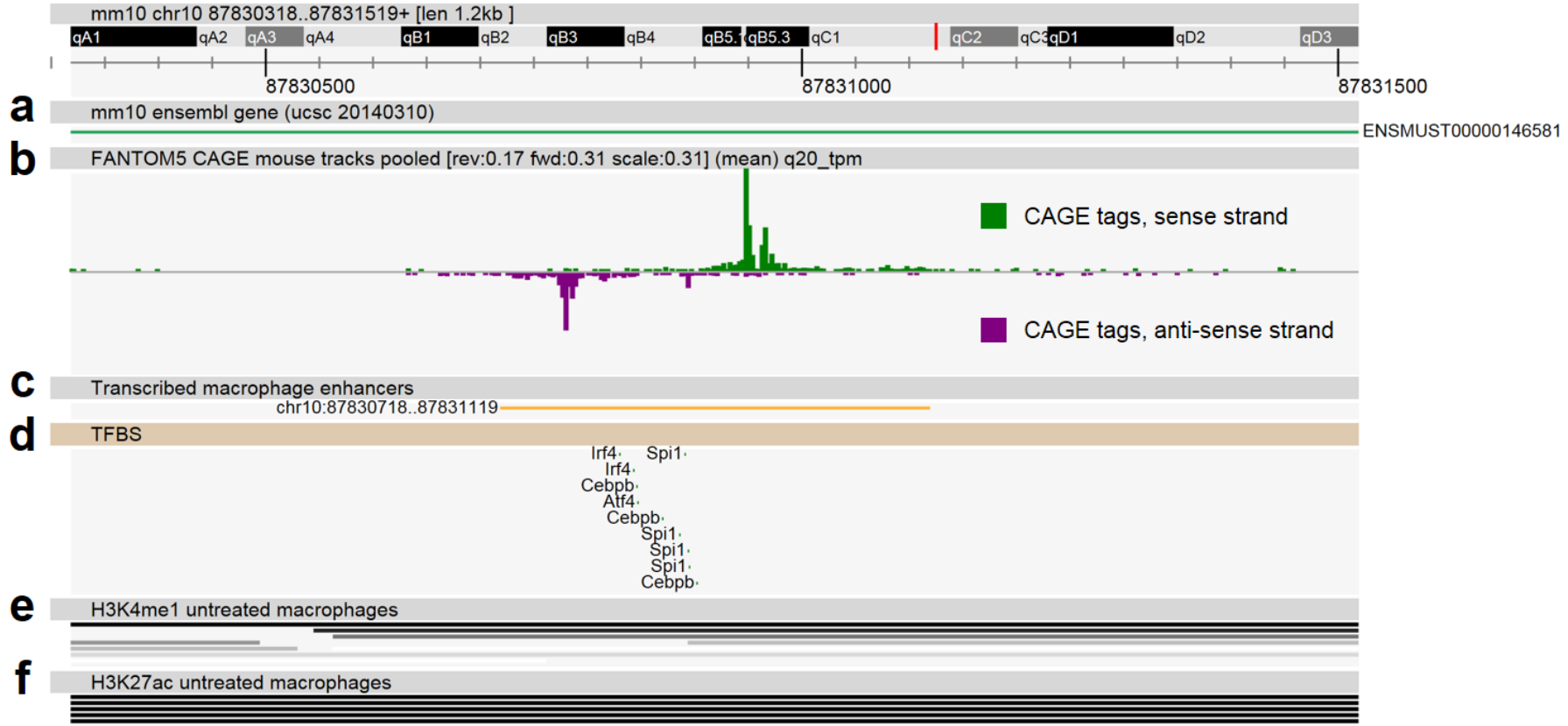

Figure 3.18. M(IL-4/IL-13) marker enhancer associated with Igf1 gene. ZENBU genome browser view shows the enhancer and 400 bp flanking regions. The enhancer is characterised by macrophage-specific eRNA expression; see also **Figure 3.17**. **a** The enhancer is located in antisense RNA Igflos. **b** CAGE signal in 184 macrophage samples, split by strand. **c** Enhancer region. **d** Summits of transcription factor binding sites; based on ChIP-seq data that were used for TFBS over-representation analysis, see 3.6.9. **e, f** Significant ChIP-seq peaks for histone marks that were used to define ChIP-seq-based enhancers (Ostuni et al., 2013).

3.2.6. Transcription factor binding sites are enriched in enhancer regions

To investigate whether our enhancer sets were enriched for known transcription factor binding sites (TFBSs), we performed an over-representation analysis of experimentally determined protein binding sites established through ChIP-seq (see 3.6.9) (Garber et al., 2012; Yue et al., 2014). The sets of macrophage-specific and non-macrophage-specific enhancers were both enriched for binding sites of general factors (p300, Tbp), as well as a range of TFs with well-established roles in macrophages, such as macrophage lineage-determining factor Spi1 (PU.1) (Ghisletti et al., 2010; Heinz et al., 2010), Cebpb, required for macrophage activation (Ruffell et al., 2009), and Rela, regulating inflammatory genes (Saliba et al., 2014) (**Table 3.3**). Interestingly, TFBSs for Spi1 overlapped 54.1% of macrophage-specific enhancers, but only 38% of non-macrophage-specific enhancers (overlap ratio of 1.4 for macrophage-specific/non-macrophage-specific enhancers). We observed similar and higher overlap ratios for other functionally important TFs in macrophages, including Stat1, Rela, Irf1, Junb, and Cebpb (Fontana et al., 2015; Martinez & Gordon, 2014; Ruffell et al., 2009; Saliba et al., 2014) (**Table 3.3**). Six out of the seven TFs in the upper part of the **Table 3.3**, except for Junb, showed macrophage-specific expression (see 3.2.3). Moreover, four TFs (Stat1, Irf1, Spi1, Cebpb) were significantly differentially expressed and up-regulated (see 3.6.10, FDR < 0.01, $\log_2$FC > 2) in our 184 macrophage samples when compared to the 744 FANTOM5 non-macrophage mouse samples (see **Table A2.1**, Appendix). Furthermore, we found that macrophage-specific enhancers associated with Rela (chr19:5931597..5931998, chr19:6157210..6157611) and Spi1 (chr2:91086328..91086729, chr2:91204688..91205089) also carried TFBSs of the corresponding TFs, suggesting the formation of enhancer-

mediated positive feedback loops, where a TF may induce its own enhancers. A genome browser view of one of these enhancers (chr2:91086328..91086729) shows a distribution of TFBSs and CAGE tags in the corresponding genomic region, which, notably, is located within an intron of the enhancer target gene Spil (**Figure 3.19**). Of note, comparison of the genome browser views shows that although all regions carry multiple TFBSs, the non-macrophage-specific enhancer in **Figure 3.14** can be characterised by higher occurrence of general enhancer-binding proteins Ctcf and p300 than the macrophage-specific enhancers in **Figure 3.18** and **Figure 3.19**, in agreement with the TFBS over-representation analysis results (**Table 3.3**).

Table 3.3. TFs regulating macrophage-specific and non-macrophage-specific enhancers. TFBSs statistically significantly over-represented in both sets and regulating at least 10% of either set were selected. Columns show TF name, average expression in macrophage samples in TPM, percentage of enhancers overlapping corresponding binding sites, and a macrophage-specific/non-macrophage-specific percentage ratio.

TF	mean TPM in macrophages	% Macrophage-specific enhancers	% Non-macrophage-specific enhancers	Ratio
Stat1	284.6	15.8	8.5	1.9
Rela	130.7	26.6	14.5	1.8
Atf4	329.4	25.5	14.3	1.8
Irf1	508.7	21.7	12.2	1.8
Junb	176.3	11.2	7.4	1.5
Spi1	599.9	54.1	38	1.4
Cebpb	647.9	48	34.8	1.4
Fosl1	4.7	8.2	10.2	0.8
Usf1	55.3	9	11.6	0.8
Bhlhe40	86.3	17.4	22.8	0.8
Ets1	5	25.2	33.6	0.8
Myc	26.8	11.9	16.9	0.7
Ep300	28.6	31.7	46.3	0.7
Max	90.1	14.8	23.9	0.6
Tbp	30.8	16	26.5	0.6
Tal1	14.6	7	11.6	0.6
Rad21	43.9	9.4	16.7	0.6
Mxi1	32.9	7.9	14.5	0.5
Tcf12	6.8	6.9	12.7	0.5
Sin3a	19.8	9.3	18.8	0.5

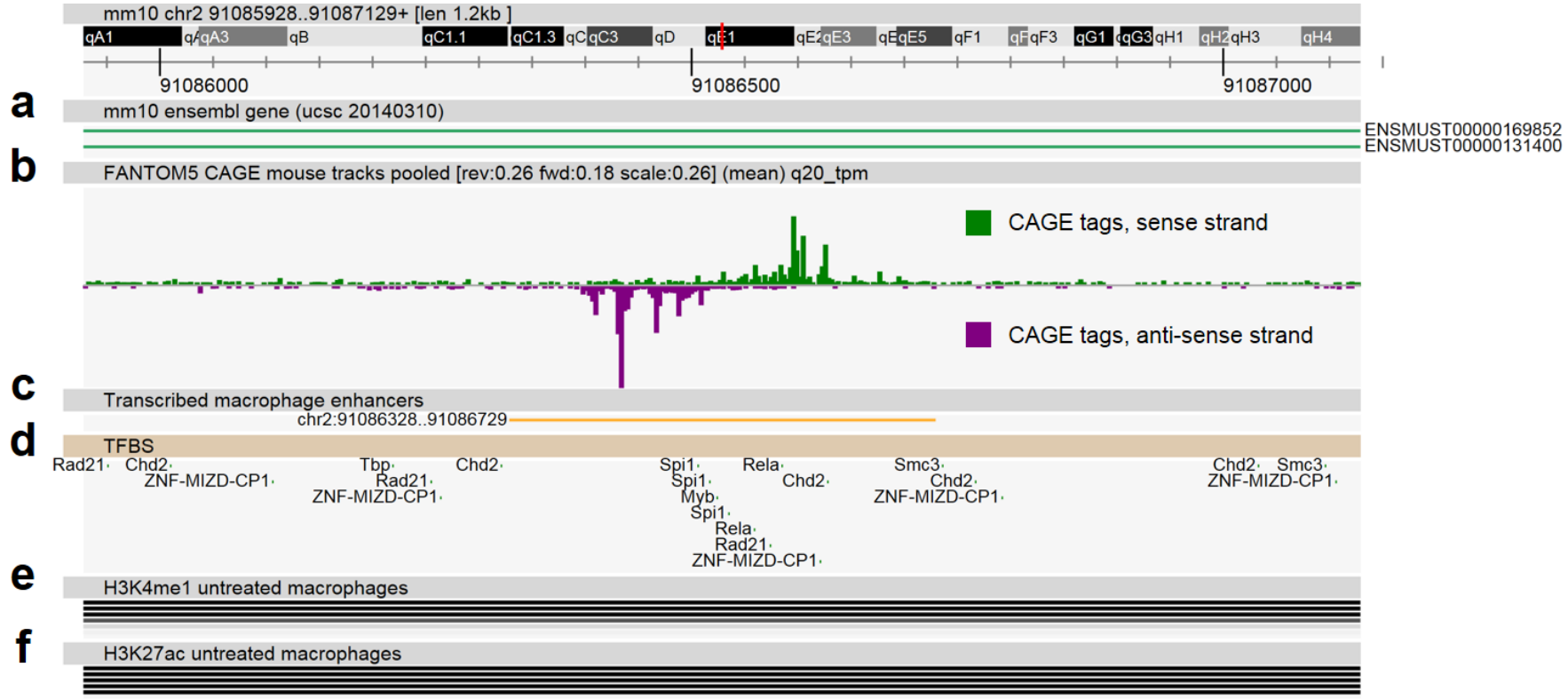

Figure 3.19. Macrophage-specific enhancer associated with Spil gene. ZENBU genome browser view shows the enhancer and 400 bp flanking regions. **a** The enhancer is located in an intron of its target gene Spil. **b** CAGE signal in 184 macrophage samples, split by strand. **c** Enhancer region. **d** Summits of transcription factor binding sites; based on ChIP-seq data that were used for TFBS over-representation analysis, see 3.6.9. **e, f** Significant ChIP-seq peaks for histone marks that were used to define ChIP-seq-based enhancers (Ostuni et al., 2013).

The E1 and E2 stimuli-responsive enhancer sets were enriched for TFBSs of known macrophage TFs including Spi1, Cebpb, Rela, and Irf and Stat families (Martinez & Gordon, 2014; Taniguchi, Ogasawara, Takaoka, & Tanaka, 2001; Tugal, Liao, & Jain, 2013) (**Table 3.4**). Interestingly, TFBSs of Stat1, Rela, and Irf1, involved in classical macrophage activation (Martinez & Gordon, 2014; Roy, Guler, et al., 2015), overlapped a higher percentage of E1 enhancers as compared to E2 and macrophage-specific enhancers (**Table 3.4**). For instance, Irf1 TFBSs overlap 21.7% of macrophage-specific enhancers, 26.7% of E2 but 44.3% of E1 enhancers. In addition, Stat1 and Irf1 were deemed M(IFN-γ)-responsive, and were significantly differentially expressed and up-regulated (FDR < 0.01, $\log_2$FC > 1) in M(IFN-γ) when compared to either control or M(IL-4/IL-13) macrophages. Taken together, these results provide an additional layer of support for our regions as functionally important macrophage enhancers and implicate key macrophage TFs in modulating their activity. These findings further reflect that enhancers are selectively activated depending on the transcriptional machinery involved in the cellular response.

Table 3.4. TFs with binding sites enriched in both E1 and E2 enhancer sets. Columns show TF name, average expression in M(IFN-γ) and M(IL-4/IL-13) macrophages in TPM, percentage of enhancers overlapping corresponding binding sites, and a M(IFN-γ)/M(IL-4/IL-13) ratio.

TF	mean TPM in M(IFN-γ)	% enhancers in M(IFN-γ)	mean TPM in M(IL-4/IL-13)	% enhancers in M(IL-4/IL-13)	Ratio
Stat1	726.3	40.9	218.6	22.9	1.8
Irf1	1345.4	44.3	426.7	26.7	1.7
Ets1	1.4	39.1	7	25.2	1.6
Jun	74.3	14.8	70	9.9	1.5
Rela	131.6	42.6	102.8	29.8	1.4
Atf4	277.3	33.9	208.3	27.5	1.2
Junb	122	13	99.7	13	1.0
Irf4	2.3	13	18.7	13.7	0.9
Spi1	766.3	52.2	681.7	56.5	0.9
Cebpb	424.6	51.3	262.9	59.5	0.9
Atf3	233.9	9.6	242.9	12.2	0.8

3.3. Discussion

In this study, we investigated the transcribed enhancer landscape in mouse BMDM and its dynamic changes during M(IFN-γ) and M(IL-4/IL-13) activation. Using CAGE data combined with ChIP-seq, we identified 8,667 actively transcribed enhancers forming 64,891 regulatory associations with protein-coding gene promoters in mouse BMDM. We highlighted tissue and stimuli specificity of both enhancers and their regulatory interactions. The enhancer-gene interactome established here supports a model of additive action of enhancers (Chepelev et al., 2012; Shlyueva et al., 2014), with higher gene expression concomitant with higher numbers of associated enhancers. Moreover, we observed a shift towards stronger enrichment for signalling pathways important for macrophage immune function in genes associated with many enhancers. Cytokine stimulation had a striking influence on enhancer transcription, which highlights the importance of enhancers in macrophage activation. In addition, we inferred potential macrophage activation marker enhancers. Finally, we find that binding sites of inflammatory TFs are enriched in enhancer regions, proposing a link between the response to stimuli and enhancer transcriptional activation.

Several studies have previously reported on enhancer landscape in mouse macrophages. Different populations of tissue macrophages were shown to be highly heterogeneous and to possess distinct sets of active enhancers, as defined by ChIP-seq profiling of histone modifications (Gosselin et al., 2014; Lavin et al., 2014). A few studies used ChIP-seq experiments to uncover enhancers that were established in macrophages *de novo* in response to a range of stimuli (Kaikkonen et al., 2013; Ostuni et al., 2013). In contrast to previous studies, we combined two complementary data types, transcriptomic (CAGE-derived) and epigenomic (ChIP-seq-derived, profiled by Ostuni et al.) data, to infer

more reliable transcribed active enhancers in mouse BMDM. We found a good overlap with three previous studies in mouse macrophages, but uncovered many novel enhancers, which can be explained by differences in the approaches used.

Ostuni et al. (2013) separated macrophage enhancer regions into different enhancer classes based on the enhancer response to a range of stimuli. Of their enhancers carrying H3K27ac active enhancer mark in naïve macrophages, 31% were found to be transcribed in our study. Of the poised not activated ChIP-seq-based enhancers, only 7.1% showed transcriptional activity in our set of 42,470 mouse enhancers. Finally, most of our CAGE-based enhancers overlapped regions carrying H3K27ac active mark either before or after stimulation. These observations support the idea of enhancer transcription being associated with histone mark-based active states of enhancers.

Importantly, our analysis extended beyond identification of enhancers and characterisation of their nearest genes. Here, instead of a widely used linear proximity-based approach (Andersson et al., 2014; Arner et al., 2015; De Santa et al., 2010), we employed TAD data to infer enhancer-gene associations. Accumulating evidence suggests that many enhancers regulate distal genes, bypassing the nearest promoter (G. Li et al., 2012; Lupianez et al., 2016). At the same time, TADs have emerged as units of chromatin organisation that favour internal DNA contacts (Rocha et al., 2015), and the majority of characterised interactions between enhancers and target promoters occur within the same TAD (Lupianez et al., 2016; Rocha et al., 2015; Symmons et al., 2014). Hence, our TAD-based approach enriched with correlation-based filtering enabled us to establish a more reliable mouse BMDM enhancer-gene interactome. Interestingly, we report higher correlation of expression in enhancers and promoters located closer to each other, which is a contradictory observation, given the above mentioned ability of enhancers to bypass the closest promoters.

Our interactome covers 8,667 actively transcribed enhancers. Of these, 70% overlap RNAPII ChIP-seq peaks in untreated mouse macrophages (Ostuni et al., 2013). Our enhancer regions show significant enrichment for binding sites of histone acetyltransferase p300, an enhancer-associated marker (Visel et al., 2009), and known inflammatory TFs. Hence, the regions identified here show a range of known enhancer properties, generally supporting our approach. Of our BMDM enhancers, 39.8% overlap a set of *cis*-regulatory elements identified in 19 non-macrophage mouse tissues (Shen et al., 2012) and most of the active enhancers show macrophage-specific eRNA expression, in line with known tissue specificity of enhancers (Kieffer-Kwon et al., 2013; Romanoski et al., 2015; Shen et al., 2012). In another recent study, a Capture Hi-C approach was employed to identify enhancers and their target promoters in mouse foetal liver cells and embryonic stem cells (Schoenfelder et al., 2015). Even though enhancers and enhancer-promoter interactions are known to be highly tissue specific, their data still support 24.8% of our 64,891 E-P pairs.

Recent reports suggested that genes regulated by multiple enhancers were higher expressed than those regulated by a single enhancer, proposing that enhancers might contribute additively to the expression of their target genes (Chepelev et al., 2012; Shlyueva et al., 2014). In support of this, we observed a steady increase of gene expression concomitant with increasing numbers of associated enhancers, with the genes not associated with any enhancers showing the lowest overall expression. A study of 12 mouse tissues has reported the enrichment for tissue-specific functions in genes associated with enhancers that transcribe eRNAs as compared to genes associated with non-transcribed enhancers (Cheng et al., 2015). Another study recently showed that genes that did not interact with distal enhancers were enriched for housekeeping genes and also suggested that cell-specific genes were extensively controlled by *cis*-regulators (Jin et al., 2013). We

showed in this study that genes associated with many enhancers were more enriched for macrophage-related functions as compared to genes associated with only few or no enhancers. This finding might reflect a more fundamental principle of genome organisation and evolution, such as the importance of multiple enhancers for fine-tuned and redundant control of cell specialisation and cell-specific responses. Indeed, according to a recent study, enhancer redundancy prevents deleterious consequences of loss-of-function mutations in individual enhancers (Osterwalder et al., 2018).

Previous studies revealed stimuli-specific epigenomic changes in enhancer regions in mouse macrophages and introduced a concept of stimuli-specific enhancer activation (Kaikkonen et al., 2013; Ostuni et al., 2013). In our study, we focused on enhancers and genes that responded to the stimuli with increased expression in order to further investigate this phenomenon. Notably, many stimuli-responsive genes were associated with stimuli-responsive enhancers, highlighting the importance of enhancer regulation in macrophage activation. As expected for such a cell-type-specific process as macrophage activation, most of the responsive enhancers showed macrophage-specific eRNA expression, and genes were enriched for macrophage-specific functions. In addition, our study suggests stimuli specificity of enhancer-gene regulatory associations in macrophages.

As an important example, we assessed 20 and 26 marker genes of classically and alternatively activated macrophages to characterise their enhancer regulation (Gordon & Martinez, 2010; Jablonski et al., 2015; Martinez & Gordon, 2014; Mosser & Edwards, 2008; Murray & Wynn, 2011). Of those, seven markers (Ccl20, Fpr2, Ido1; Chi3l3, Chi3l4, Alox12e, Chia) were not expressed in our data. For a total of 16 marker genes, we identified associated enhancers. Moreover, for 11 of them we found enhancers that might regulate these genes specifically in M(IFN-γ) or M(IL-4/IL-13) stimulation. Hence, these enhancers

present new potential markers for a particular macrophage activation status. Seven additional marker genes, identified as stimuli responsive, were not associated with any stimuli-responsive enhancer (Gpr18, Il12b, Il6, Inhba in the G1' set; Il27ra, Klf4, Myc in the G2' set). The remaining marker genes were not deemed stimuli-responsive. Of those, classically activated macrophage markers Il1b, Cd86, Marco, and Il23a and alternatively activated macrophage markers Mmp12, Tgm2, Clec4a2, Stab1, Fl3a1 were associated with at least one enhancer in macrophages. Ccr7, Retnla, Ccl17, Ccl22, Chi3l1, Cxcl13, and Ccl12 were not associated with any enhancers in macrophages.

We observed a particular genomic distribution of potential marker enhancers associated with Egr2 and Igf1 marker genes in M(IL-4/IL-13), which suggested that these regulatory DNA regions might represent super or stretch enhancers. A recent study investigated stretch enhancers in human cells and proposed that such extended regions could serve as molecular runways to attract tissue-specific TFs and focus their activity (Parker et al., 2013). Similarly to Parker et al. (2013), potential stretch enhancer regions identified here were associated with cell-type-specific genes and were demarcated by broad H3K27ac signals, specifically higher enriched in M(IL-4) as compared to M(IFN-γ) and untreated macrophages. Therefore, we propose that stretch enhancers might be involved in the regulation of macrophage activation. However, further studies are required to investigate this phenomenon in more detail.

Our approach inferred M(IFN-γ)- and M(IL-4/IL-13)-responsive enhancers that were strongly enriched for TFBSs of known inflammatory TFs. These results are in line with previous reports in mouse macrophages. For example, Spi1 (PU.1) has been extensively studied as a crucial TF involved in macrophage differentiation and transcriptional regulation (Ghisletti et al., 2010). Moreover, Spi1 was deemed a pioneering or lineage-determining TF in macrophages, which defines enhancer regions and occupies many

enhancers in macrophages (De Santa et al., 2010; Ghisletti et al., 2010; Gosselin et al., 2014; Heinz et al., 2010). Furthermore, Heinz et al. (2010) suggested that collaborative action of Spi1 with Cebpb was required for the deposition of enhancer-associated chromatin marks. Ghisletti et al. (2010) reported enrichment for NF-kB (Rel) and Irf TFs in enhancers induced by LPS in mouse macrophages. Likewise, transcribed enhancers induced by LPS and IFN-γ stimulation showed enrichment for NF-kB/Rel, Irf, and Stat1 binding motifs (De Santa et al., 2010). Taken together, our results link enhancer activation to the transcriptional programme induced by IFN-γ and IL-4/IL-13 stimuli.

3.4. Limitations

The limitations regarding the identification of CAGE-based transcribed enhancers are naturally inherited from Chapter 2. Here, we used epigenomic data to compensate for those limitations, and to establish a high-confidence transcribed enhancer set. It is important to note, however, that data by Ostuni et al. (2013), although being profiled in mouse macrophages, does not represent a perfectly matching set due to a different range of macrophage stimuli.

TAD regions used in this study were derived from mouse embryonic stem cells (Dixon et al., 2012). Recent studies on chromosomal domains reported that TADs are well-conserved across tissues and even species (Dixon et al., 2012; Rocha et al., 2015). Nevertheless, the study could have been improved if TAD data for macrophages were available to us.

We used Spearman's correlation coefficient to select correlated promoters and eRNAs within TADs. For the macrophage interactome, we calculated the correlation in all 184 macrophage samples, and required the coefficient to be positive and significant with

FDR < 10^{-4}. We believe that these requirements resulted in high-confidence interactions. Given that enhancers are presumed to be very stimuli-specific, we chose to impose an additional selection criterion for M(IFN-γ) and M(IL-4/IL-13) macrophages. As there are only 16 samples in each of the corresponding stimulations, we did not require the correlation coefficient to be significant in this second filtering. The study could have been improved if the macrophage set included more biological replicates and time points. In addition, we have restricted our analyses to TAD-based *cis*-regulatory interactions only. Still, *trans*-regulatory interactions might exist but cannot be identified through our current methodology.

More reliable enhancer-target promoter interactions could have been inferred by using additional types of experimental data, such as Hi-C or ChIA-PET, that provide genome-wide snapshots of closely located or interacting genomic regions (G. Li et al., 2014; Lieberman-Aiden et al., 2009). However, these data were not available for mouse macrophages in general, and for M(IFN-γ) and M(IL-4/IL-13) macrophages in particular.

The TFBS analysis was limited to the set of 66 TFs profiled in non-macrophage cell types (see 3.6.9); hence, more macrophage-specific TFs might be involved in regulating our enhancer regions. This limitation, again, stems from the limited availability of high-throughput data in mouse macrophages. To overcome this limitation in Chapter 4, we predicted TFBSs in enhancers using known TF binding motifs.

3.5. Conclusions

In this study, we have established a genome-wide catalogue of enhancers and enhancer-promoter regulatory interactions in mouse BMDM. In contrast to previous studies of enhancer landscape in mouse macrophages, we focused on transcribed

enhancers and employed an improved method for identification of enhancer target genes, based on location within a TAD and correlation of expression. Hence, our study represents the most comprehensive analysis of transcribed enhancer activities in mouse macrophages to date and extends current knowledge of transcriptional regulation in macrophages in general and during activation in particular.

3.6. Materials and methods

3.6.1. Data

The CAGE data set, used in Chapter 2, includes 184 BMDM samples, that were profiled by our collaborators (Roy, Schmeier, et al., 2015). These samples were used here to construct a macrophage enhancer landscape and enhancer-gene interactome. BMDM samples were cultivated for 24 hours under five different conditions, including stimulation with IL-4, IL-13, a combination of IL-4 and IL-13, IFN-γ, and untreated control macrophages. At 24 h post stimulation, BMDM were either infected with *M.tb* or left non-infected as a control. **Table 3.5** shows number of biological replicates that were profiled with CAGE at each time point.

Table 3.5. BMDM samples. Rows indicate different cultivation conditions, columns show time points in hours post stimulation, numbers of biological replicates profiled at each time point are shown.

Cell lines \ Time points		Before infection, hours after stimulation						After infection, hours after stimulation			
		0	2	4	6	12	24	28	36	48	72
Non-stimulated	Non-infected	3		1	1	1	4	3	3	3	3
	Infected							3	3	3	2
IFN-gamma	Non-infected		3	3	3	3	4	3	3	3	2
	Infected							3	3	3	3
IL-4	Non-infected		2	2	3	3	4	3	2	3	3
	Infected							3	3	3	3
IL-13	Non-infected		3	3	3	2	3	3	3	3	2
	Infected							3	2	2	3
IL-4/IL-13	Non-infected		3	3	3	3	4	3	3	3	3
	Infected							3	3	3	3

To identify high-confidence macrophage enhancers and to build enhancer-promoter interactome, we used the whole set of 184 BMDM samples. To study macrophage activation, we used a subset of 184 BMDM samples profiled at time points up to 24 h post stimulation, which included samples stimulated with IFN-γ or a combination of IL-4 and IL-13, referred to as M(IFN-γ) and M(IL-4/IL-13), as well as untreated samples as controls.

3.6.2. Enhancer and promoter sets

Expression of protein-coding genes and their promoters was derived in Chapter 2. Here, we retained only promoters with expression of at least one TPM in 10% of the 184 BMDM samples. The resulting set included 24,449 promoters of 10,767 protein-coding genes.

Enhancer regions and eRNA expression levels were derived in Chapter 2; the initial set included 42,470 transcribed mouse enhancers and was further filtered as described in 3.6.3.

3.6.3. Identification of high-confidence BMDM enhancers

First, we selected enhancers with nonzero eRNA expression in at least 10% of the 184 BMDM samples, and deemed them transcribed in mouse BMDM; the remainder of the mouse enhancers were discarded. Second, we retained only transcribed enhancers with at least 1 bp overlap with enhancer regions inferred based on ChIP-seq profiling of H3K4me1 histone mark in mouse macrophages (Ostuni et al., 2013).

3.6.4. Enhancer-promoter interactome

First, we selected pairs of high-confidence BMDM enhancers and expressed BMDM promoters that were located entirely within the same TAD, as in Chapter 2 (Dixon et al., 2012). Second, for each of these pairs, a Spearman's correlation coefficient was calculated between expression levels of an eRNA and a promoter across the 184 macrophage samples. Pairs with positive correlation coefficient and FDR < 10^{-4}, Benjamini-Hochberg procedure (Benjamini & Hochberg, 1995), were selected. We considered an enhancer to regulate a gene if it was associated with at least one of the gene's promoters.

3.6.5. Identification of macrophage-specific genes and enhancers

Normalised TPM expression data were used to calculate a z-score for each of our 184 macrophage samples for each enhancer and gene by subtracting the mean and dividing by

the standard deviation of expression values of the same feature in 744 FANTOM5 non-macrophage mouse sample (see **Table A2.1**, Appendix), as in (Yao et al., 2015). Enhancers and genes with z-score > 3 (i.e. expressed more than 3 standard deviations above the mean of the non-macrophage samples) in at least 10% of the macrophage samples were deemed macrophage specific.

3.6.6. Identification of stimuli-responsive genes and enhancers in macrophages

We calculated a z-score for each of 16 M(IFN-γ) and 16 M(IL-4/IL-13) macrophage samples for each enhancer and gene by subtracting the mean and dividing by the standard deviation of expression values of the same feature in ten non-stimulated macrophage samples, similarly to the approach for identification of macrophage-specific features. Genes and enhancers with z-score > 3 in more than 25% of the corresponding samples were deemed stimuli responsive.

We imposed an additional filtering on enhancer-gene associations between stimuli-responsive genes and enhancers in M(IFN-γ) and M(IL-4/IL-13) macrophages. First, we selected associations between M(IFN-γ)- and M(IL-4/IL-13)-responsive enhancers and genes of all our BMDM interactome associations (those significant with positive correlation coefficient and FDR < 10^{-4}, as described in 3.6.4). Second, for these associations, we calculated correlation between eRNA and gene expression in the subset of either M(IFN-γ) or M(IL-4/IL-13) samples, respectively. Only enhancer-gene associations with a positive Spearman's correlation coefficient were retained for each stimulus.

3.6.7. Identification of marker enhancers in activated macrophages

We aimed to infer potential activation marker enhancers that regulate marker genes specifically during either M(IFN-γ) or M(IL-4/IL-13) activation. To identify marker enhancers in M(IFN-γ), we first selected enhancers which were deemed M(IFN-γ) responsive, but not M(IL-4/IL-13) responsive, and were associated with known M(IFN-γ) marker genes. Second, a z-score for each of 16 M(IFN-γ) samples was calculated using 16 M(IL-4/IL-13) samples as a background. Enhancers with z-score > 3 in more than 25% of M(IFN-γ) samples were deemed potential activation marker enhancers in M(IFN-γ). The same strategy was used to infer activation marker enhancers in M(IL-4/IL-13) macrophages.

3.6.8. Gene set enrichment analyses (GSEA)

KEGG pathway maps (Kanehisa & Goto, 2000) or GO biological process ontology (Ashburner et al., 2000) were used as sets of biological terms for GSEA. GO terms and associated genes were retrieved using the R package GO.db (Carlson, 2015). We used hypergeometric distribution to calculate the probability of obtaining the same or larger overlap between a gene set of interest and each biological term (Huang da, Sherman, & Lempicki, 2009). Derived p-values were corrected for multiple testing using Benjamini-Hochberg procedure (Benjamini & Hochberg, 1995). As a background, a set of 22,543 Ensembl protein-coding genes (version 75) was used (Flicek et al., 2011).

3.6.9. Transcription factor binding analysis

Transcription factor binding site (TFBS) data from ChIP-seq experiments in mice were obtained from ENCODE (Yue et al., 2014) and HT-ChIP (Garber et al., 2012). Raw sequencing data were mapped to the mm10 genome build for each tissue and cell type separately, and peaks were called using MACS2 (Zhang et al., 2008). TFBS summits with FDR < 10^{-4} were retained.

For over-representation analysis of TFBSs in enhancer regions, we used three different background sets: the whole set of identified transcribed mouse enhancers, the subset of enhancers not transcribed in macrophages, and a set of random genomic regions located within TADs excluding gaps, repeated sequences, Ensembl coding regions, and mouse enhancers identified here. Gap and repeated sequence regions were obtained from the UCSC Table Browser (Karolchik et al., 2004) on 1 August 2016 ("gap" and "rmsk" tables of mm10 database). Significantly over-represented TFBSs were selected based on empirical p-value < 0.01 from a Monte Carlo analysis of 1,000 trials calculated as described in (North, Curtis, & Sham, 2002). We retained only TFBSs which showed p-value < 0.01 when tested against all three background sets. The corresponding TF was required to be expressed in the macrophages samples.

3.6.10. Differential expression analysis

Differential gene expression analyses were performed using the exact test implemented in edgeR (M. D. Robinson et al., 2010) and the p-values were adjusted for multiple hypothesis testing using the Benjamini-Hochberg procedure (Benjamini & Hochberg, 1995).

3.6.11. Tools

All analyses made extensive use of the Shell scripting language and the R software (http://www.R-project.org/) with the Bioconductor packages (Gentleman et al., 2004). Most of the figures were generated with ggplot2 package for R (Wickham, 2009).

All genomic regions used in the present work were either mapped to mm10 mouse genome or were converted from mm9 genomic coordinates to mm10 using the liftOver programme (https://genome.ucsc.edu/cgi-bin/hgLiftOver). All analyses made extensive use of the BEDTools utilities (Quinlan & Hall, 2010), including tools for identification of overlapping intervals and generating random genomic intervals. Genomic regions were visualised in a circular layout using the Circos software (Krzywinski et al., 2009).

Chapter 4

Transcriptionally induced enhancers play important roles in macrophage response to tuberculosis infection

4.1. Overview

Tuberculosis (TB) remains a major public health threat and cause of death worldwide (Zumla et al., 2015). Macrophages are immune cells that compose the first line of an organism's defence against *Mycobacterium tuberculosis* (*M.tb*), the causative agent of TB (Ernst, 2012). Interactions between macrophages and *M.tb* define the infection outcome. The role of macrophage enhancers in regulating these interactions remains unexplored.

In this study, we made use of bone marrow-derived macrophage (BMDM) enhancer-gene interactome established in Chapter 3 and analysed its changes during *M.tb* infection with the following objectives:

1. Characterising the involvement of transcribed enhancers in the regulation of major gene expression changes in BMDM upon *M.tb* infection;
2. Identifying the roles of enhancers with the strongest transcriptional induction in the macrophage response to *M.tb*;
3. Identifying immune transcription factors that are involved in the regulation of induced enhancers;
4. Characterising enhancer regions that acquire transcriptional activity *de novo* upon *M.tb* infection.

4.2. Results

4.2.1. Transcribed enhancers mediate macrophage responses to *M.tb* infection

We analysed the host transcriptional response to *M.tb* infection using CAGE expression data from mouse BMDM profiled at 4, 12, 24, and 48 hours post infection (see 4.6.1). Non-infected control BMDM were profiled prior to infection (0 h) and at matched time points (4, 12, 24 and 48 h). First, we analysed overall gene expression changes and found that they were the strongest at 4 h post infection and declined with time (**Figure 4.1**). Half as many differentially expressed genes (DEGs) were detected at 12 h as at 4 h, and almost no genes were significantly differentially expressed (DE) at 24 or 48 h post infection (**Figure 4.1a**) (see 4.6.3). We combined the DEGs from all time points into two unique lists of 1,384 up- and 1,604 down-regulated DEGs for further analysis.

Using CAGE expression data, we identified actively transcribed enhancers and their target genes in mouse BMDM in Chapter 3. Here, we found that many of these enhancers

acquired higher eRNA expression in response to *M.tb* infection (**Figure 4.2a**). Moreover, enhancers associated with up-regulated DEGs in infected macrophages showed an increase in eRNA expression (**Figure 4.2b**). Hence, BMDM enhancers demonstrated an overall increase in transcriptional activity upon *M.tb* infection.

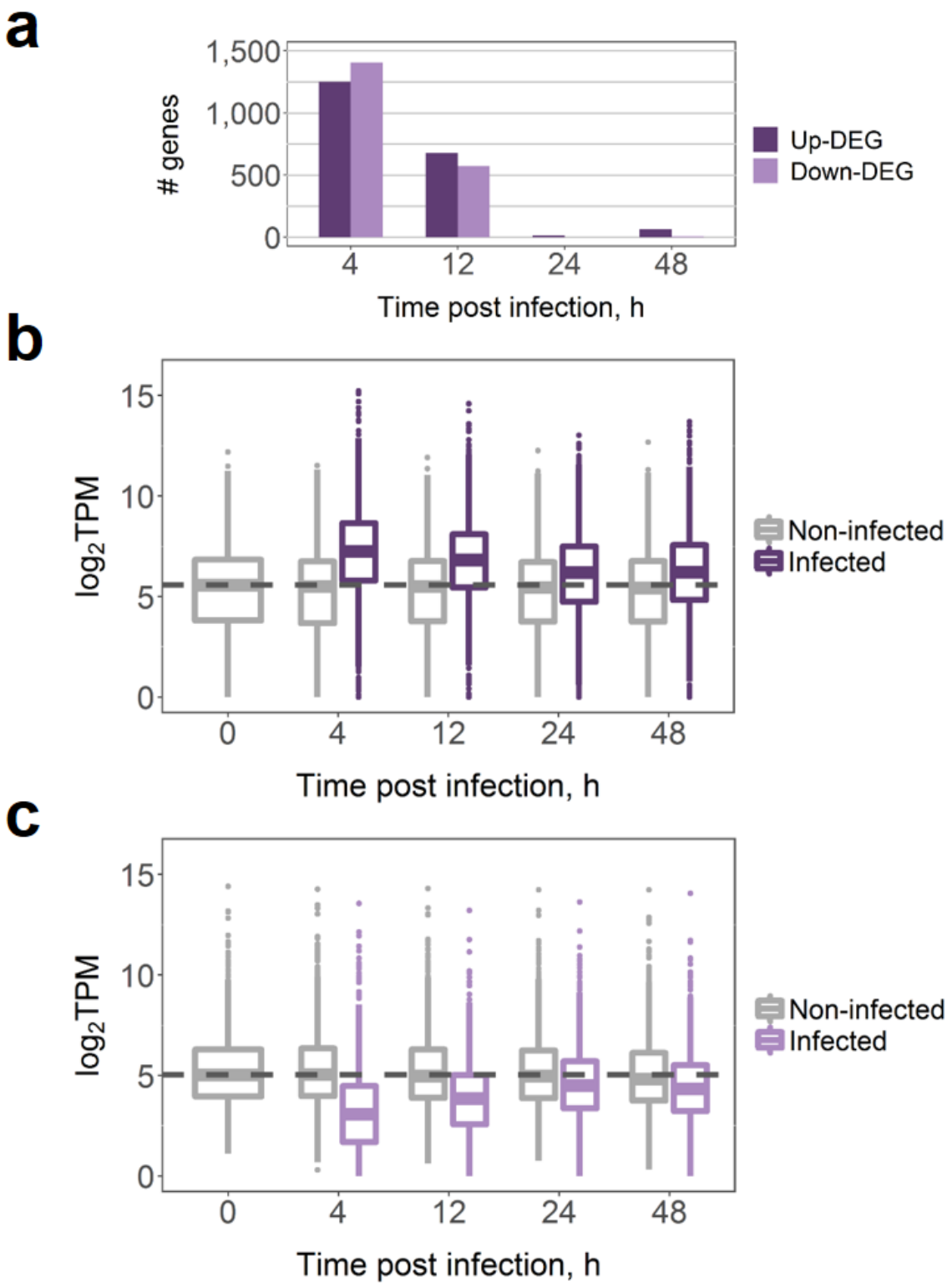

Figure 4.1. Genes show the strongest response to *M.tb* infection at 4 and 12 h post infection. **a** Numbers of differentially expressed genes (DEGs) in infected macrophages vs. macrophages prior to infection (0 h). **b** Expression of 1,384 up-regulated DEGs (DE at any time point). **c** Expression of 1,604 down-regulated DEGs (DE at any time point). In **b** and **c**, expression in TPM was averaged across replicates; dashed lines show median gene expression prior to the infection.

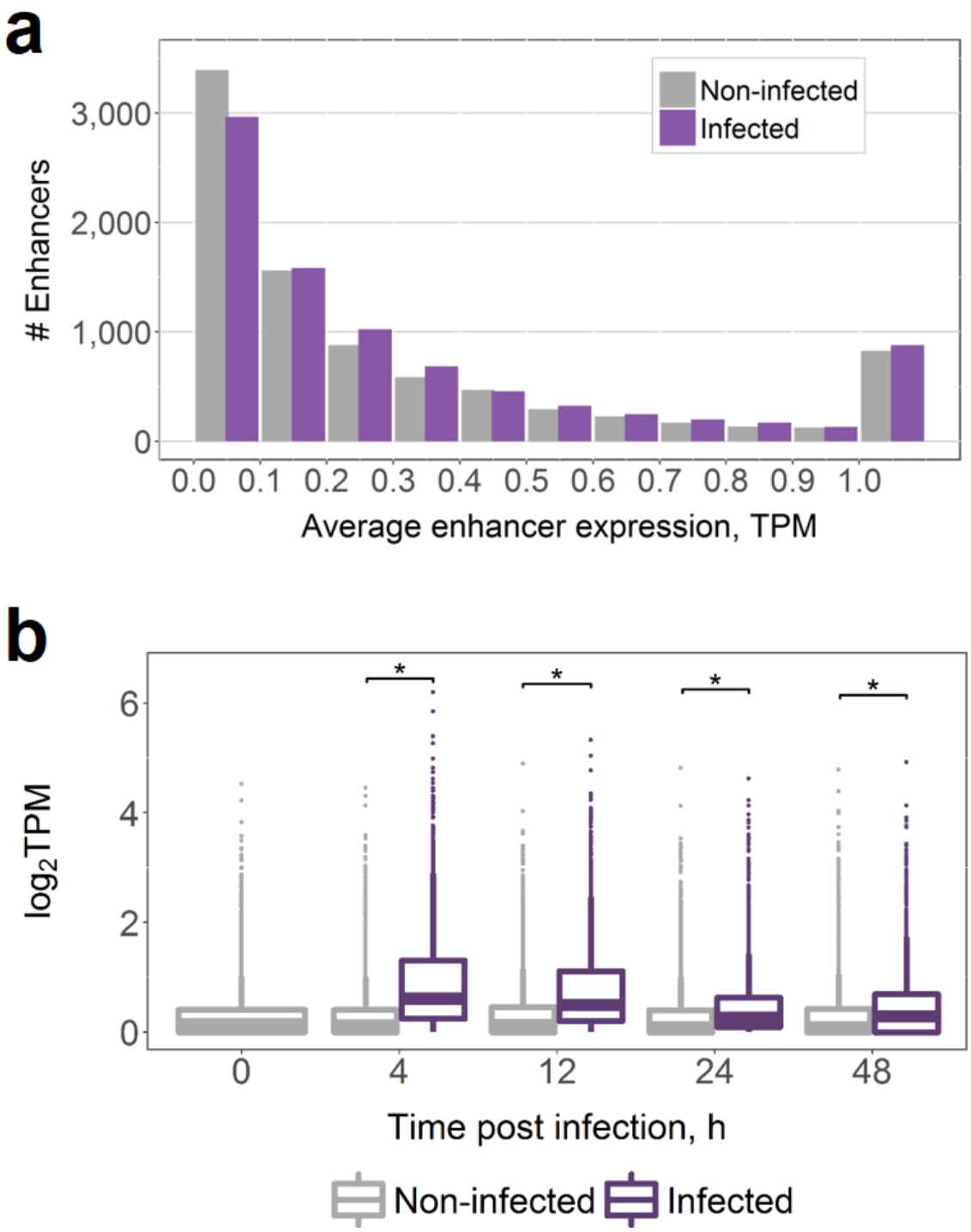

Figure 4.2. Many enhancers respond to *M.tb* infection with increased eRNA expression. a Expression of all 8,667 macrophage enhancer eRNA in non-infected and infected macrophages; each bin includes the left edge. **b** Expression of 2,999 enhancer eRNA associated with up-regulated DEGs; expression in TPM was averaged across replicates, (*) indicate paired two-sided Wilcoxon signed-rank test p-value < $2.2*10^{-16}$.

We investigated the differences in the enhancer repertoire between DEGs and non-DEGs to uncover the role of enhancers in the infection response. Genes with no transcribed enhancers composed 36.4% of up-regulated DEGs, whereas this percentage was significantly higher at 41.1% for down-regulated DEGs (Fisher's exact test two-sided p-value 0.008467) (**Figure 4.3a**). Furthermore, 41% of up-regulated DEGs, but only 34% of down-regulated DEGs were associated with more than two transcribed enhancers (Fisher's exact test two-sided p-value $7.9*10^{-5}$) (**Figure 4.3a**). Finally, non-DEGs had the highest percentage of genes with no transcribed enhancers (45%) and the lowest percentage of genes with more than two enhancers (31%) (**Figure 4.3a**). Hence, transcribed enhancers play a prominent role in up-regulation of protein-coding genes in response to *M.tb* infection.

Previously we have shown that regulation by many transcribed enhancers in BMDM was a concomitant of higher gene expression and tissue-specific function (Chapter 3). Here, we focused on up-regulated DEGs to uncover whether those genes with many enhancers showed similar properties. Indeed, as before, we observed higher expression levels in genes with more enhancers in infected macrophages (**Figure 4.3b**). Gene set enrichment analysis (GSEA, see 4.6.7) showed that DEGs with no transcribed enhancers in infected macrophages were significantly enriched in only five KEGG pathway maps with FDR < 0.05 (**Figure 4.3c**). In contrast, genes associated with more than two enhancers were significantly enriched in as many as 92 maps, and showed much stronger enrichment for more specific infection-related pathways (**Figure 4.3d**) when compared to genes with no enhancers (**Figure 4.3c**). Of note, while the 'Tuberculosis' KEGG pathway map is not shown in **Figure 4.3d** among the top 15 maps with the lowest FDR, it was nevertheless enriched with FDR = $2.4*10^{-7}$ and includes 20 DEGs associated with more than two enhancers, in contrast to only 12 genes and FDR = 0.04 for DEGs with no associated

enhancers (**Figure 4.3c**). The enrichment analyses point to the assumption that up-regulated DEGs without transcribed enhancers are functionally more diverse as opposed to those associated with more than two actively transcribed enhancers. Moreover, these results indicate that even within such a process-oriented set as the list of up-regulated DEGs, multiple enhancers are regulating the most highly expressed and functionally important genes. We repeated this analysis for all genes (as opposed to only DEGs) and their associated enhancers in infected macrophages and observed a similar trend (**Figure 4.4**), in agreement with the results of Chapter 3. In addition, we repeated GSEA for a selection of 500 genes with the highest expression in infected macrophages in each category, to avoid a size-related bias. The results in **Figure 4.5** indicate that the observed differences in functional enrichment persisted. Notably, among the top biological pathways in **Figure 4.5a,** we found three KEGG pathways of neurodegenerative diseases. It can be explained by the fact that most of the genes are shared between these pathways. Functionally, these genes are associated with mitochondrial dysfunction, and as many as 25 genes also map to the "Oxidative phosphorylation" KEGG pathway (see **Figure 4.5a**).

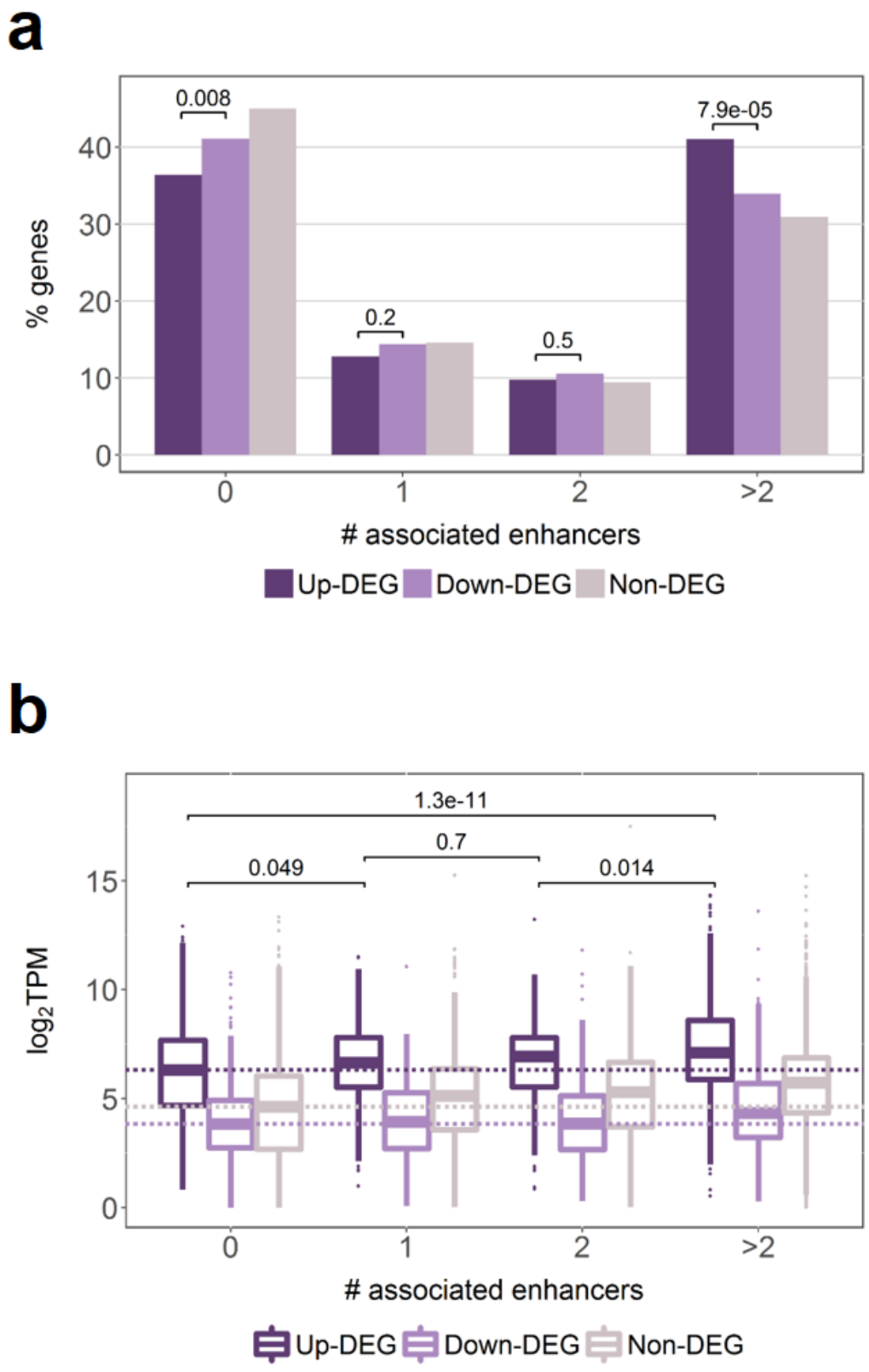

Figure 4.3. Continued on next page.

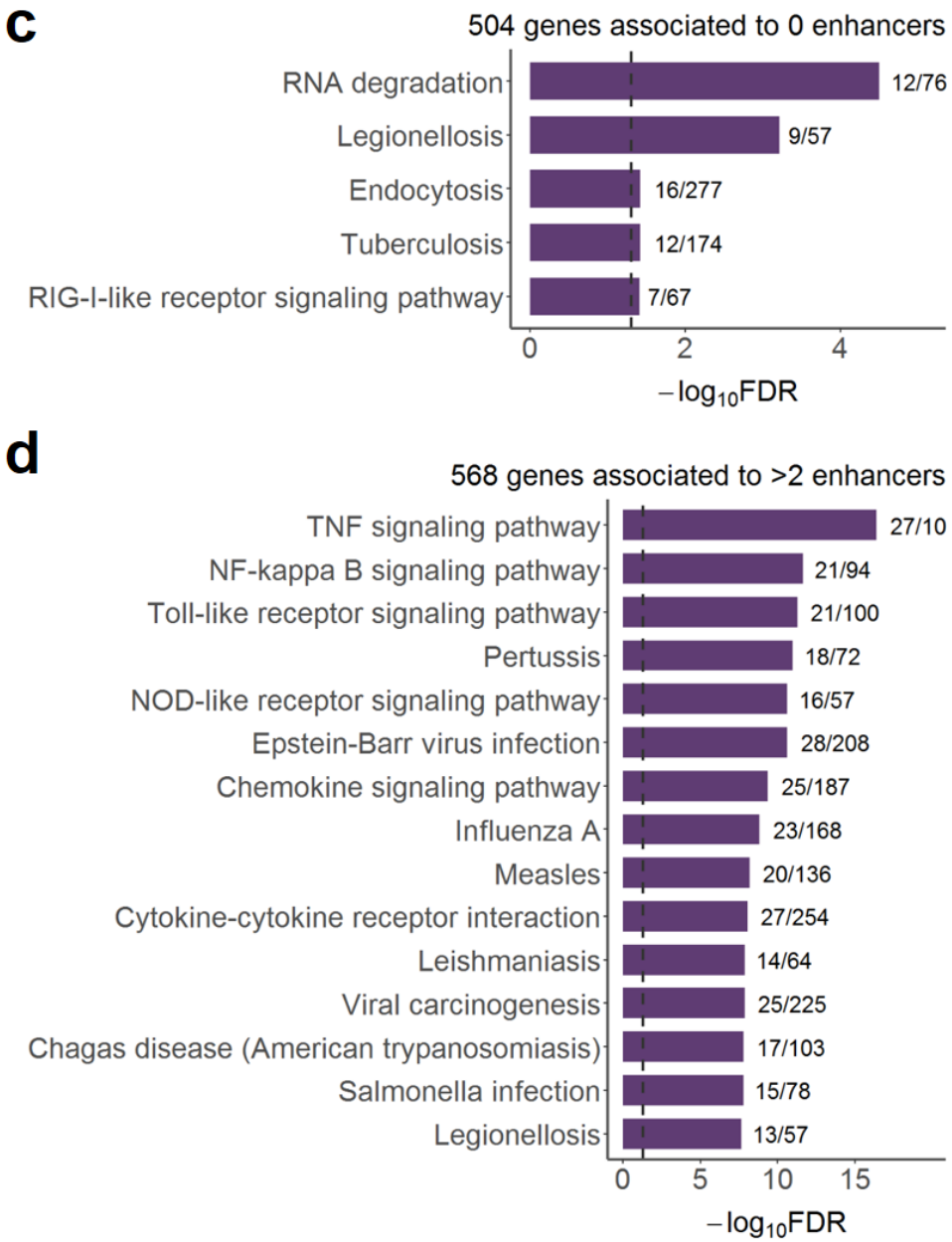

Figure 4.3. Enhancers mediate up-regulation of immune genes in macrophages upon *M.tb* infection. a Percentage of genes associated with different number of enhancers in infected macrophages; up- or down-regulated DEGs and non-DEGs are shown, numbers indicate Fisher's exact test p-values. **b** Expression of genes associated with different number of enhancers in infected macrophages; expression in TPM was averaged across infected samples, dashed lines show the median expression of genes not associated with any transcribed enhancer; numbers indicate Wilcoxon two-sided rank sum test p-values. **c** KEGG pathway maps significantly enriched for up-regulated DEGs with no associated transcribed enhancers, FDR < 0.05. **d** Top 15 KEGG pathway maps with the lowest FDR enriched for up-regulated DEGs associated with more than two transcribed enhancers. In **c** and **d,** next to the bars are the numbers of genes in the KEGG term covered by our gene list; dashed lines indicate FDR = 0.05.

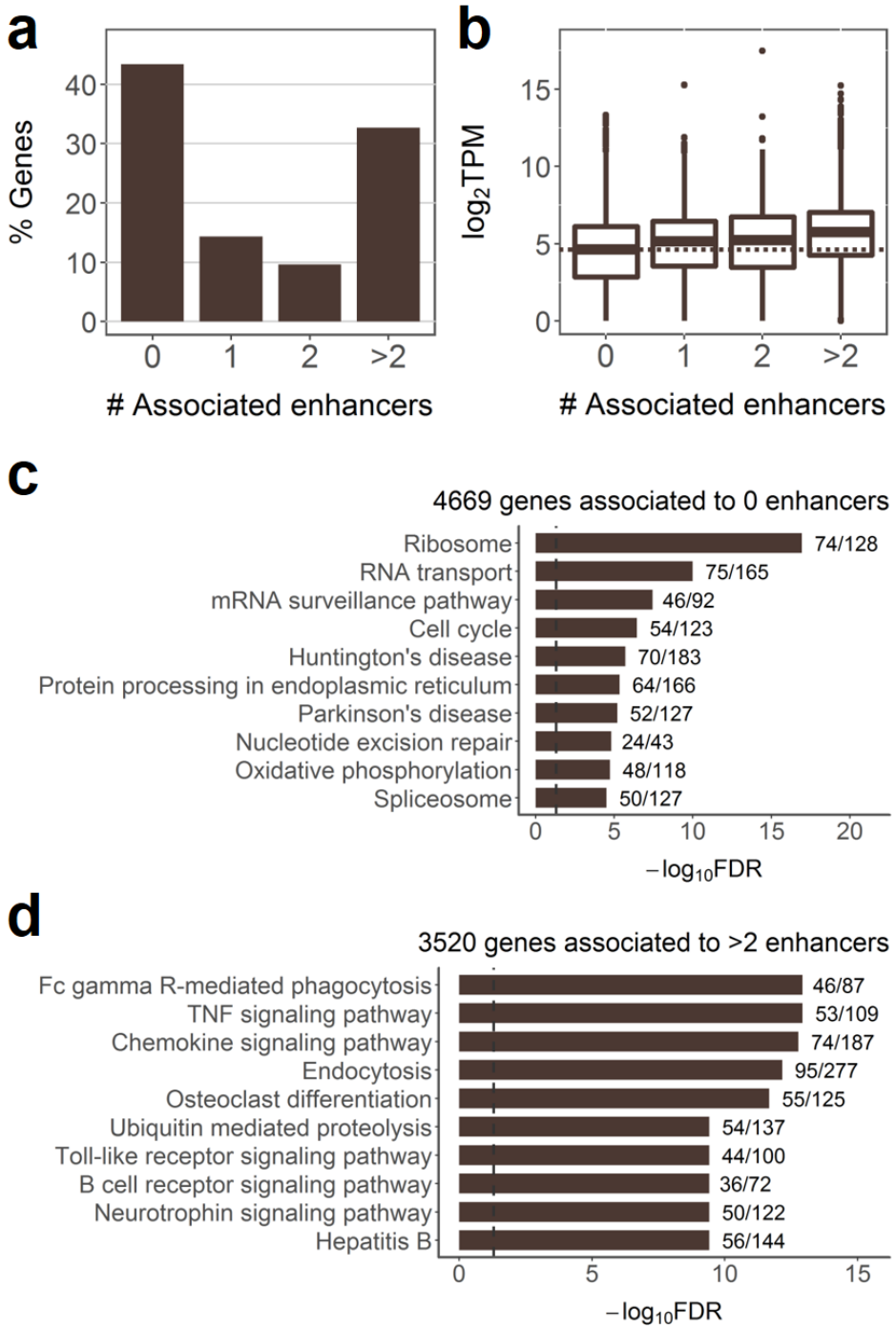

Figure 4.4. Higher number of associated enhancers is a concomitant of higher gene expression and immune functions in infected macrophages. a, b Percentage and expression of genes associated with different number of enhancers in infected macrophages; expression in TPM was averaged across infected samples, dashed line shows median expression of genes not associated with any enhancer. **c** KEGG pathway maps enriched for genes associated with no transcribed enhancers. **d** KEGG pathway maps enriched for genes associated with more than two transcribed enhancers. In **c** and **d,** top 10 maps with the lowest FDR are shown; next to the bars are the numbers of genes in the map covered by our gene list; dashed lines indicate FDR = 0.05.

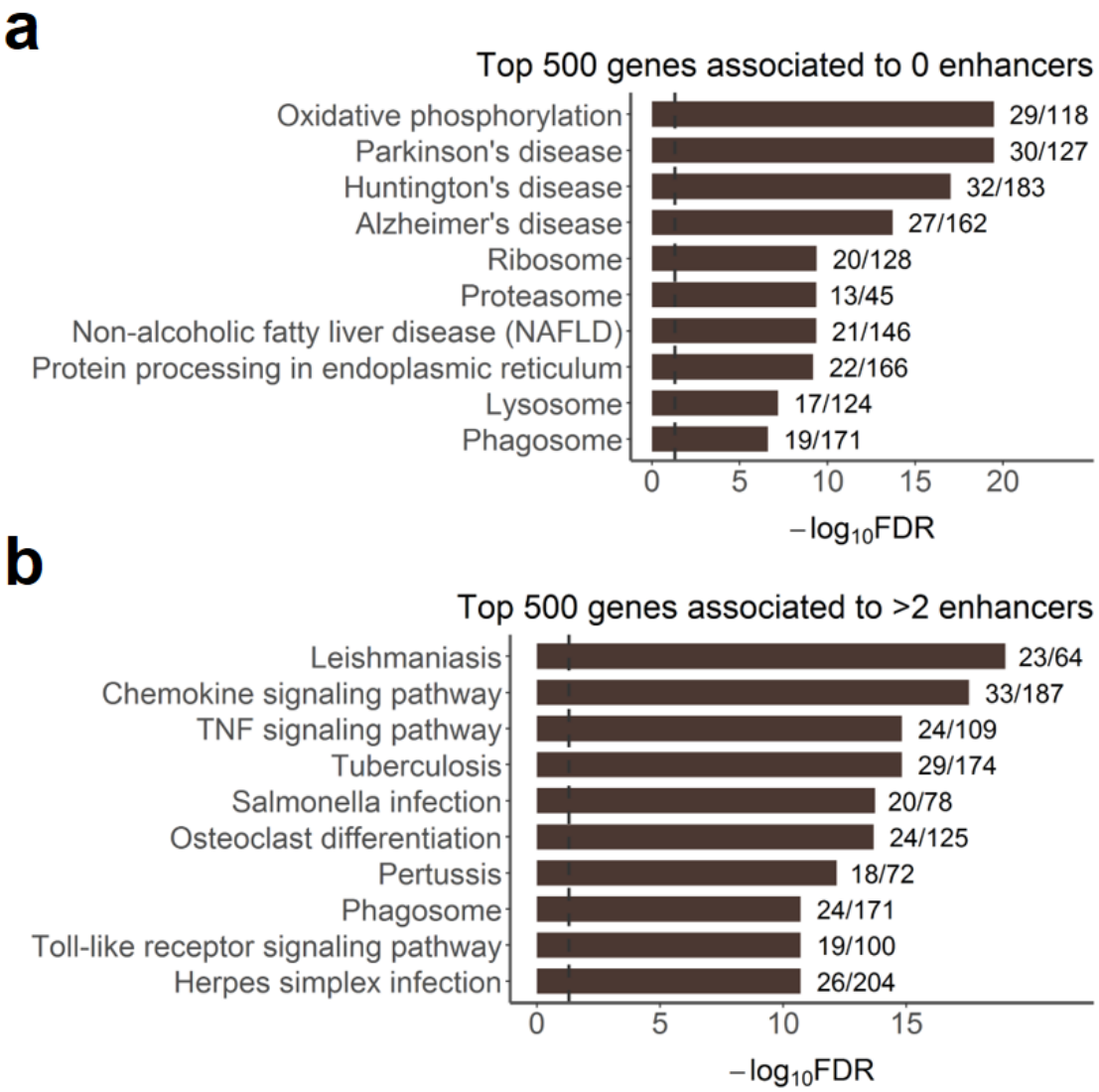

Figure 4.5. Functions of highly expressed genes associated with different number of enhancers in infected macrophages. Top 500 genes with the highest average expression in infected macrophages were selected among genes associated with no transcribed enhancers (in **a**) and genes associated with more than two transcribed enhancers (in **b**). Top 10 KEGG pathway maps with the lowest FDR are shown; next to the bars are the numbers of genes in the map covered by our gene list; dashed lines indicate FDR = 0.05.

We next compared our transcribed enhancers to a set of inflammation-sensitive macrophage super enhancers (SEs) (Hah et al., 2015). Super-enhancers (or stretch enhancers) have emerged as a sub-class of particularly potent enhancers, which are associated with higher levels of enhancer-specific histone marks and regulate key cell

identity genes (Pott & Lieb, 2015; Witte et al., 2015). Among 2,999 enhancers associated with up-regulated DEGs, 45.9% overlapped SE regions. This percentage was significantly lower at 30% for the remainder of our BMDM transcribed enhancers (as described in Chapter 3) (two-sided Fisher's exact test p-value < $2.2*10^{-16}$, odds ratio 1.98). Interestingly, of 880 up-regulated DEGs associated with transcribed enhancers, 477 were associated with enhancers overlapping SEs, and these DEGs showed a much stronger enrichment for immune-related functions, when compared to the remaining 403 DEGs for which none of their associated enhancers overlapped SEs (**Figure 4.6**).

Taken together, our findings indicate that the up-regulation of immune genes in BMDM upon *M.tb* infection is largely driven by transcribed enhancers. Comparison of the three subsets of up-regulated DEGs revealed the strongest enrichment for specific immune response pathways in up-regulated DEGs associated with SEs (**Figure 4.6b**) and the weakest enrichment in up-regulated DEGs not associated with any transcribed enhancers (**Figure 4.3c**), highlighting the functional importance of SEs in BMDM response to *M.tb* infection.

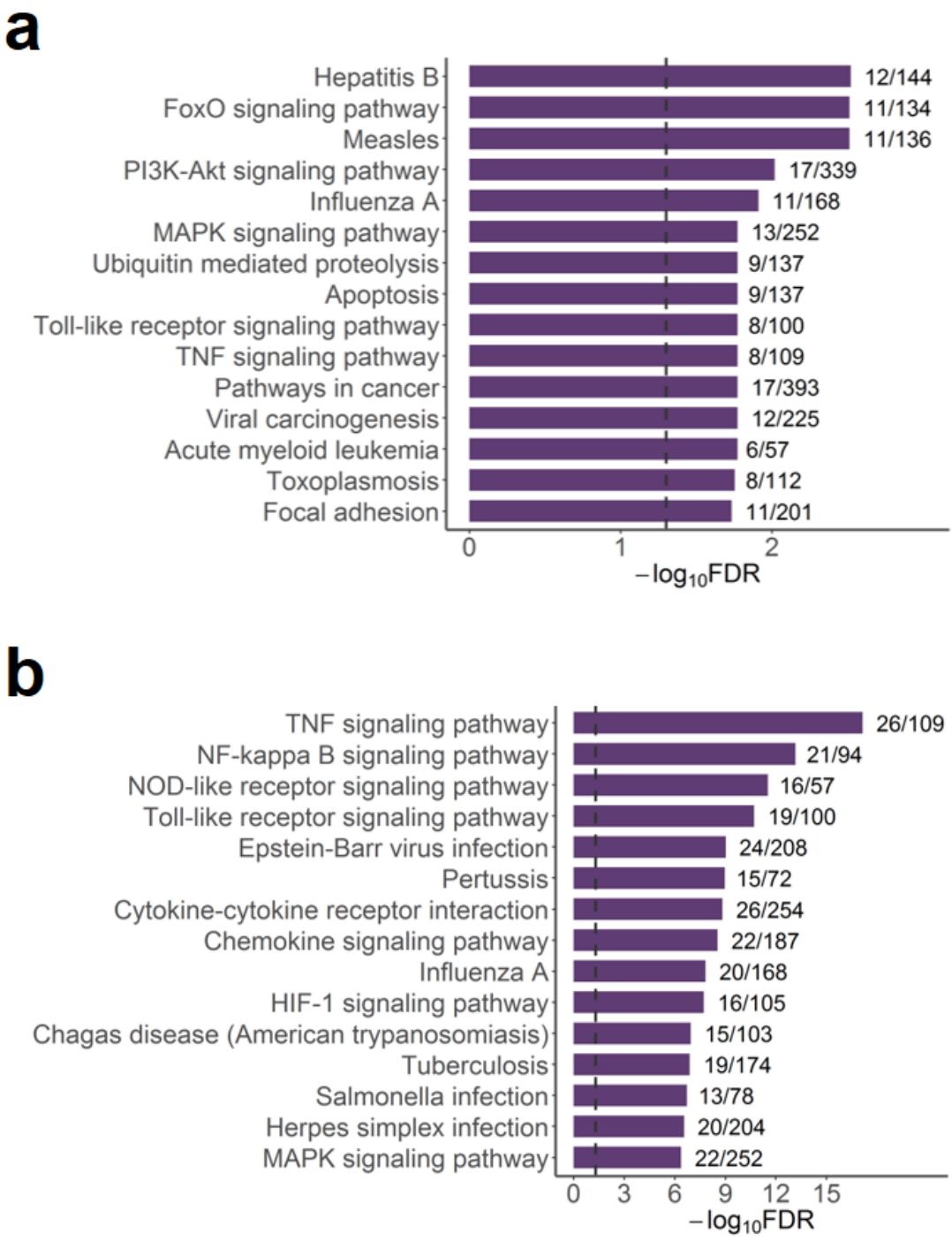

Figure 4.6. Up-regulated DEGs associated to super enhancers show more infection-specific functions. a KEGG pathway maps enriched for 403 genes associated with transcribed enhancers that do not overlap super enhancer regions. **b** KEGG pathway maps enriched for 477 genes associated with transcribed enhancers overlapping super enhancer regions. Top 15 maps with the lowest FDR are shown; next to the bars are the numbers of genes in the map covered by our gene list; dashed lines indicate FDR = 0.05.

4.2.2. Transcriptionally induced enhancers contribute substantially to the regulation of immune genes during *M.tb* infection

We further set out to investigate a subset of enhancers that targeted up-regulated DEGs and were themselves highly transcriptionally induced upon infection.

We focused on 809 DEGs that were associated to transcribed enhancers and up-regulated at 4 h post infection, because we observed the strongest transcriptional response upon infection at this time point. Of enhancers targeting these DEGs, we selected those with the highest eRNA expression at 4 h and its fold change as compared to 0 h, by requiring both these values to be in the upper quartiles of their corresponding distributions (see 4.6.4). The derived set of 257 enhancers (further referred to as induced enhancers) was associated with a total of 263 of 809 DEGs that were up-regulated at 4 h and associated with transcribed enhancers (**Figure 4.7**). We investigated expression of the induced enhancers in other mouse tissues available in FANTOM5 CAGE database (see **Table A2.1**, Appendix) (Forrest et al., 2014). Interestingly, we found that the set of enhancers showed the highest average and maximum eRNA expression, as well as the highest percentage of samples with nonzero eRNA expression in infected macrophages (statistically significant differences, with paired two-sided Wilcoxon signed-rank test p-value < $2.2*10^{-16}$, when infected macrophages were tested against each of the other tissues) (**Figure 4.8**). In addition, induced enhancers were over-represented in SE regions (Hah et al., 2015) when compared to the remainder of BMDM enhancers, with 60.7% of the induced enhancers overlapping SEs as compared to 34.7% of non-induced enhancers (two-sided Fisher's exact test p-value < $2.2*10^{-16}$, odds ratio 2.9). These findings indicate a high specificity of the induced enhancers to the BMDM *M.tb* infection response and highlight

the fact that they are likely key elements for driving the transcriptional responses of the macrophage host upon infection.

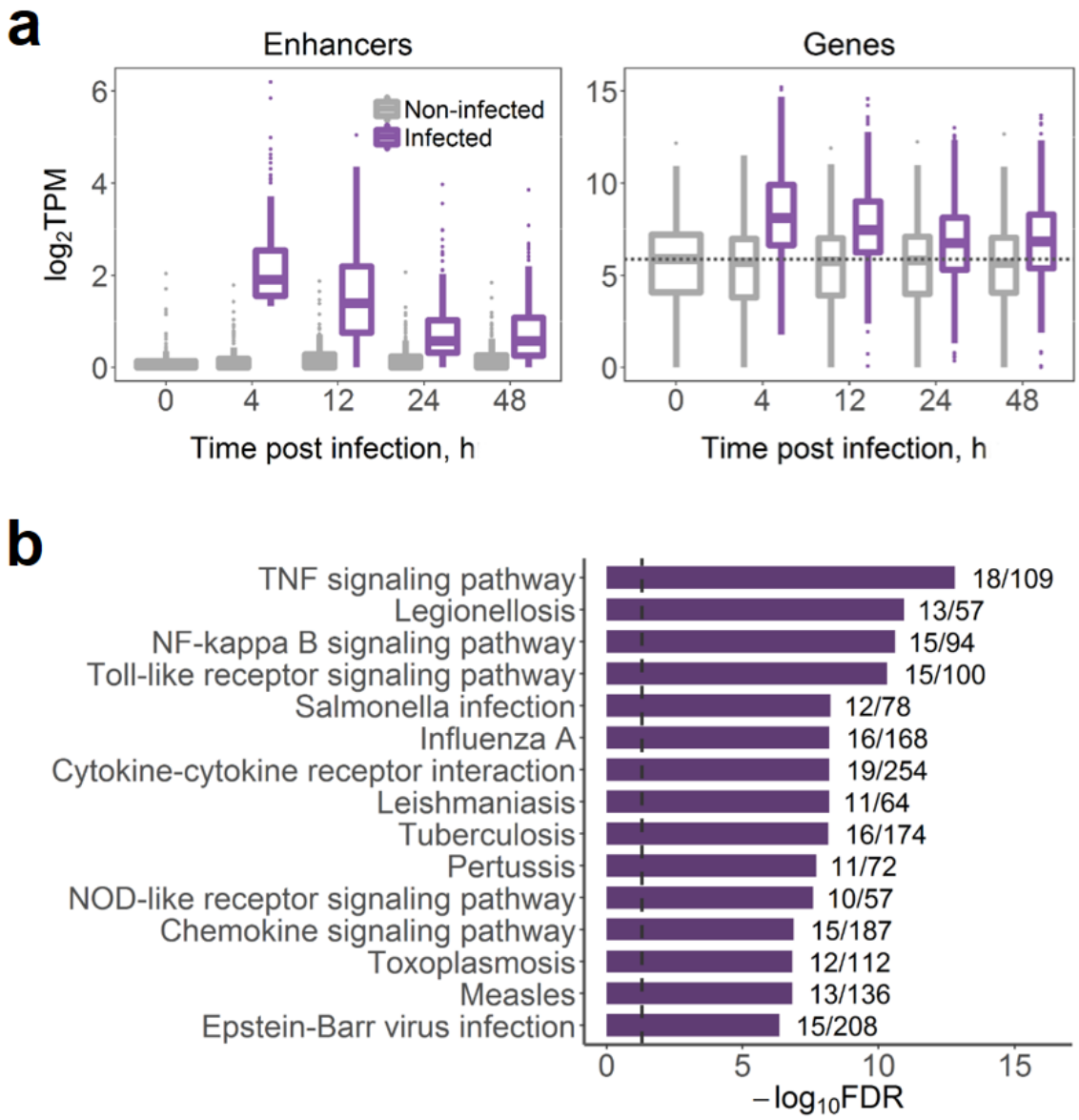

Figure 4.7. 257 induced enhancers associated with 263 DEGs up-regulated at 4 h. a Expression of enhancer eRNA and genes; dashed line shows median gene expression prior to the infection, expression in TPM was averaged across replicates. **b** Top 15 KEGG pathway maps with the lowest FDR enriched for the genes; next to the bars are the numbers of genes in the KEGG term covered by our gene list; dashed line indicates FDR = 0.05.

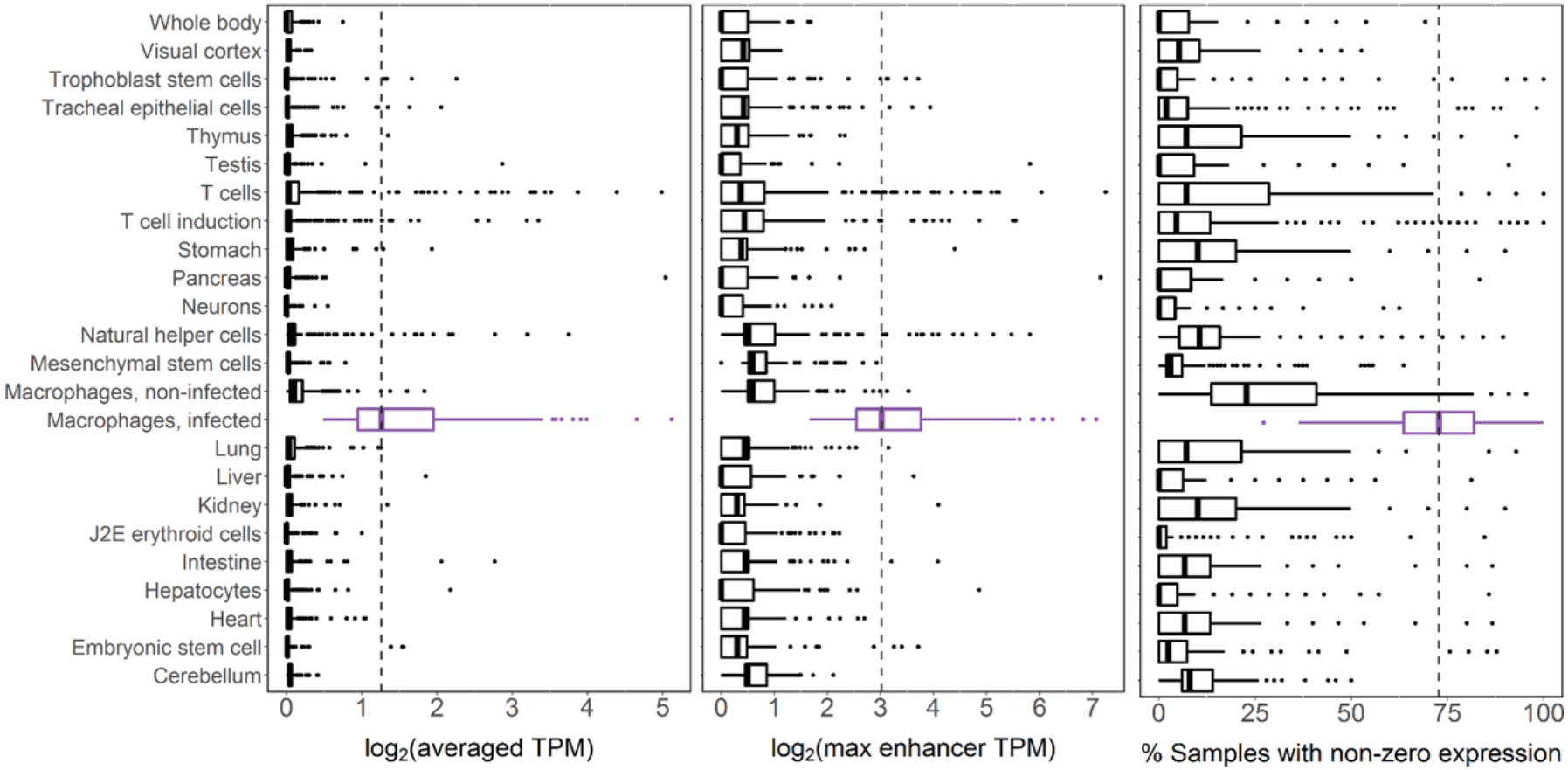

Figure 4.8. Expression of the induced enhancers in mouse tissues. Left panel: expression of each enhancer was averaged across tissue samples. Middle panel: maximum enhancer expression value in each tissue is used. Right panel: percentage of samples with nonzero expression was calculated for each enhancer in each tissue.

Next we investigated DEGs that were targeted by many induced enhancers as it stands to reason that these genes play crucial roles in the response to *M.tb*. Among the 263 DEGs, Tnfrsf1b was associated with the highest number of the induced enhancers, eight (**Figure 4.9**). Interestingly, one of these induced enhancers (chr4:145245568..145245969, **Figure 4.9b**) showed the second highest mean eRNA expression (28.79 TPM) at 4 h post infection among all enhancers targeting up-regulated DEGs. We found that induced enhancers were also significantly over-represented in the corresponding TAD (eight induced enhancers among 38 BMDM enhancers in the TAD, hypergeometric test FDR = 0.005, see 4.6.5). Interestingly, Tnfrsf1b was the only up-regulated DEG within the TAD ($\log_2$FC = 2.2 at 4 h vs. 0 h, **Figure 4.9a**) and encodes Tnf-alpha receptor type 2, which is known to interfere with apoptosis and sensitise macrophages for Tnfr1-mediated necroptosis, a programmed form of inflammatory cell death resulting from cellular damage or infiltration by pathogens (Balcewicz-Sablinska, Keane, Kornfeld, & Remold, 1998; Siegmund, Kums, Ehrenschwender, & Wajant, 2016). Given that all of Tnfrsf1b's induced enhancers coincide with a super enhancer (see **Figure 4.9c**), we hypothesise that the activation of the super enhancer upon infection is driving the process in conjunction with increased eRNA expression from the induced enhancers.

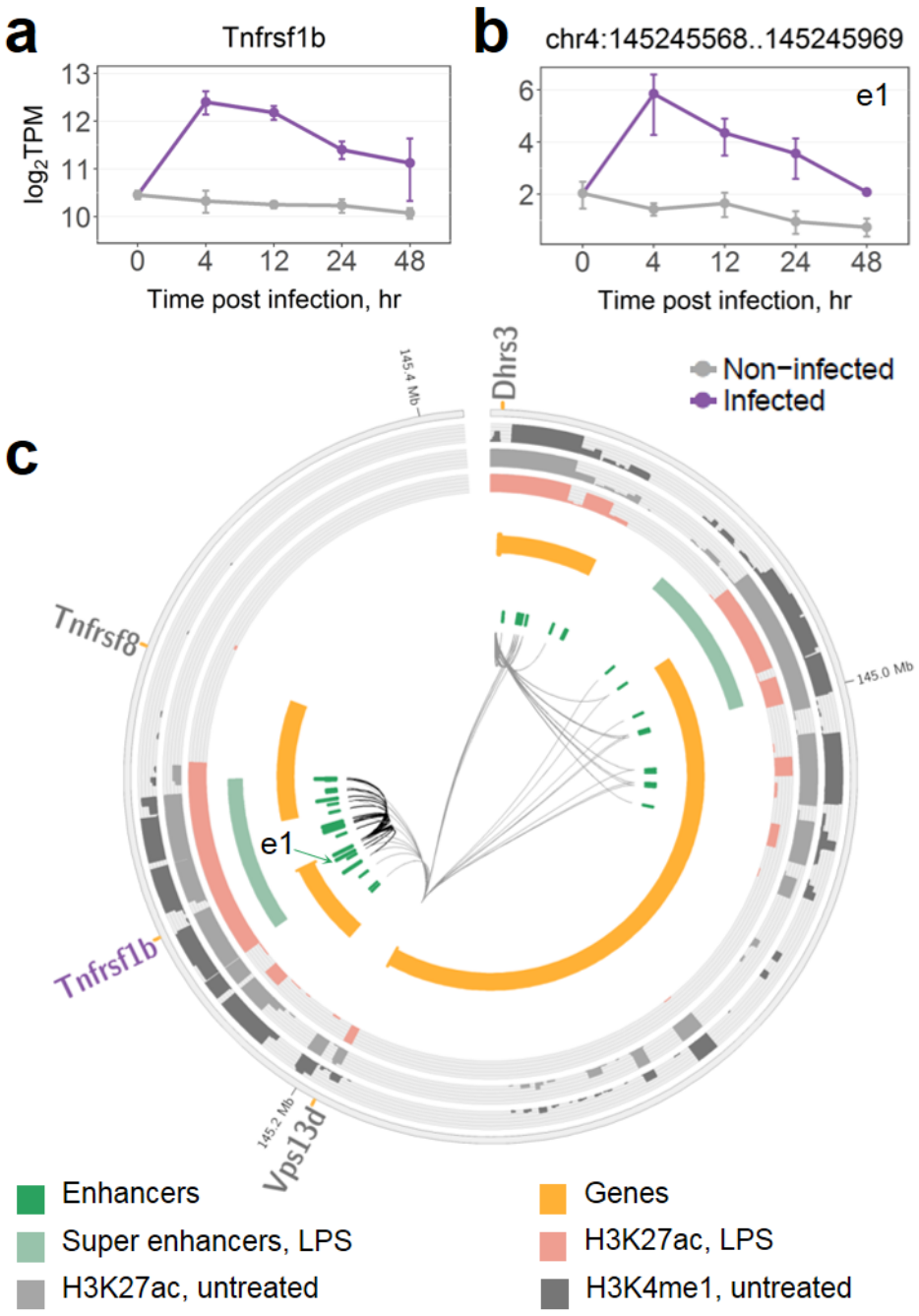

Figure 4.9. Regulation of Tnfrsf1b by induced enhancers. **a** Time-course expression of the Tnfrsf1b gene. **b** Time-course eRNA expression of Tnfrsf1b-associated induced enhancer. In **a** and **b**, data were averaged over replicates and log-transformed, error bars are the SEM. **c** TAD containing Tnfrsf1b and associated enhancers; induced enhancers are shown as longer green blocks. Genes are split into two tracks based on the strand, wide orange marks denote gene promoters. DEGs significantly up-regulated at 4 h are shown in purple and their associations with enhancers are shown as thicker black connections. SEs are shown as defined in LPS-treated macrophages (Hah et al., 2015). Histone marks are shown as defined in untreated and LPS-treated macrophages (Ostuni et al., 2013).

In another example, the TAD contained a group of three co-regulated DEGs (Irg1, Cln5, and Fbxl3) with properties similar to the above (**Figure 4.10**). First, these genes were associated with six induced enhancers each, the second highest number after Tnfrsf1b reported above. Second, among these six, the chr14:103037012..103037413 enhancer showed the highest mean eRNA expression (36.68 TPM) at 4 h post infection among all enhancers of up-regulated DEGs (**Figure 4.10b**, enhancer e2). Finally, six out of 14 enhancers in the TAD were deemed induced enhancers (significant over-representation with hypergeometric test FDR = 0.001). Of the three DEGs, Irg1 had the strongest induction of $\log_2$FC = 5.2 at 4 h vs. 0 h (**Figure 4.10a**). Irg1 was recently shown to produce itaconic acid that has antimicrobial activity and inhibits the growth of *M.tb* (Michelucci et al., 2013). While the immune functions of Cln5 ($\log_2$FC = 2) and Fbxl3 ($\log_2$FC = 1.4) are yet to be elucidated, the link between highly induced enhancers and Irg1 points to another biological process important for the host response that might be driven by transcribed enhancers. Notably, a subset of induced enhancers was, again, located within a SE (see **Figure 4.10c**), reinforcing the importance of SEs in macrophage response to *M.tb* infection.

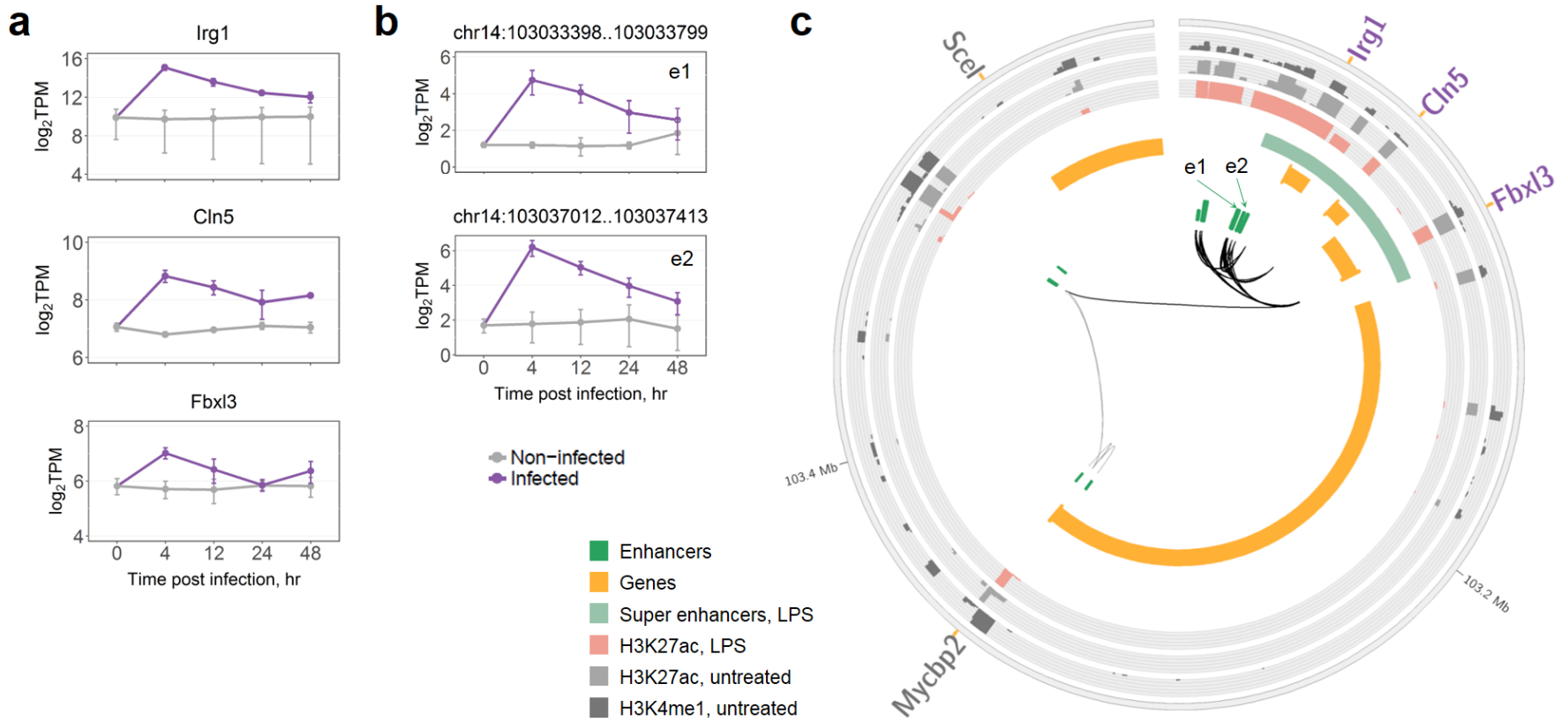

Figure 4.10. Regulation of Irg1, Cln5, and Fbxl3 genes. a Time-course expression of the genes. **b** Time-course eRNA expression of associated induced enhancers with the highest average expression at 4 h. In **a** and **b,** data were averaged over replicates and log-transformed, error bars are the SEM. **c** TAD containing the genes and associated enhancers; induced enhancers are shown as longer green blocks. Genes are split into two tracks based on the strand, wide orange marks denote gene promoters. DEGs up-regulated at 4 h are shown in purple and their associations with enhancers are shown as thicker black connections. SEs are shown as defined in LPS-treated macrophages (Hah et al., 2015). Histone marks are shown as defined in untreated and LPS-treated macrophages (Ostuni et al., 2013).

Induced enhancers were significantly over-represented with FDR < 0.05 in four more TADs, which we further investigated as potentially important *M.tb*-responsive genomic regions. One of the TADs (FDR = 0.001, five induced enhancers among eight BMDM transcribed enhancers, **Figure 4.11**) is as large as 1.2 Mb and contains multiple genes, however, only Hilpda (Hig2) was DE and up-regulated at 4 h ($log_2FC = 6$, **Figure 4.11a**). Hilpda is induced in hypoxia and is crucial to lipid accumulation in macrophages, which provides a favourable environment for dormant *M.tb* and might, thus, contribute to *M.tb* survival within the host (Daniel, Maamar, Deb, Sirakova, & Kolattukudy, 2011; Maier et al., 2017). Similarly, Itgb8 was the only up-regulated DEG ($log_2FC = 7.1$) in another TAD with five induced enhancers among 14 BMDM transcribed enhancers (FDR = 0.011, **Figure 4.12**). Although specific roles of Itgb8 in *M.tb* infection response have not yet been established, integrin alpha(v)beta8 is known to activate TGF-beta (Mu et al., 2002), an important mediator of susceptibility to *M.tb* (Reed, 1999).

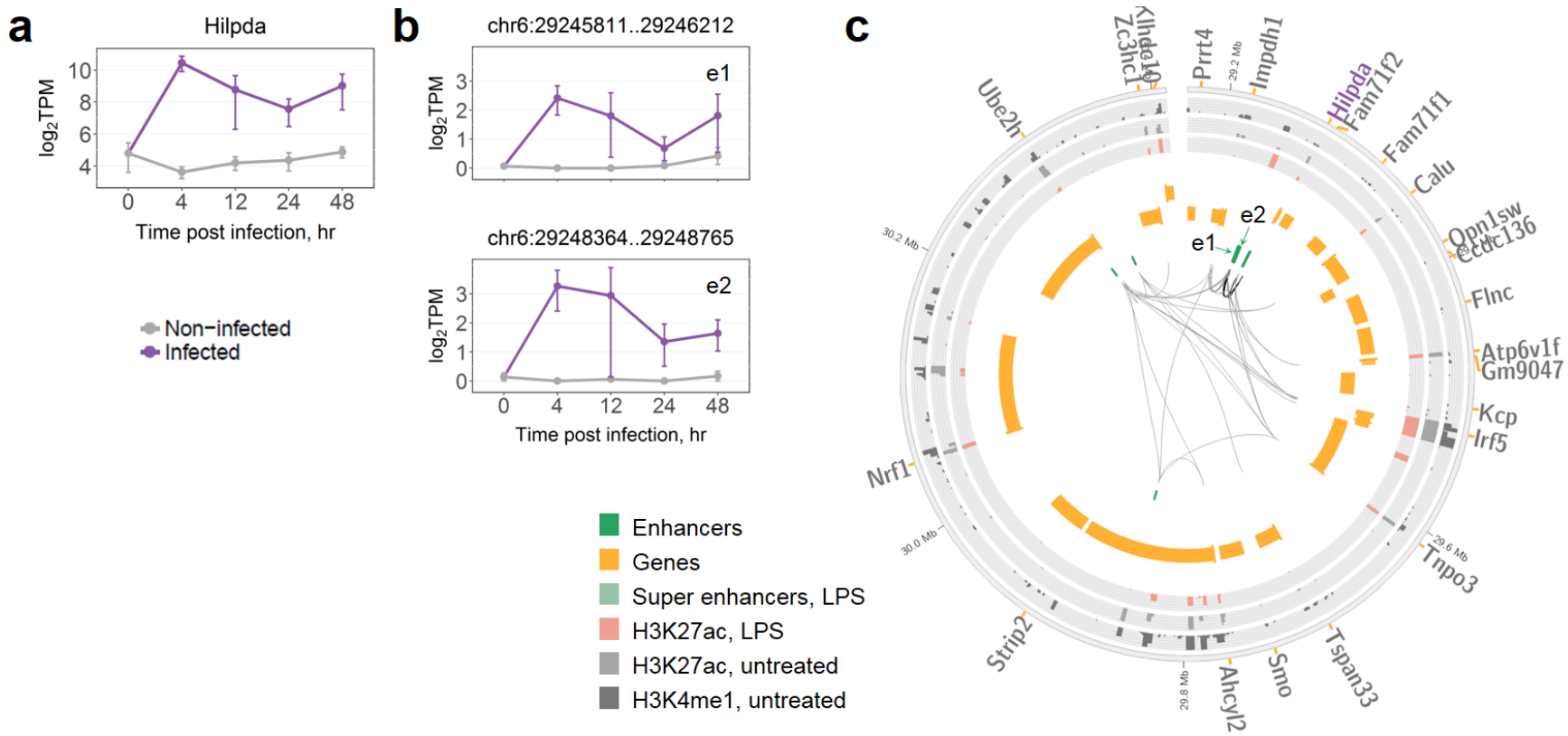

Figure 4.11. Regulation of Hilpda gene. a Time-course expression of the gene. **b** Time-course eRNA expression of associated induced enhancers with the highest average expression at 4 h. In **a** and **b,** data were averaged over replicates and log-transformed, error bars are the SEM. **c** TAD containing the gene and associated enhancers; induced enhancers are shown as longer green blocks. Genes are split into two tracks based on the strand, wide orange marks denote gene promoters. The Hilpda gene up-regulated at 4 h is shown in purple and its associations with enhancers are shown as thicker black connections. SEs are shown as defined in LPS-treated macrophages (Hah et al., 2015). Histone marks are shown as defined in untreated and LPS-treated macrophages (Ostuni et al., 2013).

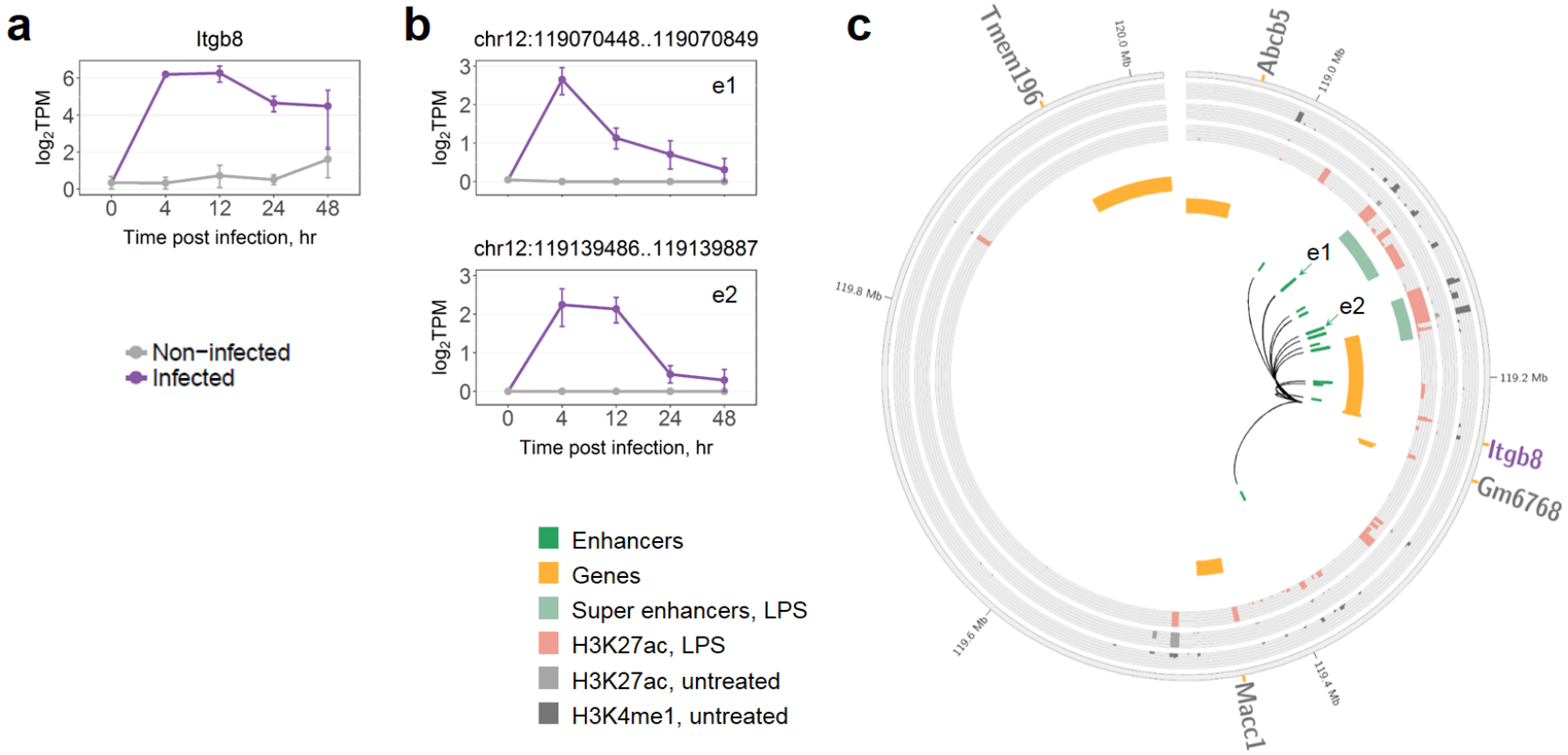

Figure 4.12. Regulation of Itgb8 gene. a Time-course expression of the gene. **b** Time-course eRNA expression of associated induced enhancers with the highest average expression at 4 h. In **a** and **b,** data were averaged over replicates and log-transformed, error bars are the SEM. **c** TAD containing the gene and associated enhancers; induced enhancers are shown as longer green blocks. Genes are split into two tracks based on the strand, wide orange marks denote gene promoters. DEGs up-regulated at 4 h are shown in purple and their associations with enhancers are shown as thicker black connections. SEs are shown as defined in LPS-treated macrophages (Hah et al., 2015). Histone marks are shown as defined in untreated and LPS-treated macrophages (Ostuni et al., 2013).

A TAD with four induced enhancers among eight BMDM transcribed enhancers (FDR = 0.012) contains three DEGs up-regulated at 4 h post infection (**Figure 4.13**). Cd38 and Bst1 (Cd157) are homologous NAD(+) metabolic enzymes up-regulated by Tnf (Iqbal & Zaidi, 2006), and Cd38 was shown to be involved in phagocytosis (Kang et al., 2012) and response to intracellular pathogen *Listeria monocytogenes* in mouse macrophages (Botta, Rivero-Nava, & Lund, 2014). The role of the third gene in that TAD, transmembrane protein Tapt1, remains to be elucidated.

Finally, a TAD with five induced enhancers among 17 BMDM transcribed enhancers (FDR = 0.02) covers four DEGs Ccl3, Ccl4, Ccl9, and Wfdc17 (**Figure 4.14**). Ccl3 and Ccl4 are macrophage-derived inflammatory chemokines that induce chemotactic mobilisation of immune cells (Griffith, Sokol, & Luster, 2014), while Wfdc17 might have the opposite function decreasing production of pro-inflammatory cytokines (Karlstetter et al., 2010).

Taken together, these examples highlight six TADs, located on six different chromosomes, which show strong responses to *M.tb* infection and contain genes with both known and previously unappreciated roles in *M.tb* infection. These genes are under the control of multiple *M.tb* induced enhancers, which might be essential for contributing to the genes' activation states.

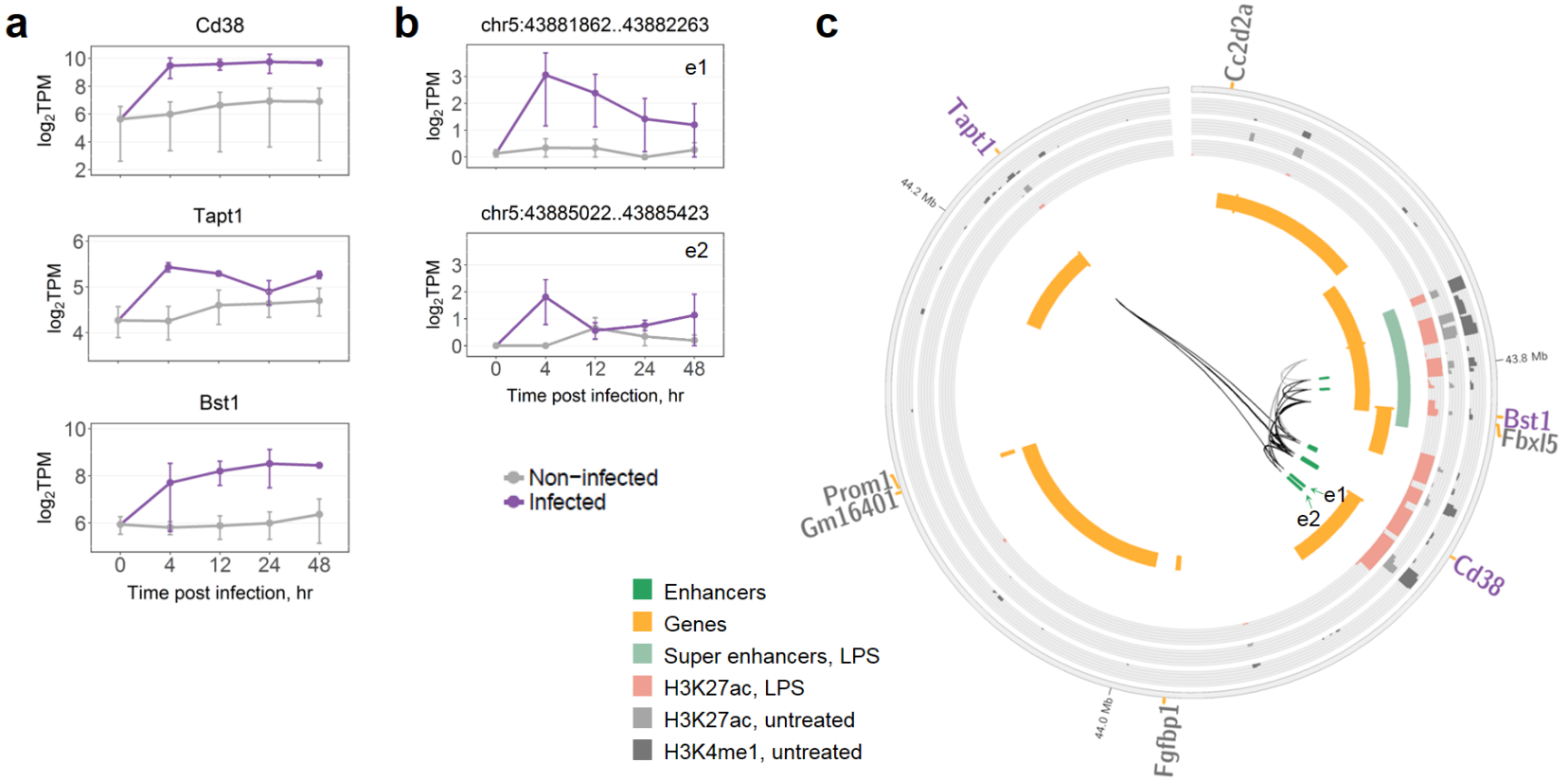

Figure 4.13. Regulation of Cd38, Bst1, and Tapt1 genes. a Time-course expression of the genes. **b** Time-course eRNA expression of associated induced enhancers with the highest average expression at 4 h. In **a** and **b,** data were averaged over replicates and log-transformed, error bars are the SEM. **c** TAD containing the genes and associated enhancers; induced enhancers are shown as longer green blocks. Genes are split into two tracks based on the strand, wide orange marks denote gene promoters. DEGs up-regulated at 4 h are shown in purple and their associations with enhancers are shown as thicker black connections. SEs are shown as defined in LPS-treated macrophages (Hah et al., 2015). Histone marks are shown as defined in untreated and LPS-treated macrophages (Ostuni et al., 2013).

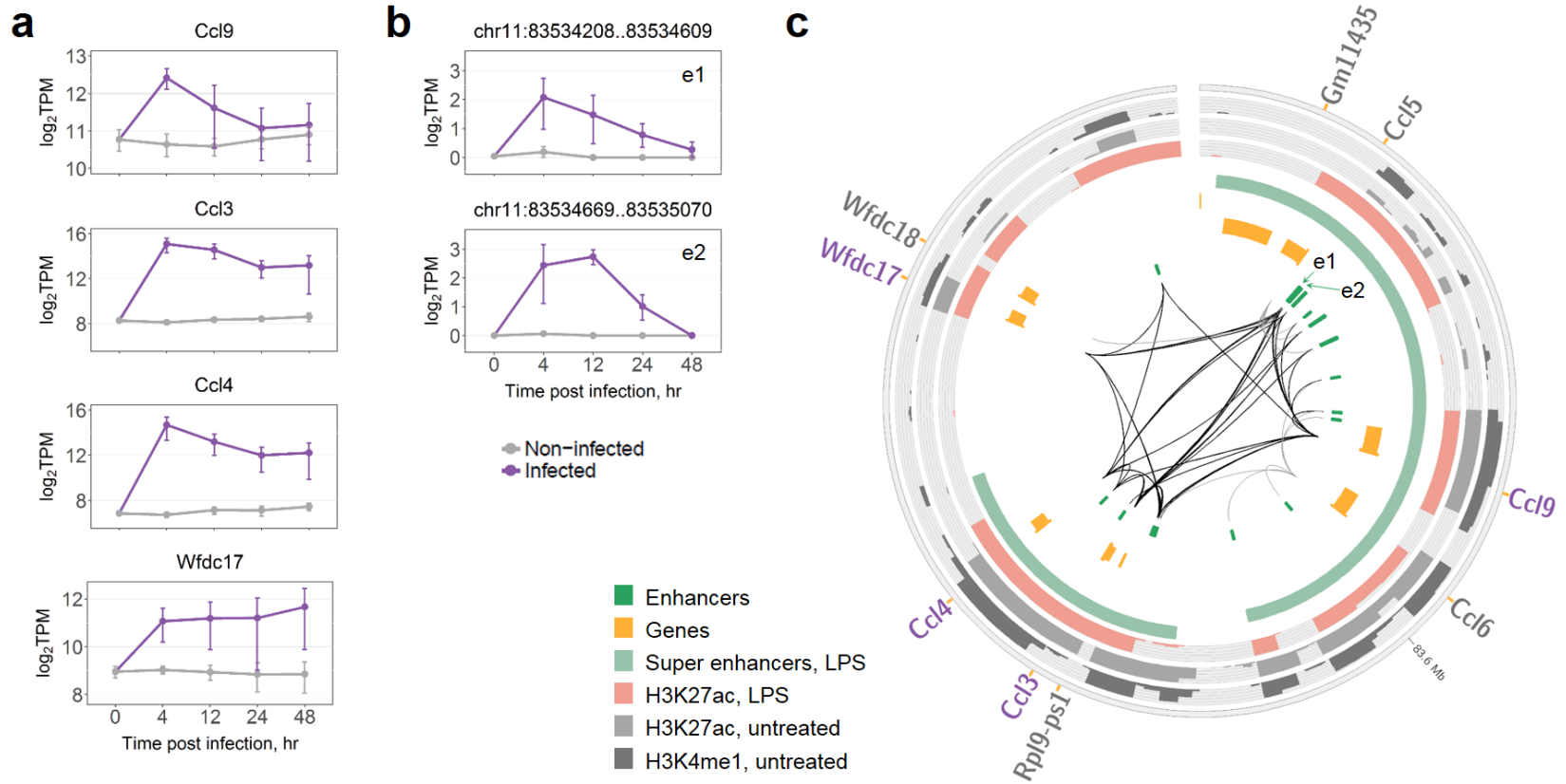

Figure 4.14. Regulation of Ccl9, Ccl3, Ccl4, and Wfdc17 genes. a Time-course expression of the genes. **b** Time-course eRNA expression of associated induced enhancers with the highest average expression at 4 h. In **a** and **b,** data were averaged over replicates and log-transformed, error bars are the SEM. **c** TAD containing the genes and associated enhancers; induced enhancers are shown as longer green blocks. Genes are split into two tracks based on the strand, wide orange marks denote gene promoters. DEGs up-regulated at 4 h are shown in purple and their associations with enhancers are shown as thicker black connections. SEs are shown as defined in LPS-treated macrophages (Hah et al., 2015). Histone marks are shown as defined in untreated and LPS-treated macrophages (Ostuni et al., 2013).

To get further insights into the capacity of induced enhancer regulation during the response to *M.tb* infection, we investigated their target DEGs that were significantly enriched in particular biological pathways (**Figure 4.7b**). The Tnf signalling pathway showed the strongest enrichment and included 18 DEGs up-regulated at 4 h and associated with the induced enhancers. Among these genes, in addition to Tnf-alpha receptor type 2 (Tnfrsf1b) reported above, we identified Tnf itself, Tnf signalling pathway mediator Traf5 and multiple effector genes targeted by induced enhancers. Tnf-alpha receptors are known to trigger the NF-kB signalling pathway, which was also enriched for DEGs regulated by induced enhancers. Among these genes, we report receptors Cd14 and Cd40, ligand Il1b, and transcription factors of canonical NF-kB signalling, Nfkb1 and Rela. In addition, among the genes known to regulate *M.tb* response and that are enriched in "Tuberculosis" KEGG pathway map, we found signal transduction mediators Irak2, Jak2, Malt1, Ripk2, and Src, and Eea1, known to be involved in phagosome maturation, which is necessary for killing of bacteria within phagosomes (Fratti, Backer, Gruenberg, Corvera, & Deretic, 2001). Notably, negative regulators of the listed signalling pathways, Nfkbia, Tnfaip3, and Socs3, were also associated with one to five induced enhancers, and showed up-regulation. Hence, we find that induced enhancers are extensively involved in the regulation of important immune signalling pathways, targeting all their components, starting from ligands and receptors, through signal transduction mediators, ending with transcription factors and pathway effector genes.

4.2.3. Transcriptionally induced enhancers are regulated by immune transcription factors

Transcription factor (TF) binding motif analysis was performed to uncover TFs potentially involved in the transcriptional activation of induced enhancers. We identified twelve significantly over-represented motifs of TFs that were differentially expressed and up-regulated at 4 h post infection (see 4.6.6, **Table 4.1**). Five of these motifs belong to the AP-1 family of TFs, among which the highest expressed one was Junb, recently reported to be an important regulator of immune genes in macrophages treated with LPS (Fontana et al., 2015). Interestingly, a negative regulator of AP-1, Jdp2, was also among the significantly over-represented motifs, although it was found only in 20.6% of the induced enhancers. Three motifs of NF-kB family were identified, among which Rela was reported above to be itself regulated by the induced enhancers, potentially forming a positive feedback loop. Both AP-1 and NF-kB families of TFs, as well as another identified TF Irf1, play important roles in macrophages and can be triggered by a range of infection response receptors including Toll-like and Nod-like receptors (Oviedo-Boyso, Bravo-Patino, & Baizabal-Aguirre, 2014; Schorey & Cooper, 2003). Rbpj, which showed the second strongest motif over-representation, is a key TF of canonical Notch signalling pathway which is known to be activated by Toll-like receptor signalling pathways (Shang, Smith, & Hu, 2016). Finally, Nfe2l2 (Nrf2) regulates genes that enhance cell survival and was shown to increase phagocytic ability of macrophages and to improve antibacterial defence (Harvey et al., 2011; Kensler, Wakabayashi, & Biswal, 2007).

Importantly, 89.1% of the 257 induced enhancers considered here carry at least one of the twelve motifs, and these enhancers target a total of 95.1% of the 263 up-regulated DEGs (**Table 4.2**). Among the motifs, AP-1 family members covered the largest

percentages of the induced enhancers and their target genes, followed by the NF-kB family and Rbpj TF, highlighting their importance in enhancer regulation of *M.tb* response. We compared this TF regulation of protein-coding genes via enhancers to TFs that bind directly to the promoters of the 263 up-regulated DEGs (see 4.6.6). In the promoters, Irfl, as well as AP-1 and NF-kB families were similarly significantly over-represented, whereas Rbpj, Nfe2l2 and Jdp2 were not deemed significant and, thus, might be specific to the transcriptionally induced enhancers. Taken together, these findings link *M.tb*-perturbed signalling pathways and their key TFs to transcriptional activation of the induced enhancers, which in turn activate their immune target DEGs.

Table 4.1. TF motifs over-represented in the induced enhancers. Columns show TF motif name, number and percentage of overlapping enhancers among the induced enhancers, average expression of the corresponding TF(s) in infected BMDM at 4 h, fold change and FDR of DE test for the corresponding TF(s) in infected BMDM at 4 h versus non-infected control at 0 h. Motifs were retained for TFs with significant up-regulation at 4 h.

TF Motif	# overlapping enhancers	Expression, TPM	log_2FC	FDR
FOSL1::JUNB	118 (45.9%)	19.4 / 523.7	5.4 / 2.6	2.7e-03 / 1e-04
RBPJ	117 (45.5%)	295.7	1.8	7.30e-03
REL	96 (37.4%)	165.3	3	4.30e-06
FOSL2::JUNB	91 (35.4%)	81.2 / 523.7	2.4 / 2.6	1.2e-06 / 1e-04
IRF1	88 (34.2%)	1099.8	2.8	1.50e-04
RELA	87 (33.9%)	309	1.7	1.00e-06
JUNB	84 (32.7%)	523.7	2.6	1.00e-04
FOSL1	80 (31.1%)	19.4	5.4	2.70e-03
FOSL2	80 (31.1%)	81.2	2.4	1.20e-06
Nfe2l2	54 (21%)	684	1.5	2.40e-03
JDP2	53 (20.6%)	67.7	2.9	4.80e-04
NFKB2	28 (10.9%)	496.3	2.7	2.50e-04

Table 4.2. TF-mediated regulation of genes via induced enhancers. Columns show individual TF motifs or their groups, number and percentage of overlapping enhancers among the induced enhancers, number and percentage of DEGs targeted by these enhancers among the 263 DEGs up-regulated at 4 h and associated with the induced enhancers.

TF Motifs	# overlapping enhancers	# target DEGs
AP-1 (FOSL1::JUNB, FOSL2::JUNB, JUNB, FOSL2, FOSL1)	128 (49.8%)	180 (68.4%)
NF-kB (REL, RELA, NFKB2)	117 (45.5%)	157 (59.7%)
RBPJ	117 (45.5%)	160 (60.8%)
IRF1	88 (34.2%)	126 (47.9%)
Nfe2l2	54 (21%)	86 (32.7%)
JDP2	53 (20.6%)	92 (35%)
Total (12 motifs)	229 (89.1%)	250 (95.1%)

4.2.4. A subset of enhancers is transcribed *de novo* upon *M.tb* infection

Interestingly, among 257 induced enhancers we found 17 enhancers that showed zero eRNA expression in all of the 22 non-infected macrophage samples. Hence, transcription of these enhancers was specifically acquired *de novo* in macrophages upon *M.tb* infection. These enhancers were associated with a total of 31 of the 263 DEGs under investigation, which included Hilpda, Il1b, Itgb8, Jak2, Src, and Tnfaip3 genes, reported above. We further set out to investigate in more detail the phenomenon of *de novo* transcription at enhancers.

We focused on enhancers that were transcriptionally silent in naïve BMDM, but acquired transcriptional activity *de novo* in *M.tb*-infected macrophages (further referred to as acquired enhancers, see 4.6.4). We hypothesised that such enhancers in non-infected

macrophages might either loop towards their target promoters without being transcriptionally active, or might form a novel DNA loop upon infection (**Figure 4.15a** and **b**). We identified 356 acquired enhancers (see 4.6.4). Their eRNA expression was the highest at 4 and 12 h post infection and declined with time (**Figure 4.15c**, left panel), in agreement with the DEG expression reported above. Notably, overall expression of the acquired enhancers in infected macrophages was lower than that of the induced enhancers (median of 0.23 TPM versus 1.73 TPM at 4 h). However, similarly to induced enhancers, acquired enhancers showed the highest expression in infected macrophages when compared to other mouse tissues (**Figure 4.16**). Thus, the transcriptional activity of the acquired enhancers demonstrates high specificity to the response of BMDM to *M.tb* infection.

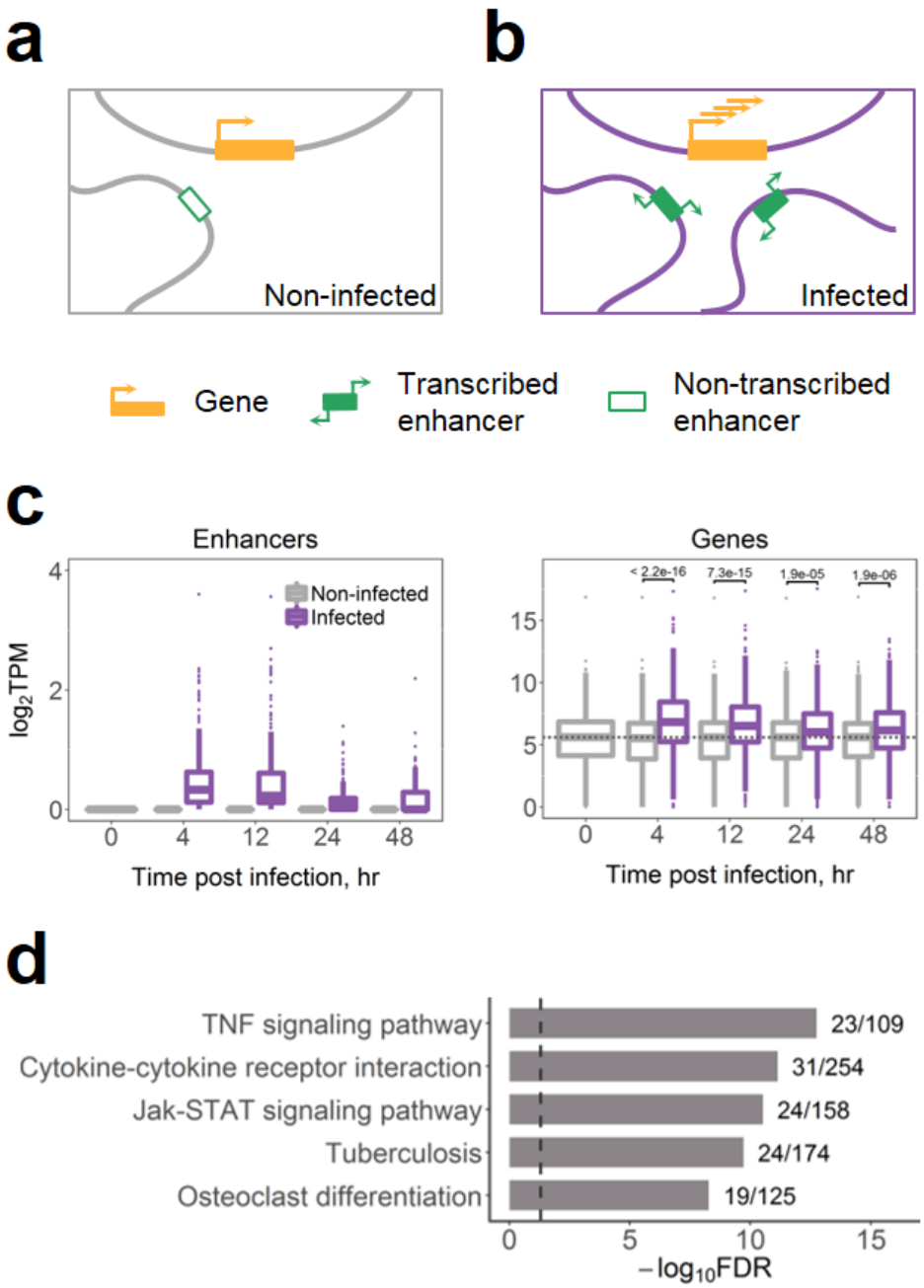

Figure 4.15. Enhancers that acquire transcriptional activity *de novo* upon *M.tb* infection. **a** and **b** show presumable changes in gene regulation upon infection: **a** In non-infected macrophages, a transcriptionally inactive enhancer loops towards its target gene, **b** Upon infection, the enhancer acquires transcriptional activity; an additional loop is formed *de novo* for another acquired transcribed enhancer; the gene expression is induced. **c** eRNA expression of 356 acquired enhancers (left) and their 526 target genes (right); dashed line shows median gene expression prior to the infection, expression in TPM was averaged across replicates, p-values of Wilcoxon two-sided rank sum tests are shown. **d** Top 5 KEGG pathway maps with the lowest FDR enriched for 526 target genes of the acquired enhancers; next to the bars are the numbers of genes in the KEGG term covered by our gene list; dashed line indicates FDR = 0.05.

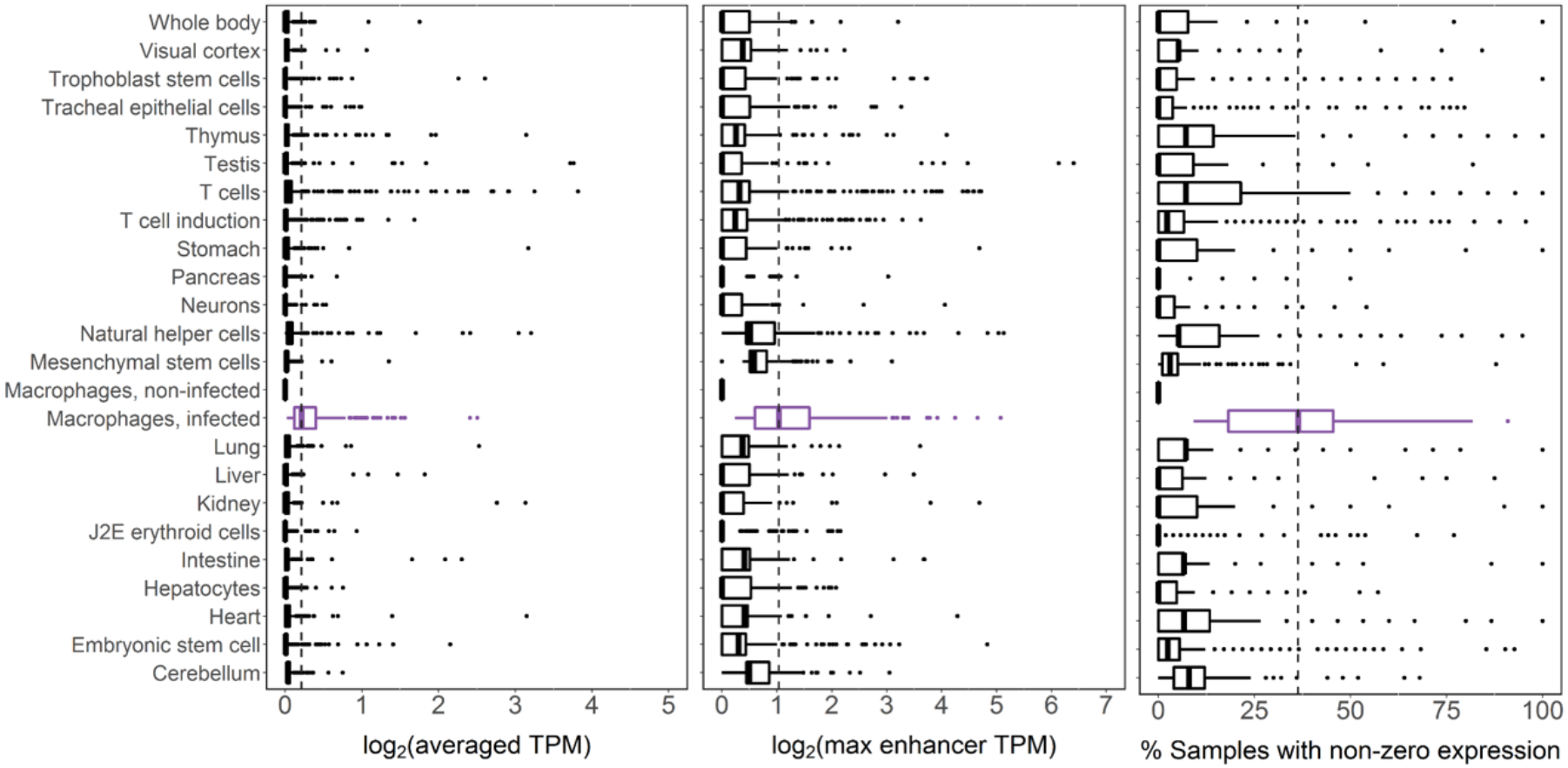

Figure 4.16. Expression of the acquired enhancers in mouse tissues. Left panel: expression of each enhancer was averaged across tissue samples. Middle panel: maximum enhancer expression value in each tissue samples is used. Right panel: percentage of samples with nonzero expression was calculated for each enhancer in each sample group.

We further compared the acquired enhancers to genomic regions carrying H3K4me1 and H3K27ac histone marks, which demarcate pre-established enhancer regions and active enhancers, respectively. We used data derived for untreated and LPS-treated macrophages (Ostuni et al., 2013). LPS (lipopolysaccharide) represents a component of bacterial membranes, which is recognised by the host and triggers a strong immune anti-bacterial response in a manner similar to *M.tb* (van Crevel, Ottenhoff, & van der Meer, 2002). Of 356 acquired enhancers, 83.1% and 99.2% overlapped H3K4me1-enriched regions in untreated and LPS-treated macrophages, respectively, indicating that most of the acquired transcribed enhancers might be established in naïve macrophages, prior to infection. Unexpectedly, as much as 63.8% of the acquired enhancers overlapped H3K27ac-enriched regions in untreated macrophages. However, this percentage was higher at 86% in LPS-treated macrophages, and the corresponding H3K27ac ChIP-seq peaks were much stronger enriched in LPS-treated as compared to untreated macrophages (**Figure 4.17**).

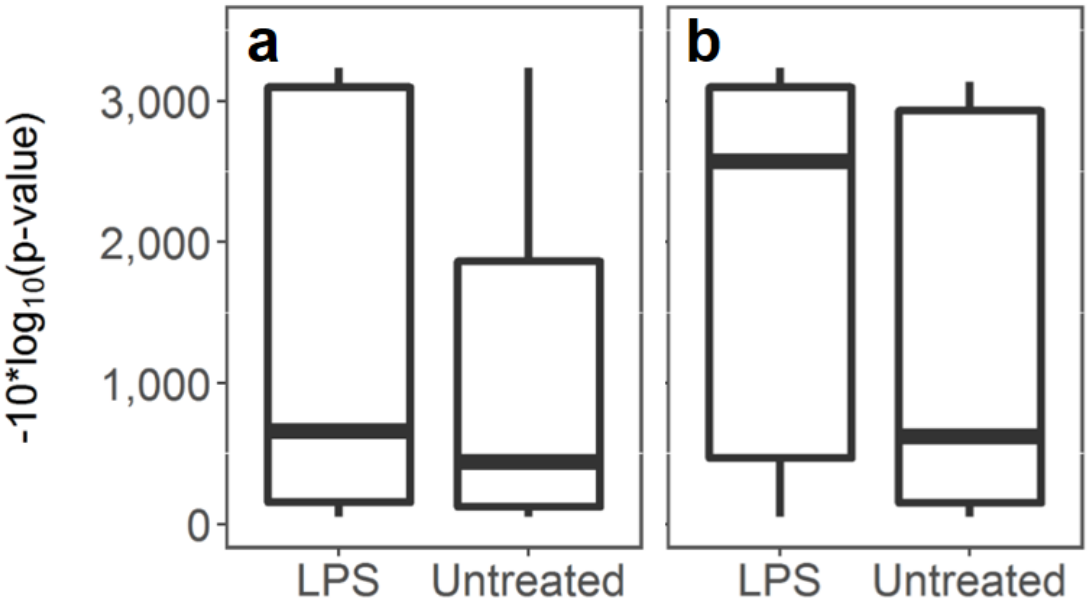

Figure 4.17. H3K27ac ChIP-seq peaks. Data from (Ostuni et al., 2013). **a** All significant H3K27ac peaks detected in untreated and LPS-treated samples. **b** A subset of peaks overlapping acquired enhancers.

4.2.5. Acquired enhancers contribute to the regulation of immune genes during *M.tb* infection

The acquired enhancers in infected macrophages were associated with a total of 526 genes. These genes showed an overall increased expression upon *M.tb* infection (**Figure 4.15c**, right panel) and, importantly, a strong enrichment for immune response-related functions (**Figure 4.15d**). For further analyses we sub selected the target DEGs that were up-regulated at 4 h post infection (251 genes, 47.7%).

First, we investigated enhancer-gene associations and found that, at maximum, a DEG was associated with six acquired enhancers. We identified five such genes (Hivep1, Itgb8, Pla2g4a, Ptgs2, and Tnfaip3), and among them Pla2g4a and Ptgs2 were co-regulated by the same set of acquired enhancers within a TAD (**Figure 4.18**). Both genes are known

to be involved in the metabolism of arachidonic acid, one of the regulators of cell death, and to play a role in infection responses (Behar, Divangahi, & Remold, 2010). While Pla2g4a showed a moderate induction of $log_2FC = 2.9$, expression of Ptgs2 was induced dramatically with $log_2FC = 11.5$ at 4 h post infection (**Figure 4.18a**).

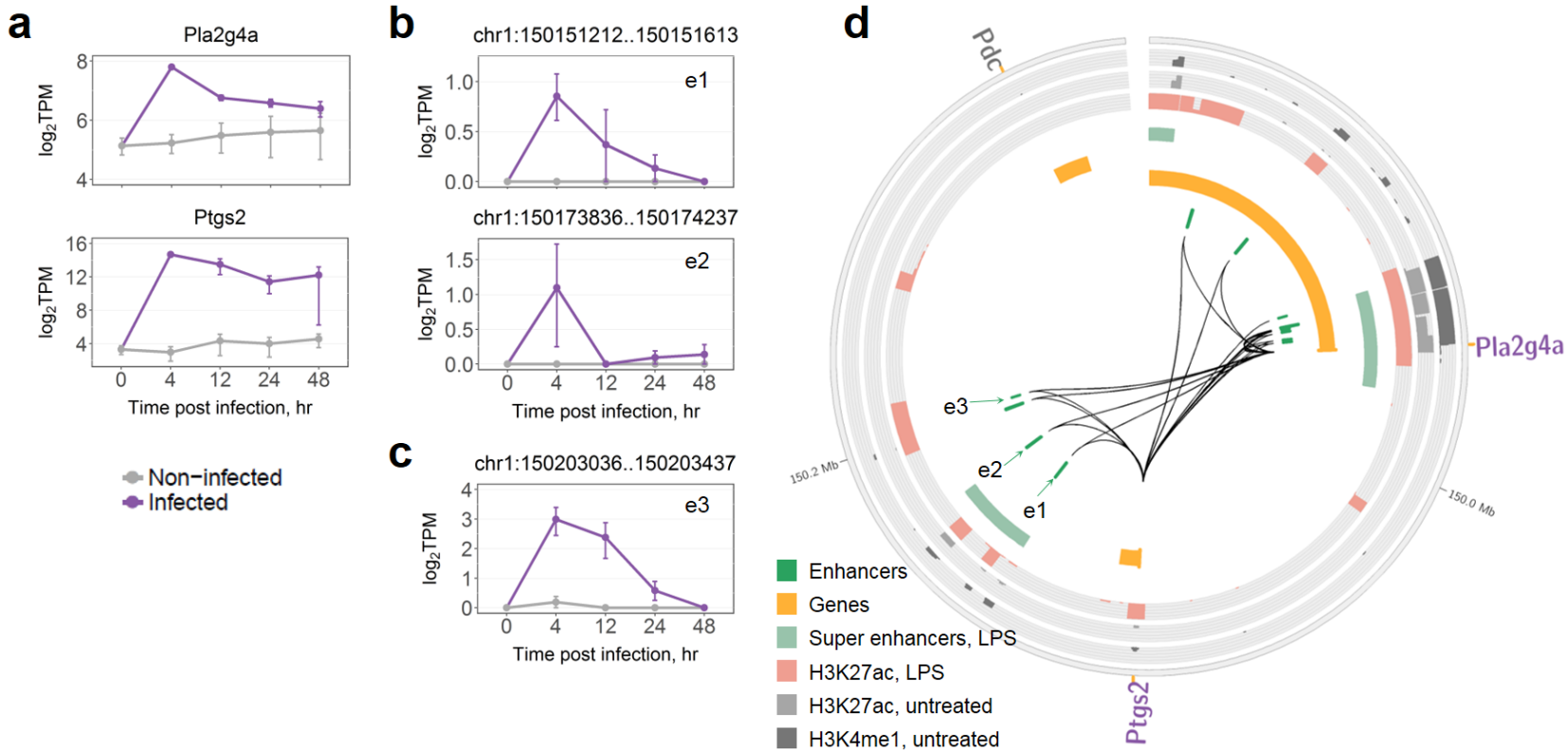

Figure 4.18. Regulation of Pla2g4a and Ptgs2 genes. a Time-course expression of the genes. **b** Time-course eRNA expression of associated acquired enhancers with the highest average expression at 4 h. **c** Time-course eRNA expression of associated induced enhancer. In **a, b,** and **c,** data were averaged over replicates and log-transformed, error bars are the SEM. **d** TAD containing the genes and associated enhancers; acquired enhancers are shown as longer green blocks. Genes are split into two tracks based on the strand, wide orange marks denote gene promoters. DEGs up-regulated at 4 h are shown in purple. SEs are shown as defined in LPS-treated macrophages (Hah et al., 2015). Histone marks are shown as defined in untreated and LPS-treated macrophages (Ostuni et al., 2013).

The strongest induction of log_2FC = 12.3 at 4 h was observed for Edn1, a DEG associated with five acquired enhancers (**Figure 4.19**). Edn1 (endothelin) is well-known as a vascular regulator, however, its particular roles in infectious diseases, including tuberculosis, are only beginning to be elucidated (Correa et al., 2014). Edn1 is co-regulated with DEG Hivep1, a transcriptional regulator for which the precise function in infected macrophages is unknown (**Figure 4.19**).

All of Pla2g4a, Ptgs2, Edn1, and Hivep1 genes were additionally associated with other enhancers, which were not classified as acquired enhancers. Among those, Edn1 and Hivep1 were associated with one enhancer that was deemed induced in our study (**Figure 4.19c**), while Pla2g4a and Ptgs2 were associated with four such induced enhancers (see **Figure 4.18c** for eRNA expression of one of them). These enhancers, in contrast to the acquired ones, showed nonzero (although very low) eRNA expression in non-infected macrophages. Notably, in infected macrophages these induced enhancers had a higher expression than the acquired enhancers associated to the same genes (**Figure 4.18** and **Figure 4.19**). Thus, up-regulation of DEGs Pla2g4a, Ptgs2, Edn1, and Hivep1 could not be attributed exclusively to activity of the acquired enhancers.

Of note, the induced enhancer of Edn1 and Hivep1 (**Figure 4.19c**) is surrounded by acquired enhancers within a region reported as a SE (Hah et al., 2015) (**Figure 4.19d**), and showed a particularly low (close to zero) expression in non-infected macrophages (similarly to two other non-acquired enhancers in that region, data not shown). Hence, the whole super enhancer region might have low or no activity in non-infected macrophages and acquire broad transcriptional activity upon *M.tb* infection.

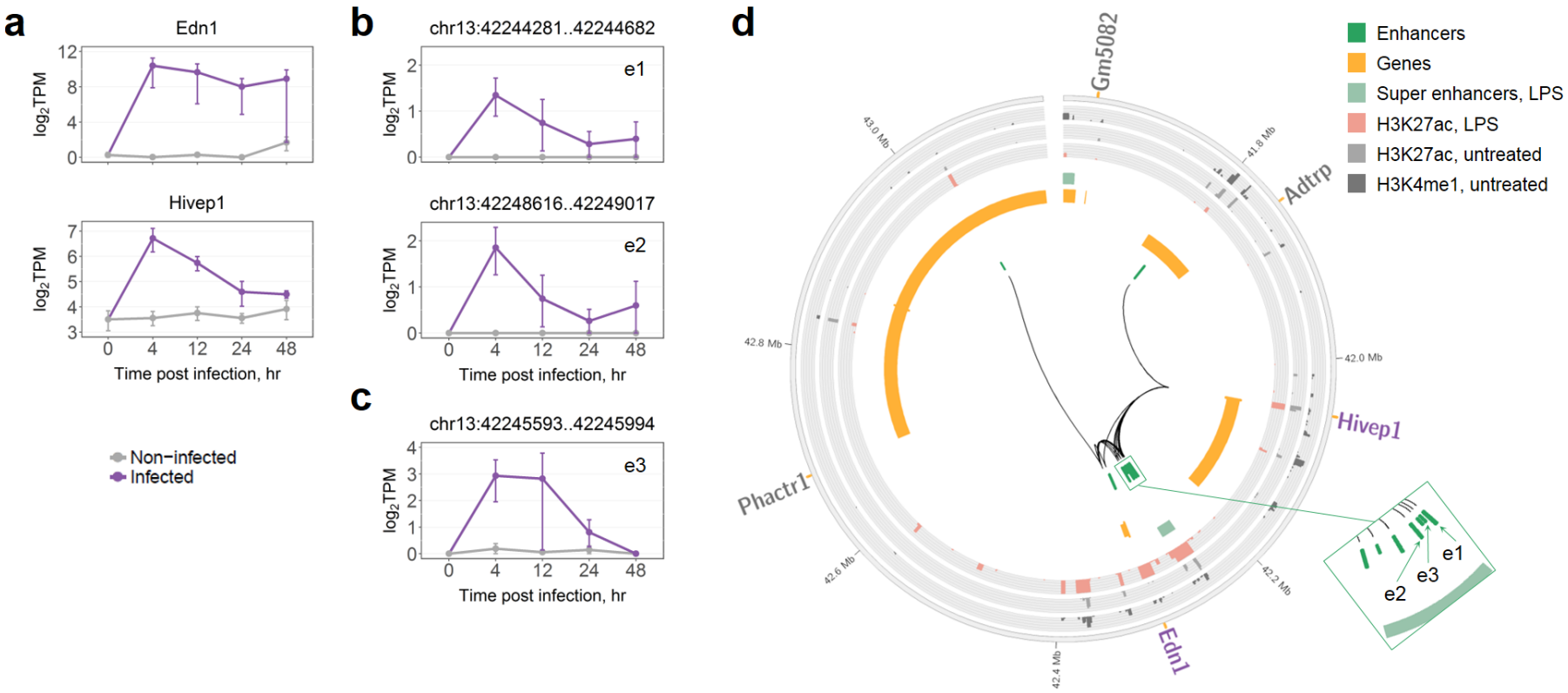

Figure 4.19. Regulation of Edn1 and Hivep1 genes. a Time-course expression of the genes. **b** Time-course eRNA expression of associated acquired enhancers with the highest average expression at 4 h. **c** Time-course eRNA expression of associated induced enhancer with the highest expression at 4 h. In **a, b,** and **c,** data were averaged over replicates and log-transformed, error bars are the SEM. **d** TAD containing the genes and associated enhancers; acquired enhancers are shown as longer green blocks. Genes are split into two tracks based on the strand, wide orange marks denote gene promoters. DEGs up-regulated at 4 h are shown in purple. SEs are shown as defined in LPS-treated macrophages (Hah et al., 2015). Histone marks are shown as defined in untreated and LPS-treated macrophages (Ostuni et al., 2013).

We further asked whether any of the 251 up-regulated DEGs were associated exclusively with acquired enhancers. We identified 22 such genes regulated by a total of 18 acquired enhancers. However, in most cases, we observed either low or inconsistent eRNA expression among replicates (data not shown). Hence, our data could not reliably infer up-regulated DEGs driven exclusively by acquired enhancers. Moreover, the 251 DEGs were associated on average with 1.6 acquired enhancers and 6.1 other enhancers, not classified as acquired. These findings suggest that upon *M.tb* infection, *de novo* transcription at enhancers targeting up-regulated DEGs is acquired in addition to already established transcriptionally active enhancers.

TF binding motif analysis of the acquired enhancers showed overall similar results to that of the induced enhancers, except for Irf1 motif which was over-represented only in induced enhancers, and three TF motifs over-represented only in acquired ones. Among these, a motif for Stat3, which is known to be involved in *M.tb* infection response (Rottenberg & Carow, 2014), overlaps 36.2% of the acquired enhancers. Macrophage-restricted TF Tfec with an overlap of 35.7% has been reported as an important regulator of IL-4 inducible genes in macrophages but was also up-regulated in response to LPS treatment (Rehli et al., 2005). Finally, the Srebf2 motif overlaps 25.3% of the acquired enhancers. Interestingly, this TF is a host gene of miR-33, a miRNA induced in macrophages by *M.tb* to inhibit pathways of autophagy, lysosomal function and fatty acid oxidation to support *M.tb* intracellular survival (Ouimet et al., 2016). Taken together, these results uncover a novel role of these TFs in the response to *M.tb* infection in BMDM.

4.3. Discussion

Macrophages represent the first line of an organism's defence against *M.tb*, and interactions between macrophages and *M.tb* define the TB infection outcome (Russell et al., 2010; Weiss & Schaible, 2015). Macrophages are equipped with a multitude of strategies to combat *M.tb*, however, the pathogen has developed a wide range of matching resistance mechanisms, allowing it to avoid destruction and to survive and proliferate inside macrophages (Guirado et al., 2013). Hence, macrophage responses need to be tightly controlled in order to eliminate the pathogen. Transcriptional enhancers have emerged as major determinants of gene expression programmes in virtually all cell-types, including macrophages. Enhancers are defined as *cis*-regulatory DNA regions that activate transcription of target genes in a distance- and orientation-independent manner (Shlyueva et al., 2014). Enhancers have been found to be extremely widespread, with an estimation of up to one million enhancers in mammalian genomes, and are required for establishing cell-type specificity and mediating cellular responses to extracellular signals (Kieffer-Kwon et al., 2013; W. Li et al., 2016; Romanoski et al., 2015; G. D. Thomas et al., 2016). Nevertheless, the role of enhancers in mediating macrophage responses to *M.tb* infection remains unexplored.

In this study, we analysed how transcriptional changes in *M.tb*-infected macrophages were driven by transcribed enhancers. We found that transcribed enhancers had a strong influence in the infection response and mediated up-regulation of many important immune protein-coding genes. The strongest macrophage response to *M.tb* was observed at 4 h post infection, hence, we elected to focus on DEGs up-regulated at this time point and to analyse their associated enhancers. We characterised highly transcriptionally induced enhancers and showed that many genes acquired *de novo* transcribed enhancers

upon *M.tb* infection. We report enhancers targeting known immune genes crucial for the genetic response of the host to *M.tb* and highlight transcription factors that are likely regulating these enhancers. These findings are extended by highlighting particular chromosomal domains carrying groups of highly transcriptionally induced enhancers and genes with previously unappreciated roles in *M.tb* infection.

Previously we have demonstrated that regulation by many enhancers was a concomitant of higher gene expression and tissue-specific functions (see Chapter 3), in agreement with a model of additive enhancer action (Chepelev et al., 2012; Shlyueva et al., 2014). Unexpectedly, here we report a similar observation for a highly function-specific set of DEGs up-regulated upon *M.tb* infection. Among these DEGs, the genes associated with more enhancers showed higher expression and more immune-specific functions, which indicates that enhancers play major roles in the macrophage response to *M.tb*.

Furthermore, our results indicate that activation of SEs might have a prominent role in regulation of macrophage responses to the pathogen. First, among all up-regulated DEGs, those associated with SEs showed the highest expression levels and strongest enrichment for immune-related functions. Second, we found that *M.tb*-induced enhancers were over-represented in SE regions. These observations are in line with our current understanding of SEs as genomic regions of extreme importance for the regulation of key genes involved in cell-specific processes and responses (Pott & Lieb, 2015; Witte et al., 2015).

Previous studies have reported on enhancers that were activated *de novo* upon stimuli. These might represent a particularly functionally important class of enhancers responsible for establishing stimuli-specific gene expression programmes. Ostuni et al. (2013) uncovered a set of latent enhancers that lacked any enhancer characteristics in

naïve mouse macrophages, but gained active enhancer marks in response to stimulation. Similarly, Kaikkonen et al. (2013) identified enhancers activated *de novo* in mouse macrophages stimulated with TLR4 agonist and, interestingly, suggested that eRNA transcription might precede H3K4me1 deposition. In this study, we asked whether any enhancers were non-transcribed in naïve macrophages and acquired *de novo* eRNA transcription upon *M.tb* infection. Interestingly, in contrast to Ostuni et al. (2013) and Kaikkonen et al. (2013), we found that most of the acquired enhancers might be already marked with H3K4me1 (hence, primed) in naïve macrophages. The remaining 60 of 356 enhancers might acquire both a H3K4me1 mark and transcriptional activity upon infection. In agreement with this idea, all 60 enhancers carried H3K4me1 histone marks in LPS-treated macrophages. Moreover, we found that 63.8% of acquired enhancers overlap H3K27ac histone marks in untreated macrophages. This is an unexpectedly large percentage, since H3K27ac is believed to demarcate active enhancers. One possible explanation is that H3K27ac-marked enhancers might have a spectrum of activation states, including those with and without eRNA production. In agreement with this hypothesis, we observe a much stronger H3K27ac enrichment in regions overlapping acquired enhancers in LPS-treated as compared to untreated macrophages. Hence, the strength of H3K27ac enrichment rather than the presence or absence of this histone mark could demarcate actively transcribed enhancers.

Our findings indicate that up-regulated genes in *M.tb*-infected macrophages might acquire *de novo* transcribed enhancers in addition to already established actively transcribed enhancers. We hypothesise that acquired enhancers might be involved in regulating their target genes via at least two different mechanisms. First, activation of acquired enhancers might involve considerable rearrangement of chromatin to allow formation of novel DNA loops between enhancers and their target promoters. Indeed,

examples of stimuli-driven dynamical changes in chromatin conformation in mouse macrophages were reported recently (Mukhopadhyay et al., 2014). A second hypothetical mechanism would involve the transcriptional activation of enhancers within pre-established chromatin loops. We found that acquired enhancers are often surrounded by other enhancers that are transcribed in naïve macrophages, including *M.tb*-induced enhancers. The fact that these enhancers, at least in some cases, are located close to each other and within SEs points to a hypothetical regulatory mechanism that involves an expansion of active enhancer regions. For instance, a few individual enhancers within a SE might be primed and generate low levels of eRNAs in naïve macrophages, while upon *M.tb* infection these individual enhancers could serve as 'seeds', and, ultimately, broader neighbour regions might acquire enhancer histone marks and stronger eRNA transcription. Such a phenomenon has been described in mouse stem cells, where seed enhancers were shown to expand into super enhancers (Factor et al., 2014). Similarly, a seed enhancer required for activation of a super enhancer has been reported in mammary glands (Shin et al., 2016). However, the associated mechanisms and abundances of such seed enhancers remain to be elucidated.

Signalling pathways regulating macrophage responses to infection have been extensively studied, and here we report *M.tb*-induced enhancers which might activate these pathways. We find that induced enhancers extensively control Tnf and NF-κB signalling pathways by targeting their components, starting from receptors (Cd14 and Cd40) and ligands (Il1b, Tnfrsf1b, Tnf), through mediators (Traf5, Irak2, Jak2, Malt1, Ripk2, and Src), ending with TFs (Nfkb1 and Rela) and numerous pathway effectors. These pathways are known to be activated upon macrophage recognition of *M.tb* and play central roles in shaping immune responses, as they mediate production of pro-inflammatory cytokines and chemokines, and regulate apoptosis (Mogensen, 2009; Wada & Penninger,

2004). Interestingly, induced enhancers also control negative feedback regulators of these pathways (Nfkbia, Tnfaip3, and Socs3), which might implicate induced enhancers in terminating the immune response.

As important examples, we highlighted genes regulated by multiple induced or acquired enhancers. We also reported TADs where induced enhancers were over-represented, as these chromosomal regions could be considerably affected by *M.tb*. Notably, in this manner we highlighted a group of genes that might be decisive in *M.tb* death versus survival balance via different mechanisms. Knowledge of regulation of these genes is extremely important for understanding *M.tb* survival strategies and the development of novel treatments. For instance, Cd38, targeted by induced enhancers, regulates the response of mouse macrophages to at least one intracellular pathogen, *Listeria monocytogenes* (Botta et al., 2014) and was shown to be involved in phagocytosis (Kang et al., 2012). Once internalised, *M.tb* is trapped in host phagosomes, where it is supposed to be ultimately eliminated (Hmama et al., 2015). For this to happen, phagosomes must undergo maturation processes and fusions with lysosomes which result in acidification and acquisition of microbicidal factors (Hmama et al., 2015). The Eea1 gene, regulated by induced enhancers, was shown to be crucial for phagosomal maturation (Kinchen & Ravichandran, 2008). Moreover, via inhibition of Eea1 recruitment, *M.tb* can interfere with phagosomal maturation and survive inside host macrophages (Fratti et al., 2001). Another gene important for *M.tb* killing is Irg1, regulated by induced enhancers. Irg1 was recently shown to encode an enzyme that produces itaconic acid, a metabolite with a strong antimicrobial activity, that can inhibit the growth of *M.tb* (Michelucci et al., 2013). In contrast, Hilpda, regulated by induced enhancers, might contribute to *M.tb* survival within the host. Hilpda was shown to induce lipid accumulation in mouse macrophages (Maier et al., 2017), and these lipids can be used by *M.tb* as a source of energy

(Daniel et al., 2011). These genes with known immune functions are often co-regulated with DEGs with previously unappreciated functions in *M.tb* infection response (such as Fbxl3, Cln5, Tapt1, Edn1, and Hivep1), and these DEGs are, thus, good candidates for further *in vitro* functional studies.

In addition to the aforementioned survival strategies, *M.tb* is known to control macrophage cell death pathways and existing evidence suggests that *M.tb* might induce necroptosis, which facilitates the spread of the pathogen (Amaral et al., 2016). We found that induced enhancers might extensively regulate Tnfrsf1b, which is known to interfere with apoptosis and sensitise macrophages for Tnfr1-mediated necroptosis (Balcewicz-Sablinska et al., 1998; Siegmund et al., 2016). Seven additional genes regulated by induced enhancers (Il1a, Il1b, Jak2, Pla2g4a, Tnf, Tnfaip3 and Traf5) map to the "Necroptosis" KEGG pathway map, hence, their associated enhancers might contribute to the activation of this process.

Finally, we investigated the transcriptional regulation of induced and acquired enhancers. We identified TFs with binding sites significantly over-represented in these enhancer sets. Importantly, most of these TFs are known to be activated in response to infection, for instance, via Toll-like and Nod-like receptors upon recognition of the pathogen. These findings provide a mechanistic link between *M.tb* infection and transcriptional activation of enhancers which mediate up-regulation of immune genes. Interestingly, we found that most of the TFBS motifs over-represented in induced enhancers were also over-represented in promoters of their target genes, indicating co-regulatory mechanisms of enhancer and promoter transcription by the same cellular machinery. There were, however, three exceptions, as Rbpj, Nfe2l2 and Jdp2 TFs were over-represented in the enhancer but not promoter regions, possibly mediating enhancer-specific transcriptional regulation of *M.tb* responses.

One of the crucial areas of TB research is the development of novel strategies for host-directed therapies, which can stimulate host antimicrobial pathways and suppress host subversion by *M.tb* (Kiran, Podell, Chambers, & Basaraba, 2016; Wallis & Hafner, 2015). Targeting disease-specific enhancers has been investigated as a therapeutic approach in cancer and autoimmune diseases (Loven et al., 2013; Peeters et al., 2015). In this study, we show that both acquired and induced enhancers regulate immune genes, which are crucial for *M.tb* survival versus elimination balance. Moreover, transcriptional activity of these enhancers is characterised by a high macrophage- and infection-specificity. Hence, these enhancers are likely good candidate regulatory genomic regions for targeted manipulation of macrophage responses to *M.tb* infection.

4.4. Limitations

SE regions used in this study were inferred in macrophages stimulated by LPS (Hah et al., 2015), due to the lack of a comparable data set for *M.tb* infection. LPS (lipopolysaccharide) represents a component of bacterial membranes which is recognised by host and triggers a strong immune anti-bacterial response (Alexander & Rietschel, 2001). A major component of *M.tb* cell wall, lipoarabinomannan, differs from LPS, but its immune recognition seems to resemble that of LPS (van Crevel et al., 2002). Therefore, although LPS treatment represents a good approximation for our study, certain differences can be expected to exist.

We focused on DEGs with significant and strong up-regulation, enhancers with the highest induction rates, and top enriched pathways. Such an approach might result in certain potentially functional and interesting genes and pathways being overlooked. However, given that this is the first, to our knowledge, study of transcribed enhancer

regulation in *M.tb*-infected macrophages, we aimed at outlining the most influential transcriptional changes. Future studies may take the results presented here and analyse in more detail enhancer-gene interactions.

We separately considered two overlapping subsets of enhancers: acquired and induced enhancers. The identification was based on eRNA expression levels before and after *M.tb* infection. However, it is important to note that there is a narrow margin separating these classes, which is influenced by the limits of expression versus noise detection by CAGE and by our sample composition. In other settings, the composition of these classes might differ from our results. For instance, some induced enhancers showed very low (close to zero) eRNA expression in non-infected macrophages, which could be, alternatively, attributed to transcriptional noise.

A more natural strategy, alternative to our approach for identifying induced enhancers, would be to calculate statistically differentially expressed eRNAs. However, due to low levels of eRNA expression and low numbers of biological replicates, the differential expression analysis yielded no statistically significant findings in most cases, making this approach not viable.

We specifically investigated DEGs regulated by many induced or acquired enhancers, as we reasoned that these genes are likely extremely important for the host response to *M.tb*. Regulation of the same gene by multiple enhancers has been described as a model of additive enhancer action and has been connected to the functional importance and high expression levels of target genes (Chepelev et al., 2012; Denisenko et al., 2017; Shlyueva et al., 2014). There are several considerations regarding this idea. First, many enhancers might be needed to achieve high transcriptional output of a gene. Second, many enhancers might be needed to ensure robust and reliable transcriptional control of key functional

genes (Osterwalder et al., 2018). Third, most of the existing data on enhancer regulation does not come from single cell profiling and we typically observe a snapshot of multiple cells, hence, the reported enhancers might actually regulate the same gene in different cells of the same population. Further studies are needed to distinguish between these possibilities, however, they are likely to co-exist.

4.5. Conclusions

M.tb triggers extensive changes in macrophage gene expression programme that are decisive for the infection outcome, yet the associated regulatory mechanisms remain largely unknown. This is the first to our knowledge study of the role of transcribed enhancers in macrophage response to *M.tb* infection. It extends current understanding of the regulation of *M.tb* responses by linking *M.tb*-responsive transcription factors to activation of transcribed enhancers, which, in turn, target protein-coding immune genes upon infection. Given the increasing promise for enhancer- and chromatin-directed therapy, this work paves the way for further targeted studies towards the host-directed therapy and novel tuberculosis treatments.

4.6. Materials and methods

4.6.1. Data

Here, the analyses were performed for a subset of 184 BMDM samples that were used in Chapter 3. This subset included infected non-stimulated macrophages profiled at 4, 12, 24, and 48 hours post infection (i.e. 28, 36, 48, and 72 h post stimulation, see **Table 3.5**), as well as non-infected untreated BMDM as controls.

4.6.2. Enhancer and promoter sets

Enhancer and promoter sets were obtained as in Chapter 3. However, of all BMDM enhancer-gene associations established in Chapter 3, we here sub-selected only those with a positive Spearman's correlation of eRNA and gene expression in infected macrophages.

4.6.3. Differential expression analysis

Differential gene expression analyses were performed using the exact test implemented in edgeR (M. D. Robinson et al., 2010). Four macrophage samples profiled prior to infection (0 h) were used as a control. The p-values were adjusted for multiple hypothesis testing using the Benjamini-Hochberg procedure (Benjamini & Hochberg, 1995). FDR ≤ 0.05 and $\log_2$ fold change > 1 (< -1) thresholds were used to select differentially expressed up- (down-) regulated genes (DEGs).

4.6.4. *M.tb*-induced and acquired enhancers

M.tb-induced enhancers were selected among those associated with DEGs up-regulated at 4 h post infection. Mean eRNA expression for these enhancers in infected macrophages at 4 h and its fold change as compared to 0 h were calculated. Enhancers were defined as induced, if both these values were in the upper quartiles of their corresponding distributions.

Acquired enhancers were defined as those with no detectable eRNA expression in each of 22 non-infected non-stimulated BMDM samples (see **Table 3.5**), and nonzero expression in any of the infected non-stimulated macrophage samples.

4.6.5. TADs enriched for enhancers

To uncover chromosomal domains that might be important in macrophage response to *M.tb*, we identified TADs (Dixon et al., 2012) that were significantly enriched for induced enhancers. A hypergeometric test was performed for each TAD by comparing the total number of BMDM enhancers in that TAD to the subset of those deemed induced. The p-values for 1,228 TADs were corrected for multiple hypothesis testing using Benjamini-Hochberg procedure (Benjamini & Hochberg, 1995). TADs with FDR < 0.05 were selected as significantly enriched for induced enhancers.

4.6.6. Transcription factor binding analysis

TF binding profiles were downloaded from JASPAR database, 7th release, 2018 (Khan et al., 2017). The Clover programme (Frith et al., 2004) was used for identification of statistically over-represented motifs. Enhancer regions were tested against three background DNA sets: 1) the whole set of identified transcribed mouse enhancers; 2) the subset of enhancers not transcribed in macrophages; 3) a set of random genomic regions located within TADs excluding gaps, repeated sequences, Ensembl coding regions, and mouse enhancers identified here. Promoter regions were tested against three similarly defined sets: 1) all promoters expressed in mouse tissues; 2) a subset of those not expressed in macrophages; 3) the same set of random genomic regions as used for enhancers. Promoters were extended by 500 bp upstream and downstream for motif analysis. Motifs with p-value < 0.01 for each of the three background sets were selected as significantly over-represented. TFs that were significantly differentially up-regulated at 4 h post infection when compared to 0 h were retained.

4.6.7. Gene set enrichment analyses (GSEA)

KEGG pathway maps (Kanehisa & Goto, 2000) were used as sets of biological terms for GSEA. We used hypergeometric distribution to calculate the probability of obtaining the same or larger overlap between a gene set of interest and each biological term (Huang da et al., 2009). Derived p-values were corrected for multiple testing using Benjamini-Hochberg procedure (Benjamini & Hochberg, 1995). As a background, a set of 22,543 Ensembl protein-coding genes (version 75) was used (Flicek et al., 2011).

4.6.8. Tools

All analyses made extensive use of the Shell scripting language and the R software (http://www.R-project.org/) with the Bioconductor packages (Gentleman et al., 2004). Most of the figures were generated with ggplot2 package for R (Wickham, 2009).

All genomic regions used in the present work were either mapped to mm10 mouse genome or were converted from mm9 genomic coordinates to mm10 using the liftOver programme (https://genome.ucsc.edu/cgi-bin/hgLiftOver). All analyses made extensive use of the BEDTools utilities (Quinlan & Hall, 2010), including tools for identification of overlapping intervals and generating random genomic intervals. Genomic regions were visualised in a circular layout using the Circos software (Krzywinski et al., 2009).

Chapter 5

Concluding remarks

5.1. Summary of findings

In this thesis, we investigated *in silico* transcribed enhancers in mouse tissues and cell lines, with a particular focus on macrophages.

In Chapter 2, we have inferred transcribed enhancers in a large collection of mouse tissues on a genome-wide scale. In Chapter 3, we focused on enhancer-mediated transcriptional regulation in mouse macrophages. We used the enhancer regions inferred in Chapter 2 to identify high-confidence transcribed enhancers and to establish a reliable enhancer-target gene interactome in mouse macrophages. Using this interactome, we characterised the roles of enhancers in guiding macrophage activation and polarisation into distinct pro- and anti-inflammatory phenotypes. In Chapter 4, we further narrowed our focus down to a subset of macrophages infected with *M.tb* to perform the first to our knowledge study of the role of transcribed enhancers in macrophage response to *M.tb* infection.

Transcription of eRNAs shows a remarkable tissue- and stimuli-specificity. In Chapter 2, we observed a dramatic difference in numbers of transcribed enhancers per tissue. In Chapter 3, more than a half of actively transcribed BMDM enhancers were deemed macrophage specific. In addition, enhancers driving M(IFN-γ) and M(IL-4/IL-13) activation, as well as the corresponding regulatory interactions, showed high stimuli-specificity. In Chapter 4, *M.tb*-induced and acquired enhancers showed substantially higher eRNA expression in infected macrophages as compared to non-infected macrophages and other tissues. These results are in agreement with the current paradigm of enhancer specificity.

Genes regulated by many transcribed enhancers show distinct properties, when compared to genes associated with a few or no transcribed enhancers. In Chapter 2, we observed that candidate targets associated with many enhancers showed higher expression levels in all tested tissues. In Chapter 3, we used stricter criteria to infer more reliable enhancer target genes. Again, we found that genes regulated by many transcribed enhancers showed higher expression levels. Importantly, these genes also possessed more immune- and macrophage-related functions. Furthermore, unexpectedly, in Chapter 4 we found that even within such a process-oriented set as the list of up-regulated DEGs, multiple enhancers regulated the most highly expressed and functionally important genes. Hence, enhancers can contribute additively to expression of their target genes, and multiple enhancers might be important for fine-tuned and redundant control of cell specialisation and cell-specific responses. Indeed, according to a recent study, enhancer redundancy prevents deleterious consequences of loss-of-function mutations in individual enhancers (Osterwalder et al., 2018).

Enhancers play important roles in macrophage responses to changing environmental conditions. In Chapter 3, cytokine stimulation had a striking impact on enhancer

transcription, and our findings highlight the importance of enhancers in macrophage activation. In Chapter 4, transcribed enhancers had a strong influence in the infection response and mediated up-regulation of many important immune protein-coding genes. In addition, we identified enhancers which specifically acquired transcriptional activity *de novo* upon infection.

Functional importance and specificity of transcribed enhancers makes them good candidate therapeutic targets. In Chapter 3, we have inferred transcribed enhancers which might drive macrophage M(IFN-γ) and M(IL-4/IL-13) activation. We individually investigated location and transcription of enhancers, which might specifically regulate known marker genes of these macrophage activation states. In Chapter 4, we reported enhancers regulating known immune genes, which are crucial for the genetic response of the host to *M.tb*. Hence, these enhancers might be potential therapeutic targets for treatment of tuberculosis or other diseases with important roles of macrophages, such as autoimmune diseases and cancer.

Finally, our results provide new insights into possible mechanisms of action of transcribed enhancers. We highlighted immune TFs which might mediate enhancer transcription, and showed that many of these TFs likely also regulate enhancer target genes, whereas a few might specifically regulate enhancers only. We found that genes seem to acquire *de novo* transcribed enhancers in addition to already established ones. Our results indicate that activation of SEs might have a prominent role in the regulation of macrophage responses to the pathogen and might start with the activity of individual 'seed' enhancers, further expanding to the whole SE region.

5.2. Future directions

Many more aspects of transcriptional control by transcribed enhancers are yet to be investigated. It seems reasonable to list the experimental verification of our results as a task of first priority. Indeed, here we have reported multiple findings, regarding both genome-level properties of enhancers, and individual enhancers regulating particular genes under particular conditions. These findings are essentially predictions, which were based on a set of assumptions of our methodology. Hence, experiments designed to test these predictions are of primary importance. Such experiments could not only verify the individual predictions, but also would prove the reliability of our approach and would justify the assumptions made here.

Once verified, our approach could further be applied to extend the present findings in macrophages. Indeed, of the macrophage data available to us, we did not study enhancer regulation in macrophages stimulated by a single interleukin – either IL-4 or IL-13. Such study would be of interest to uncover regulatory mechanisms of macrophage responses to the individual cytokines and their combination. Another prominent direction would be the investigation of enhancer regulation in infected macrophages that were cultivated under different conditions. Indeed, here we focused on untreated infected macrophages solely, whereas the data for infected M(IFN-γ), M(IL-4/IL-13), M(IL-4) and M(IL-13) macrophages are available. M(IFN-γ) are pro-inflammatory macrophages able to eliminate *M.tb*. M(IL-4/IL-13), M(IL-4), and M(IL-13) on the other hand, can serve as a niche for *M.tb* survival and proliferation. *M.tb* interferes with macrophage polarisation towards pro-inflammatory phenotypes and induces M(IL-4/IL-13)-like anti-inflammatory phenotypes. Hence, investigation into enhancer regulation of *M.tb* response in these

functionally opposed macrophage phenotypes could shed light on *M.tb* survival mechanisms and offer strategies for their suppression.

One highly important direction of further research would be feasible once additional kinds of data become available for mouse macrophages. For instance, data from 3C-based technologies would provide valuable information on physical proximity of genomic regions. It could be of use for verification of predicted enhancer target genes, and importantly, for studying the molecular mechanisms of enhancer regulation, such as chromatin remodelling upon stimulation.

In addition, further studies interesting in the context of this work could, for instance, investigate whether enhancers are involved in regulation of non-protein-coding genes, such as those transcribed into long non-coding RNAs. Alternatively, studies aiming at uncovering the differences between enhancer regulation in mouse and human macrophages would be of interest. Generally speaking, enhancer biology seems still to be in its infancy, and many more studies are needed to uncover the functional importance of eRNAs, the differences between transcribed and non-transcribed enhancers and their abundance, the properties of unidirectionally and bidirectionally transcribed enhancers, the full spectrum of enhancer-specific chromatin signatures, as well as the complete list of other distinctive properties and mechanisms associated with enhancers.

5.3. Outlook

Spatiotemporal control of gene transcription is crucial for all processes in a living organism, such as differentiation, development, homeostasis, and response to environmental changes.

The explosive growth of next-generation sequencing technologies has greatly advanced our understanding of genome organisation and regulation. Protein-coding genes used to be viewed as the most important part of the genome and the remainder was considered as non-functional DNA. High-throughput studies have overturned this theory showing the importance of non-coding DNA in regulation (The ENCODE Project Consortium, 2012). Moreover, the mammalian genome was found to be pervasively transcribed into non-coding RNAs of various classes (Djebali et al., 2012). Another unexpected discovery was made in genome-wide association studies, which have indicated that trait- and disease-associated variants are mostly located outside protein-coding regions (Farh et al., 2015; Maurano et al., 2012). These insights attracted an increased interest to non-coding regulatory DNA regions.

Since their discovery more than 30 years ago, enhancers have been viewed and studied primarily as a separate class of *cis*-regulatory DNA elements. However, recent findings suggest that this conception might require a reconsideration. Many enhancers are transcribed into potentially functional lncRNAs (Hon et al., 2017), blurring the differences between classes of non-coding RNAs. Intragenic enhancers can serve as alternative promoters of protein-coding genes (Kowalczyk et al., 2012). Furthermore, some researchers argue that enhancers and promoters share multiple common properties in terms of both architecture and function (Andersson, 2015; Andersson, Sandelin, & Danko, 2015; Kim & Shiekhattar, 2015). Indeed, they bind TFs, initiate transcription and can enhance transcription initiated from other promoters. It was suggested that enhancers and promoters might be viewed as a single class of DNA elements, with their exact activity being determined by genomic context (Andersson, 2015; Andersson et al., 2015; Kim & Shiekhattar, 2015). On the other hand, a recent study measuring enhancer and promoter activity of various DNA elements indicates that their balance might be pre-defined by

genomic sequence of the element (Mikhaylichenko et al., 2018). Either way, this prominent area of genome biology is being actively investigated, and future insights might bring a new paradigm shift.

Bibliography

Alexander, C., & Rietschel, E. T. (2001). Bacterial lipopolysaccharides and innate immunity. *Journal of Endotoxin Research, 7*(3), 167-202.

Allen, B. L., & Taatjes, D. J. (2015). The Mediator complex: a central integrator of transcription. *Nature Reviews: Molecular Cell Biology, 16*(3), 155-166. doi:10.1038/nrm3951

Amaral, E. P., Lasunskaia, E. B., & D'Imperio-Lima, M. R. (2016). Innate immunity in tuberculosis: how the sensing of mycobacteria and tissue damage modulates macrophage death. *Microbes Infect, 18*(1), 11-20. doi:10.1016/j.micinf.2015.09.005

Andersson, R. (2015). Promoter or enhancer, what's the difference? Deconstruction of established distinctions and presentation of a unifying model. *Bioessays, 37*(3), 314-323. doi:10.1002/bies.201400162

Andersson, R., Gebhard, C., Miguel-Escalada, I., Hoof, I., Bornholdt, J., Boyd, M., . . . Sandelin, A. (2014). An atlas of active enhancers across human cell types and tissues. *Nature, 507*(7493), 455-461. doi:10.1038/nature12787

Andersson, R., Sandelin, A., & Danko, C. G. (2015). A unified architecture of transcriptional regulatory elements. *Trends in Genetics, 31*(8), 426-433. doi:10.1016/j.tig.2015.05.007

Arango Duque, G., & Descoteaux, A. (2014). Macrophage cytokines: involvement in immunity and infectious diseases. *Front Immunol, 5*, 491. doi:10.3389/fimmu.2014.00491

Arner, E., Daub, C. O., Vitting-Seerup, K., Andersson, R., Lilje, B., Drablos, F., . . . Hayashizaki, Y. (2015). Transcribed enhancers lead waves of coordinated transcription in transitioning mammalian cells. *Science, 347*(6225), 1010-1014. doi:10.1126/science.1259418

Ashburner, M., Ball, C. A., Blake, J. A., Botstein, D., Butler, H., Cherry, J. M., . . . Sherlock, G. (2000). Gene ontology: tool for the unification of biology. The Gene Ontology Consortium. *Nature Genetics, 25*(1), 25-29. doi:10.1038/75556

Baer, C. E., Rubin, E. J., & Sassetti, C. M. (2015). New insights into TB physiology suggest untapped therapeutic opportunities. *Immunological Reviews, 264*(1), 327-343. doi:10.1111/imr.12267

Bakalova, R., Ewis, A., & Baba, Y. (2006). Microarray-Based Technology: Basic Principles, Advantages and Limitations. *Reviews in Cell Biology and Molecular Medicine*: Wiley-VCH Verlag GmbH & Co. KGaA.

Balcewicz-Sablinska, M. K., Keane, J., Kornfeld, H., & Remold, H. G. (1998). Pathogenic *Mycobacterium tuberculosis* evades apoptosis of host macrophages by release of TNF-R2, resulting in inactivation of TNF-alpha. *Journal of Immunology, 161*(5), 2636-2641.

Balwierz, P. J., Carninci, P., Daub, C. O., Kawai, J., Hayashizaki, Y., Van Belle, W., . . . van Nimwegen, E. (2009). Methods for analyzing deep sequencing expression data:

constructing the human and mouse promoterome with deepCAGE data. *Genome Biol, 10*(7), R79. doi:10.1186/gb-2009-10-7-r79
Banerji, J., Rusconi, S., & Schaffner, W. (1981). Expression of a beta-globin gene is enhanced by remote SV40 DNA sequences. *Cell, 27*(2 Pt 1), 299-308.
Bartel, D. P. (2004). MicroRNAs: genomics, biogenesis, mechanism, and function. *Cell, 116*(2), 281-297.
Beagrie, R. A., & Pombo, A. (2016). Gene activation by metazoan enhancers: Diverse mechanisms stimulate distinct steps of transcription. *Bioessays, 38*(9), 881-893. doi:10.1002/bies.201600032
Behar, S. M., Divangahi, M., & Remold, H. G. (2010). Evasion of innate immunity by *Mycobacterium tuberculosis*: is death an exit strategy? *Nature Reviews: Microbiology, 8*(9), 668-674. doi:10.1038/nrmicro2387
Benjamini, Y., & Hochberg, Y. (1995). Controlling the false discovery rate: a practical and powerful approach to multiple testing. *Journal of the Royal Statistical Society. Series B (Methodological), 57*(1), 289-300. doi:10.2307/2346101
Birnbaum, R. Y., Clowney, E. J., Agamy, O., Kim, M. J., Zhao, J., Yamanaka, T., . . . Ahituv, N. (2012). Coding exons function as tissue-specific enhancers of nearby genes. *Genome Research, 22*(6), 1059-1068. doi:10.1101/gr.133546.111
Bonasio, R., & Shiekhattar, R. (2014). Regulation of transcription by long noncoding RNAs. *Annual Review of Genetics, 48*, 433-455. doi:10.1146/annurev-genet-120213-092323
Bonn, S., Zinzen, R. P., Girardot, C., Gustafson, E. H., Perez-Gonzalez, A., Delhomme, N., . . . Furlong, E. E. (2012). Tissue-specific analysis of chromatin state identifies temporal signatures of enhancer activity during embryonic development. *Nature Genetics, 44*(2), 148-156. doi:10.1038/ng.1064
Borukhov, S., & Nudler, E. (2008). RNA polymerase: the vehicle of transcription. *Trends in Microbiology, 16*(3), 126-134. doi:10.1016/j.tim.2007.12.006
Botta, D., Rivero-Nava, L., & Lund, F. (2014). The NAD glycohydrolase CD38 regulates macrophage effector function and defense against *Listeria monocytogenes*. (INC7P.409). *The Journal of Immunology, 192*(1 Supplement), 186.110.
Brenner, D., Blaser, H., & Mak, T. W. (2015). Regulation of tumour necrosis factor signalling: live or let die. *Nature Reviews: Immunology, 15*(6), 362-374. doi:10.1038/nri3834
Calo, E., & Wysocka, J. (2013). Modification of enhancer chromatin: what, how, and why? *Molecular Cell, 49*(5), 825-837. doi:10.1016/j.molcel.2013.01.038
Carlson, M. (2015). GO.db: A set of annotation maps describing the entire Gene Ontology. (R package version 3.2.2).
Carninci, P., Kasukawa, T., Katayama, S., Gough, J., Frith, M. C., Maeda, N., . . . Hayashizaki, Y. (2005). The transcriptional landscape of the mammalian genome. *Science, 309*(5740), 1559-1563. doi:10.1126/science.1112014
Carninci, P., Sandelin, A., Lenhard, B., Katayama, S., Shimokawa, K., Ponjavic, J., . . . Hayashizaki, Y. (2006). Genome-wide analysis of mammalian promoter architecture and evolution. *Nature Genetics, 38*(6), 626-635. doi:10.1038/ng1789
Cheng, J. H., Pan, D. Z., Tsai, Z. T., & Tsai, H. K. (2015). Genome-wide analysis of enhancer RNA in gene regulation across 12 mouse tissues. *Scientific Reports, 5*, 12648. doi:10.1038/srep12648
Chepelev, I., Wei, G., Wangsa, D., Tang, Q., & Zhao, K. (2012). Characterization of genome-wide enhancer-promoter interactions reveals co-expression of interacting genes and modes of higher order chromatin organization. *Cell Research, 22*(3), 490-503. doi:10.1038/cr.2012.15

Cinghu, S., Yang, P., Kosak, J. P., Conway, A. E., Kumar, D., Oldfield, A. J., . . . Jothi, R. (2017). Intragenic enhancers attenuate host gene expression. *Molecular Cell, 68*(1), 104-117.e106. doi:10.1016/j.molcel.2017.09.010

Cloonan, N., Forrest, A. R., Kolle, G., Gardiner, B. B., Faulkner, G. J., Brown, M. K., . . . Grimmond, S. M. (2008). Stem cell transcriptome profiling via massive-scale mRNA sequencing. *Nature Methods, 5*(7), 613-619. doi:10.1038/nmeth.1223

Core, L. J., Martins, A. L., Danko, C. G., Waters, C. T., Siepel, A., & Lis, J. T. (2014). Analysis of nascent RNA identifies a unified architecture of initiation regions at mammalian promoters and enhancers. *Nature Genetics, 46*(12), 1311-1320. doi:10.1038/ng.3142

Core, L. J., Waterfall, J. J., & Lis, J. T. (2008). Nascent RNA sequencing reveals widespread pausing and divergent initiation at human promoters. *Science, 322*(5909), 1845-1848. doi:10.1126/science.1162228

Correa, A. F., Bailao, A. M., Bastos, I. M., Orme, I. M., Soares, C. M., Kipnis, A., . . . Junqueira-Kipnis, A. P. (2014). The endothelin system has a significant role in the pathogenesis and progression of *Mycobacterium tuberculosis* infection. *Infection and Immunity, 82*(12), 5154-5165. doi:10.1128/iai.02304-14

Creyghton, M. P., Cheng, A. W., Welstead, G. G., Kooistra, T., Carey, B. W., Steine, E. J., . . . Jaenisch, R. (2010). Histone H3K27ac separates active from poised enhancers and predicts developmental state. *Proceedings of the National Academy of Sciences, USA, 107*(50), 21931-21936. doi:10.1073/pnas.1016071107

Daniel, J., Maamar, H., Deb, C., Sirakova, T. D., & Kolattukudy, P. E. (2011). *Mycobacterium tuberculosis* uses host triacylglycerol to accumulate lipid droplets and acquires a dormancy-like phenotype in lipid-loaded macrophages. *PLoS Pathog, 7*(6), e1002093. doi:10.1371/journal.ppat.1002093

Dartois, V. (2014). The path of anti-tuberculosis drugs: from blood to lesions to mycobacterial cells. *Nature Reviews: Microbiology, 12*(3), 159-167. doi:10.1038/nrmicro3200

Davies, L. C., & Taylor, P. R. (2015). Tissue-resident macrophages: then and now. *Immunology, 144*(4), 541-548. doi:10.1111/imm.12451

De Santa, F., Barozzi, I., Mietton, F., Ghisletti, S., Polletti, S., Tusi, B. K., . . . Natoli, G. (2010). A large fraction of extragenic RNA Pol II transcription sites overlap enhancers. *PLoS Biology, 8*(5), e1000384. doi:10.1371/journal.pbio.1000384

Dekker, J. (2008). Gene regulation in the third dimension. *Science, 319*(5871), 1793-1794. doi:10.1126/science.1152850

Dekker, J., Rippe, K., Dekker, M., & Kleckner, N. (2002). Capturing chromosome conformation. *Science, 295*(5558), 1306-1311. doi:10.1126/science.1067799

Denisenko, E., Guler, R., Mhlanga, M. M., Suzuki, H., Brombacher, F., & Schmeier, S. (2017). Genome-wide profiling of transcribed enhancers during macrophage activation. *Epigenetics & Chromatin, 10*(1), 50. doi:10.1186/s13072-017-0158-9

Denisenko, E., Ho, D., Tamgue, O., Ozturk, M., Suzuki, H., Brombacher, F., . . . Schmeier, S. (2016). IRNdb: the database of immunologically relevant non-coding RNAs. *Database, 2016*, baw138. doi:10.1093/database/baw138

Dixon, J. R., Selvaraj, S., Yue, F., Kim, A., Li, Y., Shen, Y., . . . Ren, B. (2012). Topological domains in mammalian genomes identified by analysis of chromatin interactions. *Nature, 485*(7398), 376-380. doi:10.1038/nature11082

Djebali, S., Davis, C. A., Merkel, A., Dobin, A., Lassmann, T., Mortazavi, A., . . . Gingeras, T. R. (2012). Landscape of transcription in human cells. *Nature, 489*(7414), 101-108. doi:10.1038/nature11233

Draghici, S., Khatri, P., Eklund, A. C., & Szallasi, Z. (2006). Reliability and reproducibility issues in DNA microarray measurements. *Trends in Genetics, 22*(2), 101-109. doi:10.1016/j.tig.2005.12.005

Dryden, N. H., Broome, L. R., Dudbridge, F., Johnson, N., Orr, N., Schoenfelder, S., . . . Fletcher, O. (2014). Unbiased analysis of potential targets of breast cancer susceptibility loci by Capture Hi-C. *Genome Research, 24*(11), 1854-1868. doi:10.1101/gr.175034.114

Ernst, J. D. (2012). The immunological life cycle of tuberculosis. *Nature Reviews Immunology, 12*(8), 581-591. doi:10.1038/nri3259

Factor, D. C., Corradin, O., Zentner, G. E., Saiakhova, A., Song, L., Chenoweth, J. G., . . . Tesar, P. J. (2014). Epigenomic comparison reveals activation of 'seed' enhancers during transition from naive to primed pluripotency. *Cell stem cell, 14*(6), 854-863. doi:10.1016/j.stem.2014.05.005

Farh, K. K., Marson, A., Zhu, J., Kleinewietfeld, M., Housley, W. J., Beik, S., . . . Bernstein, B. E. (2015). Genetic and epigenetic fine mapping of causal autoimmune disease variants. *Nature, 518*(7539), 337-343. doi:10.1038/nature13835

Flicek, P., Amode, M. R., Barrell, D., Beal, K., Brent, S., Chen, Y., . . . Searle, S. M. (2011). Ensembl 2011. *Nucleic Acids Research, 39*(Database issue), D800-D806. doi:10.1093/nar/gkq1064

Fontana, M. F., Baccarella, A., Pancholi, N., Pufall, M. A., Herbert, D. R., & Kim, C. C. (2015). JUNB is a key transcriptional modulator of macrophage activation. *Journal of Immunology, 194*(1), 177-186. doi:10.4049/jimmunol.1401595

Forrest, A. R. R., Kawaji, H., Rehli, M., Baillie, J. K., de Hoon, M. J. L., Haberle, V., . . . Riken Pmi Clst, D. G. T. (2014). A promoter-level mammalian expression atlas. *Nature, 507*(7493), 462-470. doi:10.1038/nature13182

Fratti, R. A., Backer, J. M., Gruenberg, J., Corvera, S., & Deretic, V. (2001). Role of phosphatidylinositol 3-kinase and Rab5 effectors in phagosomal biogenesis and mycobacterial phagosome maturation arrest. *Journal of Cell Biology, 154*(3), 631-644. doi:10.1083/jcb.200106049

Frith, M. C., Fu, Y., Yu, L., Chen, J. F., Hansen, U., & Weng, Z. (2004). Detection of functional DNA motifs via statistical over - representation. *Nucleic Acids Research, 32*(4), 1372-1381. doi:10.1093/nar/gkh299

Frith, M. C., Valen, E., Krogh, A., Hayashizaki, Y., Carninci, P., & Sandelin, A. (2008). A code for transcription initiation in mammalian genomes. *Genome Research, 18*(1), 1-12. doi:10.1101/gr.6831208

Garber, M., Yosef, N., Goren, A., Raychowdhury, R., Thielke, A., Guttman, M., . . . Amit, I. (2012). A high-throughput chromatin immunoprecipitation approach reveals principles of dynamic gene regulation in mammals. *Molecular Cell, 47*(5), 810-822. doi:10.1016/j.molcel.2012.07.030

Gasteiger, G., D'Osualdo, A., Schubert, D. A., Weber, A., Bruscia, E. M., & Hartl, D. (2017). Cellular innate immunity: an old game with new players. *J Innate Immun, 9*(2), 111-125. doi:10.1159/000453397

Gaszner, M., & Felsenfeld, G. (2006). Insulators: exploiting transcriptional and epigenetic mechanisms. *Nature Reviews: Genetics, 7*(9), 703-713. doi:10.1038/nrg1925

Gentleman, R. C., Carey, V. J., Bates, D. M., Bolstad, B., Dettling, M., Dudoit, S., . . . Zhang, J. (2004). Bioconductor: open software development for computational biology and bioinformatics. *Genome Biol, 5*(10), R80. doi:10.1186/gb-2004-5-10-r80

Ghirlando, R., & Felsenfeld, G. (2016). CTCF: making the right connections. *Genes & Development, 30*(8), 881-891. doi:10.1101/gad.277863.116

Ghisletti, S., Barozzi, I., Mietton, F., Polletti, S., De Santa, F., Venturini, E., . . . Natoli, G. (2010). Identification and characterization of enhancers controlling the inflammatory gene expression program in macrophages. *Immunity, 32*(3), 317-328. doi:10.1016/j.immuni.2010.02.008

Ginhoux, F., & Guilliams, M. (2016). Tissue-resident macrophage ontogeny and homeostasis. *Immunity, 44*(3), 439-449. doi:10.1016/j.immuni.2016.02.024

Ginhoux, F., Schultze, J. L., Murray, P. J., Ochando, J., & Biswas, S. K. (2016). New insights into the multidimensional concept of macrophage ontogeny, activation and function. *Nature Immunology, 17*(1), 34-40. doi:10.1038/ni.3324

Gordon, S., & Martinez, F. O. (2010). Alternative activation of macrophages: mechanism and functions. *Immunity, 32*(5), 593-604. doi:10.1016/j.immuni.2010.05.007

Gordon, S., & Pluddemann, A. (2017). Tissue macrophages: heterogeneity and functions. *BMC Biology, 15*(1), 53. doi:10.1186/s12915-017-0392-4

Gorkin, D. U., Leung, D., & Ren, B. (2014). The 3D genome in transcriptional regulation and pluripotency. *Cell stem cell, 14*(6), 762-775. doi:10.1016/j.stem.2014.05.017

Gosselin, D., Link, V. M., Romanoski, C. E., Fonseca, G. J., Eichenfield, D. Z., Spann, N. J., . . . Glass, C. K. (2014). Environment drives selection and function of enhancers controlling tissue-specific macrophage identities. *Cell, 159*(6), 1327-1340. doi:10.1016/j.cell.2014.11.023

Griffith, J. W., Sokol, C. L., & Luster, A. D. (2014). Chemokines and chemokine receptors: positioning cells for host defense and immunity. *Annual Review of Immunology, 32*, 659-702. doi:10.1146/annurev-immunol-032713-120145

Guirado, E., Schlesinger, L., & Kaplan, G. (2013). Macrophages in tuberculosis: friend or foe. *Seminars in Immunopathology, 35*(5), 563-583. doi:10.1007/s00281-013-0388-2

Guler, R., Parihar, S. P., Savvi, S., Logan, E., Schwegmann, A., Roy, S., . . . Brombacher, F. (2015). IL-4Ralpha-dependent alternative activation of macrophages is not decisive for *Mycobacterium tuberculosis* pathology and bacterial burden in mice. *PLoS One, 10*(3), e0121070. doi:10.1371/journal.pone.0121070

Guo, Y., Xu, Q., Canzio, D., Shou, J., Li, J., Gorkin, D. U., . . . Wu, Q. (2015). CRISPR Inversion of CTCF sites alters genome topology and enhancer/promoter function. *Cell, 162*(4), 900-910. doi:10.1016/j.cell.2015.07.038

Hah, N., Benner, C., Chong, L. W., Yu, R. T., Downes, M., & Evans, R. M. (2015). Inflammation-sensitive super enhancers form domains of coordinately regulated enhancer RNAs. *Proceedings of the National Academy of Sciences, USA, 112*(3), E297-302. doi:10.1073/pnas.1424028112

Hah, N., Murakami, S., Nagari, A., Danko, C. G., & Kraus, W. L. (2013). Enhancer transcripts mark active estrogen receptor binding sites. *Genome Research, 23*(8), 1210-1223. doi:10.1101/gr.152306.112

Hantsche, M., & Cramer, P. (2016). The structural basis of transcription: 10 years after the Nobel prize in chemistry. *Angew Chem Int Ed Engl, 55*(52), 15972-15981. doi:10.1002/anie.201608066

Harvey, C. J., Thimmulappa, R. K., Sethi, S., Kong, X., Yarmus, L., Brown, R. H., . . . Biswal, S. (2011). Targeting Nrf2 signaling improves bacterial clearance by alveolar macrophages in patients with COPD and in a mouse model. *Sci Transl Med, 3*(78), 78ra32. doi:10.1126/scitranslmed.3002042

Hawn, T. R., Matheson, A. I., Maley, S. N., & Vandal, O. (2013). Host-directed therapeutics for tuberculosis: can we harness the host? *Microbiology and Molecular Biology Reviews, 77*(4), 608-627. doi:10.1128/mmbr.00032-13

Heintzman, N. D., Hon, G. C., Hawkins, R. D., Kheradpour, P., Stark, A., Harp, L. F., . . . Ren, B. (2009). Histone modifications at human enhancers reflect global cell-type-specific gene expression. *Nature, 459*(7243), 108-112. doi:10.1038/nature07829

Heintzman, N. D., Stuart, R. K., Hon, G., Fu, Y., Ching, C. W., Hawkins, R. D., . . . Ren, B. (2007). Distinct and predictive chromatin signatures of transcriptional promoters and enhancers in the human genome. *Nature Genetics, 39*(3), 311-318. doi:10.1038/ng1966

Heinz, S., Benner, C., Spann, N., Bertolino, E., Lin, Y. C., Laslo, P., . . . Glass, C. K. (2010). Simple combinations of lineage-determining transcription factors prime *cis*-regulatory elements required for macrophage and B cell identities. *Molecular Cell, 38*(4), 576-589. doi:10.1016/j.molcel.2010.05.004

Heinz, S., Romanoski, C. E., Benner, C., & Glass, C. K. (2015). The selection and function of cell type-specific enhancers. *Nature Reviews: Molecular Cell Biology, 16*(3), 144-154. doi:10.1038/nrm3949

Henriques, T., Scruggs, B. S., Inouye, M. O., Muse, G. W., Williams, L. H., Burkholder, A. B., . . . Adelman, K. (2018). Widespread transcriptional pausing and elongation control at enhancers. *Genes & Development*. doi:10.1101/gad.309351.117

Herbert, D. R., Holscher, C., Mohrs, M., Arendse, B., Schwegmann, A., Radwanska, M., . . . Brombacher, F. (2004). Alternative macrophage activation is essential for survival during schistosomiasis and downmodulates T helper 1 responses and immunopathology. *Immunity, 20*(5), 623-635.

Hmama, Z., Pena-Diaz, S., Joseph, S., & Av-Gay, Y. (2015). Immunoevasion and immunosuppression of the macrophage by *Mycobacterium tuberculosis*. *Immunological Reviews, 264*(1), 220-232.

Hnisz, D., Abraham, B. J., Lee, T. I., Lau, A., Saint-André, V., Sigova, A. A., . . . Young, R. A. (2013). Super-enhancers in the control of cell identity and disease. *Cell, 155*(4), 934-947. doi:10.1016/j.cell.2013.09.053

Hnisz, D., Schuijers, J., Lin, Charles Y., Weintraub, Abraham S., Abraham, Brian J., Lee, Tong I., . . . Young, Richard A. (2015). Convergence of developmental and oncogenic signaling pathways at transcriptional super-enhancers. *Molecular Cell, 58*(2), 362-370. doi:10.1016/j.molcel.2015.02.014

Holmqvist, P. H., & Mannervik, M. (2013). Genomic occupancy of the transcriptional co-activators p300 and CBP. *Transcription, 4*(1), 18-23. doi:10.4161/trns.22601

Hon, C. C., Ramilowski, J. A., Harshbarger, J., Bertin, N., Rackham, O. J., Gough, J., . . . Forrest, A. R. (2017). An atlas of human long non-coding RNAs with accurate 5' ends. *Nature, 543*(7644), 199-204. doi:10.1038/nature21374

Hsieh, C. L., Fei, T., Chen, Y. W., Li, T. T., Gao, Y. F., Wang, X. D., . . . Kantoff, P. W. (2014). Enhancer RNAs participate in androgen receptor-driven looping that selectively enhances gene activation. *Proceedings of the National Academy of Sciences of the United States of America, 111*(20), 7319-7324. doi:10.1073/pnas.1324151111

Huang da, W., Sherman, B. T., & Lempicki, R. A. (2009). Bioinformatics enrichment tools: paths toward the comprehensive functional analysis of large gene lists. *Nucleic Acids Research, 37*(1), 1-13. doi:10.1093/nar/gkn923

Hume, D. A. (2015). The many alternative faces of macrophage activation. *Front Immunol, 6*, 370. doi:10.3389/fimmu.2015.00370

Iqbal, J., & Zaidi, M. (2006). TNF regulates cellular NAD+ metabolism in primary macrophages. *Biochemical and Biophysical Research Communications, 342*(4), 1312-1318. doi:10.1016/j.bbrc.2006.02.109

Jablonski, K. A., Amici, S. A., Webb, L. M., Ruiz-Rosado, J. d. D., Popovich, P. G., Partida-Sanchez, S., & Guerau-de-Arellano, M. (2015). Novel markers to delineate murine

M1 and M2 macrophages. *PLoS One, 10*(12), e0145342. doi:10.1371/journal.pone.0145342

Jenkins, S. J., Ruckerl, D., Thomas, G. D., Hewitson, J. P., Duncan, S., Brombacher, F., . . . Allen, J. E. (2013). IL-4 directly signals tissue-resident macrophages to proliferate beyond homeostatic levels controlled by CSF-1. *Journal of Experimental Medicine, 210*(11), 2477-2491. doi:10.1084/jem.20121999

Jin, F., Li, Y., Dixon, J. R., Selvaraj, S., Ye, Z., Lee, A. Y., . . . Ren, B. (2013). A high-resolution map of the three-dimensional chromatin interactome in human cells. *Nature, 503*(7475), 290-294. doi:10.1038/nature12644

Kagey, M. H., Newman, J. J., Bilodeau, S., Zhan, Y., Orlando, D. A., van Berkum, N. L., . . . Young, R. A. (2010). Mediator and cohesin connect gene expression and chromatin architecture. *Nature, 467*(7314), 430-435. doi:10.1038/nature09380

Kahnert, A., Seiler, P., Stein, M., Bandermann, S., Hahnke, K., Mollenkopf, H., & Kaufmann, S. H. (2006). Alternative activation deprives macrophages of a coordinated defense program to *Mycobacterium tuberculosis*. *European Journal of Immunology, 36*(3), 631-647. doi:10.1002/eji.200535496

Kaikkonen, M. U., Spann, N. J., Heinz, S., Romanoski, C. E., Allison, K. A., Stender, J. D., . . . Glass, C. K. (2013). Remodeling of the enhancer landscape during macrophage activation is coupled to enhancer transcription. *Molecular Cell, 51*(3), 310-325. doi:10.1016/j.molcel.2013.07.010

Kanamori-Katayama, M., Itoh, M., Kawaji, H., Lassmann, T., Katayama, S., Kojima, M., . . . Hayashizaki, Y. (2011). Unamplified cap analysis of gene expression on a single-molecule sequencer. *Genome Research, 21*(7), 1150-1159. doi:10.1101/gr.115469.110

Kanehisa, M., & Goto, S. (2000). KEGG: kyoto encyclopedia of genes and genomes. *Nucleic Acids Research, 28*(1), 27-30.

Kang, J., Park, K. H., Kim, J. J., Jo, E. K., Han, M. K., & Kim, U. H. (2012). The role of CD38 in Fcgamma receptor (FcgammaR)-mediated phagocytosis in murine macrophages. *Journal of Biological Chemistry, 287*(18), 14502-14514. doi:10.1074/jbc.M111.329003

Karlstetter, M., Walczak, Y., Weigelt, K., Ebert, S., Van den Brulle, J., Schwer, H., . . . Langmann, T. (2010). The novel activated microglia/macrophage WAP domain protein, AMWAP, acts as a counter-regulator of proinflammatory response. *Journal of Immunology, 185*(6), 3379-3390. doi:10.4049/jimmunol.0903300

Karolchik, D., Hinrichs, A. S., Furey, T. S., Roskin, K. M., Sugnet, C. W., Haussler, D., & Kent, W. J. (2004). The UCSC Table Browser data retrieval tool. *Nucleic Acids Research, 32*(Database issue), D493-D496. doi:10.1093/nar/gkh103

Kawaji, H., Frith, M. C., Katayama, S., Sandelin, A., Kai, C., Kawai, J., . . . Hayashizaki, Y. (2006). Dynamic usage of transcription start sites within core promoters. *Genome Biol, 7*(12), R118. doi:10.1186/gb-2006-7-12-r118

Kensler, T. W., Wakabayashi, N., & Biswal, S. (2007). Cell survival responses to environmental stresses via the Keap1-Nrf2-ARE pathway. *Annual Review of Pharmacology and Toxicology, 47*, 89-116. doi:10.1146/annurev.pharmtox.46.120604.141046

Khan, A., Fornes, O., Stigliani, A., Gheorghe, M., Castro-Mondragon, J. A., van der Lee, R., . . . Mathelier, A. (2017). JASPAR 2018: update of the open-access database of transcription factor binding profiles and its web framework. *Nucleic Acids Research*. doi:10.1093/nar/gkx1126

Kieffer-Kwon, K. R., Tang, Z., Mathe, E., Qian, J., Sung, M. H., Li, G., . . . Casellas, R. (2013). Interactome maps of mouse gene regulatory domains reveal basic principles of transcriptional regulation. *Cell, 155*(7), 1507-1520. doi:10.1016/j.cell.2013.11.039

Kim, T. K., Hemberg, M., & Gray, J. M. (2015). Enhancer RNAs: a class of long noncoding RNAs synthesized at enhancers. *Cold Spring Harb Perspect Biol, 7*(1), a018622. doi:10.1101/cshperspect.a018622

Kim, T. K., Hemberg, M., Gray, J. M., Costa, A. M., Bear, D. M., Wu, J., . . . Greenberg, M. E. (2010). Widespread transcription at neuronal activity-regulated enhancers. *Nature, 465*(7295), 182-187. doi:10.1038/nature09033

Kim, T. K., & Shiekhattar, R. (2015). Architectural and functional commonalities between enhancers and promoters. *Cell, 162*(5), 948-959. doi:10.1016/j.cell.2015.08.008

Kinchen, J. M., & Ravichandran, K. S. (2008). Phagosome maturation: going through the acid test. *Nature Reviews: Molecular Cell Biology, 9*(10), 781-795. doi:10.1038/nrm2515

Kiran, D., Podell, B. K., Chambers, M., & Basaraba, R. J. (2016). Host-directed therapy targeting the *Mycobacterium tuberculosis* granuloma: a review. *Semin Immunopathol, 38*(2), 167-183. doi:10.1007/s00281-015-0537-x

Koch, C. M., Andrews, R. M., Flicek, P., Dillon, S. C., Karaoz, U., Clelland, G. K., . . . Dunham, I. (2007). The landscape of histone modifications across 1% of the human genome in five human cell lines. *Genome Research, 17*(6), 691-707. doi:10.1101/gr.5704207

Koch, F., Fenouil, R., Gut, M., Cauchy, P., Albert, T. K., Zacarias-Cabeza, J., . . . Andrau, J. C. (2011). Transcription initiation platforms and GTF recruitment at tissue-specific enhancers and promoters. *Nature Structural & Molecular Biology, 18*(8), 956-963. doi:10.1038/nsmb.2085

Kodzius, R., Kojima, M., Nishiyori, H., Nakamura, M., Fukuda, S., Tagami, M., . . . Carninci, P. (2006). CAGE: cap analysis of gene expression. *Nature Methods, 3*(3), 211-222. doi:10.1038/nmeth0306-211

Komili, S., & Silver, P. A. (2008). Coupling and coordination in gene expression processes: a systems biology view. *Nature Reviews: Genetics, 9*(1), 38-48. doi:10.1038/nrg2223

Kouzarides, T. (2007). Chromatin modifications and their function. *Cell, 128*(4), 693-705. doi:10.1016/j.cell.2007.02.005

Kowalczyk, M. S., Hughes, J. R., Garrick, D., Lynch, M. D., Sharpe, J. A., Sloane-Stanley, J. A., . . . Higgs, D. R. (2012). Intragenic enhancers act as alternative promoters. *Molecular Cell, 45*(4), 447-458. doi:10.1016/j.molcel.2011.12.021

Krzywinski, M., Schein, J., Birol, I., Connors, J., Gascoyne, R., Horsman, D., . . . Marra, M. A. (2009). Circos: an information aesthetic for comparative genomics. *Genome Research, 19*(9), 1639-1645. doi:10.1101/gr.092759.109

Lam, M. T., Cho, H., Lesch, H. P., Gosselin, D., Heinz, S., Tanaka-Oishi, Y., . . . Glass, C. K. (2013). Rev-Erbs repress macrophage gene expression by inhibiting enhancer-directed transcription. *Nature, 498*(7455), 511-515. doi:10.1038/nature12209

Lam, M. T., Li, W., Rosenfeld, M. G., & Glass, C. K. (2014). Enhancer RNAs and regulated transcriptional programs. *Trends in Biochemical Sciences, 39*(4), 170-182. doi:10.1016/j.tibs.2014.02.007

Laslo, P., Spooner, C. J., Warmflash, A., Lancki, D. W., Lee, H. J., Sciammas, R., . . . Singh, H. (2006). Multilineage transcriptional priming and determination of alternate hematopoietic cell fates. *Cell, 126*(4), 755-766. doi:10.1016/j.cell.2006.06.052

Lavin, Y., Winter, D., Blecher-Gonen, R., David, E., Keren-Shaul, H., Merad, M., . . . Amit, I. (2014). Tissue-resident macrophage enhancer landscapes are shaped by the local microenvironment. *Cell, 159*(6), 1312-1326. doi:10.1016/j.cell.2014.11.018

Le Dily, F., Bau, D., Pohl, A., Vicent, G. P., Serra, F., Soronellas, D., . . . Beato, M. (2014). Distinct structural transitions of chromatin topological domains correlate with

coordinated hormone-induced gene regulation. *Genes & Development, 28*(19), 2151-2162. doi:10.1101/gad.241422.114

Lee, T. I., & Young, R. A. (2013). Transcriptional regulation and its misregulation in disease. *Cell, 152*(6), 1237-1251. doi:10.1016/j.cell.2013.02.014

Lenhard, B., Sandelin, A., & Carninci, P. (2012). Metazoan promoters: emerging characteristics and insights into transcriptional regulation. *Nature Reviews: Genetics, 13*(4), 233-245. doi:10.1038/nrg3163

Levine, M., Cattoglio, C., & Tjian, R. (2014). Looping back to leap forward: transcription enters a new era. *Cell, 157*(1), 13-25. doi:10.1016/j.cell.2014.02.009

Li, G., Cai, L., Chang, H., Hong, P., Zhou, Q., Kulakova, E. V., . . . Ruan, Y. (2014). Chromatin Interaction Analysis with Paired-End Tag (ChIA-PET) sequencing technology and application. *BMC Genomics, 15 Suppl 12*, S11. doi:10.1186/1471-2164-15-s12-s11

Li, G., Ruan, X., Auerbach, R. K., Sandhu, K. S., Zheng, M., Wang, P., . . . Ruan, Y. (2012). Extensive promoter-centered chromatin interactions provide a topological basis for transcription regulation. *Cell, 148*(1-2), 84-98. doi:10.1016/j.cell.2011.12.014

Li, W., Notani, D., Ma, Q., Tanasa, B., Nunez, E., Chen, A. Y., . . . Rosenfeld, M. G. (2013). Functional roles of enhancer RNAs for oestrogen-dependent transcriptional activation. *Nature, 498*(7455), 516-520. doi:10.1038/nature12210

Li, W., Notani, D., & Rosenfeld, M. G. (2016). Enhancers as non-coding RNA transcription units: recent insights and future perspectives. *Nature Reviews: Genetics, 17*(4), 207-223. doi:10.1038/nrg.2016.4

Lieberman-Aiden, E., van Berkum, N. L., Williams, L., Imakaev, M., Ragoczy, T., Telling, A., . . . Dekker, J. (2009). Comprehensive mapping of long-range interactions reveals folding principles of the human genome. *Science, 326*(5950), 289-293. doi:10.1126/science.1181369

Long, H. K., Prescott, S. L., & Wysocka, J. (2016). Ever-changing landscapes: transcriptional enhancers in development and evolution. *Cell, 167*(5), 1170-1187. doi:10.1016/j.cell.2016.09.018

Loven, J., Hoke, H. A., Lin, C. Y., Lau, A., Orlando, D. A., Vakoc, C. R., . . . Young, R. A. (2013). Selective inhibition of tumor oncogenes by disruption of super-enhancers. *Cell, 153*(2), 320-334. doi:10.1016/j.cell.2013.03.036

Lugo-Villarino, G., Verollet, C., Maridonneau-Parini, I., & Neyrolles, O. (2011). Macrophage polarization: convergence point targeted by *Mycobacterium tuberculosis* and HIV. *Frontiers in Immunology, 2*, 43. doi:10.3389/fimmu.2011.00043

Lupianez, D. G., Spielmann, M., & Mundlos, S. (2016). Breaking TADs: how alterations of chromatin domains result in disease. *Trends in Genetics, 32*(4), 225-237. doi:10.1016/j.tig.2016.01.003

Maier, A., Wu, H., Cordasic, N., Oefner, P., Dietel, B., Thiele, C., . . . Warnecke, C. (2017). Hypoxia-inducible protein 2 Hig2/Hilpda mediates neutral lipid accumulation in macrophages and contributes to atherosclerosis in apolipoprotein E-deficient mice. *FASEB Journal, 31*(11), 4971-4984. doi:10.1096/fj.201700235R

Marioni, J. C., Mason, C. E., Mane, S. M., Stephens, M., & Gilad, Y. (2008). RNA-seq: an assessment of technical reproducibility and comparison with gene expression arrays. *Genome Research, 18*(9), 1509-1517. doi:10.1101/gr.079558.108

Martinez, F. O., & Gordon, S. (2014). The M1 and M2 paradigm of macrophage activation: time for reassessment. *F1000Prime Reports, 6*, 13. doi:10.12703/p6-13

Maurano, M. T., Humbert, R., Rynes, E., Thurman, R. E., Haugen, E., Wang, H., . . . Stamatoyannopoulos, J. A. (2012). Systematic localization of common disease-

associated variation in regulatory DNA. *Science, 337*(6099), 1190-1195. doi:10.1126/science.1222794

Melgar, M. F., Collins, F. S., & Sethupathy, P. (2011). Discovery of active enhancers through bidirectional expression of short transcripts. *Genome Biol, 12*(11), R113. doi:10.1186/gb-2011-12-11-r113

Melo, C. A., Drost, J., Wijchers, P. J., van de Werken, H., de Wit, E., Oude Vrielink, J. A., . . . Agami, R. (2013). eRNAs are required for p53-dependent enhancer activity and gene transcription. *Molecular Cell, 49*(3), 524-535. doi:10.1016/j.molcel.2012.11.021

Michel, M., Demel, C., Zacher, B., Schwalb, B., Krebs, S., Blum, H., . . . Cramer, P. (2017). TT-seq captures enhancer landscapes immediately after T-cell stimulation. *Molecular Systems Biology, 13*(3), 920. doi:10.15252/msb.20167507

Michelucci, A., Cordes, T., Ghelfi, J., Pailot, A., Reiling, N., Goldmann, O., . . . Hiller, K. (2013). Immune-responsive gene 1 protein links metabolism to immunity by catalyzing itaconic acid production. *Proc Natl Acad Sci U S A, 110*(19), 7820-7825. doi:10.1073/pnas.1218599110

Mifsud, B., Tavares-Cadete, F., Young, A. N., Sugar, R., Schoenfelder, S., Ferreira, L., . . . Osborne, C. S. (2015). Mapping long-range promoter contacts in human cells with high-resolution capture Hi-C. *Nature Genetics, 47*(6), 598-606. doi:10.1038/ng.3286

Mikhaylichenko, O., Bondarenko, V., Harnett, D., Schor, I. E., Males, M., Viales, R. R., & Furlong, E. E. M. (2018). The degree of enhancer or promoter activity is reflected by the levels and directionality of eRNA transcription. *Genes & Development*. doi:10.1101/gad.308619.117

Mogensen, T. H. (2009). Pathogen recognition and inflammatory signaling in innate immune defenses. *Clinical Microbiology Reviews, 22*(2), 240-273, Table of Contents. doi:10.1128/cmr.00046-08

Mora, A., Sandve, G. K., Gabrielsen, O. S., & Eskeland, R. (2015). In the loop: promoter-enhancer interactions and bioinformatics. *Brief Bioinform*. doi:10.1093/bib/bbv097

Mosser, D. M., & Edwards, J. P. (2008). Exploring the full spectrum of macrophage activation. *Nature Reviews: Immunology, 8*(12), 958-969. doi:10.1038/nri2448

Motakis, E., Guhl, S., Ishizu, Y., Itoh, M., Kawaji, H., de Hoon, M., . . . Babina, M. (2014). Redefinition of the human mast cell transcriptome by deep-CAGE sequencing. *Blood, 123*(17), e58-67. doi:10.1182/blood-2013-02-483792

Mousavi, K., Zare, H., Dell'orso, S., Grontved, L., Gutierrez-Cruz, G., Derfoul, A., . . . Sartorelli, V. (2013). eRNAs promote transcription by establishing chromatin accessibility at defined genomic loci. *Molecular Cell, 51*(5), 606-617. doi:10.1016/j.molcel.2013.07.022

Mu, D., Cambier, S., Fjellbirkeland, L., Baron, J. L., Munger, J. S., Kawakatsu, H., . . . Nishimura, S. L. (2002). The integrin alpha(v)beta8 mediates epithelial homeostasis through MT1-MMP-dependent activation of TGF-beta1. *Journal of Cell Biology, 157*(3), 493-507. doi:10.1083/jcb.200109100

Mukhopadhyay, S., Ramadass, A. S., Akoulitchev, A., & Gordon, S. (2014). Formation of distinct chromatin conformation signatures epigenetically regulate macrophage activation. *International Immunopharmacology, 18*(1), 7-11. doi:10.1016/j.intimp.2013.10.024

Muraille, E., Leo, O., & Moser, M. (2014). TH1/TH2 paradigm extended: macrophage polarization as an unappreciated pathogen-driven escape mechanism? *Front Immunol, 5*, 603. doi:10.3389/fimmu.2014.00603

Murakawa, Y., Yoshihara, M., Kawaji, H., Nishikawa, M., Zayed, H., Suzuki, H., . . . Hayashizaki, Y. (2016). Enhanced identification of transcriptional enhancers

provides mechanistic insights into diseases. *Trends in Genetics, 32*(2), 76-88. doi:10.1016/j.tig.2015.11.004

Murray, P. J., Allen, J. E., Biswas, S. K., Fisher, E. A., Gilroy, D. W., Goerdt, S., . . . Wynn, T. A. (2014). Macrophage activation and polarization: nomenclature and experimental guidelines. *Immunity, 41*(1), 14-20. doi:10.1016/j.immuni.2014.06.008

Murray, P. J., & Wynn, T. A. (2011). Protective and pathogenic functions of macrophage subsets. *Nature Reviews: Immunology, 11*(11), 723-737.

Natoli, G., & Andrau, J. C. (2012). Noncoding transcription at enhancers: general principles and functional models. *Annual Review of Genetics, 46*, 1-19. doi:10.1146/annurev-genet-110711-155459

Nolis, I. K., McKay, D. J., Mantouvalou, E., Lomvardas, S., Merika, M., & Thanos, D. (2009). Transcription factors mediate long-range enhancer-promoter interactions. *Proceedings of the National Academy of Sciences, USA, 106*(48), 20222-20227. doi:10.1073/pnas.0902454106

Nora, E. P., Lajoie, B. R., Schulz, E. G., Giorgetti, L., Okamoto, I., Servant, N., . . . Heard, E. (2012). Spatial partitioning of the regulatory landscape of the X-inactivation centre. *Nature, 485*(7398), 381-385. doi:10.1038/nature11049

North, B. V., Curtis, D., & Sham, P. C. (2002). A note on the calculation of empirical P values from Monte Carlo procedures. *American Journal of Human Genetics, 71*(2), 439-441. doi:10.1086/341527

Odegaard, J. I., Ricardo-Gonzalez, R. R., Goforth, M. H., Morel, C. R., Subramanian, V., Mukundan, L., . . . Chawla, A. (2007). Macrophage-specific PPARgamma controls alternative activation and improves insulin resistance. *Nature, 447*(7148), 1116-1120. doi:10.1038/nature05894

Ohmiya, H., Vitezic, M., Frith, M. C., Itoh, M., Carninci, P., Forrest, A. R., . . . Lassmann, T. (2014). RECLU: a pipeline to discover reproducible transcriptional start sites and their alternative regulation using capped analysis of gene expression (CAGE). *BMC Genomics, 15*, 269. doi:10.1186/1471-2164-15-269

Ong, C. T., & Corces, V. G. (2014). CTCF: an architectural protein bridging genome topology and function. *Nature Reviews: Genetics, 15*(4), 234-246. doi:10.1038/nrg3663

Orme, I. M., Robinson, R. T., & Cooper, A. M. (2015). The balance between protective and pathogenic immune responses in the TB-infected lung. *Nature Immunology, 16*(1), 57-63. doi:10.1038/ni.3048

Osterwalder, M., Barozzi, I., Tissieres, V., Fukuda-Yuzawa, Y., Mannion, B. J., Afzal, S. Y., . . . Pennacchio, L. A. (2018). Enhancer redundancy provides phenotypic robustness in mammalian development. *Nature, 554*(7691), 239-243. doi:10.1038/nature25461

Ostuni, R., Piccolo, V., Barozzi, I., Polletti, S., Termanini, A., Bonifacio, S., . . . Natoli, G. (2013). Latent enhancers activated by stimulation in differentiated cells. *Cell, 152*(1–2), 157-171. doi:10.1016/j.cell.2012.12.018

Ouimet, M., Koster, S., Sakowski, E., Ramkhelawon, B., van Solingen, C., Oldebeken, S., . . . Moore, K. J. (2016). *Mycobacterium tuberculosis* induces the miR-33 locus to reprogram autophagy and host lipid metabolism. *Nature Immunology, 17*(6), 677-686. doi:10.1038/ni.3434

Oviedo-Boyso, J., Bravo-Patino, A., & Baizabal-Aguirre, V. M. (2014). Collaborative action of Toll-like and NOD-like receptors as modulators of the inflammatory response to pathogenic bacteria. *Mediators Inflamm, 2014*, 432785. doi:10.1155/2014/432785

Parker, S. C., Stitzel, M. L., Taylor, D. L., Orozco, J. M., Erdos, M. R., Akiyama, J. A., . . . Collins, F. S. (2013). Chromatin stretch enhancer states drive cell-specific gene

regulation and harbor human disease risk variants. *Proceedings of the National Academy of Sciences, USA, 110*(44), 17921-17926. doi:10.1073/pnas.1317023110

Peeters, J. G., Vervoort, S. J., Tan, S. C., Mijnheer, G., de Roock, S., Vastert, S. J., . . . van Loosdregt, J. (2015). Inhibition of super-enhancer activity in autoinflammatory site-derived T cells reduces disease-associated gene expression. *Cell Rep, 12*(12), 1986-1996. doi:10.1016/j.celrep.2015.08.046

Pefanis, E., Wang, J., Rothschild, G., Lim, J., Kazadi, D., Sun, J., . . . Basu, U. (2015). RNA exosome-regulated long non-coding RNA transcription controls super-enhancer activity. *Cell, 161*(4), 774-789. doi:10.1016/j.cell.2015.04.034

Pekowska, A., Benoukraf, T., Zacarias-Cabeza, J., Belhocine, M., Koch, F., Holota, H., . . . Spicuglia, S. (2011). H3K4 tri-methylation provides an epigenetic signature of active enhancers. *EMBO Journal, 30*(20), 4198-4210. doi:10.1038/emboj.2011.295

Pennacchio, L. A., Bickmore, W., Dean, A., Nobrega, M. A., & Bejerano, G. (2013). Enhancers: five essential questions. *Nature Reviews: Genetics, 14*(4), 288-295. doi:10.1038/nrg3458

Pnueli, L., Rudnizky, S., Yosefzon, Y., & Melamed, P. (2015). RNA transcribed from a distal enhancer is required for activating the chromatin at the promoter of the gonadotropin alpha-subunit gene. *Proceedings of the National Academy of Sciences, USA, 112*(14), 4369-4374. doi:10.1073/pnas.1414841112

Pott, S., & Lieb, J. D. (2015). What are super-enhancers? *Nature Genetics, 47*(1), 8-12. doi:10.1038/ng.3167

Queval, C. J., Brosch, R., & Simeone, R. (2017). The macrophage: a disputed fortress in the battle against *Mycobacterium tuberculosis*. *Front Microbiol, 8*, 2284. doi:10.3389/fmicb.2017.02284

Quinlan, A. R., & Hall, I. M. (2010). BEDTools: a flexible suite of utilities for comparing genomic features. *Bioinformatics, 26*(6), 841-842. doi:10.1093/bioinformatics/btq033

Ramanathan, A., Robb, G. B., & Chan, S. H. (2016). mRNA capping: biological functions and applications. *Nucleic Acids Research, 44*(16), 7511-7526. doi:10.1093/nar/gkw551

Rao, S. S., Huntley, M. H., Durand, N. C., Stamenova, E. K., Bochkov, I. D., Robinson, J. T., . . . Aiden, E. L. (2014). A 3D map of the human genome at kilobase resolution reveals principles of chromatin looping. *Cell, 159*(7), 1665-1680. doi:10.1016/j.cell.2014.11.021

Reed, S. G. (1999). TGF-beta in infections and infectious diseases. *Microbes Infect, 1*(15), 1313-1325.

Rehli, M., Sulzbacher, S., Pape, S., Ravasi, T., Wells, C. A., Heinz, S., . . . Andreesen, R. (2005). Transcription factor Tfec contributes to the IL-4-inducible expression of a small group of genes in mouse macrophages including the granulocyte colony-stimulating factor receptor. *Journal of Immunology, 174*(11), 7111-7122.

Reiter, F., Wienerroither, S., & Stark, A. (2017). Combinatorial function of transcription factors and cofactors. *Current Opinion in Genetics & Development, 43*, 73-81. doi:10.1016/j.gde.2016.12.007

Robinson, M. D., McCarthy, D. J., & Smyth, G. K. (2010). edgeR: a Bioconductor package for differential expression analysis of digital gene expression data. *Bioinformatics, 26*(1), 139-140. doi:10.1093/bioinformatics/btp616

Robinson, R. T., Orme, I. M., & Cooper, A. M. (2015). The onset of adaptive immunity in the mouse model of tuberculosis and the factors that compromise its expression. *Immunological Reviews, 264*(1), 46-59. doi:10.1111/imr.12259

Rocha, P. P., Raviram, R., Bonneau, R., & Skok, J. A. (2015). Breaking TADs: insights into hierarchical genome organization. *Epigenomics, 7*(4), 523-526. doi:10.2217/epi.15.25

Romanoski, C. E., Link, V. M., Heinz, S., & Glass, C. K. (2015). Exploiting genomics and natural genetic variation to decode macrophage enhancers. *Trends in Immunology, 36*(9), 507-518. doi:10.1016/j.it.2015.07.006

Rothschild, G., & Basu, U. (2017). Lingering questions about enhancer RNA and enhancer transcription-coupled genomic instability. *Trends in Genetics, 33*(2), 143-154. doi:10.1016/j.tig.2016.12.002

Rottenberg, M. E., & Carow, B. (2014). SOCS3 and STAT3, major controllers of the outcome of infection with *Mycobacterium tuberculosis*. *Seminars in Immunology, 26*(6), 518-532. doi:10.1016/j.smim.2014.10.004

Roundtree, I. A., Evans, M. E., Pan, T., & He, C. (2017). Dynamic RNA modifications in gene expression regulation. *Cell, 169*(7), 1187-1200. doi:10.1016/j.cell.2017.05.045

Roy, S., Guler, R., Parihar, S. P., Schmeier, S., Kaczkowski, B., Nishimura, H., . . . Suzuki, H. (2015). Batf2/Irf1 induces inflammatory responses in classically activated macrophages, lipopolysaccharides, and mycobacterial infection. *Journal of Immunology, 194*(12), 6035-6044. doi:10.4049/jimmunol.1402521

Roy, S., Schmeier, S., Arner, E., Alam, T., Parihar, S. P., Ozturk, M., . . . Suzuki, H. (2015). Redefining the transcriptional regulatory dynamics of classically and alternatively activated macrophages by deepCAGE transcriptomics. *Nucleic Acids Research, 43*(14), 6969-6982. doi:10.1093/nar/gkv646

Rubin, A. J., Barajas, B. C., Furlan-Magaril, M., Lopez-Pajares, V., Mumbach, M. R., Howard, I., . . . Khavari, P. A. (2017). Lineage-specific dynamic and pre-established enhancer-promoter contacts cooperate in terminal differentiation. *Nature Genetics, 49*(10), 1522-1528. doi:10.1038/ng.3935

Ruffell, D., Mourkioti, F., Gambardella, A., Kirstetter, P., Lopez, R. G., Rosenthal, N., & Nerlov, C. (2009). A CREB-C/EBPbeta cascade induces M2 macrophage-specific gene expression and promotes muscle injury repair. *Proceedings of the National Academy of Sciences, USA, 106*(41), 17475-17480. doi:10.1073/pnas.0908641106

Russell, D. G., Barry, C. E., III, & Flynn, J. L. (2010). Tuberculosis: what we don't know can, and does, hurt us. *Science, 328*(5980), 852-856. doi:10.1126/science.1184784

Saliba, D. G., Heger, A., Eames, H. L., Oikonomopoulos, S., Teixeira, A., Blazek, K., . . . Udalova, I. A. (2014). IRF5:RelA interaction targets inflammatory genes in macrophages. *Cell Reports, 8*(5), 1308-1317. doi:10.1016/j.celrep.2014.07.034

Sanyal, A., Lajoie, B., Jain, G., & Dekker, J. (2012). The long-range interaction landscape of gene promoters. *Nature, 489*(7414), 109-113. doi:10.1038/nature11279

Schmidl, C., Hansmann, L., Lassmann, T., Balwierz, P. J., Kawaji, H., Itoh, M., . . . Rehli, M. (2014). The enhancer and promoter landscape of human regulatory and conventional T-cell subpopulations. *Blood, 123*(17), e68-e78. doi:10.1182/blood-2013-02-486944

Schmidl, C., Renner, K., Peter, K., Eder, R., Lassmann, T., Balwierz, P. J., . . . Rehli, M. (2014). Transcription and enhancer profiling in human monocyte subsets. *Blood, 123*(17), e90-99. doi:10.1182/blood-2013-02-484188

Schoenfelder, S., Furlan-Magaril, M., Mifsud, B., Tavares-Cadete, F., Sugar, R., Javierre, B. M., . . . Fraser, P. (2015). The pluripotent regulatory circuitry connecting promoters to their long-range interacting elements. *Genome Research, 25*(4), 582-597. doi:10.1101/gr.185272.114

Schorey, J. S., & Cooper, A. M. (2003). Macrophage signalling upon mycobacterial infection: the MAP kinases lead the way. *Cellular Microbiology, 5*(3), 133-142.

Schwalb, B., Michel, M., Zacher, B., Fruhauf, K., Demel, C., Tresch, A., . . . Cramer, P. (2016). TT-seq maps the human transient transcriptome. *Science, 352*(6290), 1225-1228. doi:10.1126/science.aad9841

Schwarzer, W., Abdennur, N., Goloborodko, A., Pekowska, A., Fudenberg, G., Loe-Mie, Y., . . . Spitz, F. (2017). Two independent modes of chromatin organization revealed by cohesin removal. *Nature, 551*(7678), 51-56. doi:10.1038/nature24281

Schwarzer, W., & Spitz, F. (2014). The architecture of gene expression: integrating dispersed *cis*-regulatory modules into coherent regulatory domains. *Current Opinion in Genetics & Development, 27*, 74-82. doi:10.1016/j.gde.2014.03.014

Shang, Y., Smith, S., & Hu, X. (2016). Role of Notch signaling in regulating innate immunity and inflammation in health and disease. *Protein Cell, 7*(3), 159-174. doi:10.1007/s13238-016-0250-0

Shen, Y., Yue, F., McCleary, D. F., Ye, Z., Edsall, L., Kuan, S., . . . Ren, B. (2012). A map of the *cis*-regulatory sequences in the mouse genome. *Nature, 488*(7409), 116-120. doi:10.1038/nature11243

Shin, H. Y., Willi, M., HyunYoo, K., Zeng, X., Wang, C., Metser, G., & Hennighausen, L. (2016). Hierarchy within the mammary STAT5-driven Wap super-enhancer. *Nature Genetics, 48*(8), 904-911. doi:10.1038/ng.3606

Shiraki, T., Kondo, S., Katayama, S., Waki, K., Kasukawa, T., Kawaji, H., . . . Hayashizaki, Y. (2003). Cap analysis gene expression for high-throughput analysis of transcriptional starting point and identification of promoter usage. *Proc Natl Acad Sci U S A, 100*(26), 15776-15781. doi:10.1073/pnas.2136655100

Shlyueva, D., Stampfel, G., & Stark, A. (2014). Transcriptional enhancers: from properties to genome-wide predictions. *Nature Reviews: Genetics, 15*(4), 272-286. doi:10.1038/nrg3682

Sica, A., & Mantovani, A. (2012). Macrophage plasticity and polarization: in vivo veritas. *Journal of Clinical Investigation, 122*(3), 787-795. doi:10.1172/jci59643

Siegmund, D., Kums, J., Ehrenschwender, M., & Wajant, H. (2016). Activation of TNFR2 sensitizes macrophages for TNFR1-mediated necroptosis. *Cell Death Dis, 7*(9), e2375. doi:10.1038/cddis.2016.285

Sigova, A. A., Abraham, B. J., Ji, X., Molinie, B., Hannett, N. M., Guo, Y. E., . . . Young, R. A. (2015). Transcription factor trapping by RNA in gene regulatory elements. *Science, 350*(6263), 978-981. doi:10.1126/science.aad3346

Spadaro, O., Camell, C. D., Bosurgi, L., Nguyen, K. Y., Youm, Y. H., Rothlin, C. V., & Dixit, V. D. (2017). IGF1 shapes macrophage activation in response to immunometabolic challenge. *Cell Reports, 19*(2), 225-234. doi:10.1016/j.celrep.2017.03.046

Spitz, F., & Furlong, E. E. (2012). Transcription factors: from enhancer binding to developmental control. *Nature Reviews: Genetics, 13*(9), 613-626. doi:10.1038/nrg3207

Stamm, C. E., Collins, A. C., & Shiloh, M. U. (2015). Sensing of *Mycobacterium tuberculosis* and consequences to both host and bacillus. *Immunological Reviews, 264*(1), 204-219. doi:10.1111/imr.12263

Stavreva, D. A., & Hager, G. L. (2015). Chromatin structure and gene regulation: a dynamic view of enhancer function. *Nucleus, 6*(6), 442-448. doi:10.1080/19491034.2015.1107689

Symmons, O., Uslu, V. V., Tsujimura, T., Ruf, S., Nassari, S., Schwarzer, W., . . . Spitz, F. (2014). Functional and topological characteristics of mammalian regulatory domains. *Genome Research, 24*(3), 390-400. doi:10.1101/gr.163519.113

Szutorisz, H., Dillon, N., & Tora, L. (2005). The role of enhancers as centres for general transcription factor recruitment. *Trends in Biochemical Sciences, 30*(11), 593-599. doi:10.1016/j.tibs.2005.08.006

Taniguchi, T., Ogasawara, K., Takaoka, A., & Tanaka, N. (2001). IRF family of transcription factors as regulators of host defense. *Annual Review of Immunology, 19*, 623-655. doi:10.1146/annurev.immunol.19.1.623

The ENCODE Project Consortium. (2012). An integrated encyclopedia of DNA elements in the human genome. *Nature, 489*(7414), 57-74. doi:10.1038/nature11247

Thomas, G. D., Hanna, R. N., Vasudevan, N. T., Hamers, A. A., Romanoski, C. E., McArdle, S., . . . Hedrick, C. C. (2016). Deleting an Nr4a1 super-enhancer subdomain ablates Ly6Clow monocytes while preserving macrophage gene function. *Immunity, 45*(5), 975-987. doi:10.1016/j.immuni.2016.10.011

Thomas, M. C., & Chiang, C. M. (2006). The general transcription machinery and general cofactors. *Critical Reviews in Biochemistry and Molecular Biology, 41*(3), 105-178. doi:10.1080/10409230600648736

Tugal, D., Liao, X., & Jain, M. K. (2013). Transcriptional control of macrophage polarization. *Arteriosclerosis, Thrombosis, and Vascular Biology, 33*(6), 1135-1144. doi:10.1161/atvbaha.113.301453

van Crevel, R., Ottenhoff, T. H., & van der Meer, J. W. (2002). Innate immunity to *Mycobacterium tuberculosis*. *Clinical Microbiology Reviews, 15*(2), 294-309.

Visel, A., Blow, M. J., Li, Z., Zhang, T., Akiyama, J. A., Holt, A., . . . Pennacchio, L. A. (2009). ChIP-seq accurately predicts tissue-specific activity of enhancers. *Nature, 457*(7231), 854-858. doi:10.1038/nature07730

Visel, A., Minovitsky, S., Dubchak, I., & Pennacchio, L. A. (2007). VISTA Enhancer Browser--a database of tissue-specific human enhancers. *Nucleic Acids Research, 35*(Database issue), D88-92. doi:10.1093/nar/gkl822

Wada, T., & Penninger, J. M. (2004). Mitogen-activated protein kinases in apoptosis regulation. *Oncogene, 23*(16), 2838-2849. doi:10.1038/sj.onc.1207556

Wallis, R. S., & Hafner, R. (2015). Advancing host-directed therapy for tuberculosis. *Nature Reviews: Immunology, 15*(4), 255-263. doi:10.1038/nri3813

Wang, C., Gong, B., Bushel, P. R., Thierry-Mieg, J., Thierry-Mieg, D., Xu, J., . . . Tong, W. (2014). The concordance between RNA-seq and microarray data depends on chemical treatment and transcript abundance. *Nature Biotechnology, 32*(9), 926-932. doi:10.1038/nbt.3001

Wang, D., Garcia-Bassets, I., Benner, C., Li, W., Su, X., Zhou, Y., . . . Fu, X. D. (2011). Reprogramming transcription by distinct classes of enhancers functionally defined by eRNA. *Nature, 474*(7351), 390-394. doi:10.1038/nature10006

Wang, N., Liang, H., & Zen, K. (2014). Molecular mechanisms that influence the macrophage M1–M2 polarization balance. *Front Immunol, 5*, 614. doi:10.3389/fimmu.2014.00614

Wang, Z., Gerstein, M., & Snyder, M. (2009). RNA-Seq: a revolutionary tool for transcriptomics. *Nature Reviews: Genetics, 10*(1), 57-63. doi:10.1038/nrg2484

Wang, Z., Zang, C., Rosenfeld, J. A., Schones, D. E., Barski, A., Cuddapah, S., . . . Zhao, K. (2008). Combinatorial patterns of histone acetylations and methylations in the human genome. *Nature Genetics, 40*(7), 897-903. doi:10.1038/ng.154

Weake, V. M., & Workman, J. L. (2010). Inducible gene expression: diverse regulatory mechanisms. *Nature Reviews: Genetics, 11*(6), 426-437. doi:10.1038/nrg2781

Weiss, G., & Schaible, U. E. (2015). Macrophage defense mechanisms against intracellular bacteria. *Immunological Reviews, 264*(1), 182-203.

Whyte, W. A., Orlando, D. A., Hnisz, D., Abraham, B. J., Lin, C. Y., Kagey, M. H., . . . Young, R. A. (2013). Master transcription factors and mediator establish super-enhancers at key cell identity genes. *Cell, 153*(2), 307-319. doi:10.1016/j.cell.2013.03.035

Wickham, H. (2009). *ggplot2: Elegant Graphics for Data Analysis*: Springer, New York, NY.

Witte, S., O'Shea, J. J., & Vahedi, G. (2015). Super-enhancers: asset management in immune cell genomes. *Trends in Immunology, 36*(9), 519-526. doi:10.1016/j.it.2015.07.005

Wu, H., Nord, A. S., Akiyama, J. A., Shoukry, M., Afzal, V., Rubin, E. M., . . . Visel, A. (2014). Tissue-specific RNA expression marks distant-acting developmental enhancers. *PLoS Genetics, 10*(9), 12. doi:10.1371/journal.pgen.1004610

Wu, H., & Zhang, Y. (2014). Reversing DNA methylation: mechanisms, genomics, and biological functions. *Cell, 156*(1-2), 45-68. doi:10.1016/j.cell.2013.12.019

Xu, G., Wang, J., Gao, G. F., & Liu, C. H. (2014). Insights into battles between *Mycobacterium tuberculosis* and macrophages. *Protein Cell, 5*(10), 728-736. doi:10.1007/s13238-014-0077-5

Yan, J., Chen, S. A., Local, A., Liu, T., Qiu, Y., Dorighi, K. M., . . . Ren, B. (2018). Histone H3 lysine 4 monomethylation modulates long-range chromatin interactions at enhancers. *Cell Research*. doi:10.1038/cr.2018.1

Yao, P., Lin, P., Gokoolparsadh, A., Assareh, A., Thang, M. W., & Voineagu, I. (2015). Coexpression networks identify brain region-specific enhancer RNAs in the human brain. *Nature Neuroscience, 18*(8), 1168-1174. doi:10.1038/nn.4063

Yue, F., Cheng, Y., Breschi, A., Vierstra, J., Wu, W., Ryba, T., . . . Ren, B. (2014). A comparative encyclopedia of DNA elements in the mouse genome. *Nature, 515*(7527), 355-364. doi:10.1038/nature13992

Zaret, K. S., & Carroll, J. S. (2011). Pioneer transcription factors: establishing competence for gene expression. *Genes & Development, 25*(21), 2227-2241. doi:10.1101/gad.176826.111

Zentner, G. E., Tesar, P. J., & Scacheri, P. C. (2011). Epigenetic signatures distinguish multiple classes of enhancers with distinct cellular functions. *Genome Research, 21*(8), 1273-1283. doi:10.1101/gr.122382.111

Zhang, Y., Liu, T., Meyer, C. A., Eeckhoute, J., Johnson, D. S., Bernstein, B. E., . . . Liu, X. S. (2008). Model-based analysis of ChIP-Seq (MACS). *Genome Biol., 9*(9), R137. doi:10.1186/gb-2008-9-9-r137

Zhang, Y., Wong, C. H., Birnbaum, R. Y., Li, G., Favaro, R., Ngan, C. Y., . . . Wei, C. L. (2013). Chromatin connectivity maps reveal dynamic promoter-enhancer long-range associations. *Nature, 504*(7479), 306-310. doi:10.1038/nature12716

Zumla, A., George, A., Sharma, V., Herbert, R. H., Oxley, A., & Oliver, M. (2015). The WHO 2014 global tuberculosis report--further to go. *Lancet Glob Health, 3*(1), e10-12. doi:10.1016/s2214-109x(14)70361-4

Zumla, A., Raviglione, M., Hafner, R., & von Reyn, C. F. (2013). Tuberculosis. *N Engl J Med, 368*(8), 745-755. doi:10.1056/NEJMra1200894

Appendix

Table A2.1. A full list of 969 mouse samples split by tissue. Tissues with at least ten samples were considered separately, the rest of the samples were combined together into an 'Others' category.

	Cerebellum
1	cerebellar_granule_cells_embryo_E13_biol_rep1_(E13R1).CNhs14143.13532-145G4
2	cerebellar_granule_cells_embryo_E13_biol_rep2_(E13R2).CNhs14144.13533-145G5
3	cerebellar_granule_cells_embryo_E13_biol_rep3_(E13R3).CNhs14146.13534-145G6
4	cerebellar_granule_cells_embryo_E15_biol_rep1_(E15R1).CNhs14162.13535-145G7
5	cerebellar_granule_cells_embryo_E15_biol_rep2_(E15R2).CNhs14163.13536-145G8
6	cerebellar_granule_cells_embryo_E15_biol_rep3_(E15R3).CNhs14164.13537-145G9
7	cerebellar_granule_cells_embryo_E18_biol_rep1_(E18R1).CNhs14165.13538-145H1
8	cerebellar_granule_cells_embryo_E18_biol_rep2_(E18R2).CNhs14166.13539-145H2
9	cerebellar_granule_cells_embryo_E18_biol_rep3_(E13R3).CNhs14167.13540-145H3
10	cerebellum_adult.CNhs10494.15-8B2
11	cerebellum_embryo_E11_biol_rep1_(E11R1).CNhs12956.10114-102E6
12	cerebellum_embryo_E11_biol_rep2_(E11R2).CNhs13002.10126-102F9
13	cerebellum_embryo_E11_biol_rep3_(E11R3).CNhs13014.10138-102H3
14	cerebellum_embryo_E12_biol_rep1_(E12R1).CNhs12957.10115-102E7
15	cerebellum_embryo_E12_biol_rep2_(E12R2).CNhs13003.10127-102G1
16	cerebellum_embryo_E12_biol_rep3_(E12R3).CNhs13015.10139-102H4
17	cerebellum_embryo_E13_biol_rep1_(E13R1).CNhs12958.10116-102E8
18	cerebellum_embryo_E13_biol_rep2_(E13R2).CNhs13004.10128-102G2
19	cerebellum_embryo_E13_biol_rep3_(E13R3).CNhs13016.10140-102H5
20	cerebellum_embryo_E14_biol_rep1_(E14R1).CNhs12960.10117-102E9
21	cerebellum_embryo_E14_biol_rep2_(E14R2).CNhs13005.10129-102G3
22	cerebellum_embryo_E14_biol_rep3_(E14R3).CNhs13017.10141-102H6
23	cerebellum_embryo_E15_biol_rep1_(E15R1).CNhs12961.10118-102F1
24	cerebellum_embryo_E15_biol_rep2_(E15R2).CNhs13006.10130-102G4
25	cerebellum_embryo_E15_biol_rep3_(E15R3).CNhs13018.10142-102H7
26	cerebellum_embryo_E16_biol_rep1_(E16R1).CNhs13000.10119-102F2
27	cerebellum_embryo_E16_biol_rep2_(E16R2).CNhs13007.10131-102G5
28	cerebellum_embryo_E16_biol_rep3_(E16R3).CNhs13019.10143-102H8
29	cerebellum_embryo_E17_biol_rep1_(E17R1).CNhs12818.10120-102F3
30	cerebellum_embryo_E17_biol_rep2_(E17R2).CNhs13008.10132-102G6
31	cerebellum_embryo_E17_biol_rep3_(E17R3).CNhs13020.10144-102H9
32	cerebellum_embryo_E18_biol_rep1_(E18R1).CNhs12962.10121-102F4
33	cerebellum_embryo_E18_biol_rep2_(E18R2).CNhs13009.10133-102G7
34	cerebellum_embryo_E18_biol_rep3_(E18R3).CNhs13021.10145-102I1
35	cerebellum_neonate_N00_biol_rep1_(P0R1).CNhs12963.10122-102F5
36	cerebellum_neonate_N00_biol_rep2_(P0R2).CNhs13010.10134-102G8
37	cerebellum_neonate_N00_biol_rep3_(P0R3).CNhs13022.10146-102I2
38	cerebellum_neonate_N03_biol_rep1_(P3R1).CNhs13001.10123-102F6
39	cerebellum_neonate_N03_biol_rep2_(P3R2).CNhs13011.10135-102G9
40	cerebellum_neonate_N03_biol_rep3_(P3R3).CNhs13024.10147-102I3
41	cerebellum_neonate_N06_biol_rep1_(P6R1).CNhs12819.10124-102F7
42	cerebellum_neonate_N06_biol_rep2_(P6R2).CNhs13012.10136-102H1
43	cerebellum_neonate_N06_biol_rep3_(P6R3).CNhs13025.10148-102I4
44	cerebellum_neonate_N09_biol_rep1_(P9R1).CNhs12820.10125-102F8
45	cerebellum_neonate_N09_biol_rep2_(P9R2).CNhs13013.10137-102H2
46	cerebellum_neonate_N09_biol_rep3_(P9R3).CNhs13026.10149-102I5
47	cerebellum_neonate_N30.CNhs11135.1395-42I2
48	Mouse_Granule_cells_donor1.CNhs12131.11713-123C3
49	Mouse_Granule_cells_donor2.CNhs12357.11731-123E3
50	Mouse_Granule_cells_donor3.CNhs12108.11636-122C7
	Embryonic stem cell

1	ES-46C_derived_epistem_cells_biol_rep1.CNhs14123.14375-156B1
2	ES-46C_derived_epistem_cells_biol_rep2.CNhs14124.14376-156B2
3	ES-46C_derived_epistem_cells_biol_rep3.CNhs14125.14377-156B3
4	ES-46C_derived_epistem_cells_neuronal_differentiation_day05_biol_rep1.CNhs14126.14378-156B4
5	ES-46C_derived_epistem_cells_neuronal_differentiation_day14_biol_rep1.CNhs14127.14379-156B5
6	ES-46C_embryonic_stem_cells_neuronal_differentiation_day00_biol_rep1.CNhs14104.14357-155I1
7	ES-46C_embryonic_stem_cells_neuronal_differentiation_day00_biol_rep2.CNhs14109.14362-155I6
8	ES-46C_embryonic_stem_cells_neuronal_differentiation_day01_biol_rep1.CNhs14105.14358-155I2
9	ES-46C_embryonic_stem_cells_neuronal_differentiation_day01_biol_rep2.CNhs14110.14363-155I7
10	ES-46C_embryonic_stem_cells_neuronal_differentiation_day02_biol_rep1.CNhs14106.14359-155I3
11	ES-46C_embryonic_stem_cells_neuronal_differentiation_day02_biol_rep2.CNhs14111.14364-155I8
12	ES-46C_embryonic_stem_cells_neuronal_differentiation_day03_biol_rep1.CNhs14107.14360-155I4
13	ES-46C_embryonic_stem_cells_neuronal_differentiation_day03_biol_rep2.CNhs14112.14365-155I9
14	ES-46C_embryonic_stem_cells_neuronal_differentiation_day04_biol_rep1.CNhs14108.14361-155I5
15	ES-46C_embryonic_stem_cells_neuronal_differentiation_day04_biol_rep2.CNhs14113.14366-156A1
16	ES-Ert2_embryonic_stem_cells_tamoxifen_treated_48hr_biol_rep1.CNhs14101.14354-155H7
17	ES-Ert2_embryonic_stem_cells_tamoxifen_treated_48hr_biol_rep2.CNhs14102.14355-155H8
18	ES-Ert2_embryonic_stem_cells_tamoxifen_treated_48hr_biol_rep3.CNhs14103.14356-155H9
19	ES-Ert2_embryonic_stem_cells_untreated_control_48hr_biol_rep1.CNhs14098.14351-155H4
20	ES-Ert2_embryonic_stem_cells_untreated_control_48hr_biol_rep2.CNhs14099.14352-155H5
21	ES-Ert2_embryonic_stem_cells_untreated_control_48hr_biol_rep3.CNhs14100.14353-155H6
22	ES-OS25_embryonic_stem_cells_aminitin_treatment_for_7hr_biol_rep1.CNhs14094.14348-155H1
23	ES-OS25_embryonic_stem_cells_aminitin_treatment_for_7hr_biol_rep2.CNhs14095.14349-155H2
24	ES-OS25_embryonic_stem_cells_aminitin_treatment_for_7hr_biol_rep3.CNhs14097.14350-155H3
25	ES-OS25_embryonic_stem_cells_DMSO_control_biol_rep1.CNhs14085.14339-155G1
26	ES-OS25_embryonic_stem_cells_DMSO_control_biol_rep2.CNhs14086.14340-155G2
27	ES-OS25_embryonic_stem_cells_DMSO_control_biol_rep3.CNhs14087.14341-155G3
28	ES-OS25_embryonic_stem_cells_flavopiridol_treatment_01hr_biol_rep1.CNhs14088.14342-155G4
29	ES-OS25_embryonic_stem_cells_flavopiridol_treatment_01hr_biol_rep2.CNhs14089.14343-155G5
30	ES-OS25_embryonic_stem_cells_flavopiridol_treatment_01hr_biol_rep3.CNhs14090.14344-155G6
31	ES-OS25_embryonic_stem_cells_KD_for_exosomal_component_EXOSC3_biol_rep1.CNhs14118.14371-156A6
32	ES-OS25_embryonic_stem_cells_KD_for_exosomal_component_EXOSC3_biol_rep2.CNhs14119.14372-156A7
33	ES-OS25_embryonic_stem_cells_KD_for_exosomal_component_EXOSC5_biol_rep1.CNhs14121.14373-156A8
34	ES-OS25_embryonic_stem_cells_KD_for_exosomal_component_EXOSC5_biol_rep2.CNhs14122.14374-156A9
35	ES-OS25_embryonic_stem_cells_scrambled_siRNA_control_biol_rep1.CNhs14116.14369-156A4
36	ES-OS25_embryonic_stem_cells_scrambled_siRNA_control_biol_rep2.CNhs14117.14370-156A5
37	ES-OS25_embryonic_stem_cells_untreated_control_biol_rep1.CNhs14091.14345-155G7
38	ES-OS25_embryonic_stem_cells_untreated_control_biol_rep2.CNhs14092.14346-155G8
39	ES-OS25_embryonic_stem_cells_untreated_control_biol_rep3.CNhs14093.14347-155G9
40	ES-OS25_embryonic_stem_cells_untreated_siRNA_control_biol_rep1.CNhs14114.14367-156A2
41	ES-OS25_embryonic_stem_cells_untreated_siRNA_control_biol_rep2.CNhs14115.14368-156A3
	Heart
1	heart_embryo_E11.CNhs10586.331-24E9
2	heart_embryo_E12.CNhs11015.353-12F5
3	heart_embryo_E13.CNhs11013.376-3I9
4	heart_embryo_E14.CNhs10597.403-26D4
5	heart_embryo_E15.CNhs11017.431-16C8
6	heart_embryo_E16.CNhs11021.457-17C6
7	heart_embryo_E17.CNhs11025.479-18E5

8	heart_embryo_E18.CNhs11030.1283-20G3
9	heart_neonate_N00.CNhs11213.639-21E3
10	heart_neonate_N03.CNhs11221.1349-25I2
11	heart_neonate_N10.CNhs11118.749-24G1
12	heart_neonate_N16.CNhs11209.782-15G1
13	heart_neonate_N20.CNhs11127.821-26I6
14	heart_neonate_N25.CNhs11196.1351-25D3
15	heart_neonate_N30.CNhs11202.1390-42D2
	Hepatocytes
1	hepatocytes_partial_hepatectomy_02hr_biol_rep1.CNhs14450.13583-146D1
2	hepatocytes_partial_hepatectomy_02hr_biol_rep2.CNhs14451.13584-146D2
3	hepatocytes_partial_hepatectomy_02hr_biol_rep3.CNhs14452.13585-146D3
4	hepatocytes_partial_hepatectomy_30hr_biol_rep1.CNhs14453.13586-146D4
5	hepatocytes_partial_hepatectomy_30hr_biol_rep2.CNhs14454.13587-146D5
6	hepatocytes_partial_hepatectomy_30hr_biol_rep3.CNhs14455.13588-146D6
7	hepatocytes_partial_hepatectomy_48hr_biol_rep1.CNhs14456.13589-146D7
8	hepatocytes_partial_hepatectomy_48hr_biol_rep2.CNhs14458.13590-146D8
9	hepatocytes_partial_hepatectomy_48hr_biol_rep3.CNhs14459.13591-146D9
10	hepatocytes_partial_hepatectomy_week01_biol_rep1.CNhs14460.13592-146E1
11	hepatocytes_partial_hepatectomy_week01_biol_rep2.CNhs14461.13593-146E2
12	hepatocytes_partial_hepatectomy_week01_biol_rep3.CNhs14462.13594-146E3
13	hepatocytes_sham_operation_biol_rep1.CNhs14447.13580-146C7
14	hepatocytes_sham_operation_biol_rep2.CNhs14448.13581-146C8
15	hepatocytes_sham_operation_biol_rep3.CNhs14449.13582-146C9
16	Mouse_hepatocyte_donor1.CNhs13078.11714-123C4
17	Mouse_hepatocyte_donor3.CNhs12615.11637-122C8
18	Mouse_hepatocyte_donor5.CNhs14553.11821-124F3
19	Mouse_hepatocyte_donor6.CNhs13090.11822-124F4
20	Mouse_hepatocyte_donor7.CNhs14554.11823-124F5
21	Mouse_hepatocyte_donor8.CNhs13091.11824-124F6
	Intestine
1	intestine_adult.CNhs10496.178-9A3
2	intestine_embryo_E12.CNhs11019.1251-16I5
3	intestine_embryo_E13.CNhs11010.381-16D5
4	intestine_embryo_E15.CNhs10602.976-16D8
5	intestine_embryo_E16.CNhs10585.463-22H4
6	intestine_embryo_E17.CNhs10582.482-18D3
7	intestine_embryo_E18.CNhs10526.1289-20F7
8	intestine_neonate_N00.CNhs11126.644-26D1
9	intestine_neonate_N01.CNhs11192.1322-23E9
10	intestine_neonate_N06.CNhs11102.688-20B8
11	intestine_neonate_N07.CNhs11095.720-20F2
12	intestine_neonate_N10.CNhs11098.755-23A5
13	intestine_neonate_N20.CNhs11187.827-18D1
14	intestine_neonate_N25.CNhs11121.1352-25E3
15	intestine_neonate_N30.CNhs11131.1384-42G1
	J2E erythroid cells
1	J2E_erythroblastic_leukemia_response_to_erythropoietin_00hr00min_biol_rep1.CNhs12449.13063-139I3
2	J2E_erythroblastic_leukemia_response_to_erythropoietin_00hr00min_biol_rep2.CNhs12668.13129-140G6
3	J2E_erythroblastic_leukemia_response_to_erythropoietin_00hr00min_biol_rep3_tech_rep1.CNhs12770.13195-141E9
4	J2E_erythroblastic_leukemia_response_to_erythropoietin_00hr00min_biol_rep3_tech_rep2.CNhs14547.13195-141E9
5	J2E_erythroblastic_leukemia_response_to_erythropoietin_00hr15min_biol_rep1.CNhs12644.13064-139I4
6	J2E_erythroblastic_leukemia_response_to_erythropoietin_00hr15min_biol_rep2.CNhs12669.13130-140G7

7	J2E_erythroblastic_leukemia_response_to_erythropoietin_00hr15min_biol_rep3.CNhs12771.13196-141F1
8	J2E_erythroblastic_leukemia_response_to_erythropoietin_00hr30min_biol_rep1.CNhs12645.13065-139I5
9	J2E_erythroblastic_leukemia_response_to_erythropoietin_00hr30min_biol_rep2_tech_rep1.CNhs12670.13131-140G8
10	J2E_erythroblastic_leukemia_response_to_erythropoietin_00hr30min_biol_rep2_tech_rep2.CNhs14544.13131-140G8
11	J2E_erythroblastic_leukemia_response_to_erythropoietin_00hr30min_biol_rep3.CNhs12772.13197-141F2
12	J2E_erythroblastic_leukemia_response_to_erythropoietin_00hr45min_biol_rep1.CNhs12646.13066-139I6
13	J2E_erythroblastic_leukemia_response_to_erythropoietin_00hr45min_biol_rep2.CNhs12671.13132-140G9
14	J2E_erythroblastic_leukemia_response_to_erythropoietin_00hr45min_biol_rep3.CNhs12773.13198-141F3
15	J2E_erythroblastic_leukemia_response_to_erythropoietin_01hr00min_biol_rep1.CNhs12647.13067-139I7
16	J2E_erythroblastic_leukemia_response_to_erythropoietin_01hr00min_biol_rep2.CNhs12672.13133-140H1
17	J2E_erythroblastic_leukemia_response_to_erythropoietin_01hr00min_biol_rep3.CNhs12774.13199-141F4
18	J2E_erythroblastic_leukemia_response_to_erythropoietin_01hr20min_biol_rep1.CNhs12648.13068-139I8
19	J2E_erythroblastic_leukemia_response_to_erythropoietin_01hr20min_biol_rep2.CNhs12673.13134-140H2
20	J2E_erythroblastic_leukemia_response_to_erythropoietin_01hr20min_biol_rep3.CNhs12775.13200-141F5
21	J2E_erythroblastic_leukemia_response_to_erythropoietin_01hr40min_biol_rep1.CNhs12649.13069-139I9
22	J2E_erythroblastic_leukemia_response_to_erythropoietin_01hr40min_biol_rep2.CNhs12674.13135-140H3
23	J2E_erythroblastic_leukemia_response_to_erythropoietin_01hr40min_biol_rep3.CNhs12776.13201-141F6
24	J2E_erythroblastic_leukemia_response_to_erythropoietin_02hr00min_biol_rep1.CNhs12650.13070-140A1
25	J2E_erythroblastic_leukemia_response_to_erythropoietin_02hr00min_biol_rep2.CNhs12675.13136-140H4
26	J2E_erythroblastic_leukemia_response_to_erythropoietin_02hr00min_biol_rep3_tech_rep1.CNhs12777.13202-141F7
27	J2E_erythroblastic_leukemia_response_to_erythropoietin_02hr00min_biol_rep3_tech_rep2.CNhs14548.13202-141F7
28	J2E_erythroblastic_leukemia_response_to_erythropoietin_02hr30min_biol_rep1.CNhs12651.13071-140A2
29	J2E_erythroblastic_leukemia_response_to_erythropoietin_02hr30min_biol_rep2.CNhs12676.13137-140H5
30	J2E_erythroblastic_leukemia_response_to_erythropoietin_02hr30min_biol_rep3.CNhs12778.13203-141F8
31	J2E_erythroblastic_leukemia_response_to_erythropoietin_03hr00min_biol_rep1.CNhs12450.13072-140A3
32	J2E_erythroblastic_leukemia_response_to_erythropoietin_03hr00min_biol_rep2.CNhs12677.13138-140H6
33	J2E_erythroblastic_leukemia_response_to_erythropoietin_03hr00min_biol_rep3.CNhs12779.13204-141F9
34	J2E_erythroblastic_leukemia_response_to_erythropoietin_03hr30min_biol_rep1.CNhs12451.13073-140A4
35	J2E_erythroblastic_leukemia_response_to_erythropoietin_03hr30min_biol_rep2.CNhs12678.13139-140H7
36	J2E_erythroblastic_leukemia_response_to_erythropoietin_03hr30min_biol_rep3.CNhs12780.13205-141G1
37	J2E_erythroblastic_leukemia_response_to_erythropoietin_04hr_biol_rep1.CNhs12452.13074-140A5
38	J2E_erythroblastic_leukemia_response_to_erythropoietin_04hr_biol_rep2.CNhs12679.13140-140H8

39	J2E_erythroblastic_leukemia_response_to_erythropoietin_04hr_biol_rep3.CNhs12781.13206-141G2
40	J2E_erythroblastic_leukemia_response_to_erythropoietin_06hr_biol_rep1.CNhs12453.13075-140A6
41	J2E_erythroblastic_leukemia_response_to_erythropoietin_06hr_biol_rep2.CNhs12680.13141-140H9
42	J2E_erythroblastic_leukemia_response_to_erythropoietin_06hr_biol_rep3.CNhs12782.13207-141G3
43	J2E_erythroblastic_leukemia_response_to_erythropoietin_12hr_biol_rep1.CNhs12454.13076-140A7
44	J2E_erythroblastic_leukemia_response_to_erythropoietin_12hr_biol_rep2_tech_rep1.CNhs12681.13142-140I1
45	J2E_erythroblastic_leukemia_response_to_erythropoietin_12hr_biol_rep2_tech_rep2.CNhs14546.13142-140I1
46	J2E_erythroblastic_leukemia_response_to_erythropoietin_12hr_biol_rep3.CNhs12783.13208-141G4
47	J2E_erythroblastic_leukemia_response_to_erythropoietin_24hr_biol_rep1.CNhs12455.13077-140A8
48	J2E_erythroblastic_leukemia_response_to_erythropoietin_24hr_biol_rep2.CNhs12682.13143-140I2
49	J2E_erythroblastic_leukemia_response_to_erythropoietin_24hr_biol_rep3.CNhs12784.13209-141G5
50	J2E_erythroblastic_leukemia_response_to_erythropoietin_48hr_biol_rep1.CNhs12456.13078-140A9
51	J2E_erythroblastic_leukemia_response_to_erythropoietin_48hr_biol_rep2.CNhs12683.13144-140I3
52	J2E_erythroblastic_leukemia_response_to_erythropoietin_48hr_biol_rep3.CNhs12785.13210-141G6
	Kidney
1	kidney_embryo_E14.CNhs10606.411-4I9
2	kidney_embryo_E15.CNhs10997.434-16F8
3	kidney_embryo_E16.CNhs10584.464-22A5
4	kidney_embryo_E17.CNhs11028.483-18I2
5	kidney_embryo_E18.CNhs11001.1288-20C7
6	kidney_neonate_N00.CNhs11214.646-21G7
7	kidney_neonate_N10.CNhs11206.758-6D5
8	kidney_neonate_N20.CNhs11113.832-19I1
9	kidney_neonate_N25.CNhs11122.1353-25F3
10	kidney_neonate_N30.CNhs11203.1385-42H1
	Liver
1	liver_adult_pregnant_day01.CNhs10466.508-5B2
2	liver_embryo_E12.CNhs10601.355-15F8
3	liver_embryo_E13.CNhs10524.378-3H6
4	liver_embryo_E14.CNhs10594.409-16E1
5	liver_embryo_E15.CNhs10520.433-16D7
6	liver_embryo_E16.CNhs10523.462-17F5
7	liver_embryo_E17.CNhs10510.481-18A3
8	liver_embryo_E18.CNhs10579.499-43G4
9	liver_neonate_N00.CNhs11117.641-24F4
10	liver_neonate_N03.CNhs11123.1345-25G2
11	liver_neonate_N06.CNhs11101.684-20A8
12	liver_neonate_N07.CNhs11103.716-20H2
13	liver_neonate_N10.CNhs11115.751-24B9
14	liver_neonate_N20.CNhs11220.823-25A3
15	liver_neonate_N25.CNhs11198.1368-26H1
16	liver_neonate_N30.CNhs11106.1382-42D1
	Lung
1	lung_adult.CNhs10474.28-22B1
2	lung_embryo_E12.CNhs10522.354-16G2
3	lung_embryo_E14.CNhs10604.404-26F8
4	lung_embryo_E15.CNhs11020.432-17C5
5	lung_embryo_E16.CNhs10998.458-17B6
6	lung_embryo_E17.CNhs10605.480-44A6

7	lung_embryo_E18.CNhs10583.1287-20I6
8	lung_neonate_N00.CNhs11224.640-42C6
9	lung_neonate_N06.CNhs11212.683-20E5
10	lung_neonate_N07.CNhs11111.715-19A3
11	lung_neonate_N10.CNhs11219.750-23E6
12	lung_neonate_N20.CNhs11109.822-18A4
13	lung_neonate_N25.CNhs11119.1359-25C7
14	lung_neonate_N30.CNhs11133.1394-42H2
	Macrophages
1	macrophage_bone_marrow_derived.CNhs14136.2171-50H8
2	macrophage_bone_marrow_derived_pool1.CNhs11457.3560-170A1
3	macrophage_bone_marrow_derived_pool2.CNhs11532.3632-171A1
4	macrophage_bone_marrow_derived_pool3.CNhs11632.3704-172A1
5	macrophage_TB_infection_non_stimulated_BMDM_with_Mtb_028hr(004h_after_stimulation)_biol_rep4.CNhs14347.3972-173I4
6	macrophage_TB_infection_non_stimulated_BMDM_with_Mtb_036hr(012h_after_stimulation)_biol_rep4.CNhs14348.3973-173A5
7	macrophage_TB_infection_non_stimulated_BMDM_with_Mtb_048hr(024h_after_stimulation)_biol_rep4.CNhs14349.3974-173B5
8	macrophage_TB_infection_non_stimulated_BMDM_with_Mtb_072hr(048h_after_stimulation)_biol_rep4.CNhs14350.3975-173C5
9	macrophage_TB_infection_non_stimulated_BMDM_with_Mtb_120hr(096h_after_stimulation)_biol_rep4.CNhs14351.3976-173D5
10	macrophage_TB_infection_non_stimulated_BMDM_without_Mtb_024hr_biol_rep4.CNhs14342.3967-173D4
11	macrophage_TB_infection_non-stimulated_BMDM_with_Mtb_028hr(004h_after_stimulation)_biol_rep1.CNhs11507.3607-170C6
12	macrophage_TB_infection_non-stimulated_BMDM_with_Mtb_028hr(004h_after_stimulation)_biol_rep2.CNhs11582.3679-171C6
13	macrophage_TB_infection_non-stimulated_BMDM_with_Mtb_036hr(012h_after_stimulation)_biol_rep1.CNhs11508.3608-170D6
14	macrophage_TB_infection_non-stimulated_BMDM_with_Mtb_036hr(012h_after_stimulation)_biol_rep2.CNhs11583.3680-171D6
15	macrophage_TB_infection_non-stimulated_BMDM_with_Mtb_048hr(024h_after_stimulation)_biol_rep1.CNhs11509.3609-170E6
16	macrophage_TB_infection_non-stimulated_BMDM_with_Mtb_048hr(024h_after_stimulation)_biol_rep2.CNhs11584.3681-171E6
17	macrophage_TB_infection_non-stimulated_BMDM_with_Mtb_072hr(048h_after_stimulation)_biol_rep1.CNhs11510.3610-170F6
18	macrophage_TB_infection_non-stimulated_BMDM_with_Mtb_072hr(048h_after_stimulation)_biol_rep2.CNhs11585.3682-171F6
19	macrophage_TB_infection_non-stimulated_BMDM_with_Mtb_120hr(096h_after_stimulation)_biol_rep1.CNhs11511.3611-170G6
20	macrophage_TB_infection_non-stimulated_BMDM_with_Mtb_120hr(096h_after_stimulation)_biol_rep2.CNhs11586.3683-171G6
21	macrophage_TB_infection_non-stimulated_BMDM_without_Mtb_004hr_biol_rep3.CNhs11633.3705-172B1
22	macrophage_TB_infection_non-stimulated_BMDM_without_Mtb_006hr_biol_rep3.CNhs11634.3706-172C1
23	macrophage_TB_infection_non-stimulated_BMDM_without_Mtb_012hr_biol_rep3.CNhs11635.3707-172D1
24	macrophage_TB_infection_non-stimulated_BMDM_without_Mtb_024hr_biol_rep1.CNhs11458.3561-170B1
25	macrophage_TB_infection_non-stimulated_BMDM_without_Mtb_024hr_biol_rep2.CNhs11533.3633-171B1
26	macrophage_TB_infection_non-stimulated_BMDM_without_Mtb_024hr_biol_rep3.CNhs11636.3708-172E1
27	macrophage_TB_infection_non-stimulated_BMDM_without_Mtb_028hr_biol_rep1.CNhs11459.3562-170C1
28	macrophage_TB_infection_non-stimulated_BMDM_without_Mtb_028hr_biol_rep2.CNhs11534.3634-171C1
29	macrophage_TB_infection_non-stimulated_BMDM_without_Mtb_028hr_biol_rep3.CNhs11637.3709-172F1

30 macrophage_TB_infection_non-stimulated_BMDM_without_Mtb_036hr_biol_rep1.CNhs11460.3563-170D1
31 macrophage_TB_infection_non-stimulated_BMDM_without_Mtb_036hr_biol_rep2.CNhs11535.3635-171D1
32 macrophage_TB_infection_non-stimulated_BMDM_without_Mtb_036hr_biol_rep3.CNhs14298.3710-172G1
33 macrophage_TB_infection_non-stimulated_BMDM_without_Mtb_048hr_biol_rep1.CNhs11461.3564-170E1
34 macrophage_TB_infection_non-stimulated_BMDM_without_Mtb_048hr_biol_rep2.CNhs11536.3636-171E1
35 macrophage_TB_infection_non-stimulated_BMDM_without_Mtb_048hr_biol_rep3.CNhs14299.3711-172H1
36 macrophage_TB_infection_non-stimulated_BMDM_without_Mtb_072hr_biol_rep1.CNhs11462.3565-170F1
37 macrophage_TB_infection_non-stimulated_BMDM_without_Mtb_072hr_biol_rep2.CNhs11537.3637-171F1
38 macrophage_TB_infection_non-stimulated_BMDM_without_Mtb_072hr_biol_rep3.CNhs14300.3712-172I1
39 macrophage_TB_infection_non-stimulated_BMDM_without_Mtb_120hr_biol_rep1.CNhs11463.3566-170G1
40 macrophage_TB_infection_non-stimulated_BMDM_without_Mtb_120hr_biol_rep2.CNhs11538.3638-171G1
41 macrophage_TB_infection_non-stimulated_BMDM_without_Mtb_120hr_biol_rep3.CNhs14301.3713-172A2
42 macrophage_TB_infection_stimulated_BMDM+IFNg(caMph)_with_Mtb_028hr(004h_after_stimulation)_biol_rep1.CNhs11512.3612-170H6
43 macrophage_TB_infection_stimulated_BMDM+IFNg(caMph)_with_Mtb_028hr(004h_after_stimulation)_biol_rep2.CNhs11587.3684-171H6
44 macrophage_TB_infection_stimulated_BMDM+IFNg(caMph)_with_Mtb_028hr(004h_after_stimulation)_biol_rep4.CNhs14352.3977-173E5
45 macrophage_TB_infection_stimulated_BMDM+IFNg(caMph)_with_Mtb_036hr(012h_after_stimulation)_biol_rep1.CNhs11513.3613-170I6
46 macrophage_TB_infection_stimulated_BMDM+IFNg(caMph)_with_Mtb_036hr(012h_after_stimulation)_biol_rep2.CNhs11588.3685-171I6
47 macrophage_TB_infection_stimulated_BMDM+IFNg(caMph)_with_Mtb_036hr(012h_after_stimulation)_biol_rep4.CNhs14353.3978-173F5
48 macrophage_TB_infection_stimulated_BMDM+IFNg(caMph)_with_Mtb_048hr(024h_after_stimulation)_biol_rep1.CNhs11514.3614-170A7
49 macrophage_TB_infection_stimulated_BMDM+IFNg(caMph)_with_Mtb_048hr(024h_after_stimulation)_biol_rep2.CNhs11614.3686-171A7
50 macrophage_TB_infection_stimulated_BMDM+IFNg(caMph)_with_Mtb_048hr(024h_after_stimulation)_biol_rep4.CNhs14354.3979-173G5
51 macrophage_TB_infection_stimulated_BMDM+IFNg(caMph)_with_Mtb_072hr(048h_after_stimulation)_biol_rep1.CNhs11515.3615-170B7
52 macrophage_TB_infection_stimulated_BMDM+IFNg(caMph)_with_Mtb_072hr(048h_after_stimulation)_biol_rep2.CNhs11615.3687-171B7
53 macrophage_TB_infection_stimulated_BMDM+IFNg(caMph)_with_Mtb_072hr(048h_after_stimulation)_biol_rep4.CNhs14355.3980-173H5
54 macrophage_TB_infection_stimulated_BMDM+IFNg(caMph)_with_Mtb_120hr(096h_after_stimulation)_biol_rep1.CNhs11516.3616-170C7
55 macrophage_TB_infection_stimulated_BMDM+IFNg(caMph)_with_Mtb_120hr(096h_after_stimulation)_biol_rep2.CNhs11616.3688-171C7
56 macrophage_TB_infection_stimulated_BMDM+IFNg(caMph)_with_Mtb_120hr(096h_after_stimulation)_biol_rep4.CNhs14356.3981-173I5
57 macrophage_TB_infection_stimulated_BMDM+IFNg(caMph)_without_Mtb_002hr_biol_rep1.CNhs11464.3567-170H1
58 macrophage_TB_infection_stimulated_BMDM+IFNg(caMph)_without_Mtb_002hr_biol_rep2.CNhs11539.3639-171H1
59 macrophage_TB_infection_stimulated_BMDM+IFNg(caMph)_without_Mtb_002hr_biol_rep3.CNhs11638.3714-172B2
60 macrophage_TB_infection_stimulated_BMDM+IFNg(caMph)_without_Mtb_004hr_biol_rep1.CNhs11465.3568-170I1
61 macrophage_TB_infection_stimulated_BMDM+IFNg(caMph)_without_Mtb_004hr_biol_rep2.CNhs11540.3640-171I1

62	macrophage_TB_infection_stimulated_BMDM+IFNg(caMph)_without_Mtb_004hr_biol_rep3.CNhs11639.3715-172C2
63	macrophage_TB_infection_stimulated_BMDM+IFNg(caMph)_without_Mtb_006hr_biol_rep1.CNhs11466.3569-170A2
64	macrophage_TB_infection_stimulated_BMDM+IFNg(caMph)_without_Mtb_006hr_biol_rep2.CNhs11541.3641-171A2
65	macrophage_TB_infection_stimulated_BMDM+IFNg(caMph)_without_Mtb_006hr_biol_rep3.CNhs11640.3716-172D2
66	macrophage_TB_infection_stimulated_BMDM+IFNg(caMph)_without_Mtb_012hr_biol_rep1.CNhs11467.3570-170B2
67	macrophage_TB_infection_stimulated_BMDM+IFNg(caMph)_without_Mtb_012hr_biol_rep2.CNhs11542.3642-171B2
68	macrophage_TB_infection_stimulated_BMDM+IFNg(caMph)_without_Mtb_012hr_biol_rep3.CNhs11641.3717-172E2
69	macrophage_TB_infection_stimulated_BMDM+IFNg(caMph)_without_Mtb_024hr_biol_rep1.CNhs11468.3571-170C2
70	macrophage_TB_infection_stimulated_BMDM+IFNg(caMph)_without_Mtb_024hr_biol_rep2.CNhs11543.3643-171C2
71	macrophage_TB_infection_stimulated_BMDM+IFNg(caMph)_without_Mtb_024hr_biol_rep3_.CNhs11642.3718-172F2
72	macrophage_TB_infection_stimulated_BMDM+IFNg(caMph)_without_Mtb_024hr_biol_rep4.CNhs14343.3968-173E4
73	macrophage_TB_infection_stimulated_BMDM+IFNg(caMph)_without_Mtb_028hr_biol_rep1.CNhs11469.3572-170D2
74	macrophage_TB_infection_stimulated_BMDM+IFNg(caMph)_without_Mtb_028hr_biol_rep2.CNhs11547.3644-171D2
75	macrophage_TB_infection_stimulated_BMDM+IFNg(caMph)_without_Mtb_028hr_biol_rep3.CNhs11643.3719-172G2
76	macrophage_TB_infection_stimulated_BMDM+IFNg(caMph)_without_Mtb_036hr_biol_rep1.CNhs11470.3573-170E2
77	macrophage_TB_infection_stimulated_BMDM+IFNg(caMph)_without_Mtb_036hr_biol_rep2.CNhs11548.3645-171E2
78	macrophage_TB_infection_stimulated_BMDM+IFNg(caMph)_without_Mtb_036hr_biol_rep3.CNhs14302.3720-172H2
79	macrophage_TB_infection_stimulated_BMDM+IFNg(caMph)_without_Mtb_048hr_biol_rep1.CNhs11471.3574-170F2
80	macrophage_TB_infection_stimulated_BMDM+IFNg(caMph)_without_Mtb_048hr_biol_rep2.CNhs11549.3646-171F2
81	macrophage_TB_infection_stimulated_BMDM+IFNg(caMph)_without_Mtb_048hr_biol_rep3.CNhs14303.3721-172I2
82	macrophage_TB_infection_stimulated_BMDM+IFNg(caMph)_without_Mtb_072hr_biol_rep1.CNhs11472.3575-170G2
83	macrophage_TB_infection_stimulated_BMDM+IFNg(caMph)_without_Mtb_072hr_biol_rep2.CNhs11550.3647-171G2
84	macrophage_TB_infection_stimulated_BMDM+IFNg(caMph)_without_Mtb_072hr_biol_rep3.CNhs14304.3722-172A3
85	macrophage_TB_infection_stimulated_BMDM+IFNg(caMph)_without_Mtb_120hr_biol_rep1.CNhs11473.3576-170H2
86	macrophage_TB_infection_stimulated_BMDM+IFNg(caMph)_without_Mtb_120hr_biol_rep2.CNhs11551.3648-171H2
87	macrophage_TB_infection_stimulated_BMDM+IFNg(caMph)_without_Mtb_120hr_biol_rep3.CNhs14305.3723-172B3
88	macrophage_TB_infection_stimulated_BMDM+IL-13(aaMph)_with_Mtb_028hr(004h_after_stimulation)_biol_rep1.CNhs11517.3617-170D7
89	macrophage_TB_infection_stimulated_BMDM+IL-13(aaMph)_with_Mtb_028hr(004h_after_stimulation)_biol_rep2.CNhs11617.3689-171D7
90	macrophage_TB_infection_stimulated_BMDM+IL-13(aaMph)_with_Mtb_028hr(004h_after_stimulation)_biol_rep4.CNhs14357.3982-173A6
91	macrophage_TB_infection_stimulated_BMDM+IL-13(aaMph)_with_Mtb_036hr(012h_after_stimulation)_biol_rep1.CNhs11518.3618-170E7
92	macrophage_TB_infection_stimulated_BMDM+IL-13(aaMph)_with_Mtb_036hr(012h_after_stimulation)_biol_rep2.CNhs11618.3690-171E7
93	macrophage_TB_infection_stimulated_BMDM+IL-13(aaMph)_with_Mtb_048hr(024h_after_stimulation)_biol_rep1.CNhs11519.3619-170F7

94	macrophage_TB_infection_stimulated_BMDM+IL-13(aaMph)_with_Mtb_048hr(024h_after_stimulation)_biol_rep2.CNhs11619.3691-171F7
95	macrophage_TB_infection_stimulated_BMDM+IL-13(aaMph)_with_Mtb_048hr(024h_after_stimulation)_biol_rep4.CNhs14359.3984-173C6
96	macrophage_TB_infection_stimulated_BMDM+IL-13(aaMph)_with_Mtb_072hr(048h_after_stimulation)_biol_rep1.CNhs11520.3620-170G7
97	macrophage_TB_infection_stimulated_BMDM+IL-13(aaMph)_with_Mtb_072hr(048h_after_stimulation)_biol_rep2.CNhs11620.3692-171G7
98	macrophage_TB_infection_stimulated_BMDM+IL-13(aaMph)_with_Mtb_072hr(048h_after_stimulation)_biol_rep4.CNhs14360.3985-173D6
99	macrophage_TB_infection_stimulated_BMDM+IL-13(aaMph)_with_Mtb_120hr(096h_after_stimulation)_biol_rep1.CNhs11521.3621-170H7
100	macrophage_TB_infection_stimulated_BMDM+IL-13(aaMph)_with_Mtb_120hr(096h_after_stimulation)_biol_rep2.CNhs11621.3693-171H7
101	macrophage_TB_infection_stimulated_BMDM+IL-13(aaMph)_with_Mtb_120hr(096h_after_stimulation)_biol_rep4.CNhs14361.3986-173E6
102	macrophage_TB_infection_stimulated_BMDM+IL-13(aaMph)_without_Mtb_002hr_biol_rep1.CNhs11474.3577-170I2
103	macrophage_TB_infection_stimulated_BMDM+IL-13(aaMph)_without_Mtb_002hr_biol_rep2.CNhs11552.3649-171I2
104	macrophage_TB_infection_stimulated_BMDM+IL-13(aaMph)_without_Mtb_002hr_biol_rep3.CNhs11644.3724-172C3
105	macrophage_TB_infection_stimulated_BMDM+IL-13(aaMph)_without_Mtb_004hr_biol_rep1.CNhs11475.3578-170A3
106	macrophage_TB_infection_stimulated_BMDM+IL-13(aaMph)_without_Mtb_004hr_biol_rep2.CNhs11553.3650-171A3
107	macrophage_TB_infection_stimulated_BMDM+IL-13(aaMph)_without_Mtb_004hr_biol_rep3.CNhs11645.3725-172D3
108	macrophage_TB_infection_stimulated_BMDM+IL-13(aaMph)_without_Mtb_006hr_biol_rep1.CNhs11476.3579-170B3
109	macrophage_TB_infection_stimulated_BMDM+IL-13(aaMph)_without_Mtb_006hr_biol_rep2.CNhs11554.3651-171B3
110	macrophage_TB_infection_stimulated_BMDM+IL-13(aaMph)_without_Mtb_006hr_biol_rep3.CNhs11646.3726-172E3
111	macrophage_TB_infection_stimulated_BMDM+IL-13(aaMph)_without_Mtb_012hr_biol_rep1.CNhs11477.3580-170C3
112	macrophage_TB_infection_stimulated_BMDM+IL-13(aaMph)_without_Mtb_012hr_biol_rep2.CNhs11555.3652-171C3
113	macrophage_TB_infection_stimulated_BMDM+IL-13(aaMph)_without_Mtb_012hr_biol_rep3.CNhs11647.3727-172F3
114	macrophage_TB_infection_stimulated_BMDM+IL-13(aaMph)_without_Mtb_024hr_biol_rep1.CNhs11478.3581-170D3
115	macrophage_TB_infection_stimulated_BMDM+IL-13(aaMph)_without_Mtb_024hr_biol_rep2.CNhs11556.3653-171D3
116	macrophage_TB_infection_stimulated_BMDM+IL-13(aaMph)_without_Mtb_024hr_biol_rep3.CNhs11648.3728-172G3
117	macrophage_TB_infection_stimulated_BMDM+IL-13(aaMph)_without_Mtb_024hr_biol_rep4.CNhs14344.3969-173F4
118	macrophage_TB_infection_stimulated_BMDM+IL-13(aaMph)_without_Mtb_028hr_biol_rep1.CNhs11479.3582-170E3
119	macrophage_TB_infection_stimulated_BMDM+IL-13(aaMph)_without_Mtb_028hr_biol_rep2.CNhs11557.3654-171E3
120	macrophage_TB_infection_stimulated_BMDM+IL-13(aaMph)_without_Mtb_028hr_biol_rep3.CNhs11649.3729-172H3
121	macrophage_TB_infection_stimulated_BMDM+IL-13(aaMph)_without_Mtb_036hr_biol_rep1.CNhs11480.3583-170F3
122	macrophage_TB_infection_stimulated_BMDM+IL-13(aaMph)_without_Mtb_036hr_biol_rep2.CNhs11558.3655-171F3
123	macrophage_TB_infection_stimulated_BMDM+IL-13(aaMph)_without_Mtb_036hr_biol_rep3.CNhs14306.3730-172I3
124	macrophage_TB_infection_stimulated_BMDM+IL-13(aaMph)_without_Mtb_048hr_biol_rep1.CNhs11481.3584-170G3
125	macrophage_TB_infection_stimulated_BMDM+IL-13(aaMph)_without_Mtb_048hr_biol_rep2.CNhs11559.3656-171G3

126	macrophage_TB_infection_stimulated_BMDM+IL-13(aaMph)_without_Mtb_048hr_biol_rep3.CNhs14307.3731-172A4
127	macrophage_TB_infection_stimulated_BMDM+IL-13(aaMph)_without_Mtb_072hr_biol_rep1.CNhs11482.3585-170H3
128	macrophage_TB_infection_stimulated_BMDM+IL-13(aaMph)_without_Mtb_072hr_biol_rep2.CNhs11560.3657-171H3
129	macrophage_TB_infection_stimulated_BMDM+IL-13(aaMph)_without_Mtb_072hr_biol_rep3.CNhs14308.3732-172B4
130	macrophage_TB_infection_stimulated_BMDM+IL-13(aaMph)_without_Mtb_120hr_biol_rep1.CNhs11483.3586-170I3
131	macrophage_TB_infection_stimulated_BMDM+IL-13(aaMph)_without_Mtb_120hr_biol_rep2.CNhs11561.3658-171I3
132	macrophage_TB_infection_stimulated_BMDM+IL-13(aaMph)_without_Mtb_120hr_biol_rep3.CNhs14309.3733-172C4
133	macrophage_TB_infection_stimulated_BMDM+IL-4(aaMph)_with_Mtb_028hr(004h_after_stimulation)_biol_rep1.CNhs11527.3627-170E8
134	macrophage_TB_infection_stimulated_BMDM+IL-4(aaMph)_with_Mtb_028hr(004h_after_stimulation)_biol_rep2.CNhs11627.3699-171E8
135	macrophage_TB_infection_stimulated_BMDM+IL-4(aaMph)_with_Mtb_028hr(004h_after_stimulation)_biol_rep4.CNhs14367.3992-173B7
136	macrophage_TB_infection_stimulated_BMDM+IL-4(aaMph)_with_Mtb_036hr(012h_after_stimulation)_biol_rep1.CNhs11528.3628-170F8
137	macrophage_TB_infection_stimulated_BMDM+IL-4(aaMph)_with_Mtb_036hr(012h_after_stimulation)_biol_rep2.CNhs11628.3700-171F8
138	macrophage_TB_infection_stimulated_BMDM+IL-4(aaMph)_with_Mtb_036hr(012h_after_stimulation)_biol_rep4.CNhs14368.3993-173C7
139	macrophage_TB_infection_stimulated_BMDM+IL-4(aaMph)_with_Mtb_048hr(024h_after_stimulation)_biol_rep1.CNhs11529.3629-170G8
140	macrophage_TB_infection_stimulated_BMDM+IL-4(aaMph)_with_Mtb_048hr(024h_after_stimulation)_biol_rep2.CNhs11629.3701-171G8
141	macrophage_TB_infection_stimulated_BMDM+IL-4(aaMph)_with_Mtb_048hr(024h_after_stimulation)_biol_rep4.CNhs14369.3994-173D7
142	macrophage_TB_infection_stimulated_BMDM+IL-4(aaMph)_with_Mtb_072hr(048h_after_stimulation)_biol_rep1.CNhs11530.3630-170H8
143	macrophage_TB_infection_stimulated_BMDM+IL-4(aaMph)_with_Mtb_072hr(048h_after_stimulation)_biol_rep2.CNhs11630.3702-171H8
144	macrophage_TB_infection_stimulated_BMDM+IL-4(aaMph)_with_Mtb_072hr(048h_after_stimulation)_biol_rep4.CNhs14370.3995-173E7
145	macrophage_TB_infection_stimulated_BMDM+IL-4(aaMph)_with_Mtb_120hr(096h_after_stimulation)_biol_rep1.CNhs11531.3631-170I8
146	macrophage_TB_infection_stimulated_BMDM+IL-4(aaMph)_with_Mtb_120hr(096h_after_stimulation)_biol_rep2.CNhs11631.3703-171I8
147	macrophage_TB_infection_stimulated_BMDM+IL-4(aaMph)_with_Mtb_120hr(096h_after_stimulation)_biol_rep4.CNhs14371.3996-173F7
148	macrophage_TB_infection_stimulated_BMDM+IL-4(aaMph)_without_Mtb_002hr_biol_rep1.CNhs11494.3597-170B5
149	macrophage_TB_infection_stimulated_BMDM+IL-4(aaMph)_without_Mtb_002hr_biol_rep2.CNhs11572.3669-171B5
150	macrophage_TB_infection_stimulated_BMDM+IL-4(aaMph)_without_Mtb_002hr_biol_rep3.CNhs11655.3744-172E5
151	macrophage_TB_infection_stimulated_BMDM+IL-4(aaMph)_without_Mtb_004hr_biol_rep1.CNhs11495.3598-170C5
152	macrophage_TB_infection_stimulated_BMDM+IL-4(aaMph)_without_Mtb_004hr_biol_rep2.CNhs11573.3670-171C5
153	macrophage_TB_infection_stimulated_BMDM+IL-4(aaMph)_without_Mtb_004hr_biol_rep3.CNhs14259.3745-172F5
154	macrophage_TB_infection_stimulated_BMDM+IL-4(aaMph)_without_Mtb_006hr_biol_rep1.CNhs11496.3599-170D5
155	macrophage_TB_infection_stimulated_BMDM+IL-4(aaMph)_without_Mtb_006hr_biol_rep2.CNhs11574.3671-171D5
156	macrophage_TB_infection_stimulated_BMDM+IL-4(aaMph)_without_Mtb_006hr_biol_rep3.CNhs14260.3746-172G5
157	macrophage_TB_infection_stimulated_BMDM+IL-4(aaMph)_without_Mtb_012hr_biol_rep1.CNhs11497.3600-170E5

158 macrophage_TB_infection_stimulated_BMDM+IL-4(aaMph)_without_Mtb_012hr_biol_rep2.CNhs11575.3672-171E5
159 macrophage_TB_infection_stimulated_BMDM+IL-4(aaMph)_without_Mtb_012hr_biol_rep3.CNhs14261.3747-172H5
160 macrophage_TB_infection_stimulated_BMDM+IL-4(aaMph)_without_Mtb_024hr_biol_rep1.CNhs11498.3601-170F5
161 macrophage_TB_infection_stimulated_BMDM+IL-4(aaMph)_without_Mtb_024hr_biol_rep2.CNhs11576.3673-171F5
162 macrophage_TB_infection_stimulated_BMDM+IL-4(aaMph)_without_Mtb_024hr_biol_rep3.CNhs14262.3748-172I5
163 macrophage_TB_infection_stimulated_BMDM+IL-4(aaMph)_without_Mtb_024hr_biol_rep4.CNhs14346.3971-173H4
164 macrophage_TB_infection_stimulated_BMDM+IL-4(aaMph)_without_Mtb_028hr_biol_rep1.CNhs11502.3602-170G5
165 macrophage_TB_infection_stimulated_BMDM+IL-4(aaMph)_without_Mtb_028hr_biol_rep2.CNhs11577.3674-171G5
166 macrophage_TB_infection_stimulated_BMDM+IL-4(aaMph)_without_Mtb_028hr_biol_rep3.CNhs14263.3749-172A6
167 macrophage_TB_infection_stimulated_BMDM+IL-4(aaMph)_without_Mtb_036hr_biol_rep1.CNhs11503.3603-170H5
168 macrophage_TB_infection_stimulated_BMDM+IL-4(aaMph)_without_Mtb_036hr_biol_rep2.CNhs11578.3675-171H5
169 macrophage_TB_infection_stimulated_BMDM+IL-4(aaMph)_without_Mtb_036hr_biol_rep3.CNhs14264.3750-172B6
170 macrophage_TB_infection_stimulated_BMDM+IL-4(aaMph)_without_Mtb_048hr_biol_rep1.CNhs11504.3604-170I5
171 macrophage_TB_infection_stimulated_BMDM+IL-4(aaMph)_without_Mtb_048hr_biol_rep2.CNhs11579.3676-171I5
172 macrophage_TB_infection_stimulated_BMDM+IL-4(aaMph)_without_Mtb_048hr_biol_rep3.CNhs14265.3751-172C6
173 macrophage_TB_infection_stimulated_BMDM+IL-4(aaMph)_without_Mtb_072hr_biol_rep1.CNhs11505.3605-170A6
174 macrophage_TB_infection_stimulated_BMDM+IL-4(aaMph)_without_Mtb_072hr_biol_rep2.CNhs11580.3677-171A6
175 macrophage_TB_infection_stimulated_BMDM+IL-4(aaMph)_without_Mtb_072hr_biol_rep3.CNhs14266.3752-172D6
176 macrophage_TB_infection_stimulated_BMDM+IL-4(aaMph)_without_Mtb_120hr_biol_rep1.CNhs11506.3606-170B6
177 macrophage_TB_infection_stimulated_BMDM+IL-4(aaMph)_without_Mtb_120hr_biol_rep2.CNhs11581.3678-171B6
178 macrophage_TB_infection_stimulated_BMDM+IL-4(aaMph)_without_Mtb_120hr_biol_rep3.CNhs14267.3753-172E6
179 macrophage_TB_infection_stimulated_BMDM+IL-4/IL-13(aaMph)_with_Mtb_028hr(004h_after_stimulation)_biol_rep1.CNhs11522.3622-170I7
180 macrophage_TB_infection_stimulated_BMDM+IL-4/IL-13(aaMph)_with_Mtb_028hr(004h_after_stimulation)_biol_rep2.CNhs11622.3694-171I7
181 macrophage_TB_infection_stimulated_BMDM+IL-4/IL-13(aaMph)_with_Mtb_028hr(004h_after_stimulation)_biol_rep4.CNhs14362.3987-173F6
182 macrophage_TB_infection_stimulated_BMDM+IL-4/IL-13(aaMph)_with_Mtb_036hr(012h_after_stimulation)_biol_rep1.CNhs11523.3623-170A8
183 macrophage_TB_infection_stimulated_BMDM+IL-4/IL-13(aaMph)_with_Mtb_036hr(012h_after_stimulation)_biol_rep2.CNhs11623.3695-171A8
184 macrophage_TB_infection_stimulated_BMDM+IL-4/IL-13(aaMph)_with_Mtb_036hr(012h_after_stimulation)_biol_rep4.CNhs14363.3988-173G6
185 macrophage_TB_infection_stimulated_BMDM+IL-4/IL-13(aaMph)_with_Mtb_048hr(024h_after_stimulation)_biol_rep1.CNhs11524.3624-170B8
186 macrophage_TB_infection_stimulated_BMDM+IL-4/IL-13(aaMph)_with_Mtb_048hr(024h_after_stimulation)_biol_rep2.CNhs11624.3696-171B8
187 macrophage_TB_infection_stimulated_BMDM+IL-4/IL-13(aaMph)_with_Mtb_048hr(024h_after_stimulation)_biol_rep4.CNhs14364.3989-173H6
188 macrophage_TB_infection_stimulated_BMDM+IL-4/IL-13(aaMph)_with_Mtb_072hr(048h_after_stimulation)_biol_rep1.CNhs11525.3625-170C8
189 macrophage_TB_infection_stimulated_BMDM+IL-4/IL-13(aaMph)_with_Mtb_072hr(048h_after_stimulation)_biol_rep2.CNhs11625.3697-171C8

190	macrophage_TB_infection_stimulated_BMDM+IL-4/IL-13(aaMph)_with_Mtb_072hr(048h_after_stimulation)_biol_rep4.CNhs14365.3990-173I6
191	macrophage_TB_infection_stimulated_BMDM+IL-4/IL-13(aaMph)_with_Mtb_120hr(096h_after_stimulation)_biol_rep1.CNhs11526.3626-170D8
192	macrophage_TB_infection_stimulated_BMDM+IL-4/IL-13(aaMph)_with_Mtb_120hr(096h_after_stimulation)_biol_rep2.CNhs11626.3698-171D8
193	macrophage_TB_infection_stimulated_BMDM+IL-4/IL-13(aaMph)_with_Mtb_120hr(096h_after_stimulation)_biol_rep4.CNhs14366.3991-173A7
194	macrophage_TB_infection_stimulated_BMDM+IL-4/IL-13(aaMph)_without_Mtb_002hr_biol_rep1.CNhs11484.3587-170A4
195	macrophage_TB_infection_stimulated_BMDM+IL-4/IL-13(aaMph)_without_Mtb_002hr_biol_rep2.CNhs11562.3659-171A4
196	macrophage_TB_infection_stimulated_BMDM+IL-4/IL-13(aaMph)_without_Mtb_002hr_biol_rep3.CNhs11650.3734-172D4
197	macrophage_TB_infection_stimulated_BMDM+IL-4/IL-13(aaMph)_without_Mtb_004hr_biol_rep1.CNhs11485.3588-170B4
198	macrophage_TB_infection_stimulated_BMDM+IL-4/IL-13(aaMph)_without_Mtb_004hr_biol_rep2.CNhs11563.3660-171B4
199	macrophage_TB_infection_stimulated_BMDM+IL-4/IL-13(aaMph)_without_Mtb_004hr_biol_rep3.CNhs11651.3735-172E4
200	macrophage_TB_infection_stimulated_BMDM+IL-4/IL-13(aaMph)_without_Mtb_006hr_biol_rep1.CNhs11486.3589-170C4
201	macrophage_TB_infection_stimulated_BMDM+IL-4/IL-13(aaMph)_without_Mtb_006hr_biol_rep2.CNhs11564.3661-171C4
202	macrophage_TB_infection_stimulated_BMDM+IL-4/IL-13(aaMph)_without_Mtb_006hr_biol_rep3.CNhs11652.3736-172F4
203	macrophage_TB_infection_stimulated_BMDM+IL-4/IL-13(aaMph)_without_Mtb_012hr_biol_rep1.CNhs11487.3590-170D4
204	macrophage_TB_infection_stimulated_BMDM+IL-4/IL-13(aaMph)_without_Mtb_012hr_biol_rep2.CNhs11565.3662-171D4
205	macrophage_TB_infection_stimulated_BMDM+IL-4/IL-13(aaMph)_without_Mtb_012hr_biol_rep3.CNhs11653.3737-172G4
206	macrophage_TB_infection_stimulated_BMDM+IL-4/IL-13(aaMph)_without_Mtb_024hr_biol_rep1.CNhs11488.3591-170E4
207	macrophage_TB_infection_stimulated_BMDM+IL-4/IL-13(aaMph)_without_Mtb_024hr_biol_rep2.CNhs11566.3663-171E4
208	macrophage_TB_infection_stimulated_BMDM+IL-4/IL-13(aaMph)_without_Mtb_024hr_biol_rep3.CNhs11654.3738-172H4
209	macrophage_TB_infection_stimulated_BMDM+IL-4/IL-13(aaMph)_without_Mtb_024hr_biol_rep4.CNhs14345.3970-173G4
210	macrophage_TB_infection_stimulated_BMDM+IL-4/IL-13(aaMph)_without_Mtb_028hr_biol_rep1.CNhs11489.3592-170F4
211	macrophage_TB_infection_stimulated_BMDM+IL-4/IL-13(aaMph)_without_Mtb_028hr_biol_rep2.CNhs11567.3664-171F4
212	macrophage_TB_infection_stimulated_BMDM+IL-4/IL-13(aaMph)_without_Mtb_028hr_biol_rep3.CNhs14254.3739-172I4
213	macrophage_TB_infection_stimulated_BMDM+IL-4/IL-13(aaMph)_without_Mtb_036hr_biol_rep1.CNhs11490.3593-170G4
214	macrophage_TB_infection_stimulated_BMDM+IL-4/IL-13(aaMph)_without_Mtb_036hr_biol_rep2.CNhs11568.3665-171G4
215	macrophage_TB_infection_stimulated_BMDM+IL-4/IL-13(aaMph)_without_Mtb_036hr_biol_rep3.CNhs14255.3740-172A5
216	macrophage_TB_infection_stimulated_BMDM+IL-4/IL-13(aaMph)_without_Mtb_048hr_biol_rep1.CNhs11491.3594-170H4
217	macrophage_TB_infection_stimulated_BMDM+IL-4/IL-13(aaMph)_without_Mtb_048hr_biol_rep2.CNhs11569.3666-171H4
218	macrophage_TB_infection_stimulated_BMDM+IL-4/IL-13(aaMph)_without_Mtb_048hr_biol_rep3.CNhs14256.3741-172B5
219	macrophage_TB_infection_stimulated_BMDM+IL-4/IL-13(aaMph)_without_Mtb_072hr_biol_rep1.CNhs11492.3595-170I4
220	macrophage_TB_infection_stimulated_BMDM+IL-4/IL-13(aaMph)_without_Mtb_072hr_biol_rep2.CNhs11570.3667-171I4
221	macrophage_TB_infection_stimulated_BMDM+IL-4/IL-13(aaMph)_without_Mtb_072hr_biol_rep3.CNhs14257.3742-172C5

222	macrophage_TB_infection_stimulated_BMDM+IL-4/IL-13(aaMph)_without_Mtb_120hr_biol_rep1.CNhs11493.3596-170A5
223	macrophage_TB_infection_stimulated_BMDM+IL-4/IL-13(aaMph)_without_Mtb_120hr_biol_rep2.CNhs11571.3668-171A5
224	macrophage_TB_infection_stimulated_BMDM+IL-4/IL-13(aaMph)_without_Mtb_120hr_biol_rep3.CNhs14258.3743-172D5
	Mesenchymal stem cells
1	Mouse_Mesenchymal_stem_cells_-_bone_marrow_derived_donor1.CNhs12628.11717-123C7
2	Mouse_Mesenchymal_stem_cells_-_bone_marrow_derived_donor2.CNhs12633.11735-123E7
3	Mouse_Mesenchymal_stem_cells_-_bone_marrow_derived_donor3.CNhs12616.11640-122D2
4	ST2_(Mesenchymal_stem_cells)_cells_differentiation_to_adipocytes_00hr15min_biol_rep1_(015mA1).CNhs13114.12308-130F4
5	ST2_(Mesenchymal_stem_cells)_cells_differentiation_to_adipocytes_00hr15min_biol_rep2_(015mA2).CNhs13243.12430-132A9
6	ST2_(Mesenchymal_stem_cells)_cells_differentiation_to_adipocytes_00hr15min_biol_rep3_(015mA3).CNhs13292.12552-133F5
7	ST2_(Mesenchymal_stem_cells)_cells_differentiation_to_adipocytes_00hr30min_biol_rep1_(030mA1).CNhs13115.12309-130F5
8	ST2_(Mesenchymal_stem_cells)_cells_differentiation_to_adipocytes_00hr30min_biol_rep2_(030mA2).CNhs13244.12431-132B1
9	ST2_(Mesenchymal_stem_cells)_cells_differentiation_to_adipocytes_00hr30min_biol_rep3_(030mA3).CNhs13293.12553-133F6
10	ST2_(Mesenchymal_stem_cells)_cells_differentiation_to_adipocytes_01hr_biol_rep1_(001hA1).CNhs13116.12310-130F6
11	ST2_(Mesenchymal_stem_cells)_cells_differentiation_to_adipocytes_01hr_biol_rep2_(001hA2).CNhs13245.12432-132B2
12	ST2_(Mesenchymal_stem_cells)_cells_differentiation_to_adipocytes_01hr_biol_rep3_(001hA3).CNhs13295.12554-133F7
13	ST2_(Mesenchymal_stem_cells)_cells_differentiation_to_adipocytes_02hr_biol_rep1_(002hA1).CNhs13117.12311-130F7
14	ST2_(Mesenchymal_stem_cells)_cells_differentiation_to_adipocytes_02hr_biol_rep2_(002hA2).CNhs13247.12433-132B3
15	ST2_(Mesenchymal_stem_cells)_cells_differentiation_to_adipocytes_02hr_biol_rep3_(002hA3).CNhs13296.12555-133F8
16	ST2_(Mesenchymal_stem_cells)_cells_differentiation_to_adipocytes_03hr_biol_rep1_(003hA1).CNhs13118.12312-130F8
17	ST2_(Mesenchymal_stem_cells)_cells_differentiation_to_adipocytes_03hr_biol_rep2_(003hA2).CNhs13248.12434-132B4
18	ST2_(Mesenchymal_stem_cells)_cells_differentiation_to_adipocytes_03hr_biol_rep3_(003hA3).CNhs13297.12556-133F9
19	ST2_(Mesenchymal_stem_cells)_cells_differentiation_to_adipocytes_06hr_biol_rep1_(006hA1).CNhs13120.12313-130F9
20	ST2_(Mesenchymal_stem_cells)_cells_differentiation_to_adipocytes_06hr_biol_rep2_(006hA2).CNhs13249.12435-132B5
21	ST2_(Mesenchymal_stem_cells)_cells_differentiation_to_adipocytes_06hr_biol_rep3_(006hA3).CNhs13298.12557-133G1
22	ST2_(Mesenchymal_stem_cells)_cells_differentiation_to_adipocytes_12hr_biol_rep1_(012hA1).CNhs13121.12314-130G1
23	ST2_(Mesenchymal_stem_cells)_cells_differentiation_to_adipocytes_12hr_biol_rep2_(012hA2).CNhs13250.12436-132B6
24	ST2_(Mesenchymal_stem_cells)_cells_differentiation_to_adipocytes_12hr_biol_rep3_(012hA3).CNhs13299.12558-133G2
25	ST2_(Mesenchymal_stem_cells)_cells_differentiation_to_adipocytes_18hr_biol_rep1_(018hA1).CNhs13122.12315-130G2
26	ST2_(Mesenchymal_stem_cells)_cells_differentiation_to_adipocytes_18hr_biol_rep2_(018hA2).CNhs13251.12437-132B7
27	ST2_(Mesenchymal_stem_cells)_cells_differentiation_to_adipocytes_18hr_biol_rep3_(018hA3).CNhs13300.12559-133G3
28	ST2_(Mesenchymal_stem_cells)_cells_differentiation_to_adipocytes_24hr_biol_rep1_(024hA1).CNhs13123.12316-130G3
29	ST2_(Mesenchymal_stem_cells)_cells_differentiation_to_adipocytes_24hr_biol_rep2_(024hA2).CNhs13252.12438-132B8
30	ST2_(Mesenchymal_stem_cells)_cells_differentiation_to_adipocytes_24hr_biol_rep3_(024hA3).CNhs13301.12560-133G4

31	ST2_(Mesenchymal_stem_cells)_cells_differentiation_to_adipocytes_36hr_biol_rep1_(036hA1).CNhs13124.12317-130G4
32	ST2_(Mesenchymal_stem_cells)_cells_differentiation_to_adipocytes_36hr_biol_rep2_(036hA2).CNhs13253.12439-132B9
33	ST2_(Mesenchymal_stem_cells)_cells_differentiation_to_adipocytes_36hr_biol_rep3_(036hA3).CNhs13302.12561-133G5
34	ST2_(Mesenchymal_stem_cells)_cells_differentiation_to_adipocytes_day02_biol_rep1_(048hA1).CNhs13125.12318-130G5
35	ST2_(Mesenchymal_stem_cells)_cells_differentiation_to_adipocytes_day02_biol_rep2_(048hA2).CNhs13254.12440-132C1
36	ST2_(Mesenchymal_stem_cells)_cells_differentiation_to_adipocytes_day02_biol_rep3_(048hA3).CNhs13303.12562-133G6
37	ST2_(Mesenchymal_stem_cells)_cells_differentiation_to_adipocytes_day03_biol_rep1_(072hA1).CNhs13126.12319-130G6
38	ST2_(Mesenchymal_stem_cells)_cells_differentiation_to_adipocytes_day03_biol_rep2_(072hA2).CNhs13255.12441-132C2
39	ST2_(Mesenchymal_stem_cells)_cells_differentiation_to_adipocytes_day03_biol_rep3_(072hA3).CNhs13304.12563-133G7
40	ST2_(Mesenchymal_stem_cells)_cells_differentiation_to_adipocytes_day04_biol_rep1_(096hA1).CNhs13127.12320-130G7
41	ST2_(Mesenchymal_stem_cells)_cells_differentiation_to_adipocytes_day04_biol_rep2_(096hA2).CNhs13256.12442-132C3
42	ST2_(Mesenchymal_stem_cells)_cells_differentiation_to_adipocytes_day04_biol_rep3_(096hA3).CNhs13305.12564-133G8
43	ST2_(Mesenchymal_stem_cells)_cells_differentiation_to_adipocytes_day05_biol_rep1_(120hA1).CNhs13128.12321-130G8
44	ST2_(Mesenchymal_stem_cells)_cells_differentiation_to_adipocytes_day05_biol_rep2_(120hA2).CNhs13257.12443-132C4
45	ST2_(Mesenchymal_stem_cells)_cells_differentiation_to_adipocytes_day05_biol_rep3_(120hA3).CNhs13306.12565-133G9
46	ST2_(Mesenchymal_stem_cells)_cells_differentiation_to_adipocytes_day06_biol_rep1_(144hA1).CNhs13129.12322-130G9
47	ST2_(Mesenchymal_stem_cells)_cells_differentiation_to_adipocytes_day06_biol_rep2_(144hA2).CNhs13258.12444-132C5
48	ST2_(Mesenchymal_stem_cells)_cells_differentiation_to_adipocytes_day06_biol_rep3_(144hA3).CNhs13307.12566-133H1
49	ST2_(Mesenchymal_stem_cells)_cells_differentiation_to_osteocytes_00hr15min_biol_rep1_(015mB1).CNhs13130.12323-130H1
50	ST2_(Mesenchymal_stem_cells)_cells_differentiation_to_osteocytes_00hr15min_biol_rep2_(015mB2).CNhs13259.12445-132C6
51	ST2_(Mesenchymal_stem_cells)_cells_differentiation_to_osteocytes_00hr15min_biol_rep3_(015mB3).CNhs13308.12567-133H2
52	ST2_(Mesenchymal_stem_cells)_cells_differentiation_to_osteocytes_00hr30min_biol_rep1_(030mB1).CNhs13131.12324-130H2
53	ST2_(Mesenchymal_stem_cells)_cells_differentiation_to_osteocytes_00hr30min_biol_rep2_(030mB2).CNhs13260.12446-132C7
54	ST2_(Mesenchymal_stem_cells)_cells_differentiation_to_osteocytes_00hr30min_biol_rep3_(030mB3).CNhs13309.12568-133H3
55	ST2_(Mesenchymal_stem_cells)_cells_differentiation_to_osteocytes_01hr_biol_rep1_(001hB1).CNhs13132.12325-130H3
56	ST2_(Mesenchymal_stem_cells)_cells_differentiation_to_osteocytes_01hr_biol_rep2_(001hB2).CNhs13261.12447-132C8
57	ST2_(Mesenchymal_stem_cells)_cells_differentiation_to_osteocytes_01hr_biol_rep3_(001hB3).CNhs13310.12569-133H4
58	ST2_(Mesenchymal_stem_cells)_cells_differentiation_to_osteocytes_02hr_biol_rep1_(002hB1).CNhs13133.12326-130H4
59	ST2_(Mesenchymal_stem_cells)_cells_differentiation_to_osteocytes_02hr_biol_rep2_(002hB2).CNhs13262.12448-132C9
60	ST2_(Mesenchymal_stem_cells)_cells_differentiation_to_osteocytes_02hr_biol_rep3_(002hB3).CNhs13311.12570-133H5
61	ST2_(Mesenchymal_stem_cells)_cells_differentiation_to_osteocytes_03hr_biol_rep1_(003hB1).CNhs13134.12327-130H5
62	ST2_(Mesenchymal_stem_cells)_cells_differentiation_to_osteocytes_03hr_biol_rep2_(003hB2).CNhs13263.12449-132D1

63 ST2_(Mesenchymal_stem_cells)_cells_differentiation_to_osteocytes_03hr_biol_rep3_(003hB3).CNhs13312.12571-133H6
64 ST2_(Mesenchymal_stem_cells)_cells_differentiation_to_osteocytes_06hr_biol_rep1_(006hB1).CNhs13135.12328-130H6
65 ST2_(Mesenchymal_stem_cells)_cells_differentiation_to_osteocytes_06hr_biol_rep2_(006hB2).CNhs13264.12450-132D2
66 ST2_(Mesenchymal_stem_cells)_cells_differentiation_to_osteocytes_06hr_biol_rep3_(006hB3).CNhs13313.12572-133H7
67 ST2_(Mesenchymal_stem_cells)_cells_differentiation_to_osteocytes_12hr_biol_rep1_(012hB1).CNhs13136.12329-130H7
68 ST2_(Mesenchymal_stem_cells)_cells_differentiation_to_osteocytes_12hr_biol_rep2_(012hB2).CNhs13265.12451-132D3
69 ST2_(Mesenchymal_stem_cells)_cells_differentiation_to_osteocytes_12hr_biol_rep3_(012hB3).CNhs13314.12573-133H8
70 ST2_(Mesenchymal_stem_cells)_cells_differentiation_to_osteocytes_18hr_biol_rep1_(018hB1).CNhs13137.12330-130H8
71 ST2_(Mesenchymal_stem_cells)_cells_differentiation_to_osteocytes_18hr_biol_rep2_(018hB2).CNhs13266.12452-132D4
72 ST2_(Mesenchymal_stem_cells)_cells_differentiation_to_osteocytes_18hr_biol_rep3_(018hB3).CNhs13315.12574-133H9
73 ST2_(Mesenchymal_stem_cells)_cells_differentiation_to_osteocytes_24hr_biol_rep1_(024hB1).CNhs13138.12331-130H9
74 ST2_(Mesenchymal_stem_cells)_cells_differentiation_to_osteocytes_24hr_biol_rep2_(024hB2).CNhs13267.12453-132D5
75 ST2_(Mesenchymal_stem_cells)_cells_differentiation_to_osteocytes_24hr_biol_rep3_(024hB3).CNhs13316.12575-133I1
76 ST2_(Mesenchymal_stem_cells)_cells_differentiation_to_osteocytes_36hr_biol_rep1_(036hB1).CNhs13139.12332-130I1
77 ST2_(Mesenchymal_stem_cells)_cells_differentiation_to_osteocytes_36hr_biol_rep2_(036hB2).CNhs13268.12454-132D6
78 ST2_(Mesenchymal_stem_cells)_cells_differentiation_to_osteocytes_36hr_biol_rep3_(036hB3).CNhs13317.12576-133I2
79 ST2_(Mesenchymal_stem_cells)_cells_differentiation_to_osteocytes_day02_biol_rep1_(048hB1).CNhs13140.12333-130I2
80 ST2_(Mesenchymal_stem_cells)_cells_differentiation_to_osteocytes_day02_biol_rep2_(048hB2).CNhs13269.12455-132D7
81 ST2_(Mesenchymal_stem_cells)_cells_differentiation_to_osteocytes_day02_biol_rep3_(048hB3).CNhs13319.12577-133I3
82 ST2_(Mesenchymal_stem_cells)_cells_differentiation_to_osteocytes_day03_biol_rep1_(072hB1).CNhs13141.12334-130I3
83 ST2_(Mesenchymal_stem_cells)_cells_differentiation_to_osteocytes_day03_biol_rep2_(072hB2).CNhs13271.12456-132D8
84 ST2_(Mesenchymal_stem_cells)_cells_differentiation_to_osteocytes_day03_biol_rep3_(072hB3).CNhs13320.12578-133I4
85 ST2_(Mesenchymal_stem_cells)_cells_differentiation_to_osteocytes_day04_biol_rep1_(096hB1).CNhs13142.12335-130I4
86 ST2_(Mesenchymal_stem_cells)_cells_differentiation_to_osteocytes_day04_biol_rep2_(096hB2).CNhs13272.12457-132D9
87 ST2_(Mesenchymal_stem_cells)_cells_differentiation_to_osteocytes_day04_biol_rep3_(096hB3).CNhs13321.12579-133I5
88 ST2_(Mesenchymal_stem_cells)_cells_differentiation_to_osteocytes_day05_biol_rep1_(120hB1).CNhs13144.12336-130I5
89 ST2_(Mesenchymal_stem_cells)_cells_differentiation_to_osteocytes_day05_biol_rep2_(120hB2).CNhs13273.12458-132E1
90 ST2_(Mesenchymal_stem_cells)_cells_differentiation_to_osteocytes_day05_biol_rep3_(120hB3).CNhs13322.12580-133I6
91 ST2_(Mesenchymal_stem_cells)_cells_differentiation_to_osteocytes_day06_biol_rep1_(144hB1).CNhs11940.12337-130I6
92 ST2_(Mesenchymal_stem_cells)_cells_differentiation_to_osteocytes_day06_biol_rep2_(144hB2).CNhs13274.12459-132E2
93 ST2_(Mesenchymal_stem_cells)_cells_differentiation_to_osteocytes_day06_biol_rep3_(144hB3).CNhs13323.12581-133I7
94 ST2_(Mesenchymal_stem_cells)_cells_medium_change_(without_induction)_00hr_biol_rep1_(000hC4).CNhs11939.12338-130I7

95	ST2_(Mesenchymal_stem_cells)_cells_medium_change_(without_induction)_00hr_biol_rep2_(000hC5).CNhs13275.12460-132E3
96	ST2_(Mesenchymal_stem_cells)_cells_medium_change_(without_induction)_00hr_biol_rep3_(000hC6).CNhs13324.12582-133I8
97	ST2_(Mesenchymal_stem_cells)_cells_medium_change_(without_induction)_day06_biol_rep1_(144hC1).CNhs14197.12347-131A7
98	ST2_(Mesenchymal_stem_cells)_cells_medium_change_(without_induction)_day06_biol_rep2_(144hC2).CNhs14198.12469-132F3
99	ST2_(Mesenchymal_stem_cells)_cells_medium_change_(without_induction)_day06_biol_rep3_(144hC3).CNhs14199.12591-134A8
	Natural helper cells
1	natural_helper_cells_IL2_treated_day15_biol_rep1_tech_rep1.CNhs12576.12247-129H6
2	natural_helper_cells_IL2_treated_day15_biol_rep1_tech_rep2.CNhs14330.12247-129H6
3	natural_helper_cells_IL2_treated_day15_biol_rep2_tech_rep1.CNhs12508.12248-129H7
4	natural_helper_cells_IL2_treated_day15_biol_rep2_tech_rep2.CNhs14334.12248-129H7
5	natural_helper_cells_IL2_treated_day15_biol_rep3_tech_rep1.CNhs12509.12249-129H8
6	natural_helper_cells_IL2_treated_day15_biol_rep3_tech_rep2.CNhs14335.12249-129H8
7	natural_helper_cells_IL33_treated_01hr_biol_rep1_tech_rep1.CNhs12579.12253-129I3
8	natural_helper_cells_IL33_treated_01hr_biol_rep1_tech_rep2.CNhs14332.12253-129I3
9	natural_helper_cells_IL33_treated_01hr_biol_rep2_tech_rep2.CNhs14338.12254-129I4
10	natural_helper_cells_IL33_treated_01hr_biol_rep3_tech_rep2.CNhs14339.12255-129I5
11	natural_helper_cells_IL33_treated_day02_biol_rep1_tech_rep2.CNhs14336.12250-129H9
12	natural_helper_cells_IL33_treated_day02_biol_rep2_tech_rep2.CNhs14337.12251-129I1
13	natural_helper_cells_IL33_treated_day02_biol_rep3_tech_rep1.CNhs12578.12252-129I2
14	natural_helper_cells_IL33_treated_day02_biol_rep3_tech_rep2.CNhs14331.12252-129I2
15	natural_helper_cells_naive_biol_rep1_tech_rep2.CNhs14340.12256-129I6
16	natural_helper_cells_naive_biol_rep2_tech_rep1.CNhs12515.12257-129I7
17	natural_helper_cells_naive_biol_rep2_tech_rep2.CNhs14341.12257-129I7
18	natural_helper_cells_naive_biol_rep3_tech_rep1.CNhs12580.12258-129I8
19	natural_helper_cells_naive_biol_rep3_tech_rep2.CNhs14333.12258-129I8
	Neurons
1	Mouse_Neurons_-_cortical_donor1.CNhs12025.11724-123D5
2	Mouse_Neurons_-_cortical_donor2.CNhs11947.11742-123F5
3	Mouse_Neurons_-_cortical_donor3.CNhs12112.11647-122D9
4	Mouse_Neurons_-_dorsal_spinal_cord_donor1.CNhs12630.11720-123D1
5	Mouse_Neurons_-_dorsal_spinal_cord_donor2.CNhs12635.11738-123F1
6	Mouse_Neurons_-_dorsal_spinal_cord_donor3.CNhs12618.11643-122D5
7	Mouse_Neurons_-_hippocampal_donor1.CNhs12133.11721-123D2
8	Mouse_Neurons_-_hippocampal_donor2.CNhs12359.11739-123F2
9	Mouse_Neurons_-_hippocampal_donor3.CNhs12110.11644-122D6
10	Mouse_Neurons_-_raphe_donor1.CNhs12631.11722-123D3
11	Mouse_Neurons_-_raphe_donor2.CNhs12636.11740-123F3
12	Mouse_Neurons_-_raphe_donor3.CNhs12619.11645-122D7
13	Mouse_Neurons_-_striatal_donor1.CNhs12134.11723-123D4
14	Mouse_Neurons_-_striatal_donor2.CNhs12360.11741-123F4
15	Mouse_Neurons_-_striatal_donor3.CNhs12111.11646-122D8
16	Mouse_Neurons_-_substantia_nigra_donor4_tech_rep1.CNhs12612.11489-119E4
17	Mouse_Neurons_-_substantia_nigra_donor4_tech_rep2.CNhs12821.11489-119E4
18	Mouse_Neurons_-_substantia_nigra_donor5.CNhs12614.11490-119E5
19	Mouse_Neurons_-_substantia_nigra_donor6.CNhs12643.11770-123I6
20	Mouse_Neurons_-_ventral_spinal_cord_donor1.CNhs12632.11725-123D6
21	Mouse_Neurons_-_ventral_spinal_cord_donor2.CNhs12638.11743-123F6
22	Mouse_Neurons_-_ventral_spinal_cord_donor3.CNhs12113.11648-122E1
23	Neurons_-_spiral_ganglion_pool1.CNhs14147.11959-126C6
24	Neurons_-_substantia_nigra_donor5_tech_rep2.CNhs12923.11490-119E5
	Others
1	adrenal_gland_adult.CNhs10508.49-24D7
2	adrenal_gland_embryo_E14.CNhs11038.406-44C5
3	adrenal_gland_embryo_E16.CNhs11004.1254-43D6

4 adrenal_gland_embryo_E17.CNhs11043.1263-45I1
5 adrenal_gland_embryo_E18.CNhs11026.1262-18F5
6 adrenal_gland_neonate_N00.CNhs11191.1311-23C1
7 adrenal_gland_neonate_N25.CNhs11223.1377-27I3
8 amnion_adult_pregnant_day17.5.CNhs10488.583-22A8
9 aorta_adult.CNhs10498.46-23H1
10 Mouse_Aortic_Smooth_Muscle_cells_-_differentiated_biol_rep1.CNhs11055.11484-119D8
11 Mouse_Aortic_Smooth_Muscle_cells_-_differentiated_biol_rep2.CNhs11056.11485-119D9
12 Mouse_Aortic_Smooth_Muscle_cells_donor1.CNhs11297.11299-117B3
13 Astrocytes_donor1.CNhs11915.11710-123B9
14 Mouse_Astrocytes_-_cerebellar_donor1.CNhs13077.11708-123B7
15 Mouse_Astrocytes_-_cerebellar_donor2.CNhs12076.11550-120C2
16 Mouse_Astrocytes_-_hippocampus_donor1.CNhs12129.11709-123B8
17 Mouse_Astrocytes_-_hippocampus_donor2.CNhs12077.11551-120C3
18 Mouse_Astrocytes_-_hippocampus_donor3.CNhs12106.11632-122C3
19 Mouse_Astrocytes_donor2.CNhs12078.11552-120C4
20 Mouse_Astrocytes_donor3.CNhs12107.11633-122C4
21 Mouse_CD19+_B_Cells_donor1.CNhs13531.11856-125A2
22 bone_(os_femoris)_adult.CNhs10483.56-12G2
23 bone_(os_femoris)_neonate_N02.CNhs11227.1985-43F5
24 bone_(os_femoris)_neonate_N16.CNhs11225.1525-43A6
25 bone_(os_femoris)_neonate_N20.CNhs11195.1350-25C3
26 Mouse_Cardiac_Myocytes_donor1.CNhs12355.11711-123C1
27 Mouse_Cardiac_Myocytes_donor2.CNhs12356.11729-123E1
28 Mouse_Cardiac_Myocytes_donor3.CNhs12353.11634-122C5
29 cecum_adult.CNhs10467.37-13H4
30 colon_adult.CNhs10468.36-18H7
31 corpora_quadrigemina_adult.CNhs10501.16-22A4
32 corpus_striatum_adult.CNhs10487.19-21D8
33 corpus_striatum_neonate_N00.CNhs11226.630-43F1
34 cortex_adult.CNhs10473.12-14D5
35 cortex_neonate_N30.CNhs11107.1392-42F2
36 diencephalon_adult.CNhs10482.20-12F2
37 diencephalon_neonate_N30.CNhs11201.1388-42B2
38 CD326+_enterocyte_pool1.CNhs13542.11848-124I3
39 CD326+_enterocyte_pool2.CNhs13197.11849-124I4
40 CD326++_enterocyte_isolated_from_mice_treated_with_RANKL_day03_pool2.CNhs13210.11853-124I8
41 epididymis_adult.CNhs10490.58-23B2
42 epididymis_and_seminiferous_tubule_neonate_N00.CNhs11218.1310-23B1
43 epididymis_and_seminiferous_tubule_neonate_N30.CNhs11199.1387-42A2
44 eyeball_adult.CNhs10484.31-12G4
45 eyeball_embryo_E12.CNhs11016.345-16C6
46 eyeball_embryo_E14.CNhs10521.399-16E2
47 eyeball_embryo_E15.CNhs10593.426-16C9
48 eyeball_embryo_E17.CNhs11023.1261-18D4
49 eyeball_neonate_N00.CNhs11207.633-15C6
50 eyeball_neonate_N01.CNhs11140.1532-43E7
51 eyeball_neonate_N02.CNhs11205.1551-44G8
52 eyeball_neonate_N16.CNhs11188.777-19A2
53 Mouse_Embryonic_fibroblasts_donor1.CNhs12130.11712-123C2
54 mouse_fibroblast_cell_line:_CRL-1658_NIH/3T3.CNhs11093.1830-49C7
55 Follicle_Associated_Epithelium_pool2.CNhs13211.10262-104D1
56 Follicle_Associated_Epithelium_pool3.CNhs13200.10263-104D2
57 forelimb_embryo_E11.CNhs10596.335-25E2
58 forelimb_embryo_E12.CNhs10600.359-14H2
59 forelimb_embryo_E13.CNhs10589.384-1E2
60 forelimb_embryo_E14.CNhs10577.413-26A8
61 forelimb_embryo_E15.CNhs11007.437-20E7

62 forelimb_embryo_E17.CNhs10598.1517-43C4
63 forelimb_embryo_E18.CNhs11008.1520-43B5
64 gonad_embryo_E13.CNhs11044.1564-45I6
65 granulocyte_macrophage_progenitor_GMP_biol_rep3.CNhs11928.12129-128D5
66 hematopoietic_stem_cell_bone_marrow_derived_adult_2years.CNhs14157.11958-126C5
67 hematopoietic_stem_cell_bone_marrow_derived_newborn_2-3months.CNhs14156.11957-126C4
68 hematopoietic_stem_cell_fetal_liver_derived_embryo_E12.5.CNhs14153.11953-126B9
69 hematopoietic_stem_cell_fetal_liver_derived_embryo_E14.5.CNhs14154.11954-126C1
70 hematopoietic_stem_cell_fetal_liver_derived_embryo_E19.5.CNhs14155.11955-126C2
71 hematopoietic_stem_cell_placenta_derived_embryo_E10.5.CNhs14150.11950-126B6
72 hematopoietic_stem_cell_placenta_derived_embryo_E11.5.CNhs14152.11952-126B8
73 hematopoietic_stem_cellaorta-gonad-mesonephros_(AGM)_region_derived_embryo_E11.5.CNhs14151.11951-126B7
74 Mouse_hepatic_Sinusoidal_Endothelial_Cells_donor1.CNhs13209.11830-124G3
75 Mouse_hepatic_Stellate_Cells_(lipocyte)_donor1.CNhs13196.11825-124F7
76 hippocampus_adult.CNhs10478.13-16E8
77 hippocampus_neonate_N00.CNhs11228.627-43G1
78 Ileum_epithelium_pool1.CNhs13199.10252-104B9
79 Inner_ear_stem_cells_1st_generation_stem_cells_pool1.CNhs11929.12215-129E1
80 intestinal_mucosa_adult.CNhs10506.860-29I3
81 accessory_axillary_lymph_node_adult.CNhs10475.1063-29H9
82 mammary_gland_adult_lactating_day02.CNhs10480.595-22B6
83 mammary_gland_adult_pregnant_day19.CNhs10476.588-5H2
84 medulla_oblongata_adult.CNhs10477.17-12C2
85 medulla_oblongata_neonate_N30.CNhs11200.1396-42A3
86 CD41+_megakaryocyte_cancer_donor1.CNhs13079.11774-124A1
87 CD41+_megakaryocyte_cancer_donor2.CNhs13213.11776-124A3
88 CD41+_megakaryocyte_cancer_donor3.CNhs13506.11778-124A5
89 CD41+_megakaryocyte_control_donor1.CNhs13212.11775-124A2
90 CD41+_megakaryocyte_control_donor2.CNhs13214.11777-124A4
91 CD41+_megakaryocyte_control_donor3.CNhs13201.11779-124A6
92 Mouse_Meningeal_cells_donor1.CNhs12132.11716-123C6
93 Mouse_Meningeal_cells_donor2.CNhs12358.11734-123E6
94 Mouse_Meningeal_cells_donor3.CNhs12109.11639-122D1
95 Mesoderm_embryo_E8.5.CNhs14148.11947-126B3
96 Mouse_Microglia_donor1.CNhs12629.11718-123C8
97 Mouse_Microglia_donor2.CNhs12634.11736-123E8
98 Mouse_Microglia_donor3.CNhs12617.11641-122D3
99 Universal_RNA_-_Mouse_Normal_Tissues_Biochain_pool1.CNhs10613.10008-101B6
100 Clontech_Mouse_Universal_Reference_Total_RNA_pool1.CNhs10609.10001-101A3
101 SABiosciences_XpressRef_Mouse_Universal_Total_RNA_pool1.CNhs10611.10003-101A7
102 muscle_(biceps_femoris)_neonate_N30.CNhs11129.1389-42C2
103 neurospheres_-_enteric_neuron_derived_biol_rep1.CNhs13087.11810-124E1
104 neurospheres_-_enteric_neuron_derived_biol_rep2.CNhs13088.11811-124E2
105 neurospheres_-_enteric_neuron_derived_biol_rep3.CNhs13089.11812-124E3
106 neurospheres_-_parasympathetic_neuron_derived_biol_rep1.CNhs13084.11807-124D7
107 neurospheres_-_parasympathetic_neuron_derived_biol_rep2.CNhs13085.11808-124D8
108 neurospheres_-_parasympathetic_neuron_derived_biol_rep3.CNhs13086.11809-124D9
109 neurospheres_-_sympathetic_neuron_derived_biol_rep1.CNhs13081.11804-124D4
110 neurospheres_-_sympathetic_neuron_derived_biol_rep2.CNhs13082.11805-124D5
111 neurospheres_-_sympathetic_neuron_derived_biol_rep3.CNhs13083.11806-124D6
112 olfactory_brain_adult.CNhs10489.18-22I9
113 osteoclast_bone_marrow_derived.CNhs14137.2379-69A1
114 ovary_adult.CNhs10507.91-2I7
115 ovary_embryo_E18.CNhs11040.505-44H7
116 ovary_neonate_N00.CNhs11217.1299-22I4
117 oviduct_adult_pregnant_day01.CNhs10500.988-6G6
118 pituitary_gland_adult.CNhs10493.21-1G8
119 pituitary_gland_embryo_E12.CNhs11018.346-16E6

120	pituitary_gland_embryo_E13.CNhs11009.370-44C7
121	pituitary_gland_embryo_E14.CNhs11037.398-44A5
122	pituitary_gland_embryo_E15.CNhs10592.427-16B9
123	pituitary_gland_embryo_E16.CNhs11036.449-43F6
124	pituitary_gland_embryo_E17.CNhs11039.1265-44F5
125	pituitary_gland_neonate_N00.CNhs11190.1308-22E9
126	placenta_adult_pregnant_day10.CNhs10472.539-13I7
127	placenta_adult_pregnant_day17.CNhs10464.577-18G3
128	Pre-hematopoietic_stem_cell_aorta-gonad-mesonephros_(AGM)_region_derived_embryo_E9.5.CNhs14149.11948-126B4
129	prostate_adult.CNhs10470.859-1F8
130	Mouse_Renal_epithelial_cells_donor1.CNhs14555.11727-123D8
131	Mouse_Schwann_donor1.CNhs12507.11728-123D9
132	Mouse_Schwann_donor2.CNhs12573.11746-123F9
133	Mouse_Schwann_donor3.CNhs12115.11651-122E4
134	skin_adult.CNhs10492.30-1C3
135	skin_neonate_N00.CNhs11124.650-25G4
136	skin_neonate_N03.CNhs11215.662-22H3
137	skin_neonate_N06.CNhs11097.693-20I5
138	skin_neonate_N10.CNhs11108.762-6C4
139	small_intestine_neonate_N16.CNhs11114.790-21I1
140	spinal_cord_adult.CNhs10505.24-13C9
141	spleen_adult.CNhs10465.25-2G2
142	spleen_embryo_E16.CNhs11035.461-43C1
143	spleen_embryo_E18.CNhs11011.1271-21F2
144	spleen_neonate_N10.CNhs11116.752-24D1
145	spleen_neonate_N20.CNhs11112.824-19H1
146	spleen_neonate_N25.CNhs11099.1354-25G3
147	submandibular_gland_adult.CNhs10469.59-29C1
148	tongue_adult.CNhs10499.32-1B4
149	TSt-4/DLL1_feeder_cells_biol_rep1.CNhs13407.12971-138H1
150	TSt-4/DLL1_feeder_cells_biol_rep2.CNhs13408.12987-138I8
151	TSt-4/DLL1_feeder_cells_biol_rep3.CNhs13409.13003-139B6
152	urinary_bladder_adult.CNhs10481.879-12E4
153	uterus_adult.CNhs10509.92-27E5
154	uterus_adult_pregnant_day19.CNhs10497.590-15F5
155	vagina_adult.CNhs10502.89-27D5
156	vesicular_gland_adult.CNhs10491.51-27F8
	Pancreas
1	pancreas_adult.CNhs10486.34-16E4
2	pancreas_embryo_E14.CNhs11012.405-44F4
3	pancreas_embryo_E15.CNhs11042.1556-45F2
4	pancreas_embryo_E16.CNhs11003.460-26E5
5	pancreas_embryo_E17.CNhs10599.1558-45G3
6	pancreas_embryo_E18.CNhs10580.1535-43I7
7	pancreas_neonate_N00.CNhs11105.645-26G9
8	pancreas_neonate_N01.CNhs11138.1531-43D7
9	pancreas_neonate_N02.CNhs11139.1539-43D8
10	pancreas_neonate_N16.CNhs11136.787-43B6
11	pancreas_neonate_N25.CNhs11094.1555-45E2
12	pancreas_neonate_N30.CNhs11182.1548-44H5
	Stomach
1	stomach_adult.CNhs10503.33-1H6
2	stomach_embryo_E12.CNhs10588.356-43E3
3	stomach_embryo_E15.CNhs10603.1252-16G8
4	stomach_embryo_E16.CNhs11022.459-17D4
5	stomach_embryo_E17.CNhs11006.1035-18D5
6	stomach_embryo_E18.CNhs10999.1286-20C6
7	stomach_neonate_N03.CNhs11193.1340-24B8

8	stomach_neonate_N07.CNhs11210.718-18A9
9	stomach_neonate_N25.CNhs11104.1355-25E4
10	stomach_neonate_N30.CNhs11134.1386-42I1
	T cell induction
1	EBF_KO_HPCs_induced_to_T_cell_00hr00min_biol_rep1.CNhs11058.12972-138H2
2	EBF_KO_HPCs_induced_to_T_cell_00hr00min_biol_rep2.CNhs12980.12988-138I9
3	EBF_KO_HPCs_induced_to_T_cell_00hr00min_biol_rep3.CNhs13687.13004-139B7
4	EBF_KO_HPCs_induced_to_T_cell_00hr30min_biol_rep1.CNhs12231.12973-138H3
5	EBF_KO_HPCs_induced_to_T_cell_00hr30min_biol_rep2.CNhs12981.12989-139A1
6	EBF_KO_HPCs_induced_to_T_cell_00hr30min_biol_rep3.CNhs13688.13005-139B8
7	EBF_KO_HPCs_induced_to_T_cell_01hr_biol_rep1.CNhs12232.12974-138H4
8	EBF_KO_HPCs_induced_to_T_cell_01hr_biol_rep2.CNhs12982.12990-139A2
9	EBF_KO_HPCs_induced_to_T_cell_01hr_biol_rep3.CNhs13689.13006-139B9
10	EBF_KO_HPCs_induced_to_T_cell_02hr_biol_rep1.CNhs12233.12975-138H5
11	EBF_KO_HPCs_induced_to_T_cell_02hr_biol_rep2.CNhs12984.12991-139A3
12	EBF_KO_HPCs_induced_to_T_cell_02hr_biol_rep3.CNhs13690.13007-139C1
13	EBF_KO_HPCs_induced_to_T_cell_04hr_biol_rep1.CNhs12234.12976-138H6
14	EBF_KO_HPCs_induced_to_T_cell_04hr_biol_rep2.CNhs12985.12992-139A4
15	EBF_KO_HPCs_induced_to_T_cell_04hr_biol_rep3.CNhs13691.13008-139C2
16	EBF_KO_HPCs_induced_to_T_cell_06hr_biol_rep1.CNhs12235.12977-138H7
17	EBF_KO_HPCs_induced_to_T_cell_06hr_biol_rep2.CNhs12986.12993-139A5
18	EBF_KO_HPCs_induced_to_T_cell_06hr_biol_rep3.CNhs13587.13009-139C3
19	EBF_KO_HPCs_induced_to_T_cell_08hr_biol_rep1.CNhs12236.12978-138H8
20	EBF_KO_HPCs_induced_to_T_cell_08hr_biol_rep2.CNhs12987.12994-139A6
21	EBF_KO_HPCs_induced_to_T_cell_08hr_biol_rep3.CNhs13588.13010-139C4
22	EBF_KO_HPCs_induced_to_T_cell_10hr_biol_rep1.CNhs12237.12979-138H9
23	EBF_KO_HPCs_induced_to_T_cell_10hr_biol_rep2.CNhs12988.12995-139A7
24	EBF_KO_HPCs_induced_to_T_cell_10hr_biol_rep3.CNhs13589.13011-139C5
25	EBF_KO_HPCs_induced_to_T_cell_12hr_biol_rep1.CNhs12238.12980-138I1
26	EBF_KO_HPCs_induced_to_T_cell_12hr_biol_rep2.CNhs12989.12996-139A8
27	EBF_KO_HPCs_induced_to_T_cell_12hr_biol_rep3.CNhs13590.13012-139C6
28	EBF_KO_HPCs_induced_to_T_cell_24hr_biol_rep1.CNhs12239.12981-138I2
29	EBF_KO_HPCs_induced_to_T_cell_24hr_biol_rep2.CNhs12990.12997-139A9
30	EBF_KO_HPCs_induced_to_T_cell_24hr_biol_rep3.CNhs13591.13013-139C7
31	EBF_KO_HPCs_induced_to_T_cell_day02_biol_rep1.CNhs12240.12982-138I3
32	EBF_KO_HPCs_induced_to_T_cell_day02_biol_rep2.CNhs12991.12998-139B1
33	EBF_KO_HPCs_induced_to_T_cell_day02_biol_rep3.CNhs13592.13014-139C8
34	EBF_KO_HPCs_induced_to_T_cell_day03_biol_rep1.CNhs11059.12983-138I4
35	EBF_KO_HPCs_induced_to_T_cell_day03_biol_rep2.CNhs13684.12999-139B2
36	EBF_KO_HPCs_induced_to_T_cell_day03_biol_rep3.CNhs13593.13015-139C9
37	EBF_KO_HPCs_induced_to_T_cell_day04_biol_rep1.CNhs12241.12984-138I5
38	EBF_KO_HPCs_induced_to_T_cell_day04_biol_rep2.CNhs13686.13000-139B3
39	EBF_KO_HPCs_induced_to_T_cell_day04_biol_rep3.CNhs13595.13016-139D1
40	EBF_KO_HPCs_induced_to_T_cell_day05_biol_rep1.CNhs12242.12985-138I6
41	EBF_KO_HPCs_induced_to_T_cell_day05_biol_rep2.CNhs12992.13001-139B4
42	EBF_KO_HPCs_induced_to_T_cell_day05_biol_rep3.CNhs13596.13017-139D2
43	EBF_KO_HPCs_induced_to_T_cell_day06_biol_rep1.CNhs11060.12986-138I7
44	EBF_KO_HPCs_induced_to_T_cell_day06_biol_rep2.CNhs12993.13002-139B5
45	EBF_KO_HPCs_induced_to_T_cell_day06_biol_rep3.CNhs13597.13018-139D3
	T cells
1	CD4+CD25+_regulatory_T_cells_antiCD3_CD28_stimulation_06hr_pool1_(BalbcA).CNhs14158.11943-126A8
2	CD4+CD25+_regulatory_T_cells_antiCD3_CD28_stimulation_06hr_pool1_(C57BL_6J).CNhs14159.11944-126A9
3	CD4+CD25+_regulatory_T_cells_PMA_and_ionomycin_stimulation_02hr_pool1_(BalbcA).CNhs14160.11946-126B2
4	CD4+CD25+_regulatory_T_cells_PMA_and_ionomycin_stimulation_02hr_pool1_(C57BL_6J).CNhs14142.11945-126B1
5	CD4+CD25+_regulatory_T_cells_pool1_(C57BL_6J).CNhs13913.11814-124E5

6	CD4+CD25+_regulatory_T_cells_pool2_(Balb_cAJcl).CNhs13221.11818-124E9
7	CD4+CD25-CD44-_naive_conventional_T_cells_antiCD3_CD28_stimulation_06hr_pool1_(C57BL_6J).CNhs13218.11815-124E6
8	CD4+CD25-CD44-_naive_conventional_T_cells_antiCD3_CD28_stimulation_06hr_pool2_(Balb_cAJcl).CNhs13225.11819-124F1
9	CD4+CD25-CD44-_naive_conventional_T_cells_PMA_and_ionomycin_stimulation_02hr_pool1_(C57BL_6J).CNhs13219.11816-124E7
10	CD4+CD25-CD44-_naive_conventional_T_cells_PMA_and_ionomycin_stimulation_02hr_pool2_(Balb_cAJcl).CNhs13226.11820-124F2
11	CD4+CD25-CD44-_naive_conventional_T_cells_pool1_(C57BL_6J).CNhs13217.11813-124E4
12	CD4+CD25-CD44-_naive_conventional_T_cells_pool2_(Balb_cAJcl).CNhs13220.11817-124E8
13	Mouse_CD4+_T_Cells_donor1.CNhs13509.11854-124I9
14	Mouse_CD8+_T_Cells_donor1.CNhs13511.11855-125A1
	Testis
1	testis_adult.CNhs10504.57-7G5
2	testis_embryo_E13.CNhs11031.389-23F5
3	testis_embryo_E15.CNhs11034.443-27C5
4	testis_embryo_E16.CNhs11033.470-26G5
5	testis_embryo_E17.CNhs11029.486-18I5
6	testis_embryo_E18.CNhs11027.503-18G5
7	testis_neonate_N00.CNhs11189.1300-22B7
8	testis_neonate_N07.CNhs11222.726-26I4
9	testis_neonate_N10.CNhs11204.763-44D9
10	testis_neonate_N20.CNhs11110.839-18H3
11	testis_neonate_N30.CNhs11130.1391-42E2
	Thymus
1	thymus_adult.CNhs10471.38-12B5
2	thymus_embryo_E14.CNhs11041.402-44I4
3	thymus_embryo_E15.CNhs11005.430-45I2
4	thymus_embryo_E16.CNhs11002.456-26C5
5	thymus_embryo_E17.CNhs10581.478-18C1
6	thymus_embryo_E18.CNhs10595.1273-19G4
7	thymus_neonate_N02.CNhs11181.1541-43F8
8	thymus_neonate_N03.CNhs11137.2104-43C7
9	thymus_neonate_N06.CNhs11197.681-26C4
10	thymus_neonate_N07.CNhs11211.713-19D3
11	thymus_neonate_N10.CNhs11194.748-24E4
12	thymus_neonate_N20.CNhs11186.820-7A2
13	thymus_neonate_N25.CNhs11125.1362-25G7
14	thymus_neonate_N30.CNhs11132.1393-42G2
	Tracheal epithelial cells
1	Tracheal_epithelial_cells_differentiation_to_ciliated_epithelial_cells_000hr_biol_rep1.CNhs13739.13367-143G1
2	Tracheal_epithelial_cells_differentiation_to_ciliated_epithelial_cells_000hr_biol_rep2.CNhs13740.13368-143G2
3	Tracheal_epithelial_cells_differentiation_to_ciliated_epithelial_cells_000hr_biol_rep3.CNhs13741.13369-143G3
4	Tracheal_epithelial_cells_differentiation_to_ciliated_epithelial_cells_004hr_biol_rep1.CNhs13742.13370-143G4
5	Tracheal_epithelial_cells_differentiation_to_ciliated_epithelial_cells_004hr_biol_rep2.CNhs13743.13371-143G5
6	Tracheal_epithelial_cells_differentiation_to_ciliated_epithelial_cells_004hr_biol_rep3.CNhs13744.13372-143G6
7	Tracheal_epithelial_cells_differentiation_to_ciliated_epithelial_cells_008hr_biol_rep1.CNhs13745.13373-143G7
8	Tracheal_epithelial_cells_differentiation_to_ciliated_epithelial_cells_008hr_biol_rep2.CNhs13746.13374-143G8

9	Tracheal_epithelial_cells_differentiation_to_ciliated_epithelial_cells_008hr_biol_rep3.CNhs13747.13375-143G9
10	Tracheal_epithelial_cells_differentiation_to_ciliated_epithelial_cells_012hr_biol_rep1.CNhs13696.13376-143H1
11	Tracheal_epithelial_cells_differentiation_to_ciliated_epithelial_cells_012hr_biol_rep2.CNhs13748.13377-143H2
12	Tracheal_epithelial_cells_differentiation_to_ciliated_epithelial_cells_012hr_biol_rep3.CNhs13749.13378-143H3
13	Tracheal_epithelial_cells_differentiation_to_ciliated_epithelial_cells_016hr_biol_rep1.CNhs13750.13379-143H4
14	Tracheal_epithelial_cells_differentiation_to_ciliated_epithelial_cells_016hr_biol_rep2.CNhs13751.13380-143H5
15	Tracheal_epithelial_cells_differentiation_to_ciliated_epithelial_cells_016hr_biol_rep3.CNhs13752.13381-143H6
16	Tracheal_epithelial_cells_differentiation_to_ciliated_epithelial_cells_020hr_biol_rep1.CNhs13697.13382-143H7
17	Tracheal_epithelial_cells_differentiation_to_ciliated_epithelial_cells_020hr_biol_rep2.CNhs13753.13383-143H8
18	Tracheal_epithelial_cells_differentiation_to_ciliated_epithelial_cells_020hr_biol_rep3.CNhs13754.13384-143H9
19	Tracheal_epithelial_cells_differentiation_to_ciliated_epithelial_cells_024hr_biol_rep1.CNhs13755.13385-143I1
20	Tracheal_epithelial_cells_differentiation_to_ciliated_epithelial_cells_024hr_biol_rep2.CNhs13756.13386-143I2
21	Tracheal_epithelial_cells_differentiation_to_ciliated_epithelial_cells_024hr_biol_rep3.CNhs13757.13387-143I3
22	Tracheal_epithelial_cells_differentiation_to_ciliated_epithelial_cells_030hr_biol_rep1.CNhs13758.13388-143I4
23	Tracheal_epithelial_cells_differentiation_to_ciliated_epithelial_cells_030hr_biol_rep2.CNhs13759.13389-143I5
24	Tracheal_epithelial_cells_differentiation_to_ciliated_epithelial_cells_030hr_biol_rep3.CNhs13760.13390-143I6
25	Tracheal_epithelial_cells_differentiation_to_ciliated_epithelial_cells_036hr_biol_rep1.CNhs13762.13391-143I7
26	Tracheal_epithelial_cells_differentiation_to_ciliated_epithelial_cells_036hr_biol_rep2.CNhs13763.13392-143I8
27	Tracheal_epithelial_cells_differentiation_to_ciliated_epithelial_cells_036hr_biol_rep3.CNhs13764.13393-143I9
28	Tracheal_epithelial_cells_differentiation_to_ciliated_epithelial_cells_042hr_biol_rep1.CNhs13765.13394-144A1
29	Tracheal_epithelial_cells_differentiation_to_ciliated_epithelial_cells_042hr_biol_rep2.CNhs13766.13395-144A2
30	Tracheal_epithelial_cells_differentiation_to_ciliated_epithelial_cells_042hr_biol_rep3.CNhs13767.13396-144A3
31	Tracheal_epithelial_cells_differentiation_to_ciliated_epithelial_cells_048hr_biol_rep1.CNhs13768.13397-144A4
32	Tracheal_epithelial_cells_differentiation_to_ciliated_epithelial_cells_048hr_biol_rep2.CNhs13769.13398-144A5
33	Tracheal_epithelial_cells_differentiation_to_ciliated_epithelial_cells_048hr_biol_rep3.CNhs13770.13399-144A6
34	Tracheal_epithelial_cells_differentiation_to_ciliated_epithelial_cells_054hr_biol_rep1.CNhs13771.13400-144A7
35	Tracheal_epithelial_cells_differentiation_to_ciliated_epithelial_cells_054hr_biol_rep2.CNhs13772.13401-144A8
36	Tracheal_epithelial_cells_differentiation_to_ciliated_epithelial_cells_054hr_biol_rep3.CNhs13773.13402-144A9
37	Tracheal_epithelial_cells_differentiation_to_ciliated_epithelial_cells_060hr_biol_rep1.CNhs13774.13403-144B1
38	Tracheal_epithelial_cells_differentiation_to_ciliated_epithelial_cells_060hr_biol_rep2.CNhs13775.13404-144B2
39	Tracheal_epithelial_cells_differentiation_to_ciliated_epithelial_cells_060hr_biol_rep3.CNhs13776.13405-144B3
40	Tracheal_epithelial_cells_differentiation_to_ciliated_epithelial_cells_066hr_biol_rep1.CNhs13777.13406-144B4

41	Tracheal_epithelial_cells_differentiation_to_ciliated_epithelial_cells_066hr_biol_rep2.CNhs13778.13407-144B5
42	Tracheal_epithelial_cells_differentiation_to_ciliated_epithelial_cells_066hr_biol_rep3.CNhs13779.13408-144B6
43	Tracheal_epithelial_cells_differentiation_to_ciliated_epithelial_cells_072hr_biol_rep1.CNhs13780.13409-144B7
44	Tracheal_epithelial_cells_differentiation_to_ciliated_epithelial_cells_072hr_biol_rep2.CNhs13781.13410-144B8
45	Tracheal_epithelial_cells_differentiation_to_ciliated_epithelial_cells_072hr_biol_rep3.CNhs13782.13411-144B9
46	Tracheal_epithelial_cells_differentiation_to_ciliated_epithelial_cells_084hr_biol_rep1.CNhs13783.13412-144C1
47	Tracheal_epithelial_cells_differentiation_to_ciliated_epithelial_cells_084hr_biol_rep2.CNhs13784.13413-144C2
48	Tracheal_epithelial_cells_differentiation_to_ciliated_epithelial_cells_084hr_biol_rep3.CNhs13786.13414-144C3
49	Tracheal_epithelial_cells_differentiation_to_ciliated_epithelial_cells_096hr_biol_rep1.CNhs13787.13415-144C4
50	Tracheal_epithelial_cells_differentiation_to_ciliated_epithelial_cells_096hr_biol_rep2.CNhs13788.13416-144C5
51	Tracheal_epithelial_cells_differentiation_to_ciliated_epithelial_cells_096hr_biol_rep3.CNhs13789.13417-144C6
52	Tracheal_epithelial_cells_differentiation_to_ciliated_epithelial_cells_120hr_biol_rep1.CNhs13790.13418-144C7
53	Tracheal_epithelial_cells_differentiation_to_ciliated_epithelial_cells_120hr_biol_rep2.CNhs13791.13419-144C8
54	Tracheal_epithelial_cells_differentiation_to_ciliated_epithelial_cells_120hr_biol_rep3.CNhs13792.13420-144C9
	Trophoblast stem cells
1	trophoblast_stem_cell_line_B1_differentiation_day00_biol_rep1.CNhs13526.13297-142H3
2	trophoblast_stem_cell_line_B1_differentiation_day01_biol_rep1.CNhs13527.13298-142H4
3	trophoblast_stem_cell_line_B1_differentiation_day02_biol_rep1.CNhs13528.13299-142H5
4	trophoblast_stem_cell_line_B1_differentiation_day03_biol_rep1.CNhs13529.13300-142H6
5	trophoblast_stem_cell_line_B1_differentiation_day04_biol_rep1.CNhs13635.13301-142H7
6	trophoblast_stem_cell_line_B1_differentiation_day05_biol_rep1.CNhs13636.13302-142H8
7	trophoblast_stem_cell_line_B1_differentiation_day06_biol_rep1.CNhs13530.13303-142H9
8	trophoblast_stem_cell_line_R1AB_differentiation_day00_biol_rep1.CNhs13481.13283-142F7
9	trophoblast_stem_cell_line_R1AB_differentiation_day01_biol_rep1.CNhs13514.13284-142F8
10	trophoblast_stem_cell_line_R1AB_differentiation_day02_biol_rep1.CNhs13515.13285-142F9
11	trophoblast_stem_cell_line_R1AB_differentiation_day03_biol_rep1.CNhs13516.13286-142G1
12	trophoblast_stem_cell_line_R1AB_differentiation_day04_biol_rep1.CNhs13517.13287-142G2
13	trophoblast_stem_cell_line_R1AB_differentiation_day05_biol_rep1.CNhs13518.13288-142G3
14	trophoblast_stem_cell_line_R1AB_differentiation_day06_biol_rep1.CNhs13482.13289-142G4
15	trophoblast_stem_cell_line_Rybp_differentiation_day00_biol_rep1.CNhs13519.13290-142G5
16	trophoblast_stem_cell_line_Rybp_differentiation_day01_biol_rep1.CNhs13520.13291-142G6
17	trophoblast_stem_cell_line_Rybp_differentiation_day02_biol_rep1.CNhs13521.13292-142G7
18	trophoblast_stem_cell_line_Rybp_differentiation_day03_biol_rep1.CNhs13522.13293-142G8
19	trophoblast_stem_cell_line_Rybp_differentiation_day04_biol_rep1.CNhs13523.13294-142G9
20	trophoblast_stem_cell_line_Rybp_differentiation_day05_biol_rep1.CNhs13524.13295-142H1
21	trophoblast_stem_cell_line_Rybp_differentiation_day06_biol_rep1.CNhs13525.13296-142H2
	Visual cortex
1	visual_cortex_-_Mecp_knockout_neonate_N15_donor1.CNhs13040.10244-104B1
2	visual_cortex_-_Mecp_knockout_neonate_N15_donor2.CNhs13041.10245-104B2
3	visual_cortex_-_Mecp_knockout_neonate_N15_donor3.CNhs13821.10350-105D8
4	visual_cortex_-_Mecp_knockout_neonate_N30_donor1.CNhs13042.10246-104B3
5	visual_cortex_-_Mecp_knockout_neonate_N30_donor2.CNhs13043.10247-104B4
6	visual_cortex_-_Mecp_knockout_neonate_N30_donor3.CNhs13044.10248-104B5
7	visual_cortex_-_Mecp_knockout_neonate_N60-70_donor1.CNhs13045.10249-104B6
8	visual_cortex_-_Mecp_knockout_neonate_N60-70_donor2.CNhs13046.10250-104B7
9	visual_cortex_-_Mecp_knockout_neonate_N60-70_donor3.CNhs13048.10251-104B8
10	visual_cortex_-_wildtype_neonate_N15_donor1.CNhs13031.10235-104A1

11	visual_cortex_-_wildtype_neonate_N15_donor2.CNhs13032.10236-104A2
12	visual_cortex_-_wildtype_neonate_N15_donor3.CNhs13033.10237-104A3
13	visual_cortex_-_wildtype_neonate_N15_donor5.CNhs13820.10349-105D7
14	visual_cortex_-_wildtype_neonate_N30_donor1.CNhs13034.10238-104A4
15	visual_cortex_-_wildtype_neonate_N30_donor2.CNhs13035.10239-104A5
16	visual_cortex_-_wildtype_neonate_N30_donor3.CNhs13036.10240-104A6
17	visual_cortex_-_wildtype_neonate_N60-70_donor1.CNhs13037.10241-104A7
18	visual_cortex_-_wildtype_neonate_N60-70_donor2.CNhs13038.10242-104A8
19	visual_cortex_-_wildtype_neonate_N60-70_donor3.CNhs13039.10243-104A9
	Whole body
1	whole_body_embryo_E11.CNhs11014.324-5I8
2	whole_body_embryo_E12.CNhs10587.857-27C9
3	whole_body_embryo_E13.CNhs10512.372-23H2
4	whole_body_embryo_E14.5.CNhs10578.420-27D2
5	whole_body_embryo_E14.CNhs10519.395-14B1
6	whole_body_embryo_E16.CNhs10514.453-14F2
7	whole_body_embryo_E17.5.CNhs10513.490-9F9
8	whole_body_embryo_E17.CNhs10517.475-3I5
9	whole_body_embryo_E18.CNhs10516.493-3B3
10	whole_body_neonate_N00.CNhs10525.657-19C2
11	whole_body_neonate_N01.CNhs10576.659-23C6
12	whole_body_neonate_N06.CNhs10515.692-21D1
13	whole_body_neonate_N10.CNhs10518.761-6B4

MASSEY UNIVERSITY
GRADUATE RESEARCH SCHOOL

STATEMENT OF CONTRIBUTION TO DOCTORAL THESIS CONTAINING PUBLICATIONS

(To appear at the end of each thesis chapter/section/appendix submitted as an article/paper or collected as an appendix at the end of the thesis)

We, the candidate and the candidate's Principal Supervisor, certify that all co-authors have consented to their work being included in the thesis and they have accepted the candidate's contribution as indicated below in the *Statement of Originality*.

Name of Candidate: Elena Denisenko

Name/Title of Principal Supervisor: Dr Sebastian Schmeier

Name of Published Research Output and full reference:

Denisenko E, Guler R, Mhlanga MM, Suzuki H, Brombacher F, Schmeier S. Genome-wide profiling of transcribed enhancers during macrophage activation. Epigenetics & chromatin. 2017;10:50

In which Chapter is the Published Work: Chapter 3

Please indicate either:

- The percentage of the Published Work that was contributed by the candidate:

  and / or

- Describe the contribution that the candidate has made to the Published Work:

  The candidate has performed all computational analyses. The results were interpreted by the candidate and the supervisor. The candidate drafted the manuscript with input from all authors.

Elena Denisenko
Digitally signed by Elena Denisenko
DN: cn=Elena Denisenko, o=Massey University, ou=INMS, email=elena.denisenko.w@gmail.com, c=NZ
Date: 2017.11.21 17:21:32 +13'00'

Candidate's Signature

21/11/2017
Date

Sebastian Schmeier
Digitally signed by Sebastian Schmeier
Date: 2018.02.13 10:34:43 +13'00'

Principal Supervisor's signature

13/02/2018
Date